Studies in the Chemistry of Marine Natural Products

A thesis submitted in partial fulfilment of the

requirements for the Degree

of

Doctor of Philosophy in Chemistry

in the University of Canterbury

by

Sarah Jane Herbison Hickford

University of Canterbury

Christchurch, New Zealand

2007

Contents

Abstract

Compounds from the marine environment exhibit a wide variety of biological activities, and thus hold much promise as potential drugs. The halichondrins, isolated from the Kaikoura sponge *Lissodendoryx* sp. are no exception to this, demonstrating potent anticancer activity. Novel cytotoxic compounds have also been isolated from the Chatham Rise sponge *Lamellomorpha strongylata*. Knowledge of the cellular origins of such compounds is desirable, in order to establish if the sponge or associated micro-organisms are producing the compounds of interest. Siderophores are also important molecules, which are produced on demand by bacteria in order to obtain sufficient iron necessary for their growth. Knowledge of the biosynthesis of these compounds has potential for the control of undesirable bacteria, such as the anthrax-causing pathogen *Bacillus anthracis.*

Cell separation studies have been carried out on *Lamellomorpha strongylata,* locating a swinholide in sponge-associated filamentous bacteria and theonellapeptolides in sponge-associated unicellular bacteria. A microscopic analysis of dissociated cells from *Lissodendoryx* sp. was also undertaken.

The structures of four new halichondrins (**3.13** ï **3.16**), isolated from *Lissodendoryx* sp., have been determined from spectral data. All of these compounds are very similar to known B series halichondrins, with differences occurring only beyond carbon 44. As biological activity has been shown to be derived from the portion of the molecule between carbons 1 and 35, they all retain good activity in the P388 assay as expected.

A new siderophore, petrobactin sulfonate (**4.2**), was characterised, along with three cyclic imide siderophore derivatives (**4.3** ï **4.5**). Petrobactin sulfonate is the first marine siderophore containing a sulfonated 3,4-dihydroxy aromatic ring. The structures were elucidated from spectral data, resulting in a revision of the NMR assignments of petrobactin.

Acknowledgements

I would like to thank my supervisors, Professor John Blunt and Professor Murray Munro, for their amazing support and encouragement throughout the time I have been working on my Ph.D. research, and for providing solutions for each new logistical challenge I put before them. I would also like to thank my associate supervisor, Professor Alison Butler, for welcoming me into her group at the University of California at Santa Barbara (UCSB), and providing me with a siderophore project.

I would like to thank the wonderfully helpful technical staff at the University of Canterbury and at UCSB, whose expertise made it all possible. I would particularly like to thank Gill Ellis for running the P388 assays and helping with the cell separation work (and so much more!), Bruce Clark and Marie Squire for mass spectrometric analyses, Atta Shirazi for assistance with NMR analyses at UCSB, and Jan McKenzie for help with SEM and TEM.

I would also like to thank the Cancer Society, Canterbury-West Coast Division, for a Postgraduate Scholarship in Cancer Research.

Thanks must also go to the amazing students and Post Docs in the Marine Group who have come and gone over the time of this research. Your friendship and support made coming into the Department a pleasure.

I would also like to thank my family and friends, who have encouraged me every step of the way, and looked after the children so I could continue to study. Particular thanks must go to Mum and to Jan and Ron in this respect, who have nurtured and delighted in Samantha, Blake and Bradley, and have spent so much time bringing them back and forth across town. Nothing was ever too much trouble. Thank you to Samantha, for writing me lovely cards to take to work, to Blake for always running to give me a hug, and to Bradley for being the model baby while I was writing up this thesis.

The biggest thank you must of course go to Mike, for so much more than I could ever write in words. Your constant love, encouragement and support have made it all possible.

I would like to dedicate this thesis to the memory of my Dad

J. Keith Herbison

1924 ï 1987

You always believed I could do it

And also to the memory of

Jean M. Herbison

1923 ï 2007

A dearly loved Aunt and mentor

Abbreviations

br	broad (spectral)
$^{\circ}$C	degrees Celsius
calcd	calculated
CIGAR	constant time inverse-detection gradient accordion rescaled (NMR)
cm	centimetre(s)
CMF-ASW	calcium magnesium free artificial seawater
conc	concentration
COSY	correlation spectroscopy (NMR)
δ	chemical shift in parts per million downfield from TMS (NMR)
d	doublet (NMR)
dd	doublet of doublets (NMR)
DMSO	dimethyl sulfoxide
DNA	deoxyribonucleic acid
ESIMS	electrospray ionisation mass spectrometry
FAB	fast atom bombardment (in mass spectrometry)
g	gradient (NMR); gram(s)
GTP	guanosine 5'-triphosphate
GDP	guanosine 5'-diphosphate
H_2O	water
HMBC	heteronuclear multiple bond correlation (NMR)
HPLC	high-performance liquid chromatography
HRFABMS	high-resolution fast atom bombardment mass spectrometry
HSQC	heteronuclear single quantum correlation (NMR)
Hz	hertz
J	coupling constant (NMR)
kDa	kilo Daltons
L	litre(s)
LCMS	liquid chromotography mass spectrometry
LCMSMS	tandem liquid chromotography mass spectrometry
LRFABMS	low resolution fast atom bombardment mass spectrometry
μ	micro
m	multiplet (spectral); milli

M	moles per litre
mmu	milli mass units
MAPs	microtubule associated proteins
MDR	multidrug resistance
MeOH	methanol
mol	mole(s)
MS	mass spectrometry
MTOC	microtubule organising centres
m/z	mass to charge ratio (in mass spectrometry)
n	nano
NMR	nuclear magnetic resonance
NOE	nuclear Overhauser effect (NMR)
NOESY	nuclear Overhauser effect spectroscopy (NMR)
NSCLC	non small cell lung cancer
ODS	octadecyl silane
P-gp	p-glycoprotein
ppm	parts per million (NMR)
rt	room temperature
ROESY	rotating-frame NOE spectroscopy (NMR)
RP-HPLC	reverse phase high performance liquid chromatography
s	singlet (NMR); second(s)
SEM	scanning electron microscopy
t	triplet (NMR)
TEM	transmission electron microscopy
TFA	trifluoroacetic acid
TLC	thin layer chromatography
TMS	tetramethylsilane
TOCSY	total correlation spectroscopy (NMR)
UV	ultraviolet

CHAPTER 1. Introduction.

1.1 General introduction

The marine environment represents a huge, and still largely untapped, resource for the discovery of novel natural products due to its vast biological diversity. Although having around one fifth the average biomass of terrestrial habitats, it is conservatively estimated that between 0.5 and 10 million of the world's total estimated 12.5 to 30 million species are accounted for by marine macrofauna alone.[1] In addition, although biomass decreases exponentially with depth, species diversity has been shown to increase.[1] Thus, a strong case can be made for the search for novel compounds in species from deep marine habitats. Thousands of secondary metabolites (compounds not involved in primary metabolism) have been isolated to date from marine organisms, often with unprecedented structures. Many of these are derived from sessile organisms, such as sponges, ascidians and soft corals, and arguably act as chemical defences to deter predators or discourage epibiosis.[2,3]

The need for new drugs is constantly growing. Diseases such as Alzheimerôs and arthritis continue to deny those affected quality of life, heart disease is prevalent, absolute cures for cancer and AIDS have not been found, drug-resistant strains of bacteria have evolved, cancers have developed multi-drug resistance, and the threat of bioterrorism is an increasing concern. The use of marine-derived secondary metabolites in these applications has been explored with much success. Within the Marine Chemistry Group at the University of Canterbury, of the thousands of marine organisms collected, extracted and screened in the group's in-house assays for antitumour, antiviral and antimicrobial activity, many with promising activity have been identified. These include the halichondrins from the Kaikoura deep water sponge *Lissodendoryx* sp. and a variety of novel compounds isolated from the Chatham Rise sponge *Lamellomorpha strongylata.* Terrain models of the Kaikoura and Chatham Rise areas are given in Figures 1.1.2 and 1.1.2, respectively.

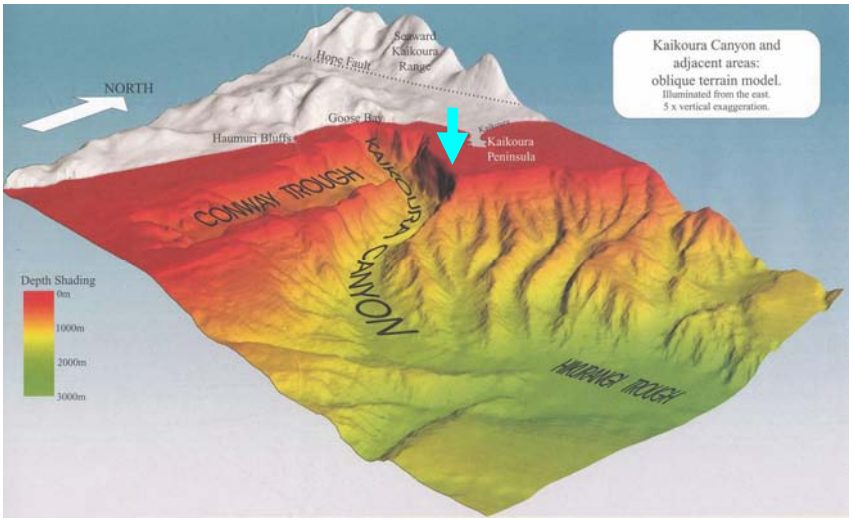

Figure 1.1.1 Oblique terrain model showing the underwater topography surrounding the Kaikoura Peninsula. The blue arrow indicates the collection site of *Lissodendoryx* sp.. Image courtesy of NIWA.

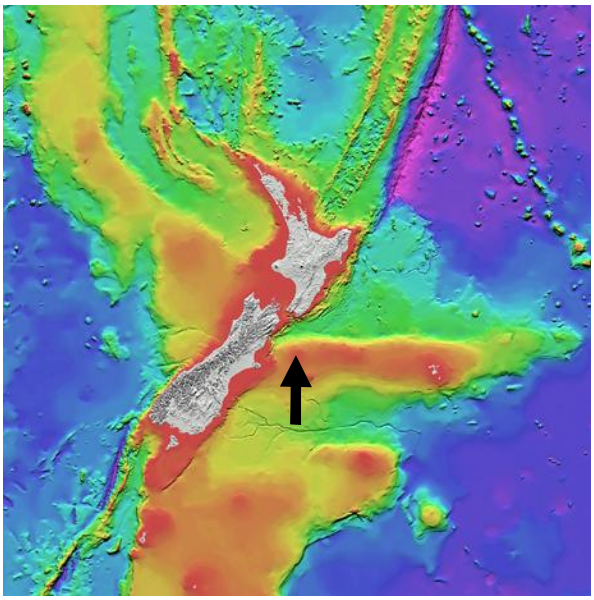

Figure 1.1.2 Terrain model showing the underwater topography surrounding New Zealand. The arrow indicates the collection site of *Lamellomorpha strongylata* on the Mernoo bank, Chatham Rise. Image courtesy of NIWA.

The use of marine natural products dates back to pre-Roman times with the utilisation of precursors from a mucus secretion of the hypobranchial gland of marine snails of the genus *Murex* (Fig. 1.1.3) to obtain the highly prized pigment Tyrian purple, the main component of which is 6,6-dibromoindigo (**1.1**).[4] While the study of natural products has been a major focus of the discipline of chemistry for over a century, most of the effort has been on natural products derived from terrestrial sources. This emphasis began to change after the 1950s when the impact and significance of Werner Bergmannôs pioneering work on natural products from the marine environment was recognised. Bergmann started his work on marine natural products in 1933, and

published the 50th article in his ñMarine Productò series in 1961. The work for which he is widely recognised was the isolation and characterisation in the early 1950s of the non-ribose nucleosides, spongothymidine (**1.2**) and spongouridine (**1.3**), from the Caribbean sponge *Tethya crypta*. Within a decade of these discoveries, the biomedical importance of non-ribose nucleosides was being realised, and the development of drugs such as Ara-C, Ara-A and AZT (**1.4**) can be traced directly back to Bergmannôs work.

Figure 1.1.3 Two of the source organisms of the precursors for the pigment Tyrian purple, *Murex brandaris* and *M. trunculus.* (Image: www.dutly.ch/indigohtml)

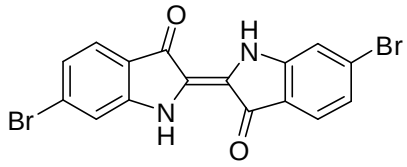

1.1 6,6'-dibromoindigo

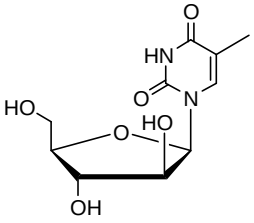

1.2 spongothymidine

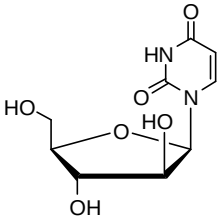

1.3 spongouridine

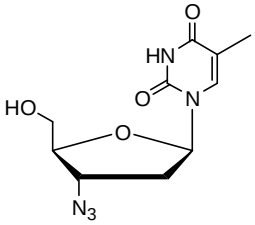

1.4 AZT

The delayed onset of more extensive research into marine natural products was partly a consequence of the relatively limited access that biologists and chemists had to that part of the marine environment beyond the sub-tidal zones. This was remedied by the popularisation of SCUBA that dramatically enhanced the ability to collect in the aquatic environment, as well as opening up possibilities for marine environmental chemistry. SCUBA was followed in turn by the use of ROVs and various submersibles that have allowed access to very much deeper water. Along with the enhanced collecting

opportunities came the recognition that most of the biodiversity on earth was actually present in the oceans.

From the recognition of the importance of marine natural products in the 1950s the field progressed steadily with the next champion being Paul Scheuer, sometimes referred to as the father of marine natural products, who began his work at the University of Hawaii at Manoa in 1950. Joining Scheuer as leaders in the field were Ken Rinehart, working at the University of Illinois from 1954, and John Faulkner, working at Scripps Institution of Oceanography, UCSD, from 1968. Sadly, all three are recently deceased, but they have left an extensive legacy from their work in the field of marine natural products. Paul Scheuer published around 300 papers, including a report of the new anticancer compound kahalalide F (**1.5**) from the Sacoglossan mollusc *Elysia rufescens* and the green alga *Bryopsis* sp.,[5,6] which is not susceptible to multidrug resistance (MDR) mechanisms (*vide infra*) and is currently in clinical trials, predominantly for the treatment of prostate cancers.[7] Ken Rinehart published over 400 papers, including the isolation of didemnin B (**1.6**),[8] an anticancer and antiviral agent from the ascidian *Tridemnum solidum*, which was the first marine natural product to enter clinical trials. John Faulkner published over 350 papers in the areas of natural product chemistry and chemical ecology, including the discovery of over 100 halogenated compounds. His work on the anti-inflammatory terpenoid manoalide (**1.7**), first isolated by Scheuer from the Western Pacific sponge *Luffariella variabilis*,[9] led to the discovery of a new class of anti-inflammatory compounds,[10-12] and his work on opisthobranchs (shell-less molluscs) led to the theory that their co-existence with toxic food sources resulted in the evolution of their shell-less state.

Further development of the studies on marine natural products from the 1970s onwards was assisted by advances in spectroscopic methods and separation science that allowed for the rapid isolation and characterisation of the many new structural types being found from the sea. Since then, the number of groups undertaking research in the area has grown rapidly, as reflected by the rapid increase in marine natural product publications, and the establishment of marine natural products as a separate focal point at conferences. Currently, the studies on marine natural products are carried out by a wide range of research groups (in excess of 150) scattered across at least 40 countries. Research in the marine natural products area is characterised by a sense of unity, with many of the current leaders of the field being able to trace an academic ancestry back to having worked for, or with, Scheuer, Rinehart or Faulkner.[13]

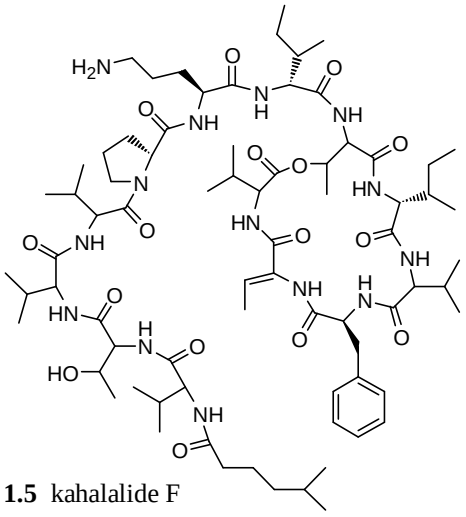

1.5 kahalalide F

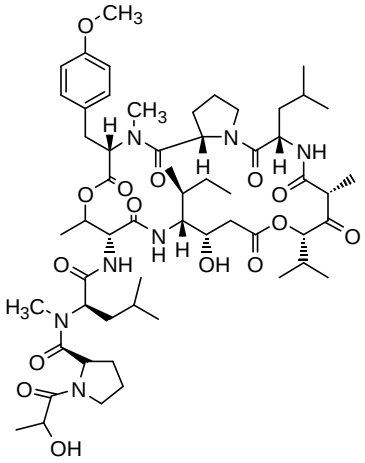

1.6 didemnin B

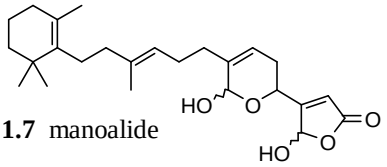

1.7 manoalide

The marine environment has yielded many compounds with potent biological activity. The analgesic ziconotide (Prialt®), a 25-residue peptide from the marine snail *Conus magus*, has recently been approved for use as an analgesic and is the first marine natural product to reach the commercial sector. Ecteinascidin 743 (**1.8**), an antimitotic anticancer agent from the ascidian *Ecteinascida turbinata* first reported in consecutive papers by Rinehart *et al.* and Wright *et al.*,[14,15] is predicted to follow later this year. In addition, there are currently a significant number of very interesting marine natural products, or their synthetic derivatives, that are in clinical or preclinical trials for the treatment of cancer, analgesia, allergy and cognitive diseases.[7]

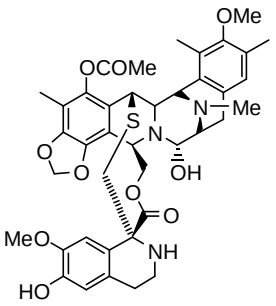

1.8 ecteinascidin 743

1.2 Sponges

Sponges are sessile marine organisms, classified in the phylum Porifera (meaning ñpore-bearingò). There are over 9000 species known, mostly marine, in habitats ranging from the intertidal zone to deeper than 8500 m.[16] They range in size from a few millimetres to two metres high. The body of a sponge has an outer and an inner layer separated by an acellular gel layer, the mesohyl. The outer layer is comprised of a tightly packed layer of pinacocytes. In the gel layer are spicules (supportive needles made of calcium carbonate or silica that are secreted by sclerocytes) and/or spongin fibres (a flexible skeletal material made from protein that is secreted by spongocytes), along with spherulous cells (cells with multiple large vesicles containing course granular material). The inner layer of the sponge is made up of flagellated cells called choanocytes.

Adult sponges are filter-feeders. Water is drawn into the organism through incurrent pores surrounded by myocytes and porocytes, which can contract to regulate the flow through the sponge. The water then passes the flagellated choanocytes that line the inside of the sponge. The beating flagella propel water through the sponge, while nutrients are absorbed *via* the collars of the choanocytes. Archeocytes subsequently transport the nutrients from the choanocyte collars to other cells in the sponge. The water then exits the sponge through the osculum, which is often lined with spicules. Spicules may also penetrate the outer layer of the sponge (Fig. 1.2.1)

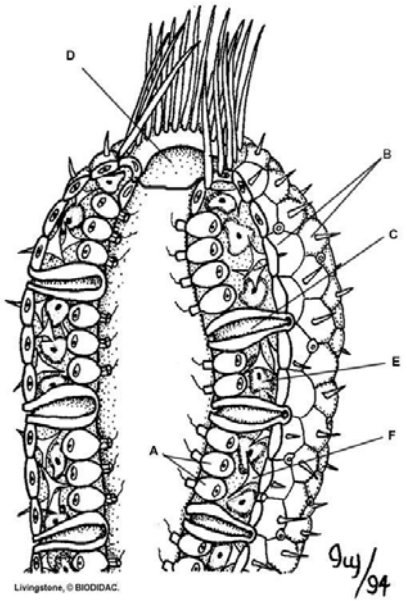

Figure 1.2.1 A diagram of a sponge, showing choanocytes (A), pinacocytes (B), incurrent pores (C), the osculum (D), archeocytes (E) and spicules (F). (Image: www.biologycorner.com)

Spicules are found in many shapes and sizes (large spicules are called megascleres, and small ones microscleres) and have structural and defence functions. Their diversity has proven useful in the classification of sponges.

Sponges are a rich source of new marine natural products, many of which are bioactive. Of all the new compounds reported by the end of 2001, 38 % were obtained from sponges (Fig. 1.2.1).

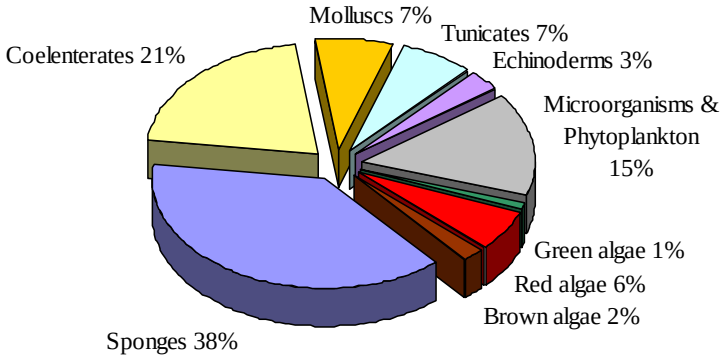

Figure 1.2.1 Distribution of marine natural products by phylum, 2001[17]

1.3 Compounds derived from *Lamellomorpha strongylata*

In 1997, four classes of compound were isolated from the marine sponge *Lamellomorpha strongylata*, collected by benthic dredging in deep water (80-100 m) along the top of the Mernoo Bank within the Chatham Rise convergence zone off the east coast of the South Island of New Zealand. Compounds isolated were from the calyculin, calyculinamide, swinholide and theonellapeptolide classes.[18,19]

1.3.1 Calyculins and calyculinamides

The anticancer compound calyculin A was first reported by Fusetani in 1986, isolated from the sponge *Discodermia calyx*.[20] Two years later, Fusetani reported the structures of calyculins B, C and D from the same sponge,[21] and other calyculins have been described subsequently. The known calyculins A, B, E and F were isolated from *Lamellomorpha strongylata*. In addition, two new calyculin derivatives, calyculinamides A and B, were isolated from this sponge. These structures are given in Chapter 2 (**2.1 - 2.6**).

1.3.2 Swinholides

The potent cytotoxic macrolide swinholide A was first isolated in Kashmanôs group from the sponge *Theonella swinhoei*, collected in the Red Sea.[22,23] It has subsequently been isolated from an Okinawan population of the same sponge,[24] when it was recognised as a dimer, and more recently still from sponge-associated heterotrophic bacteria[25] and marine cyanobacteria collected in Fiji.[26] The new swinholide H was isolated from *Lamellomorpha strongylata*. Swinholide I was reported in 2006.[27] The structure of swinholide H is given in Chapter 2 (**2.7**).

1.3.3 Theonellapeptolides

A variety of theonellapeptolides have been reported by Kitagawa *et al.* from an Okinawan sponge of the genus *Theonella*.[28-31] Theonellapeptolide IIIe was isolated from *Lamellomorpha strongylata,* and showed modest cytotoxicity (7.4 μg/mL) against the P-388 cell line. The structure of theonellapeptolide IIIe is given in Chapter 2 (**2.8**).

1.4 Halichondrins

The halichondrins, potent antitumour polyether macrolides, were first isolated by Uemura *et al.* from the Japanese sponge *Halichondria okadai*. The structure of norhalichondrin A (**3.1**) was determined by NMR and X-ray crystallography and reported in 1985.[32] The following year, Uemura reported the structures of seven further halichondrins from the same sponge, the most active of which was halichondrin B (**1.9**).[33] The structures of ten halichondrins from the B series were reported in 1991 by the Marine Group at the University of Canterbury from the New Zealand sponge *Lissodendoryx* sp. (see chapter 3), and halichondrins have also been isolated from various other sponges, including the halistatins from the east Indian sponge *Phakellia carteri*,[34] and halichondrin B and homohalichondrin B from *Axinella* sp., collected in Palau.[35] The halichondrins are characterised by a large 22-membered lactone ring (C1-C30), two exocyclic methylenes, at C19 and C26, an unusual tricyclo ring system (C8-C14) and a number of pyranose and furanose rings.

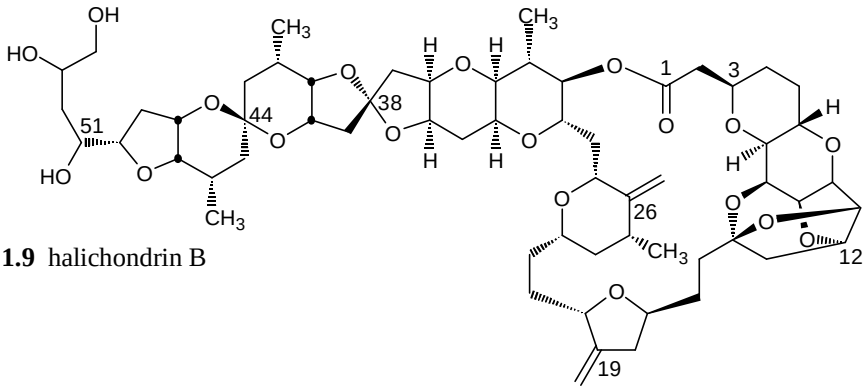

1.9 halichondrin B

As is the case for other marine natural products, the halichondrins occur at very low levels in the sponge. *Lissodendoryx* sp. is the highest yielding sponge, producing approximately 1.6 mg of total halichondrins per kilogram of wet sponge.[33-35] In an attempt to address the supply problem, several groups have attempted the synthesis of halichondrin B. The total synthesis of halichondrin B and norhalichondrin B was reported by Kishi in 1991.[36] Unfortunately, it involves close to 50 steps in the longest linear sequence, rendering it unsuitable for the commercial supply of the halichondrins. This is the only total synthesis reported to date, however Kishiôs group at Harvard University, along with other synthetic groups including that of Steven Burke at the University of Wisconsin-Madison and Andrew Phillips at the University of Colorado at Boulder, continue to attempt the synthesis of halichondrin B in fewer steps and with higher yields. The recent discovery that the truncated halichondrin B analogue NSC 707389 (**3.12**)[37] retains the activity of the parent compound[38] can only serve to increase the likelihood of the development of a commercially viable synthesis.

The halichondrins are cytotoxic at subnanomolar concentrations, preventing tubulin polymerisation and microtubule assembly by inhibiting the binding of GTP to tubulin.[39] They have also been shown to interfere with the binding of the vinca alkaloids to tubulin, binding in the vinca domain,[40] and induce apoptosis *via* a mitotic prophase stall.[41] Again, like kahalalide F (**1.5**), these compounds have the advantage of not being recognised by MDR mechanisms (*vide infra*). A recent publication proposes a tubulin binding site for halichondrin B and its analogue NSC 707389 between the two heterodimers, leading to the formation of highly unstable, small aberrant tubulin polymers rather than the massive stable structures observed with the vinca alkaloids.[38] The halichondrins are active against selected sensitive melanoma, colon, ovarian, lung and breast cancer cell lines.

In order to understand the mode of action of the halichondrins, it is necessary to investigate the nature of cancer, chemotherapy and the cell cycle, and understand tubulin, the formation of microtubules, and how these microtubules might be disrupted by an anticancer agent.

1.5 Cancer

In western countries, cancer is second only to heart disease as the biggest cause of death.[42] Cancer is a generic term for over 200 diseases with shared characteristics, including uncontrolled cellular proliferation. Normal cells demonstrate contact inhibition, where cell proliferation ceases once cells come into contact with one another. In contrast, cancer cells continue to proliferate until all available resources are exhausted. Thus, the fine balance between cell production and cell death is lost, and an over production of cells results at the expense of the host tissues. This proliferation can interfere with surrounding organs, disrupting their function, and ultimately lead to the death of the patient. A complicating feature of cancer is its ability to spread to other locations in the body, a process known as metastasis. Thus, secondary tumours are also observed to disrupt bodily functions at many different locations. This renders surgical removal of the tumours impractical, and chemotherapy (involving the use of drugs) becomes the treatment of choice.

1.6 Chemotherapy

The ultimate aim for chemotherapy is to specifically target cancer cells whilst leaving healthy cells untouched. In order to achieve this, a unique feature of the cancer cells must be exploited. Unfortunately, the differences between cancer cells and healthy cells seem to be very slight. However, as mentioned previously, cancer cells show an increase in cell growth and division. Thus, it may be possible to target the process of segregation of chromosomes prior to cell replication (mitosis) in these cells. Prolonged disruption of the cell cycle has been found to result in apoptosis, or programmed cell death. In other words, if the cell is not viable, it commits suicide.[43,44] Although mitosis also occurs in healthy cells, it has been demonstrated that it is possible to obtain selectivity towards the more frequently dividing cancer cells. Common side effects

associated with chemotherapy, such as hair loss, neutropenia (decrease in neutrophils in the blood) and peripheral neuropathy (loss of peripheral nerve function) are a result of these types of cells also demonstrating rapid replication.[45]

1.7 Cell cycle

The cell cycle is composed of three parts: interphase, mitosis and cytokinesis (Fig. 1.7.1). During interphase, the cytoplasmic material doubles in the G_1 (gap) phase, the chromosomes are replicated in the S (synthesis) phase, and tubulin and other molecules necessary for mitosis are synthesised in the G_2 phase. During mitosis, the chromosomes are divided between two daughter cells. Finally, during cytokinesis, the daughter cells separate to give two new cells, with actin and myosin microfilaments acting to pinch the cells apart.

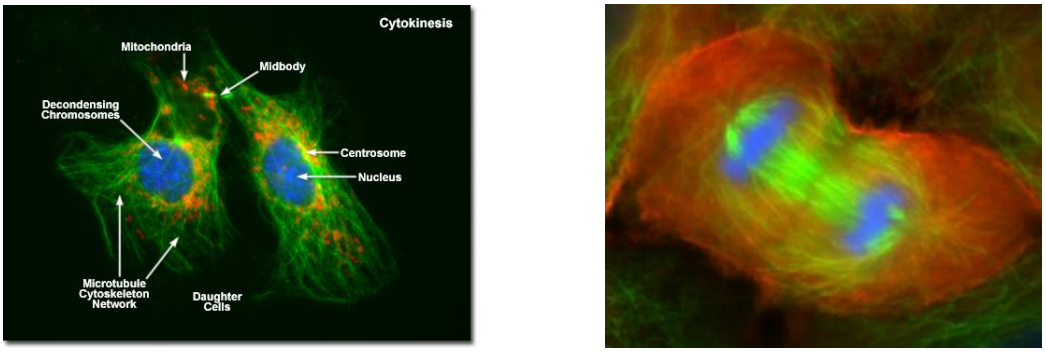

a. b.

Figure 1.7.1 (a) A digital fluorescence micrograph of an animal cell in the late stages of cytokinesis. (Image: www.molecularexpressions.com) (b) Fluorescence micrograph of a mammalian cell undergoing cytokinesis. (Image: http://biology-web.nmsu.edu/shuster-lab)

1.7.1 Mitosis

Mitosis occurs in five phases: prophase, prometaphase, metaphase, anaphase and telophase. The mitotic spindle is formed in the first of these phases. This is comprised of four different types of microtubule: astral rays, pole-to-pole microtubules, microtubules that bind to kinetochores, and microtubules that interact with chromosome arms (Fig. 1.7.2).

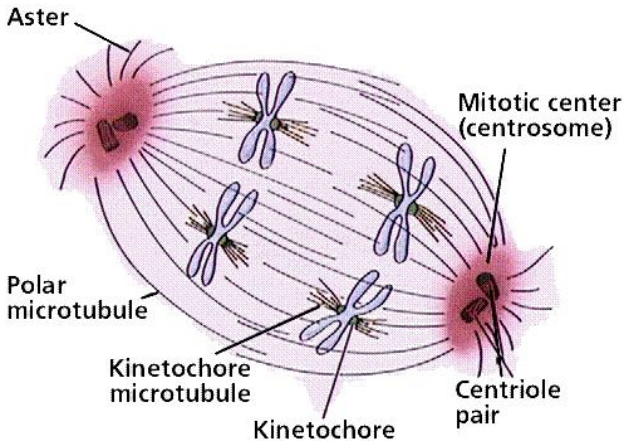

Figure 1.7.2 The four different types of microtubule: astral rays, pole-to-pole microtubules, microtubules that bind to kinetochores, and microtubules that interact with chromosome arms. (Image: www.emc.maricopa.edu)

Kinetochores are DNA-protein complexes that form on centromers.[46] As will be discussed below, microtubules attached to the kinetochore lengthen during prophase and shorten during anaphase. This is achieved by the addition or removal of tubulin dimers. The tubulin is sourced from cytoskeletal microtubules, which are observed to disassemble at the beginning of mitosis and reassemble following the dispersion of the mitotic spindle after mitosis has occurred. This borrowing of cytoskeletal tubulin is also thought to be the reason why cells appear rounded during mitosis.

1.7.2 Prophase

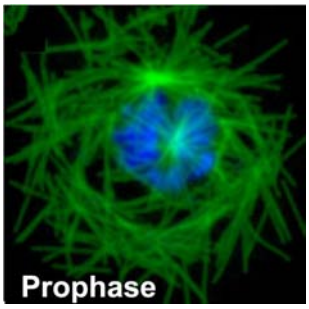

This is the longest phase, taking ~60% of the total time required for mitosis. During this phase, the chromatin condenses so that the individual chromosomes become visible, the centrioles move to opposite ends of the cell, and the spindle forms. A fluorescent micrograph of a cell during this phase is shown. (This and subsequent mitosis images: http://valelab.ucsf.edu/research)

1.7.3 Pro-metaphase

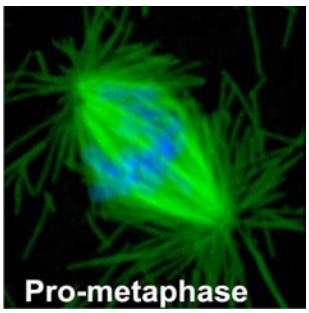

During this phase, microtubules attach to the centre of the chromosomes at a point known as the kinetochore, and the nuclear envelope breaks down.

1.7.4 Metaphase

During this phase, chromosomes move to align with the mid plane (or equator) between the centrosomes.

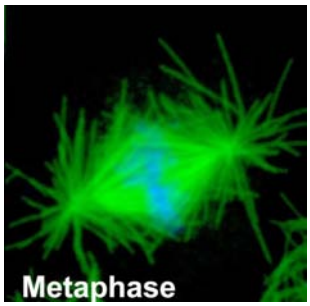

1.7.5 Anaphase

This is the most rapid phase of mitosis. As soon as the chromosomes are aligned with the equator, the microtubules begin to decay, separating the daughter chromosomes.

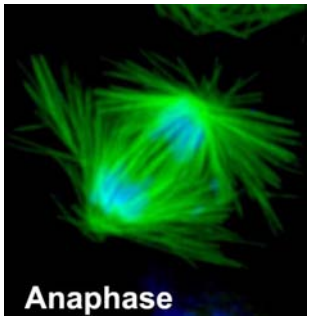

1.7.6 Telophase

During this phase, the chromosomes reach the opposite poles of the cell, and new nuclear envelopes form.

1.8 Tubulin

Tubulin is found in every nucleated cell in the body. It is comprised of two similar spherical proteins, α- and β-tubulin, each with a molecular weight of about 50 kDa. The α- and β-tubulin proteins combine to form αβ soluble heterodimers. Two molecules of guanosine triphosphate (GTP) bind to each of these heterodimers. One of these is tightly bound and cannot be removed without denaturing the heterodimer, while the other is freely exchangeable with unbound GTP. This exchangeable GTP molecule is thought to be crucial for the regulation of tubulin function.[47]

The αβ-tubulin heterodimers are able to combine in a head to tail arrangement to form a protofilament, a long protein fibre composed of alternating α- and β-tubulin. During polymerisation, the exchangeable GTP is hydrolysed to guanosine diphosphate (GDP).

The non-exchangeable guanosine nucleotide appears to be on α-tubulin, while the exchangeable nucleoside has been localised to the β-tubulin subunit.[48]

1.8.1 αβ-Tubulin heterodimer

The structure of the αβ-tubulin heterodimer was determined *via* electron crystallography by Eva Nogales, Sharon Wolf and Kenneth Downing from the Lawrence Berkeley National Laboratory, and reported in Nature in 1998.[49,50] This confirmed the location of the non-exchangeable guanosine nucleotide sites on α- and β-tubulin, respectively. An example of the amino acid sequences of pig brain α- and β-tubulin is given in Fig. 1.8.1.

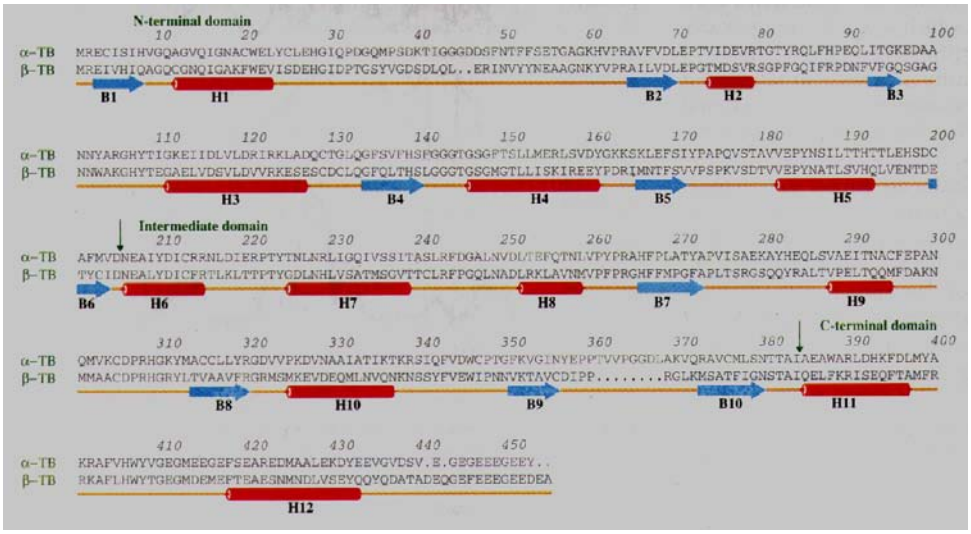

Figure 1.8.1 Amino acid sequences of pig brain α- and β-tubulin. Strands are shown as blue arrows, and helices are denoted in red.[49]

The α- and β-tubulins were found to share 40% amino-acid sequence identity, whilst existing in several isotype forms. Six α- and six β-tubulin isotypes have been described in mammals.[51] The structures of α- and β-tubulin were found to be basically identical, with each monomer being formed by a core of two β-sheets surrounded by α-helices (Fig. 1.8.2).

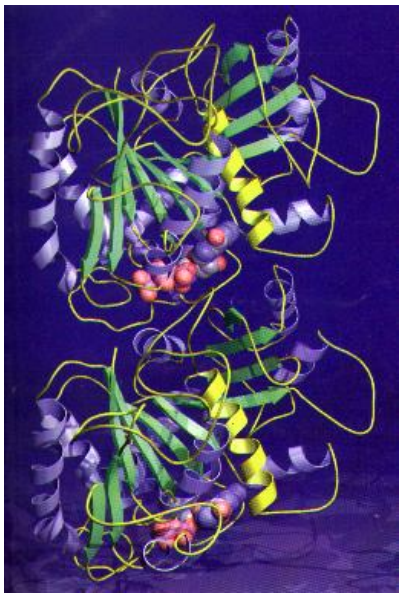

Figure 1.8.2 Ribbon diagram of the αβ-tubulin heterodimer, with the α-subunit on top and the β-subunit underneath. Strands are denoted with green arrows, and helices by blue and yellow spirals. GTP (pink molecule) in the non-exchangeable (top) and exchangeable (bottom) sites is also shown.[49]

1.8.2 Microtubules

Microtubules are dynamic pipe-like fibres. They are insoluble, and have a variety of roles in the cell, including the provision of an internal scaffold, cellular transport, and the formation of the mitotic spindle. Microtubule assembly occurs *via* the grouping together of protofilaments (typically 12 or 13) to form a C-shaped protein sheet. This sheet then curls to form a microtubule, where the external diameter is ~24 nm and the internal bore is ~15 nm.

The dynamic nature of the microtubules is crucial to their function. They are in constant equilibrium, with dimers continually adding to and leaving from each end. This process is a finely balanced equilibrium, with net addition from the positive (+) end of the microtubule (capped by β-tubulin) and net loss from the negative (-) end (capped by α-tubulin). This length control of the microtubule is vital for its intracellular function. The microtubule is said to be treadmilling when it is simultaneously gaining dimers at one end and losing them from the other (Fig. 1.8.3). This phenomenon is believed to be critical for the polar movement of chromosomes during anaphase (*vide infra*).[51]

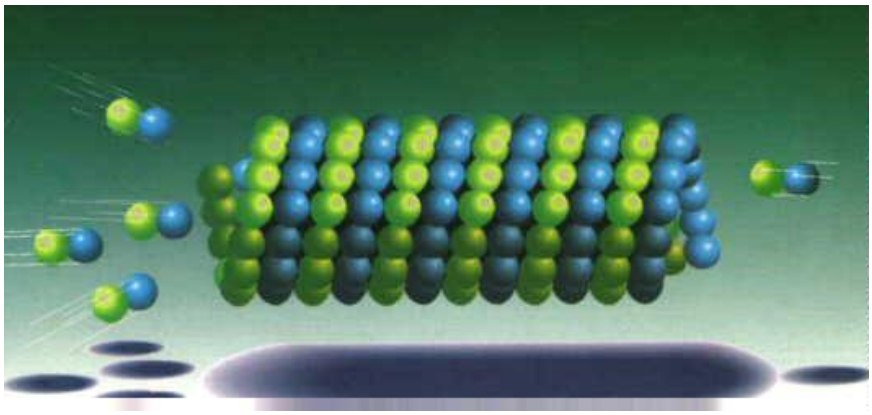

Figure 1.8.3 A schematic diagram showing the dynamic nature of microtubules, with αβ-tubulin heterodimers constantly joining and leaving each end. Net addition occurs at the + end (left hand side), and net loss from the ï end (right hand side). α-tubulin is shown in blue, and β-tubulin in green. (Image: http://python.rice.edu)

1.8.3 MAPs and MTOCs

A number of proteins, known as Microtubule Associated Proteins (MAPs), are associated with the microtubules. These have a mass of ~200 kDa, and their exact purpose is unknown. However, microtubules are observed to form faster in their presence, and they also appear to provide protection from depolymerisation by Ca^{2+} ions and at low temperatures.

Microtubule Organising Centres (MTOCs) are crucial in the formation of the microtubules. All microtubules initially begin to grow from one of these centres. In most cells, the major type of MTOC is the cell centre or centrosome, which contains two microtubular structures called centrioles.

1.8.4 γ-Tubulin

γ-Tubulin is a third type of tubulin protein. It is similar to both α- and β-tubulin, and its presence is essential for microtubule growth *in vivo*. It is thought that an aggregation of γ-tubulin on the surface of the MTOC, perhaps in the form of a ring or short cylinder, acts as a site of nucleation for incoming αβ-tubulin heterodimers.

1.9 Targeting microtubules

1.9.1 Rationale

Microtubules are intimately involved in cell replication. On entering mitosis, microtubule growth/decay increases 20 to 100-fold, thus making them highly sensitive to interference.[44] If prevention of the formation or decay of the microtubules were achieved, this would have the effect of preventing the separation of the chromosomes. Thus, the cell would be prevented from reproducing, and in the case of cancerous cells, the tumour would not be able to grow. Such anticancer agents are known as spindle poisons. Of course, as discussed earlier, microtubules have a variety of other roles in the cell. The abundant amount of tubulin in neurons and the role of microtubules in axonal transport are thought to contribute to the neurological toxicity of tubulin-binding agents in the clinic.[51]

1.9.2 Spindle poisons

Spindle poisons have been described in several classes, determined according to their binding site on the αβ-tubulin heterodimer. Although some of these compounds bind to sites which are as yet uncharacterised, others are known to bind to:

tubulin sulfhydryl groups

the colchicine binding site

the vinca alkaloid binding site

the rhizoxin / maytansine binding site (or the vinca domain)

Cytochalasin A (**1.10**) is a fungal metabolite that acts by forming a covalent adduct with the sulfhydryl groups of tubulin. Thus, the alkaloid is able to prevent microtubule assembly. Interestingly, its binding has also been shown to block the colchicine binding site.[42]

Colchicine (**1.11**) was originally purified early in the 19th century from the meadow saffron *Colchicum autumnale*, and has long been associated with its binding to tubulin, once being known as the ñcolchicine binding proteinò. It is a highly toxic and highly soluble alkaloid that has a long history as a treatment for gout, a treatment that remains today, along with that of familial Mediterranean fever and cirrhosis of the liver. It is also being investigated as a treatment for primary Sclerosimy cholangitis, a liver

disease.[52] It exhibits temperature-dependent strong binding to the αβ-tubulin heterodimer, and thus hinders microtubule assembly.[53]

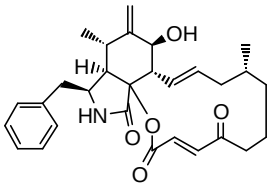

1.10 cytochalasin A

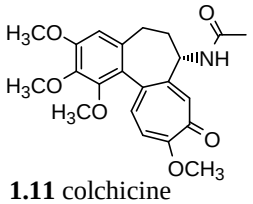

1.11 colchicine

The vinca alkaloid binding site is that defined by the binding of the vinca alkaloids vinblastine (**1.12**) and vincristine (**1.13**) on the αβ-tubulin heterodimer. It has been localised to the central region of β-tubulin,[54] preventing the binding of β-tubulin GTP. When vinca alkaloid-poisoned αβ-tubulin heterodimers are incorporated into the microtubule polymer, further microtubule growth is prevented. Thus, endwise poisoning blocks the region involved in heterodimer attachment, halting the polymerisation process and suppressing the dynamic instability of microtubules necessary for their mitotic function.[42]

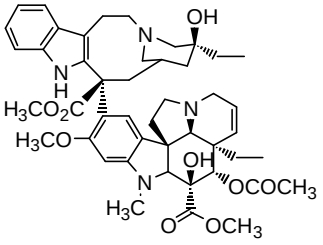

1.12 vinblastine

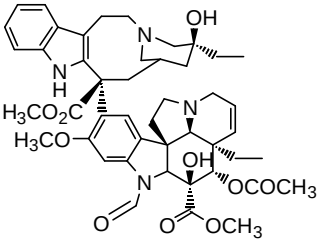

1.13 vincristine

The vinca domain is a distinct site which appears to lie between the vinca site and the exchangeable GTP site. Vinca domain binders may affect these other sites through a slight overlap. Again, the binding of these agents prevents the formation of the mitotic spindle. Agents which act at this site include rhizoxin (**1.14**) from the fungus *Rhizopus chinensis*, maytansine (**1.15**) from the plants *Maytensus* sp. and *Putterlickia verrucosa*,[48] and the marine sponge-derived halichondrins, for example halichondrin B (**1.9**).

Another well known antimitotic drug is Taxol® (**1.16**), also known as paclitaxel, isolated from the bark of the western yew tree *Taxus brevifolia*[55] along with other members of the *Taxus* family, and also from a culture of a fungus, *Taxomyces adreanae*, found growing on *T. brevifolia*.[56] Interest in the compound increased dramatically eight

years after it was first reported, when it was discovered that it acts by stabilising microtubules, thus preventing their depolymerisation, rather than destabilising them as was the case for all the other antimitotic compounds then known.[57] It also causes a prolonged blockage at metaphase in the cell cycle, thus triggering apoptosis (programmed cell death). Taxol® is now used clinically in the treatment of ovarian and breast cancer.[43] However, due to its low water solubility, delivery is achieved in an oil (Cremophor), which can cause cardiac and allergy problems at high doses. Treatment with Taxol® cannot be combined with radiotherapy as it acts by blocking the cell cycle between G_2 and mitosis in both tumour and non-tumour cells, and healthy cells have been shown to be more sensitive to radiation in these phases of the cell cycle.[45]

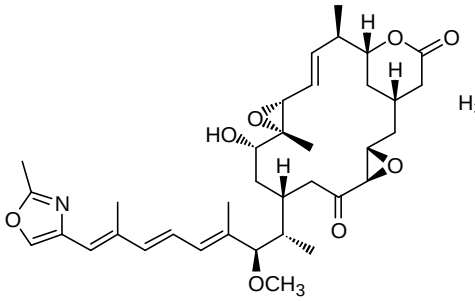

1.14 rhizoxin

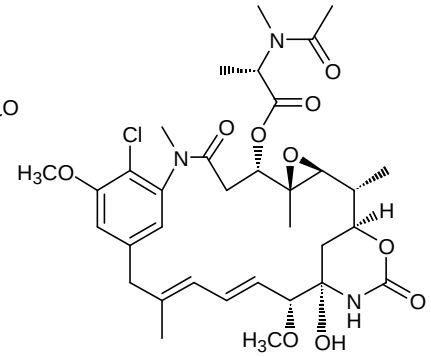

1.15 maytansine

Taxotere (**1.17**), or docetaxel, discovered as a late stage intermediate in a Taxol® synthetic strategy, has a similar mode of action to Taxol® but with a four-fold increase in potency and improved water solubility. It is produced semi-synthetically from a precursor readily obtained from yew tree needles, thus ameliorating the supply problem, and clinical trials are in progress.[43] Binding of taxotere to the αβ-tubulin heterodimer has been investigated *via* electron crystallography (Fig. 1.9.1), indicating that binding occurs on β-tubulin in an intermediate domain between the amino-terminal and carboxy-terminal domains.[49]

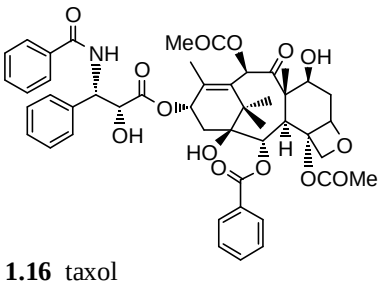

1.16 taxol

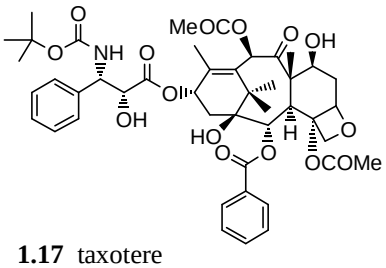

1.17 taxotere

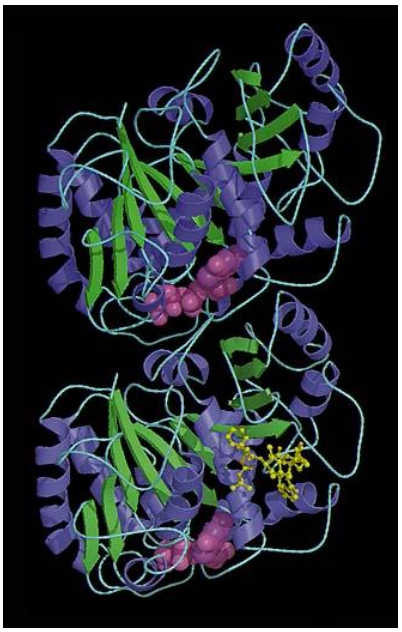

Figure 1.9.1 Ribbon diagram of the αβ-tubulin heterodimer determined by electron crystallography, with the α-subunit on top and the β-subunit underneath, showing the binding of taxotere (yellow molecule) in an intermediate domain of β-tubulin. Strands are denoted with green arrows, helices by blue spirals and GTP is in pink.[49]

1.10 Multidrug resistance

The phenomenon of multidrug resistance (MDR) was first reported in the late 1960ôs and early 1970ôs.[58] It represents the major cause of cancer treatment failure. Many cancers do not respond to treatment with some antimitotic agents. In addition to this, however, some types of cancers respond initially to treatment with a particular drug, but then acquire resistance to it, and also to other drugs that had not previously been used. Thus, the tumour acquires resistance to a variety of chemotherapeutic agents following the administration of a single agent.[45,59] This appears to be due to the over-expression of a family of related genes which code for transporters and actively pump the drugs out of the cell.[60]

1.10.1 Multiple proposed MDR mechanisms

Multiple mechanisms for multidrug resistance have been investigated. One such mechanism is the formation of mutant β-tubulin, resulting in tumours resistant to Taxol®.[61] Some resistant cell lines have been shown to contain tubulin alterations, encompassing total tubulin content, tubulin polymerisation, or tubulin isotype content. For example, the taxane resistant cell line KPTA5 has been shown to have an increased

incidence of the class IVa tubulin isotype.[51] Other mechanisms include the existence of a glutathione conjugate export pump,[62] the presence of a multidrug resistance-associated protein (MRP) which is a 190 kDa membrane glycoprotein and is an efficient transporter of vinca alkaloids but not of taxanes,[51] the existence of a lung cancer resistance protein (LRP-56) whose presence is not entirely definitive but whose over-expression is implicated in MDR leukaemia and ovarian cancer,[58] and finally, the removal of a drug *via* the P-glycoprotein (P-gp) efflux pump. P-gp is a 170 kDa (1280-amino acid) transmembrane glycoprotein, expressed on the plasma membrane of tumour cells, and is currently the best characterised drug transporter. It is likely that resistant cancers express more than one mechanism of resistance to any particular drug.[59]

1.10.2 P-Glycoprotein pump

P-gp is thought to function as a transmembrane pore-forming protein,[58] and is encoded by the *mdr*1 gene. P-gp is found to be increased or over-expressed in many drug resistant cells. It is expressed both as an acquired mechanism (in the case of leukaemias, lymphomas, breast and ovarian carcinomas, where *mdr*1 is not expressed at diagnosis, but appears after relapse from remission) and inherently (in the case of colorectal and renal cancers, where *mdr*1 is highly expressed from the outset).[59] Both the vinca alkaloids and the taxanes are good substrates for this pump.[51]

1.10.3 Combating MDR

One method used to thwart MDR is to co-administer a compound that will block the efflux pump. These compounds are called chemosensitisers, an example of which is the cyclosporin analogue PSC833. Although PSC833 has been shown to restore the sensitivity of previously drug-resistant cell lines to anticancer agents, its use is recommended as a matter of course in the clinical administration of drugs known to cause MDR, in order to prevent the onset of MDR.[63] Another method to combat MDR involves the use of a polymer drug conjugate. It has been found that the use of doxorubicin in a polymer drug conjugate decreased the level of MDR usually experienced by the free drug against MDR cell lines. This is due to the fact that cellular uptake of the polymer drug conjugate is restricted to the process of endocytosis, due to its size, resulting in at least a partial bypass of the P-gp efflux pump that would otherwise remove the drug from the cell. Further, the combination of such conjugates with chemosensitisers restored almost completely the sensitivity of these cell lines to that of parental lines.[64] A much simpler solution for overcoming MDR, however, is to

select drugs that are not susceptible to removal by these mechanisms. One such compound is isohomohalichondrin B (**3.3**).

1.11 Marine siderophores

Most micro-organisms require iron for growth. Although iron is one of the most abundant elements in the earthôs crust, it is present at very low levels in surface seawater. Under aqueous aerobic conditions, iron is present in the +3 oxidation state which renders it highly insoluble. In addition, over 99% of the dissolved iron is complexed by organic ligands. In order to obtain iron, micro-organisms produce siderophores (Greek for iron carrier), high affinity iron chelators which bind iron(III) and facilitate its transport into the cell. Siderophore production has been shown to increase under low iron conditions and decrease under high iron concentrations.[65] High-affinity receptor proteins which recognise siderophore ï iron(III) complexes and transport them into the cell have also been shown to be regulated by iron levels.[65]

Although hundreds of siderophores from terrestrial sources have been isolated, relatively few marine siderophores have been characterised to date. Examples from the marine environment include aerobactin (**1.18**), isolated from a *Vibrio* sp. in Margo Haygoodôs laboratory,[66] petrobactin (**1.19**), isolated from *Marinobacter hydrocarbonoclasticus* in Alison Butlerôs laboratory,[67,68] and the sulfonated siderophore pseudoalterobactin A (**1.20**), isolated from a marine *Pseudoalteromonas* sp. by Kaneo Kanohôs group in Japan.[69]

Petrobactin has also been identified as a virulence-associated siderophore produced by *Bacillus anthracis* (the anthrax-causing pathogen) under iron-deficient conditions.[70] A recent publication has characterised a key enzyme involved in the biosynthesis of petrobactin.[71] This is an exciting development, as it opens up the possibility of targeting the enzyme for the purpose of developing a new anti-infective agent.

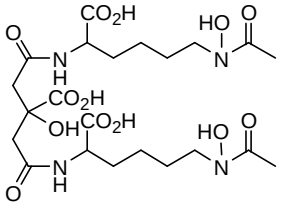

1.18 aerobactin

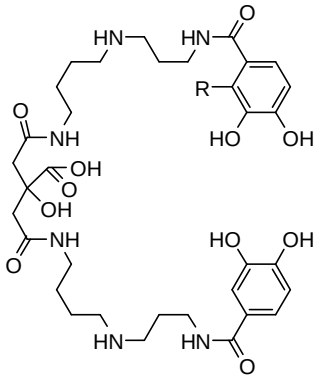

1.19 petrobactin

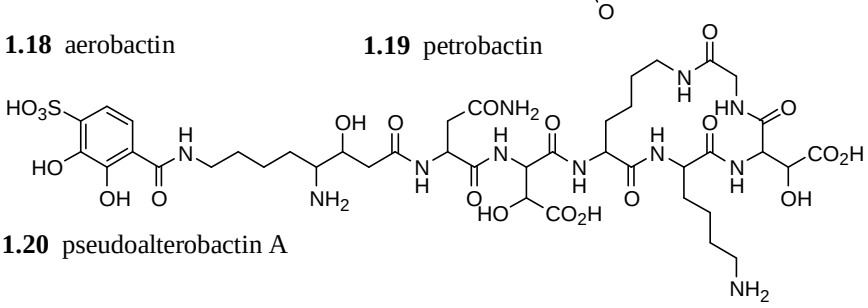

1.20 pseudoalterobactin A

1.12 Thesis aims

The research presented in this thesis falls into the following three categories:

i) Cell separation studies on the New Zealand marine sponges *Lamellomorpha strongylata*, collected in deep water (80-100 m) along the Chatham Rise, and *Lissodendoryx* sp., collected in deep water (~100 m) off the Kaikoura Peninsula.

ii) Characterisation of new halichondrins from the New Zealand marine sponge *Lissodendoryx* sp..

iii) Characterisation of siderophores from the oil-degrading marine bacterium *Marinobacter hydrocarbonoclasticus.*

CHAPTER 2. Cell Separation Studies.

2.1 Introduction

There has been considerable debate over the last decade as to the ecological origin of many of the compounds isolated from marine organisms. Are they synthesised by the organism itself or by a symbiont? Research has shown that cytotoxic components, originally isolated from the sponge *Theonella swinhoei* (Order Lithistida, Family Theonellidae), are in fact derived from bacterial symbionts.[25] For such a compound to be considered as a potential drug candidate, the logistics of its supply must be assessed. Thus, it is desirable to know the cellular origin of the natural product when considering available options for large scale production. Having established the source of a bioactive molecule, production *via* tissue culture or genome transfer becomes an option. This would serve to ameliorate the supply problems of compounds which typically occur at extremely low levels in the source organisms, and also greatly simplify the extraction process. Ecological considerations are also relevant here. Further research has indicated that marine organisms may synthesise bioactive molecules on demand for the purpose of chemical defence against predation and epibiosis.[2,3] Thus, it may be possible to manipulate an organism in order to optimise its production of bioactive molecules.

Cell separation techniques have been applied to the Chatham Rise sponge *Lamellomorpha strongylata* (Order Epipolasida, Family Jaspidae) and the Kaikoura sponge *Lissodendoryx* sp. (Order Poecilosclerida, Family Myxillidae). A sample of *Lamellomorpha strongylata* collected from Spirits Bay, Northland, will also be discussed.

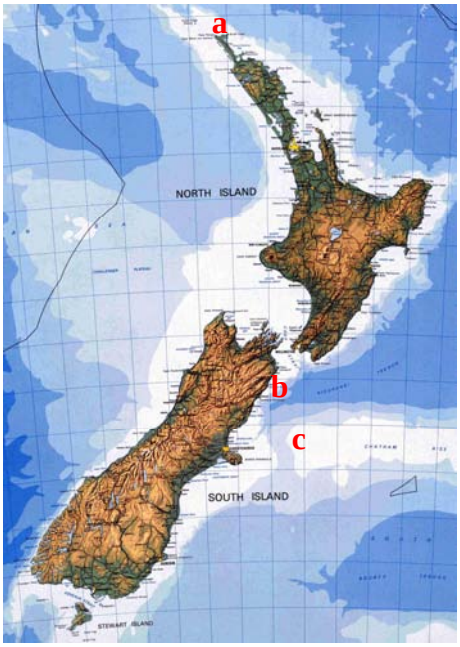

Figure 2.1.1 Map of New Zealand showing the collection sites at (a) Spirits Bay, (b) Kaikoura and (c) the Chatham Rise. Image courtesy of NIWA.

2.2 *Lamellomorpha strongylata*

Figure 2.2.1 *Lamellomorpha strongylata*. Image courtesy of Marine Group photo archive, University of Canterbury.

A wide variety of compounds have been isolated from the sponge *Lamellomorpha strongylata*, collected in deep water (80-100m) on the Chatham Rise, including the known cytotoxic calyculins A (**2.1**), B (**2.2**), E (**2.5**) and F (**2.6**), the new cytotoxic compounds calyculinamide A (**2.3**) and B (**2.4**) and swinholide H (**2.7**), as well as several novel theonellapeptolides (e.g. **2.8**).[18,19]

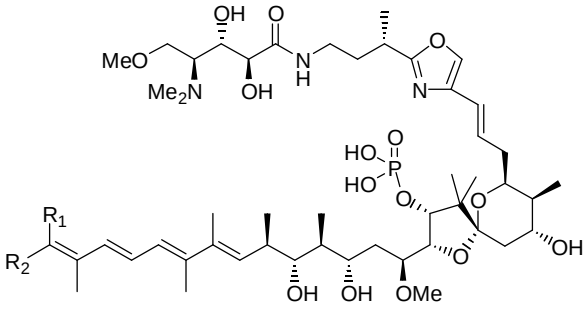

2.1 calyculin A (R_1 = CN, R_2 = H)
2.2 calyculin B (R_1 = H, R_2 = CN)
2.3 calyculinamide A (R_1 = $CONH_2$, R_2 = H)
2.4 calyculinamide B (R_1 = H, R_2 = $CONH_2$)

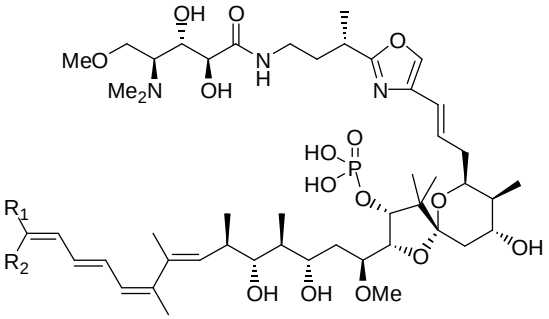

2.5 calyculin E (R_1 = CN, R_2 = H)
2.6 calyculin F (R_1 = H, R_2 = CN)

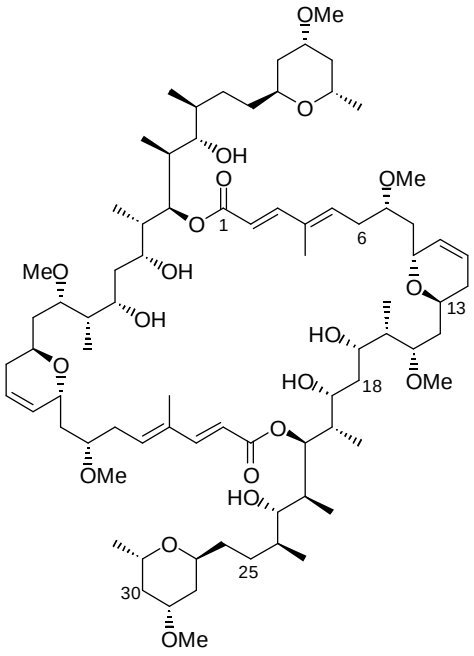

2.7 swinholide H

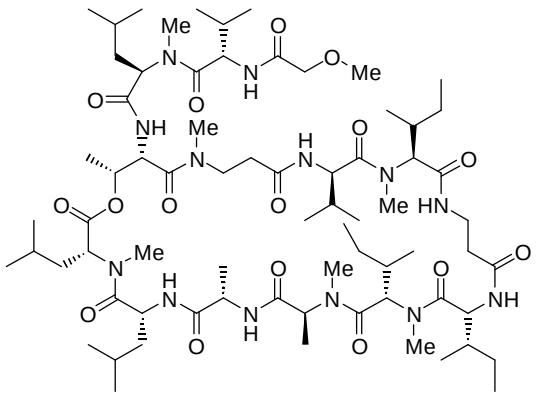

2.8 theonellapeptolide IIIe

It would be interesting to know if all of these compounds could be isolated from sponge cells or if they would be found in cells of symbiotic bacteria. The aim of this section of work was to locate these compounds within discrete cell types.

2.2.1 Introductory analyses

Six duplicate (twelve in total) samples of *Lamellomorpha strongylata* were preserved in fixative by a Post Doctoral Fellow in the Marine Group, Eric Dumdei, in 1987. In each set of six samples, three were diced sponge pieces and three were whole pieces of sponge. Various combinations of formaldehyde, glutaraldehyde and cacodylate were used as the fixative.

The first work carried out on this sponge was a microscopic examination (100 x, immersion) of the twelve fixed sponge samples. The most striking feature of these samples was the presence of large quantities of filamentous heterotrophic bacteria, which were observed throughout the organism (Fig. 2.2.2).

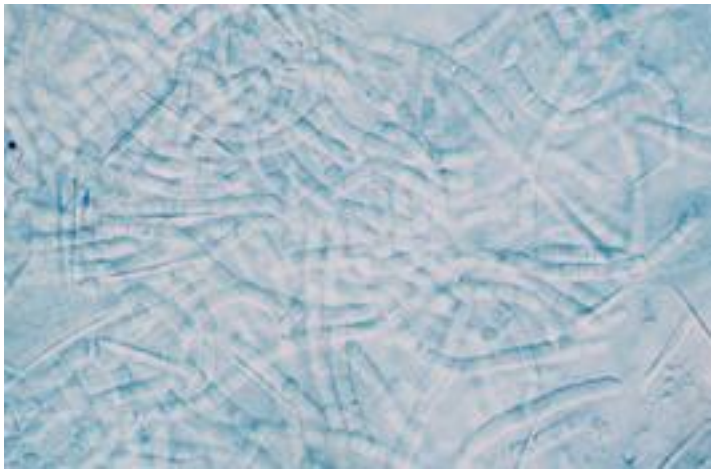

Figure 2.2.2 SEM image of the filamentous bacteria observed in *Lamellomorpha strongylata*, where the average segment length of the filaments is 4 μm

In order to assess the feasibility of detecting the secondary metabolites found in *Lamellomorpha strongylata* in a crude extract, a sub-sample from the early stages of an extraction carried out by Eric Dumdei was analysed by analytical HPLC on ODS-silica (methanol/water, 9:1). In this extraction, 800 g of sponge (95CR 2-16) was blended in 600 mL methanol/water (4:1) for 5 minutes. The resultant slurry was left to stand for 20 minutes, before being filtered through celite under vacuum. The resultant filtrate was then stored in a freezer. I transferred 0.5 mL of this filtrate into an aluminium foil-covered vial in order to preserve the light sensitive calyculins and calyculinamides, and analysed it by HPLC on an analytical ODS-silica column (methanol/water, 9:1). Peaks

in the HPLC spectrum corresponding to theonellapeptolide IIId and IIIe (**2.8**) were apparent, at retention times of 15.01 and 18.31 minutes (at 216 nm), respectively. Low level peaks at the correct retention times for calyculinamide A (**2.3**) and B (**2.4**) (with retention times of 4.21 and 4.48 minutes (at 340 nm), respectively) and for calyculin A (**2.1**) and B (**2.2**) (which co-elute in 90% methanol/water at 5.65 minutes (340 nm)) were observed. Another low level peak eluting at 28.89 minutes (at 270 nm) indicated the presence of a swinholide. Standard samples of these compounds were run immediately after the crude sponge extract. Excellent agreement in retention times was observed in all cases.

In order to establish the continued presence of the secondary metabolites under the conditions of the fixative, a whole portion (0.96 g) of fixed sponge was extracted and analysed. The sponge material was minced, sonicated in distilled water, freeze-dried, ground and then extracted with methanol and dichloromethane. The resultant extract was dried under nitrogen, and analysed by ^{1}H NMR spectroscopy and analytical HPLC on ODS-silica (methanol/water, 9:1). Light protection was achieved throughout this extraction with the use of aluminium foil.

Low level signals were observed in the ^{1}H NMR spectrum which may be consistent with the presence of swinholide-like and theonellapeptolide-like compounds. However, stronger evidence in support of the presence of these compounds was obtained from the HPLC spectrum. UV maxima at expected retention times for theonellapeptolide IIId and IIIe (**2.8**) (14.98 and 18.21 minutes at 216 nm, respectively) and a swinholide (28.79 minutes at 270 nm) were observed. No calyculin- or calyculinamide-like material was detected by either spectroscopic technique. It was initially thought that this might be due to acetal formation in these compounds in the presence of formaldehyde (Fig. 2.2.3). However, if acetal formation had occurred, peaks should still be observed at 340 nm in the HPLC spectrum, but with slightly different retention times than those for the calyculins and calyculinamides. No peaks were seen at this wavelength, suggesting that the calyculins and calyculinamides are being degraded under the conditions of the fixative.

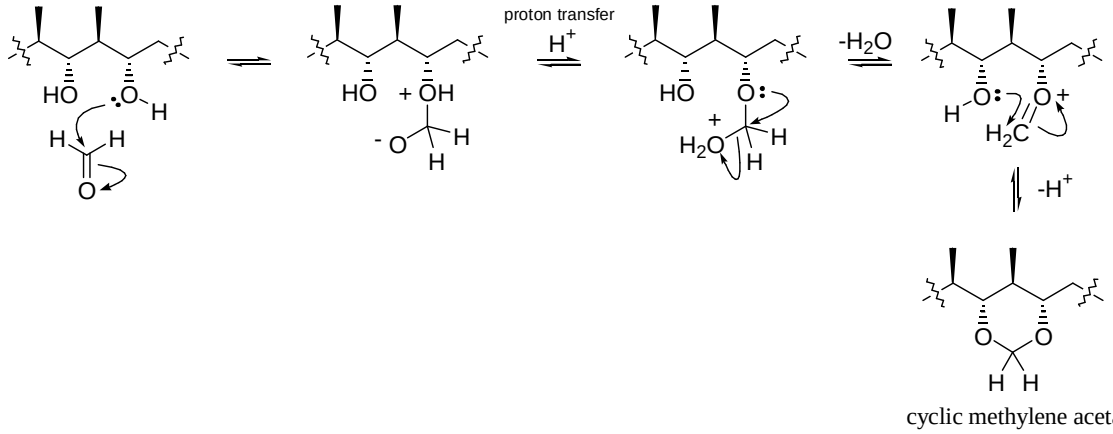

Figure 2.2.3 Mechanism for the formation of a cyclic methylene acetal in the presence of formaldehyde in molecules containing a 1,3 diol functionality, such as the calyculins and the calyculinamides

2.2.2 Analysis of the filamentous bacteria

One of the diced fixed sponge samples was selected for initial cell dissociation studies. This sample (10.43 g) was washed three times in calcium-magnesium free artificial seawater (CMF-ASW) to remove all traces of the fixative. Calcium and magnesium are excluded from the artificial seawater as they promote cell aggregation. The sample was then dissociated in a small Virtis blender for three time intervals of two minutes each in CMF-ASW. The resultant slurry was examined under a microscope (100 x, immersion) after each two minute period in order to monitor the extent of dissociation. It was then filtered through 75 µm mesh in order to remove any clumps of undissociated cells which might be present. The material retained on the filter was re-examined under the microscope. As there were still large quantities of undissociated filamentous and sponge cells apparent, this material was returned to the Virtis, blended for a further ten minutes in CMF-ASW, then re-filtered through 75 µm mesh.

The filtered dissociated cells were combined, and centrifuged at 1100 rpm (200 x g) for five minutes. Close inspection of the resultant pellet showed the formation of two layers. These layers were separated by repeatedly swirling off and re-centrifuging the top layer (filamentous bacteria) from the bottom layer (spicules and clumps of undissociated yellow sponge cells). The resultant homogeneous sample of filamentous heterotrophic bacteria cells was centrifuged twice more in Milli-Q® H_2O in order to remove the CMF-ASW. All the supernatants from above the pellets were combined and stored for subsequent analysis. A sub-sample of the filamentous heterotrophic bacteria cells was removed for reference and stored in CMF-ASW. The remainder of the sample

was freeze-dried and ground to give 144.6 mg of material. This was sonicated in methanol for five minutes and then passed through a 0.2 µm filter. The material collected on the filter was extracted and filtered twice more, and the filtrates combined and dried under nitrogen to give a 7.4 mg sample. This was analysed by ^{1}H NMR spectroscopy and analytical HPLC on ODS-silica (methanol/water, 9:1). Light protection was achieved throughout with the use of aluminium foil.

Signals in the ^{1}H NMR spectrum consistent with the presence of theonellapeptolides, including those due to amide protons of the amino acids above 6.5 ppm, were apparent (Fig 2.2.4). The presence of theonellapeptolides IIId and IIIe (**2.8**) was also indicated by the HPLC spectrum (Fig 2.2.5), with the observance of signals with retention times of 17.11 and 20.90 minutes, respectively (at 216 nm). No evidence indicating the presence of calyculins, calyculinamides or swinholides was found.

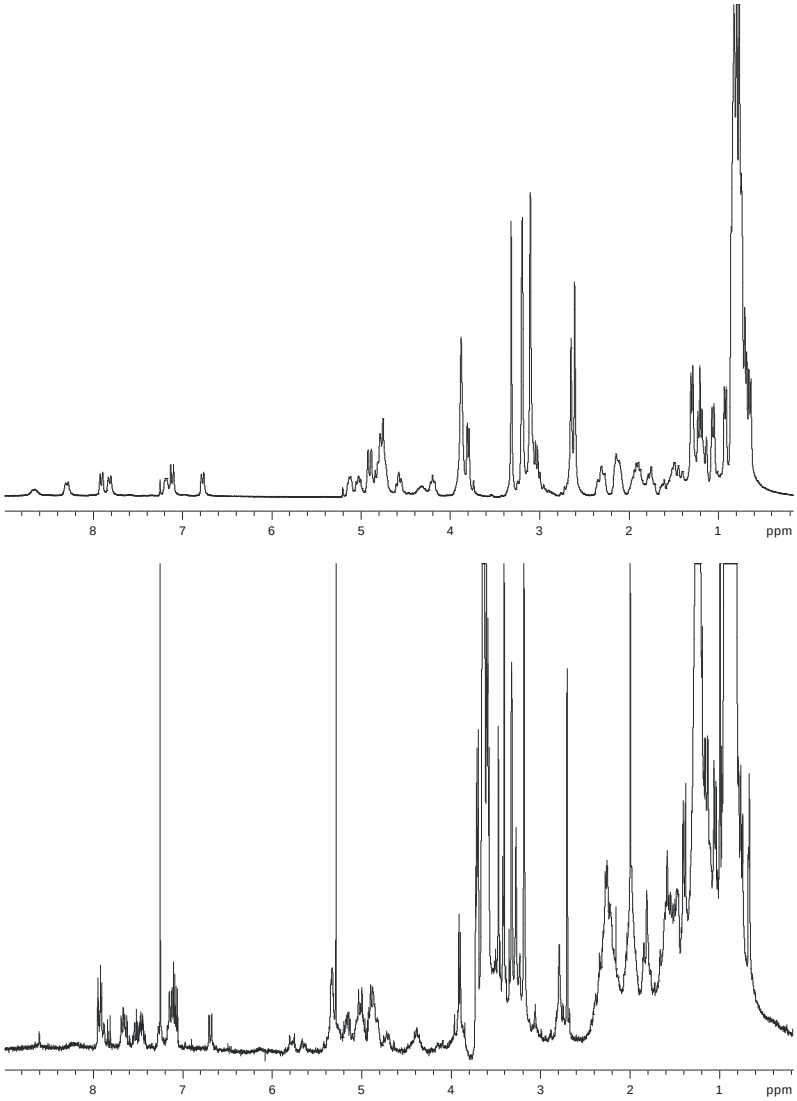

Figure 2.2.4 ^{1}H NMR spectra of theonellapeptolide IIIe (top) and the homogeneous filamentous heterotrophic bacteria sample (bottom)

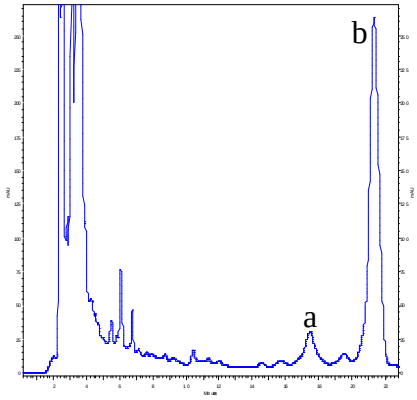

Figure 2.2.5 HPLC chromatogram of the homogeneous sample of filamentous heterotrophic bacteria cells at 219 nm showing theonellapeptolides IIId (a) and IIIe (b) (**2.8**)

Purification of the components of the filamentous bacteria extract was then carried out *via* preparative HPLC on ODS-silica ($MeOH/H_2O$, 9:1). Three peaks were collected (fractions 3-5) and dried down to give 1.8, 1.3 and 3.8 mg of material, respectively. The fractions were then analysed *via* ^1H NMR spectroscopy, analytical HPLS on ODS-silica ($MeOH/H_2O$, 9:1) and LRFABMS. The ^1H NMR spectra of these three fractions indicated the presence of peptide-like compounds. From the retention times of fractions 3 and 5 in the HPLC spectra (17.11 and 20.90 minutes, respectively (at 216 nm)), fraction 3 was identified as theonellapeptolide IIId and fraction 5 as theonellapeptolide IIIe (**2.8**). This was confirmed by LRFABMS. (Theonellapeptolide IIId (fraction 3): LRFABMS, *m/z* 1536.9 $[M + Cs]^+$ (calcd for $C_{70}H_{125}N_{13}O_{16}Cs$, 1536.8); theonellapeptolide IIIe (fraction 5): LRFABMS, *m/z* 1550.9 $[M + Cs]^+$ (calcd for $C_{71}H_{127}N_{13}O_{16}Cs$, 1550.9)). Fraction 4 appears to be an unknown theonellapeptolide. It eluted at 19.11 minutes (216 nm) and was determined to be isobaric with theonellapeptolide IIIe (**2.8**) by LRFABMS.

The filamentous bacteria stained Gram positive. Scanning electron microscopy (SEM) and transmission electron microscopy (TEM) was carried out on a pure sample of the filamentous heterotrophic bacteria. Two of the resultant micrographs are shown in Figure 2.2.6.

(a) (b)

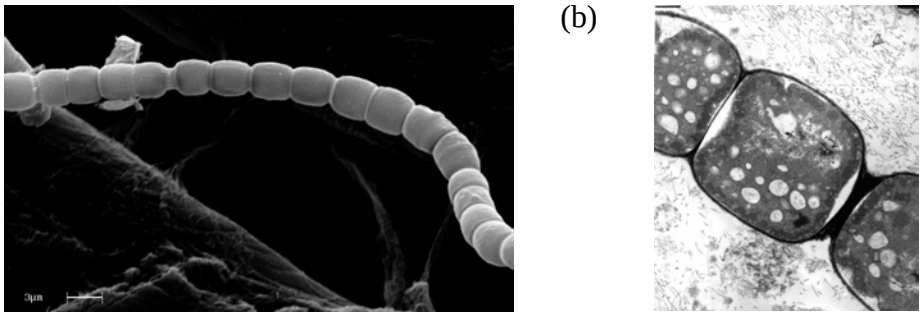

Figure 2.2.6 SEM (a) and TEM (b) micrographs of filamentous heterotrophic bacteria from *Lamellomorpha strongylata* (~ 4 μm segment length)

2.2.3 Analysis of the sponge cells

The combined supernatants from above the pellets formed on centrifugation of the dissociated cells at 1100 rpm (200 x g) were re-centrifuged at 1900 rpm (600 x g) for 5 minutes in an attempt to obtain a sample of dissociated sponge cells. Microscopic inspection of the resultant pellet (100 x, immersion) revealed extensive contamination of the sample with single segments of the filamentous bacteria and no obvious sponge cells. The problems encountered with this sample are likely to be a result of dissociating fixed sponge, rather than blending and filtering fresh sponge and then fixing the resultant cells. Extensive blending was required in order to obtain a reasonable quantity of dissociated filamentous bacteria cells. Any sponge cells that were dissociated in this process could well have been destroyed by subsequent blending. In addition, undissociated sponge cells were noted in the material retained on the filter after blending, as well as in the lower layer of the pellet obtained after centrifugation at 1100 rpm. No further work was carried out on this sample.

Unfortunately, due to considerable logistical constraints involved in the collection of the sponge from the Chatham Rise, and the need to process the material immediately following its collection, it was not possible to obtain fresh sponge to continue this work.

2.2.4 Analysis of the unicellular bacteria

The combined supernatants from above the pellets formed on centrifugation of the dissociated cells at 1900 rpm (600 x g) were re-centrifuged at 5000 rpm (4100 x g) for 5 minutes. The resultant pellets were inspected under a microscope (100 x, immersion).

This again revealed contamination from single segments of the filamentous bacteria, but to a lesser extent than that seen in the 1900 rpm pellet. The pellets were combined and re-centrifuged in Milli-Q® H_2O. An upper yellow-coloured layer and a lower black-coloured layer were observed in the resultant pellet. Microscopic investigation showed that the lower layer was comprised of spicule fragments, single segments of filamentous bacteria (along with a few short chains) and a small quantity of sponge cells. The upper layer consisted of very small cells (~ 1 µm in diameter), which were identified as unicellular bacteria. The two layers were separated by repeatedly swirling off and re-centrifuging (in Milli-Q® H_2O) the top less-densely pelleted layer. The resultant pellet was freeze-dried, ground, sonicated in MeOH for 20 minutes, filtered through a 0.2 µm filter, and dried under N_2 to give a sample of 2.5 mg. This was analysed by ^{1}H NMR and analytical HPLC on ODS-silica (MeOH/H_2O, 9:1). Light protection was achieved throughout with the use of aluminium foil.

The presence of theonellapeptolides was apparent in the HPLC spectrum, as expected, due to contamination of the sample with single segments of filamentous heterotrophic bacteria. However, the presence of a swinholide was also indicated in this spectrum (Fig. 2.2.6), with the observance of a peak eluting at 32.5 minutes (270 nm). This retention time was not indicative of swinholide H (**2.7**), however, which elutes at 31.9 minutes. It was postulated that this swinholide could be swinholide dimethylene acetal (**2.9**), formed as a result of the presence of formaldehyde in the fixative used (Fig. 2.2.3).

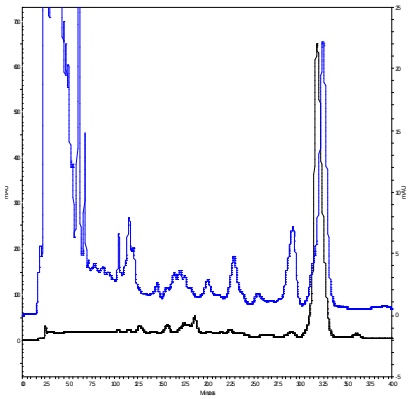

Figure 2.2.6 HPLC chromatogram of the unicellular bacteria sample at 270nm (blue) showing swinholide H dimethylene acetal (**2.9**) eluting at 32.5 minutes, overlaid with that of swinholide H (black) (**2.7**), which elutes at 31.9 minutes

Analysis of the ^{1}H NMR spectrum (run in $CDCl_3$) revealed swinholide-like resonances, along with low level peptide signals. The swinholide-like resonances were consistent

with the presence of swinholide H dimethylene acetal (**2.9**), by comparison with those for both swinholide H (**2.7**) and swinholide H diacetonide (**2.10**). As the ^{1}H NMR spectrum was done on the whole extract obtained from the unicellular bacteria cell pellet, only the most intense signals belonging to the swinholide-like material were apparent. The chemical shifts of these ^{1}H NMR signals are presented in Table 2.2.1, along with the corresponding signals for swinholide H (**2.7**) and swinholide H diacetonide (**2.10**).

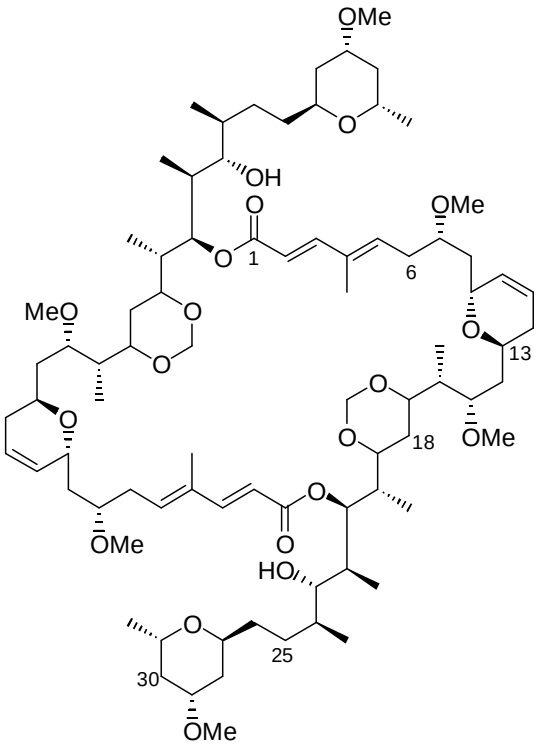

2.9 swinholide H dimethylene acetal

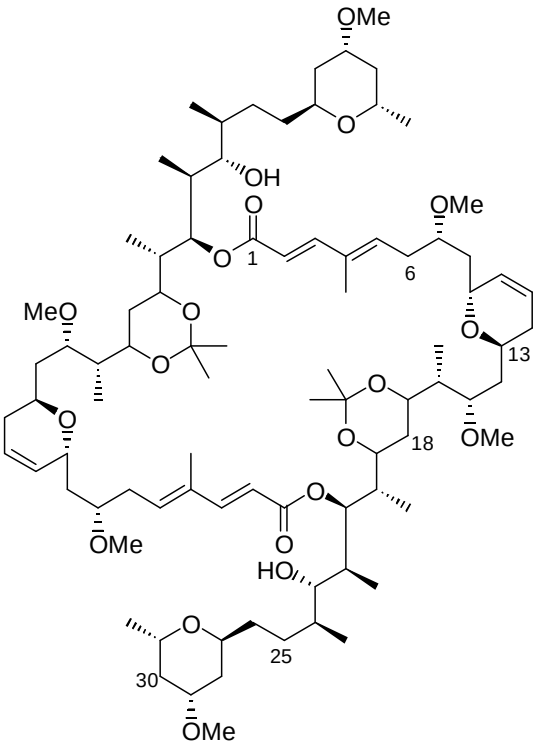

2.10 swinholide H diacetonide

From the observed ^{1}H NMR chemical shifts (Table 2.2.1), it appears that the H13 and 22-Me protons in swinholide H dimethylene acetal are in environments which bear more resemblance to those in swinholide H than its diacetonide, whilst the opposite is true of the 15-OMe, 16-Me, 20-Me and 24-Me protons in swinholide H dimethylene acetal, whose environments are more akin to the corresponding protons in swinholide H diacetonide. In order to gain some insight into the three dimensional structures of the swinholides in question, the X-ray coordinates for swinholide A[72] were imported into Chem3D Pro™. The changes required to obtain the structures for swinholide H (**13**), swinholide H dimethylene acetal (**15**) and swinholide H diacetonide (**16**) were made on the resultant 3D structure, and each was then energy minimised. The 3D arrangement of the atoms in each molecule was then compared. This indicated that the H13 and 22-Me protons in swinholide H dimethylene acetal are in environments similar to those in

swinholide H, and the 15-OMe, 16-Me, 20-Me and 24-Me protons in swinholide H dimethylene acetal are in environments similar to the corresponding protons in swinholide H diacetonide, thus supporting the observed chemical shifts shown in Table 2.2.1.

Confirmation of the presence of swinholide H dimethylene acetal (**2.9**) was obtained by LRFABMS (*m/z* 1440.9 [M], calcd for $C_{82}H_{136}O_{20}$, 1440.96). Scanning electron microscopy (SEM) and transmission electron microscopy (TEM) was carried out on a sample of the unicellular bacterium from *Lamellomorpha strongylata*. A TEM micrograph is shown in Figure 2.2.7.

Table 2.2.1 ^{1}H NMR (300 MHz) chemical shift data for swinholide H (**2.7**), swinholide H dimethylene acetal (**2.9**) and swinholide H diacetonide (**2.10**)[a]

position	**2.7**	**2.9**	**2.10**
13	3.48	3.48	3.62
7-OMe	3.43	3.42	3.41
15-OMe	3.36	3.29	3.29
29-OMe	3.33	3.33	3.33
4-Me	1.82	1.82	1.82
16-Me	0.80	0.75	0.74
20-Me	0.93	0.87	0.89
22-Me	0.85	0.85	0.82
24-Me	0.96	1.00	0.99
31-Me	1.19	1.20	1.19

[a]Values in ppm relative to C*H*Cl_3 (δ7.26).

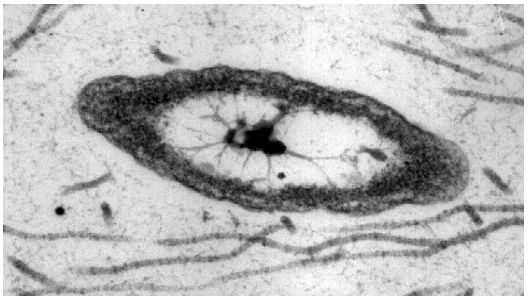

Figure 2.2.7 TEM micrograph of a unicellular bacterium from *Lamellomorpha strongylata* (~ 1 μm length)

2.2.5 Geographically distinct population of *Lamellomorpha strongylata*

Another sample of *Lamellomorpha strongylata* was subsequently supplied by the National Institute of Water and Atmospheric Research (NIWA). This was a frozen sample that had been collected at Spirits Bay, Northland, New Zealand. Like the Chatham Rise specimen, it was also reported to contain filamentous heterotrophic bacteria, but had no biological activity. Microscopic analysis revealed the presence of filamentous bacteria in low levels only (in comparison to that associated with the Chatham Rise specimen), and apparently only on the surface of the sponge. TEM analysis of the bacteria from the northern *Lamellomorpha strongylata* was undertaken, however the cells had unfortunately been damaged in the freezing process, as feared. This prohibited any meaningful comparison of the filamentous bacteria from the two geographically distinct populations of *Lamellomorpha strongylata*.

2.2.6 Summary and future directions

The theonellapeptolides isolated from *Lamellomorpha strongylata* have been located in the sponge-associated filamentous heterotrophic bacteria, while a swinholide has been found in symbiotic unicellular bacteria. Two of the known theonellapeptolides, IIId and IIIe (**2.8**), were identified *via* ^{1}H NMR, HPLC and LRFABMS, along with another unreported theonellapeptolide isobaric with IIIe. The swinholide was identified as swinholide H di-methylene acetal (**2.9**) *via* an analysis of its 3-D structure, a comparison of its NMR data with that obtained for swinholide H diacetonide (**2.10**) and MS data. These findings are consistent with research carried out on the Lithistid sponge *Theonella swinhoei* from Palau, where a peptide (P951) and swinholide A were found to be located solely in associated filamentous heterotrophic bacteria and unicellular

heterotrophic bacteria, respectively. In this case, no major metabolites were located in the sponge cells or in the cyanobacterial cells, which were the final two of four discrete cell populations observed in the sponge.[25]

Should a sufficient quantity of live *Lamellomorpha strongylata* become available in the future, it would be interesting to attempt cell dissociation of the sponge and associated symbionts without the use of chemical fixatives, in order to localise the calyculins and calyculinamides (which are suspected to degrade in the presence of fixative) within discrete cell populations. Dissociation of whole fixed sponge was not conducive to the obtention of intact sponge cells, so dissociation of fresh sponge is likely to achieve a higher yield of sponge cells for analysis. These cells could be preserved in liquid nitrogen and then separated into homogeneous cells types quickly, using centrifugation or density gradients, without the use of fixatives. Alternatively, microwave fixation may be an option. In the event that one or more of the secondary metabolites are located in sponge cells, ecological experiments, involving wounding or the introduction of parasites to the sponge, for example, could then be carried out in order to determine whether or not production of the bioactive molecule(s) is enhanced by placing the source organism under environmental stress. Aquaculture trials to determine optimal conditions for sponge growth and secondary metabolite production could also be undertaken.

Although it seems likely that the sponge-associated filamentous heterotrophic bacteria and unicellular bacteria are the producing organisms of the theonellapeptolides and swinholides, respectively (Ockhamôs razor states the simplest solution tends to be the correct one), it is possible that the localisation of the compounds within these cells may be misleading, and that they are merely being stored in the cells in question. Genetic studies to identify the producing gene cluster, such as is currently being explored in several groups around the world, would clarify this point.[73]

2.3 *Lissodendoryx* sp.

Figure 2.3.1 *Lissodendoryx* sp.. Image courtesy of Marine Group photo archive, University of Canterbury.

A major hurdle for the development of the halichondrins as anticancer drugs has been the supply issue. Kishiôs total synthesis of halichondrin B published in 1992 is still the only method reported to date, but as it involves close to 50 steps in the longest linear sequence it is not likely to be an economically viable option for the supply of the halichondrins.[36] However, more recently it has been found that a portion of the right hand side of the molecule retains the activity of the whole (see chapter 3 (**3.12)**), thus opening up the possibility of a commercially viable synthesis of this smaller molecule. In addition, Kishiôs group at Harvard University, along with other synthetic groups including that of Steven Burke at the University of Wisconsin-Madison, continue to publish syntheses of portions of halichondrin B in fewer steps and with higher yields, and exciting progress is being made in Andrew Phillipsô group at the University of Colorado at Boulder on a total synthesis of the halichondrins in under 30 steps.[74]

Another option that has been investigated for the large scale production of the halichondrins is aquaculture. Initial aquaculture trials have indicated variable levels of the halichondrins in the sponge as a result of differing environmental conditions.[75] These trials also suggest, however, that enhanced production of the compounds can be achieved by stressing the sponge. The establishment of the cellular location of the halichondrins in the sponge itself, or in its microbial symbionts, is therefore extremely pertinent.

2.3.1 Microscopic analysis

Six small samples of fixed *Lissodendoryx* sp. (I 1-3 and II 1-3) were supplied by NIWA. Microscopic investigation (100 x, immersion) of the fixative solutions revealed cell debris only, with no sign of intact sponge cells. Small slices of each sample were taken, washed three times in CMF-ASW, and inspected under the microscope. Intact sponge cells were found in all six samples. Samples I 1-3 and II 1-3 were combined to give two larger samples (I and II), and dissociated with a razor blade. The two samples were then filtered through 100 µm mesh in order to remove any clumps of undissociated cells, and made up to ~7 mL with CMF-ASW. Six 10 mL discontinuous Percoll® gradients were prepared, by sequentially layering 2 mL of 60%, 45%, 30%, 15% and 5% Percoll®, in CMF-ASW, into centrifuge tubes. Samples I and II (3 x 2 mL from each) were then loaded onto the top of the density gradients, and centrifuged at 600 rpm for 10 minutes. Bands of cells were apparent at the density interfaces of the Percoll® layers. These were isolated individually by pipette, and combined in each series (I and II) to give samples I 1-8 and II 1-6. These samples were centrifuged twice in fresh CMF-ASW in order to remove the Percoll®, and investigated microscopically.

In series I, most of the cellular material was located in samples 1-3. Cell debris, collagen, archeocytes, and very small cells (possibly bacteria clumps) were found in sample 1. Sample 2 contained a few clumps of undissociated cells, along with choanocytes, archeocytes, spherulous cells and pinacocytes. Larger cells still were found in sample 3 (choanocytes, archeocytes and spherulous cells, plus at least three other cell types). Samples 4-7 had much lower cell densities than the earlier samples, containing decreasing quantities of archeocytes and spherulous cells, along with spicule fragments. Sample 8 consisted mainly of ñrocksò (bits of stone quartz chips, and spicules).

In series II, very small archeocytes, collagen and possibly bacteria cells were again found in sample 1. Sample 2 contained choanocytes, archeocytes, cell debris and a few spherulous cells. Cell size continued to increase into sample 3, with the presence of archeocytes, spherulous cells, choanocytes and pinacocytes. Samples 4 and 5 contained progressively larger archeocytes, and sample 6 again consisted mainly of ñrocksò.

2.3.2 Analysis of fixed sponge material

Four additional fixed sponge samples, each in a different fixative, were subsequently supplied by NIWA for assessment of the survival of the halichondrins when exposed to fixative. The fixatives used were Davidsonôs, IG4F, 10% formaldehyde, and 1.9% formaldehyde/1.5% glutaraldehyde. A series of experiments involving soaking and washing samples of this fixed sponge material (in both CMF ASW and distilled water) and extracting it before submitting samples for assay indicated that detection of the halichondrins in fixed sponge *via* the P388 assay was not possible due to the activity of the fixatives themselves in the assay and the difficulty in effectively removing the fixatives from the sponge material. Thus, spectroscopic detection (NMR, HPLC, MS) is required.

Spectroscopic investigations of extracts of these four samples of fixed *Lissodendoryx* sp. were inconclusive. Although halichondrin-sized molecules were detected by MS analysis, the presence of the halichondrins was not able to be confirmed by ^{1}H NMR due to insufficient quantities in the small samples supplied to date.

4 g samples of each of the four *Lissodendoryx* sp. fixed sponge samples were taken. Each was chopped with a razor blade, sonicated in Milli-Q® H_2O, freeze dried and placed on the hi-vac for 8 hours. The samples were then weighed, ground, extracted with 25 mL 3:1 MeOH:CH_2Cl_2, and centrifuged at 3000 rpm for 10 minutes. Spectroscopic investigations of these four samples were inconclusive. All four samples showed evidence of halichondrin-sized molecules by MS, however no exact match to any of the known halichondrins was observed. The presence of the halichondrins was not able to be confirmed by ^{1}H NMR due to insufficient quantities in the samples available. This may not have been the case had the Capillary NMR probe, used in the analyses discussed in Chapter 3, been available at the time this work was done. Degradation of the samples over time meant that it was not possible to re-analyse the samples after the purchase of the CapNMR probe.

2.3.3 Summary and future directions

Halichondrin-sized molecules have been observed in samples of fixed *Lissodendoryx* sp., however definitive identification has not yet been achieved. As was encountered in the dissociation of *Lamellomorpha strongylata*, dissociation of the sponge *Lissodendoryx* sp. after fixation proved to be very destructive of the sponge cells present. Ideally, the sponge should be dissociated fresh, and the resultant cells preserved in liquid nitrogen. These cells could subsequently be fixed, once it has been established that the halichondrins survive exposure to the fixatives used. Alternatively, microwave fixation could be investigated, or the cells could be studied quickly without fixation.

Once a suitable protocol has been established, further investigation is needed on larger quantities of sponge in order to enable spectroscopic identification (*via* analytical HPLC on ODS-silica, ^{1}H NMR and MS) of the halichondrins in homogenous cell samples, obtained *via* centrifugation and/or Percoll® density gradients. Determination of the cell type in which the halichondrins are located, by SEM and TEM, should then be undertaken. The identification of particular halichondrins and their relative abundance should also be possible.

CHAPTER 3. New Halichondrins.

3.1 Introduction

An ongoing project in the Marine Chemistry Group at the University of Canterbury has been a study of the halichondrin series of compounds (complex polyether macrolides) which were first isolated from the Japanese sponge *Halichondria okadai* Kadota.[32,33] The major halichondrin component isolated from this sponge, and the first to be characterised, was norhalichondrin A (**3.1**).

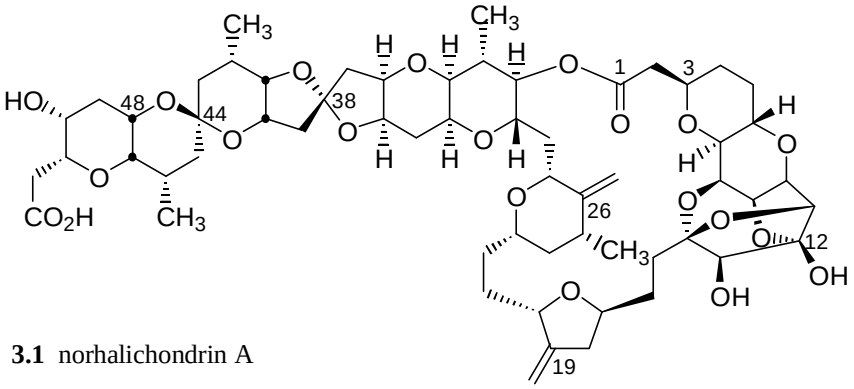

3.1 norhalichondrin A

The halichondrins are classified in three series (A, B or C) according to the degree of oxygenation at the C12 and C13 positions of the tricyclo ring system.

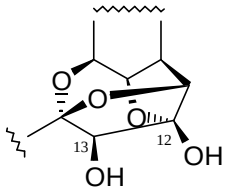

halichondrin A

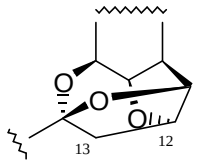

halichondrin B

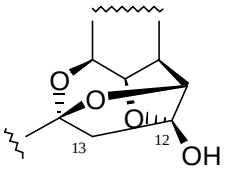

halichondrin C

These compounds have subsequently been isolated from other sponges, including B series halichondrins from the bright yellow sponge *Lissodendoryx* sp. (Family Myxillidae, Order Poecilosclerida) which is found in deep water (~ 100 m) off the Kaikoura Peninsula.[76] Although still occurring at very low levels, relatively speaking the Kaikoura source of the halichondrins is rich. *Lissodendoryx* sp. has been found to contain approximately 1.6 mg of total halichondrins per kg of wet sponge. Two of the known halichondrins isolated from the Kaikoura sponge, halichondrin B (**3.2**) and isohomohalichondrin B (**3.3**), have been investigated by the National Cancer Institute (NCI) in the USA and the pharmaceutical company PharmaMar S.A. in Spain, respectively, for their extremely promising anticancer activity. Halichondrin B is an

antimitotic agent, active against selected sensitive melanoma, colon, ovarian, lung and breast cancer cell lines.

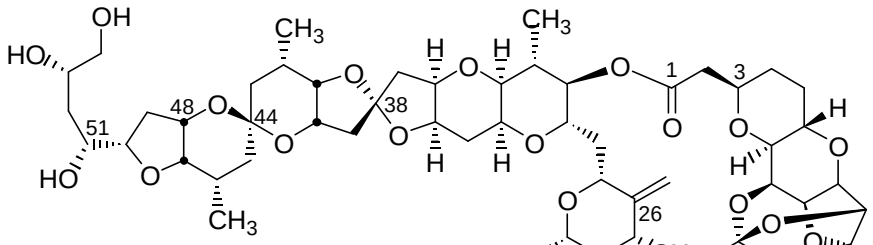

3.2 halichondrin B

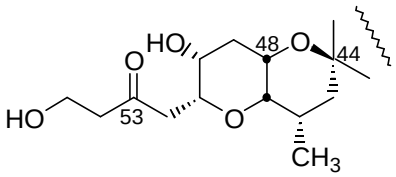

3.3 isohomohalichondrin B

In addition to halichondrin B (**3.2**) and isohomohalichondrin B (**3.3**), the other known halichondrins isolated to date from *Lissodendoryx* sp., which are all from the B series, are shown below (**3.4** ï **3.11**). Compounds **3.5**, **3.10** and **3.11** are thought to be artefacts of the isolation process.[76]

Following the total synthesis of halichondrin B (**3.2**) and norhalichondrin B (**3.1**) in 1992,[36] it was discovered that synthetically derived analogues based on the fragment from C1 to C30 had cytotoxic activity similar to that of halichondrin B.[77-83] One of these simplified analogues, the macrocyclic ketone NSC 707389 (**3.12**), is currently in clinical trials, having replaced halichondrin B as the lead candidate of this class of compounds due to its comparable activity and relative ease of supply.[38] In further studies, NSC 707389 was found to be consistently more potent than halichondrin B in its interactions with tubulin.[38]

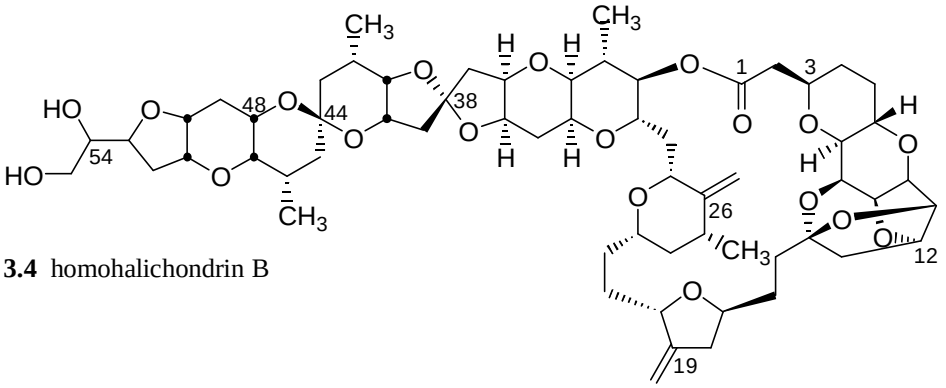

3.4 homohalichondrin B

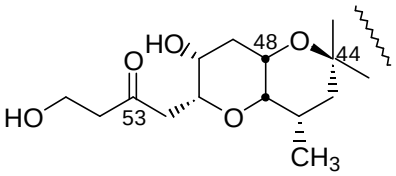

3.5 38-*epi* isohomohalichondrin B (artefact)

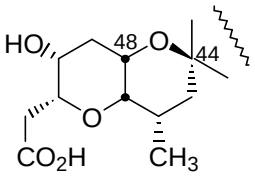

3.6 norhalichondrin B

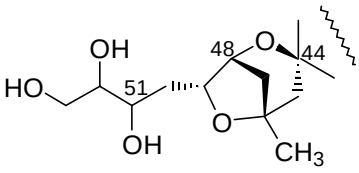

3.7 neonorhalichondrin B

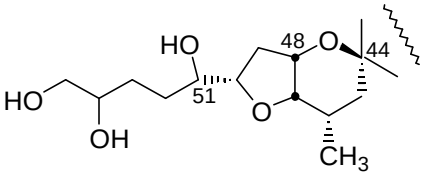

3.8 neohomohalichondrin B

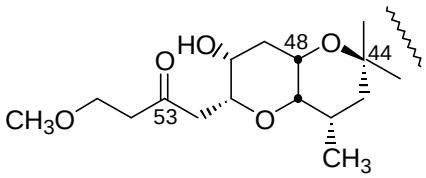

3.9 55-methoxyisohomohalichondrin B

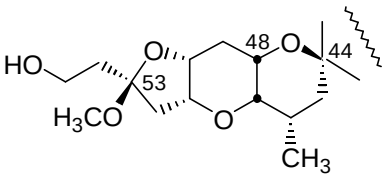

3.10 53-methoxyneoisohomohalichondrin B (artefact)

3.11 53-*epi* 53-methoxyneoisohomohalichondrin B (artefact)

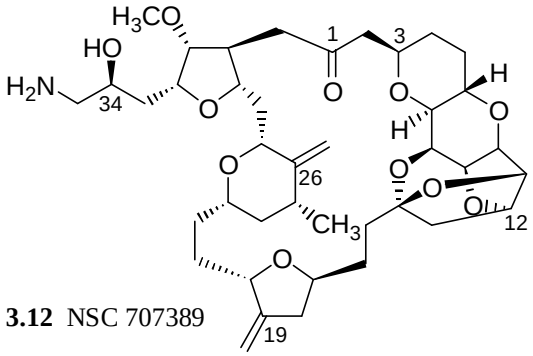

3.12 NSC 707389

3.2 Isolation of new halichondrins from *Lissodendoryx* sp.

The halichondrins occur at extremely low levels in *Lissodendoryx* sp. One tonne of the sponge was collected in 1995 in order to supply halichondrin B (310 mg) and isohomohalichondrin B (~300 mg) for further trials. During the final purification of isohomohalichondrin B by preparative HPLC on ODS-silica (CH_3CN/H_2O, 7:3 or 9:1), twelve 2.5 L bottles of side cut residue were accumulated. The residue from each of these bottles was dried down individually, weighed, and analysed by ^1H NMR and analytical HPLC on ODS-silica (CH_3CN/H_2O, 7:3 and 9:1). Signals in the ^1H NMR spectra characteristic of the halichondrins (for example, those between 4.7 and 5 ppm corresponding to the 19=CH_2 and 26=CH_2 exocyclic methylenes) were observed in the extracts of all twelve bottles. In the HPLC spectra, halichondrin-like peaks, which exhibit end absorption only, were also seen.

This side cut residue was processed, after initial analysis with DIOL TLC (4% $MeOH/CH_2Cl_2$), on preparative and analytical HPLC ODS-silica columns, eluting with 55% CH_3CN/H_2O and 70% CH_3CN/H_2O respectively, to give five pure fractions (**SH3 116.2**, **116.4**, **118.2**, **118.3** and **118.4**). Analysis of these fractions *via* analytical HPLC on ODS-silica (CH_3CN/H_2O, 7:3), ^1H NMR and LCMS established that these were all new halichondrins. Table 3.2.1 depicts the masses of the five new halichondrins, interspersed with those of the known halichondrins. The HPLC chromatograms of the five new halichondrins are shown in Figure 3.2.1.

Using a 5 mg/mL solution of quinine in the ^1H NMR solvent (deuterated chloroform containing 0.1% d5-pyridine), it was established that there were approximate sample sizes of between 50 and 110 µg. The quantity of the compounds was estimated according to the formula:

$$(MW/\#H) \times (\text{total integral for } \#H)/(\text{integral for } C\mathbf{H}Cl_3) \times CF$$

where MW is the molecular weight of the compound, #H is the number of protons in the selected resonances used, ñtotal integral for #Hò is the sum of the integrals for the selected resonances, and CF is the calibration factor that had previously been determined from a standard solution containing quinine (5 mg/mL) in the same $CDCl_3$ solvent. #H was typically ~10, with resonances selected on the basis of their resolution from other resonances and from the solvent peak.

Using these estimated masses, the five samples were submitted for P388 assay (a murine leukaemia cell line) at known concentration, yielding results in ng/mL. All five of the new halichondrins showed very potent P388 activity. Individual sample masses, along with their P388 activities, are given in Table 3.2.2. The P388 activities of three known halichondrins are also included for the purpose of comparison.

Table 3.2.1 Exact masses of the halichondrins isolated from *Lissodendoryx* sp.

Compound	Number	Exact Mass
SH3 116.2	**3.13**	1020.51
SH3 118.2	**3.15**	1076.53
SH3 118.3	**3.16**	1092.57
norhalichondrin B	**3.6**	1094.54
neonorhalichondrin B (minor 2)	**3.7**	1096.56
SH3 118.4	**3.17**	not determined
halichondrin B	**3.2**	1110.58
homohalichondrin B	**3.4**	1122.58
isohomohalichondrin B	**3.3**	1122.58
38-epi isohomohalichondrin B (artefact)	**3.5**	1122.58
neohomohalichondrin B (minor 1)	**3.8**	1124.59
55-methoxyisohomohalichondrin B (LP2)	**3.9**	1136.59
53-methoxyneoisohomohalichondrin B (LP1)	**3.10**	1136.59
53-epi 53-methoxyneoisohomohalichondrin B (LP3)	**3.11**	1136.59
SH3 116.4	**3.14**	1140.54

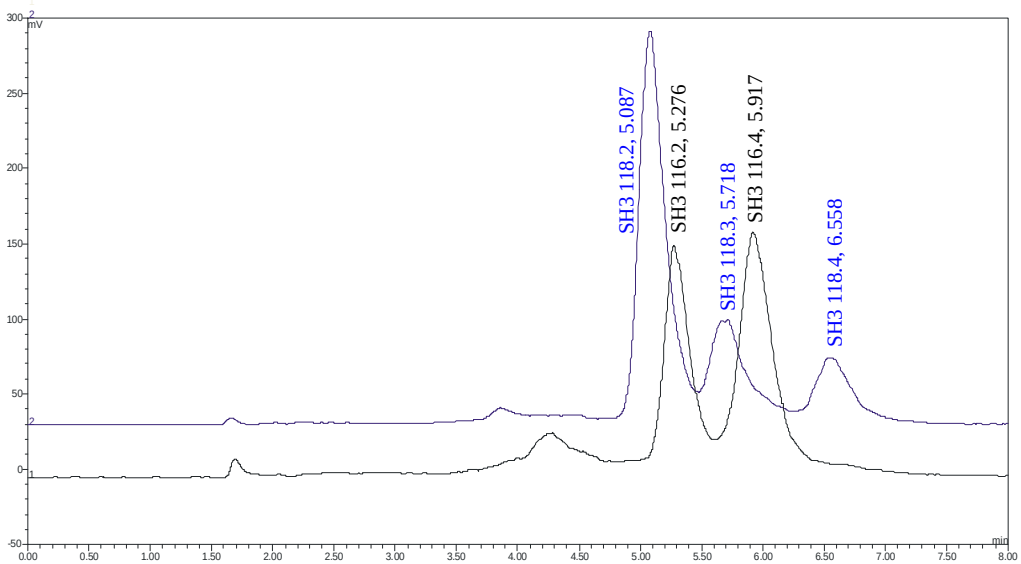

Figure 3.2.1 The ELSD HPLC chromatograms of the SH3 116.x (black) and SH3 118.x (blue) series of new halichondrins, with retention times in minutes

Table 3.2.2 Estimated sample masses and *in vitro* cytotoxicities of selected halichondrins

Compound	Sample Mass (μg)	P388 IC_{50} (ng/mL)
SH3 116.2	50	1.1
SH3 116.4	55	2.0
SH3 118.2	110	1.1
SH3 118.3	88	0.76
SH3 118.4	50	0.51
halichondrin B		0.78
homohalichondrin B		0.22
isohomohalichondrin B		0.18

3.3 Structure elucidation of SH3 116.2 (3.13)

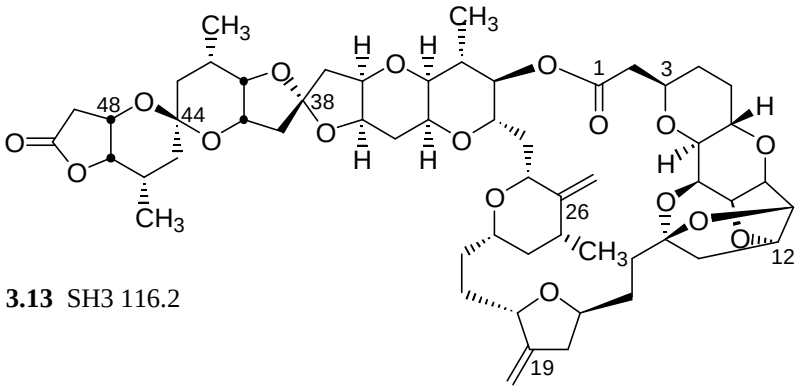

3.13 SH3 116.2

SH3 116.2 (**3.13**) was the second most polar of the five new halichondrin derivatives (Fig. 3.3.1). High-resolution LCMS (*m/z* 1038.5372 $[M+NH_4]^+$, ϕ = -5.4 mmu), in combination with NMR data (Table 3.3.1), gave the molecular formula $C_{56}H_{76}O_{17}$ (19 double bond equivalents). This is 90 mass units less than that observed for halichondrin B (**3.2**), corresponding to the replacement of the terminal chain from carbon 51 in halichondrin B with a carboxyl moiety, thus converting the terminal ring to a ɔ-lactone. The NMR assignments were confirmed by gCOSY, TOCSY, ROESY and HSQC 2D experiments, in addition to comparisons with the known NMR shifts for halichondrin B. The ^{1}H NMR spectrum is shown in Figure 3.3.1. Due to the small sample size, no ^{13}C NMR spectrum was obtained. The ^{13}C data reported in Table 3.3.1 were obtained from the HSQC experiment (Fig. 3.3.2).

The observed ^{1}H NMR shifts for SH3 116.2 showed excellent agreement with those of halichondrin B up to C45 (Table 3.3.1). The connectivity of the remainder of the molecule was established *via* gCOSY and TOCSY data (Fig. 3.3.3). The presence of a large geminal coupling constant of 17 Hz for the methylene protons at C49 (ŭ 2.50, 2.66) is consistent with the attachment of a carboxyl moiety at C50.[84]

H47 (ŭ 4.21) and H48 (ŭ 4.26) were determined to be *cis* from the small 2 Hz coupling constant observed for H48, and the relative stereochemistry of these protons was established *via* observed ROESY correlations between H46 (ŭ 2.43) and both H47 and H48 (Fig. 3.3.3). This stereochemistry is consistent with that observed for halichondrin B (**3.2**). The gCOSY, TOCSY and ROESY spectra, along with selected correlations, are shown in Figures 3.3.4, 3.3.5 and 3.3.6, respectively.

Table 3.3.1 ^{1}H and ^{13}C NMR chemical shift data for halichondrin B (**3.2**) and SH3 116.2 (**3.13**)[a]

	halichondrin B		SH3 116.2	
position	C	H	C[b]	H
1	171.2		*c*	
2	40.4	2.35, 2.60	40.4	2.35, 2.59
3	73.7	3.86	73.7	3.88
4	30.7	1.37, 1.75	30.6	1.38, 1.75
5	30.0	1.35, 2.08	30.0	1.37, 2.09
6	68.2	4.34	68.3	4.33
7	77.7	2.94	77.7	2.94
8	74.3	4.33	74.3	4.32
9	73.8	4.04	73.8	4.05
10	76.5	4.20	76.5	4.19
11	82.1	4.60	82.1	4.59
12	81.1	4.68	81.1	4.68
13	48.3	1.94, 2.15	48.3	1.94, 2.16
14	110.1		*c*	
15	34.4	1.62, 2.18	34.4	1.62, 2.16
16	28.2	1.42, 2.16	28.2	1.43, 2.17
17	75.5	4.10	75.2	4.10
18	38.7	2.26, 2.80	38.6	2.27, 2.79
19	151.8		*c*	
19=CH2	104.4	4.92, 4.98	*c*	4.91, 4.99
20	75.4	4.37	75.3	4.37
21	29.5	1.40, 1.88	29.6	1.40, 1.88
22	32.0	1.60, 1.60	32.0	1.61, 1.61
23	74.9	3.53	74.8	3.54
24	43.4	1.04, 1.70	43.4	1.04, 1.70
25	35.9	2.20	36.0	2.20
25-Me	18.0	1.07	18.0	1.07
26	151.6		*c*	
26=CH2	104.2	4.77, 4.81	*c*	4.76, 4.81
27	73.5	3.54	73.5	3.53
28	36.9	1.94, 2.02	36.9	1.94, 2.02
29	71.2	4.21	71.2	4.21
30	76.9	4.63	76.9	4.65
31	36.6	2.04	36.5	2.04
31-Me	15.1	0.99	15.0	1.00
32	77.5	3.18	77.5	3.19
33	66.3	3.80	66.3	3.81
34	29.1	1.79, 2.13	29.1	1.80, 2.13
35	75.0	4.10	75.2	4.10
36	76.2	4.10	76.2	4.10
37	43.5	1.92, 2.35	43.4	1.92, 2.36
38	112.5		*c*	
39	42.7	2.24, 2.24	42.7	2.22, 2.22
40	71.7	4.00	71.7	3.98
41	79.0	3.63	79.1	3.63
42	25.6	2.23	25.4	2.23
42-Me	17.6	0.94	17.5	0.94
43	36.6	1.29, 1.52	36.2	1.35, 1.47
44	97.5		*c*	
45	36.9	1.42, 1.50	36.1	1.37, 1.58
46	25.7	2.35	25.5	2.43
46-Me	17.8	0.99	17.2	1.06
47	80.2	3.61	81.0	4.21
48	71.7	4.05	68.8	4.26
49	35.9	1.9, 2.32	38.6	2.50, 2.66
50	79.8	4.08	*c*	
51	73.0	3.80		
52	37.2	1.62, 1.79		
53	70.4	4.02		
54	66.9	3.54, 3.61		

[a] Values in ppm relative to C**H**Cl_3 (ŭ 7.25) and **C**DCl_3 (ŭ 77.0). [b] Values obtained from HSQC spectrum. [c] Values not detected.

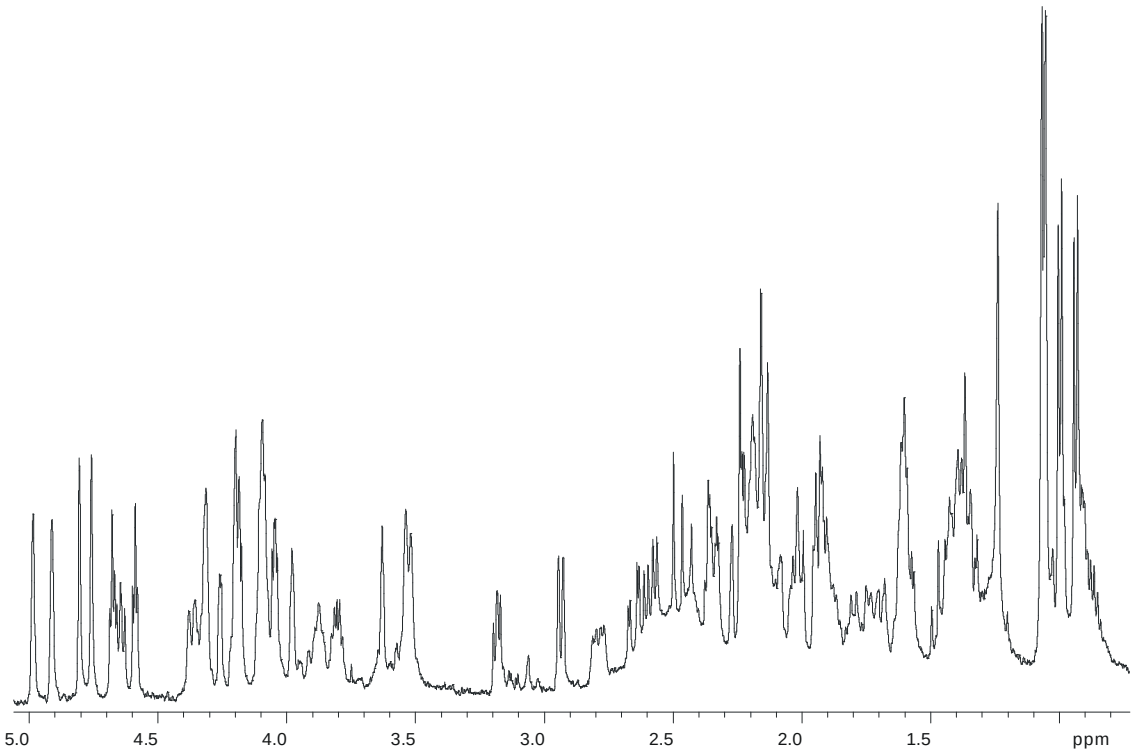

Figure 3.3.1 The ^{1}H NMR spectrum of SH3 116.2 (**3.13**)

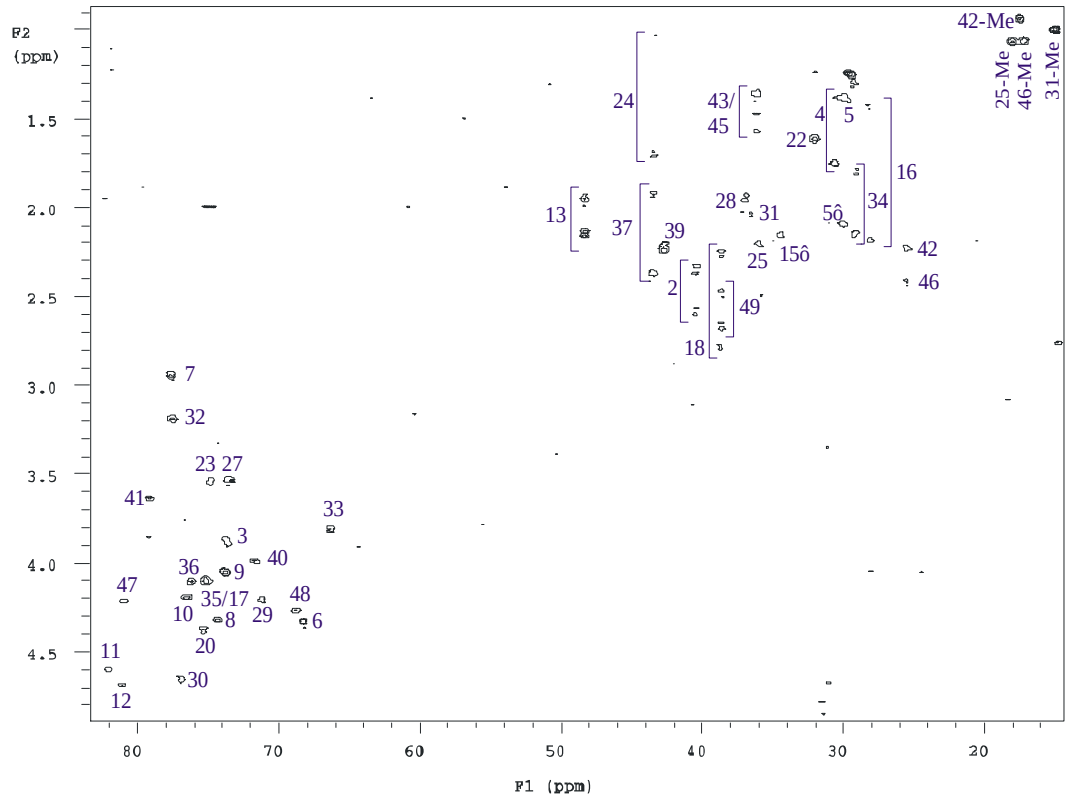

Figure 3.3.2 The HSQC NMR spectrum of SH3 116.2 (**3.13**)

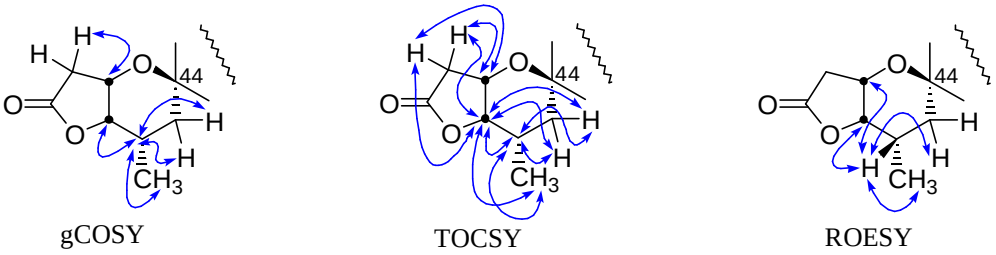

Figure 3.3.3 gCOSY, TOCSY and selected ROESY correlations for the C44-C50 region of SH3 116.2 (**3.13**)

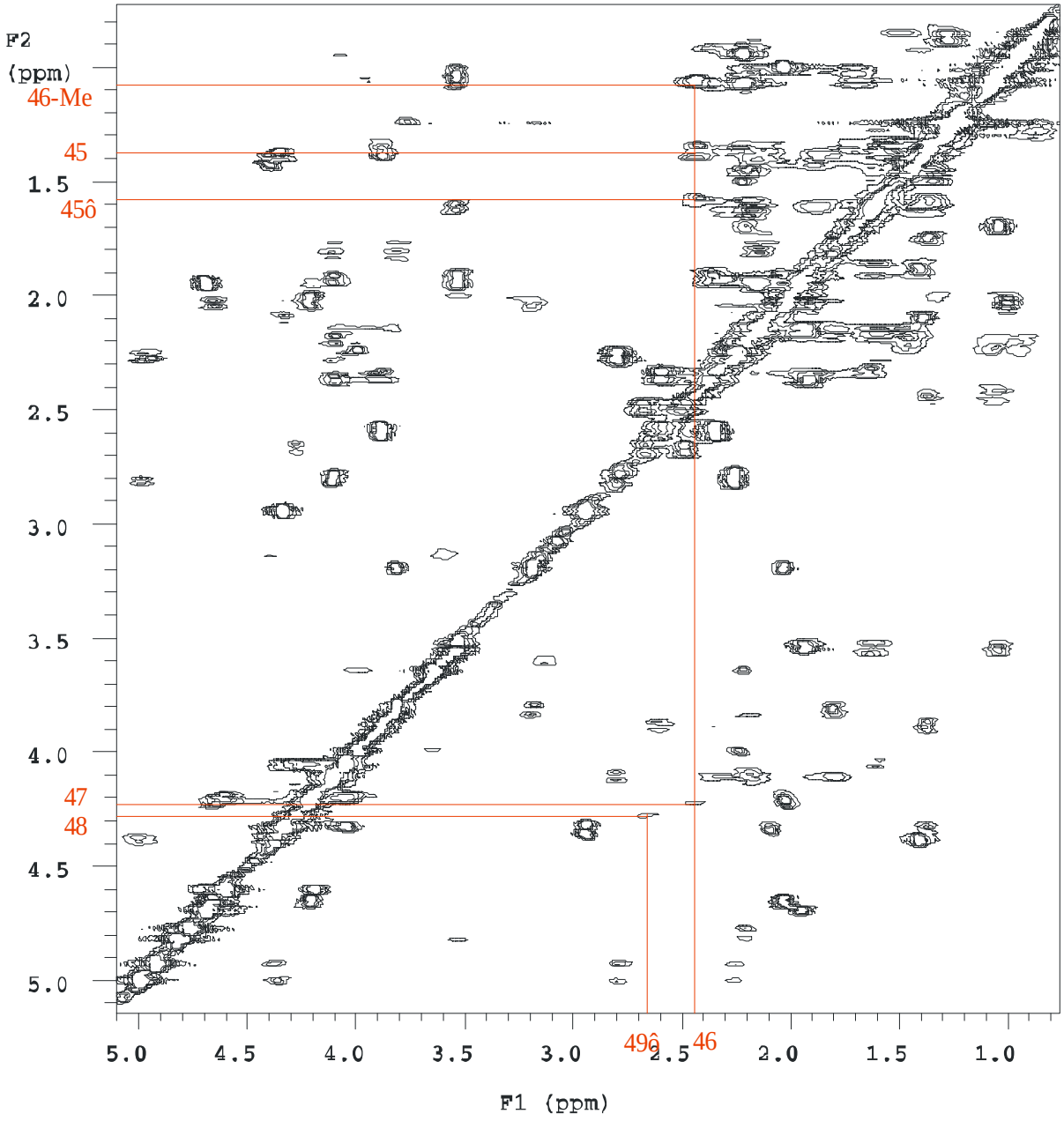

Figure 3.3.4 The gCOSY NMR spectrum of SH3 116.2 (**3.13**), showing selected correlations

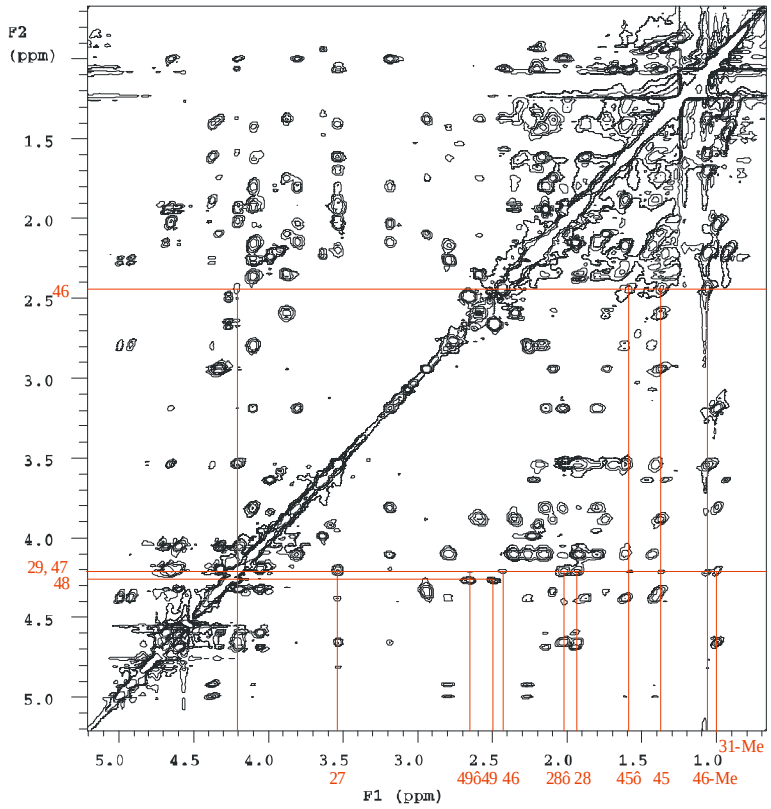

Figure 3.3.5 The TOCSY NMR spectrum of SH3 116.2 (**3.13**)

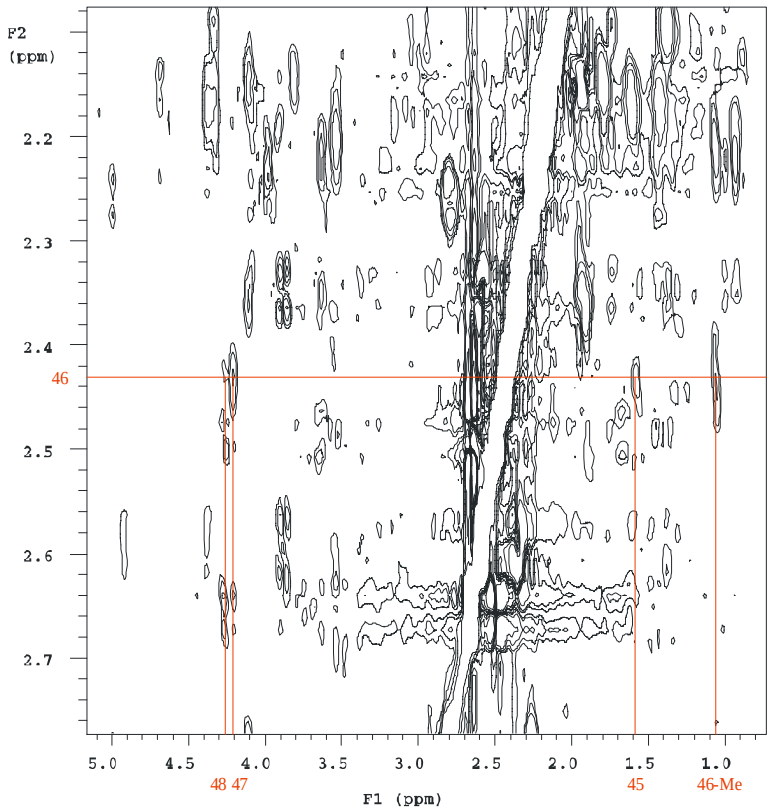

Figure 3.3.6 The ROESY NMR spectrum of SH3 116.2 (**3.13**)

3.4 Structure elucidation of SH3 116.4 (3.14)

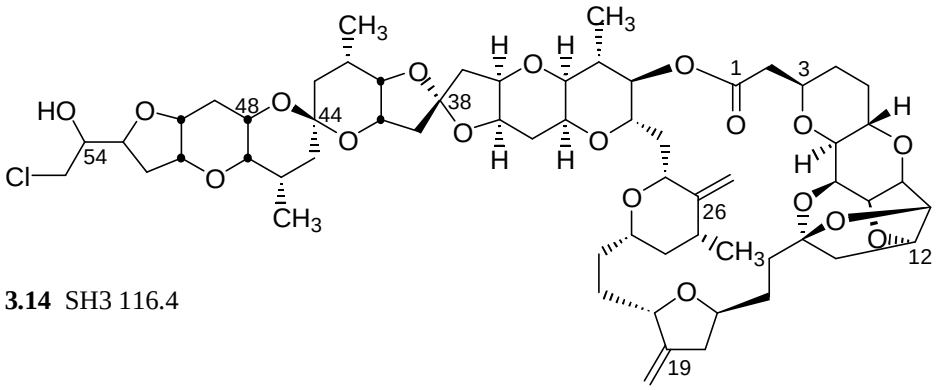

3.14 SH3 116.4

SH3 116.4 (**3.14**) was the second least polar of the five new halichondrin derivatives (Fig. 3.3.1). High-resolution LCMS (*m/z* 1179.5001 $[M+K]^+$, φ = -6.1 mmu), in combination with NMR data (Table 3.4.1), gave the molecular formula $C_{61}H_{85}ClO_{18}$ (19 double bond equivalents). This is 18 mass units more than that observed for homohalichondrin B (**3.4**), corresponding to the replacement of the terminal (C55) hydroxyl group in homohalichondrin B with chlorine. The presence of chlorine in a molecule from the halichondrin family is unprecedented to date. The NMR assignments were confirmed by gCOSY, TOCSY, ROESY, HSQC and CIGAR[85] 2D experiments, in addition to comparisons with the known NMR shifts for homohalichondrin B. The ^{1}H NMR spectrum is shown in Figure 3.4.1. Due to the small sample size, no ^{13}C NMR spectrum was obtained. The ^{13}C data reported in Table 3.4.1 were obtained from the HSQC and CIGAR (Fig. 3.4.2) experiments. The CIGAR experiment was primarily used to obtain the ^{13}C NMR chemical shift for position 26, and to confirm the ^{13}C NMR chemical shifts around the methyl groups, using the typically prominent $^2J_{CH}$ and $^3J_{CH}$ correlations observed.

As the chemical shifts on the right hand side of SH3 116.4 were very similar to those of SH3 116.2, the HSQC for SH3 116.4 was printed with the same scale as that of SH3 116.2, copied onto a transparency, and overlaid. This proved to be a very efficient means of establishing the known portion of the molecule, the parts of the molecule where change was beginning to occur, and the parts of the molecule which were in totally different steric and electronic environments to those of the known halichondrin. Once the similarity to homohalichondrin B (**3.4**) was established, these HSQC spectra were also overlaid, revealing that only positions 53-55 varied between the two molecules (Fig. 3.4.3).

Table 3.4.1 ^{1}H and ^{13}C NMR chemical shift data for homohalichondrin B (**3.4**) and SH3 116.4 (**3.14**)[a]

	homohalichondrin B		SH3 116.4	
position	C	H	C[b]	H
1	171.2		*c*	
2	40.4	2.34, 2.58	40.3	2.35, 2.58
3	73.6	3.88	73.6	3.87
4	30.7	1.34, 1.72	30.7	1.36, 1.74
5	30.0	1.38, 2.08	29.9	1.37, 2.08
6	68.2	4.34	68.2	4.32
7	77.7	2.94	77.6	2.93
8	74.3	4.32	74.3	4.32
9	73.8	4.04	73.8	4.05
10	76.5	4.20	76.5	4.18
11	82.1	4.58	82.1	4.58
12	81.1	4.68	81.2	4.67
13	48.3	1.94, 2.16	48.3	1.94, 2.13
14	110.1		*c*	
15	34.4	1.60, 2.16	34.4	1.62, 2.15
16	28.1	1.40, 2.16	28.1	1.40, 2.17
17	75.4	4.10	75.3	4.09
18	38.7	2.26, 2.79	38.7	2.25, 2.79
19	151.8		*c*	
19=CH2	104.5	4.91, 4.98	*c*	4.91, 4.98
20	75.0	4.38	75.3	4.36
21	29.0	1.44, 1.88	29.4	1.42, 1.89
22	32.0	1.60, 1.60	32.0	1.60, 1.60
23	74.8	3.52	74.8	3.53
24	43.4	1.05, 1.70	43.2	1.05, 1.68
25	35.9	2.20	35.9	2.20
25-Me	18.0	1.06	18.0	1.06
26	151.5		151.7	
26=CH2	104.2	4.75, 4.80	*c*	4.75, 4.80
27	73.5	3.54	73.6	3.53
28	36.9	1.94, 2.02	36.9	1.92, 2.00
29	71.2	4.20	71.3	4.18
30	76.6	4.65	76.9	4.64
31	36.8	2.04	36.3	2.04
31-Me	15.0	0.99	15.0	0.98
32	77.5	3.17	77.5	3.17
33	66.5	3.78	66.4	3.79
34	29.4	1.80, 2.14	29.1	1.79, 2.13
35	75.3	4.10	75.3	4.09
36	76.3	4.10	76.3	4.10
37	43.4	1.90, 2.35	43.5	1.91, 2.35
38	112.4		*c*	
39	42.5	2.21, 2.21	42.6	2.19, 2.19
40	70.8	3.92	70.8	3.92
41	79.4	3.60	79.5	3.58
42	25.8	2.32	25.7	2.32
42-Me	17.7	0.93	17.6	0.92
43	36.5	1.29,1.45	36.9	1.33, 1.45
44	96.6		*c*	
45	36.8	1.42, 1.42	36.9	1.44, 1.44
46	28.9	2.18	28.7	2.18
46-Me	17.1	0.90	17.1	0.90
47	72.8	3.06	72.8	3.06
48	63.6	3.53	63.6	3.53
49	31.4	1.79, 2.15	31.4	1.79, 2.19
50	74.7	3.90	74.7	3.90
51	76.3	4.04	76.4	4.06
52	37.2	2.02, 2.02	37.9	2.02, 2.02
53	79.8	4.25	77.3	4.38
54	72.0	3.57	72.6	3.66
55	65.6	3.69, 3.69	45.9	3.55, 3.55

[a] Values in ppm relative to C**H**Cl_3 (ŭ 7.25) and **C**DCl_3 (ŭ 77.0). [b] Values obtained from HSQC and CIGAR spectra. [c] Values not detected.

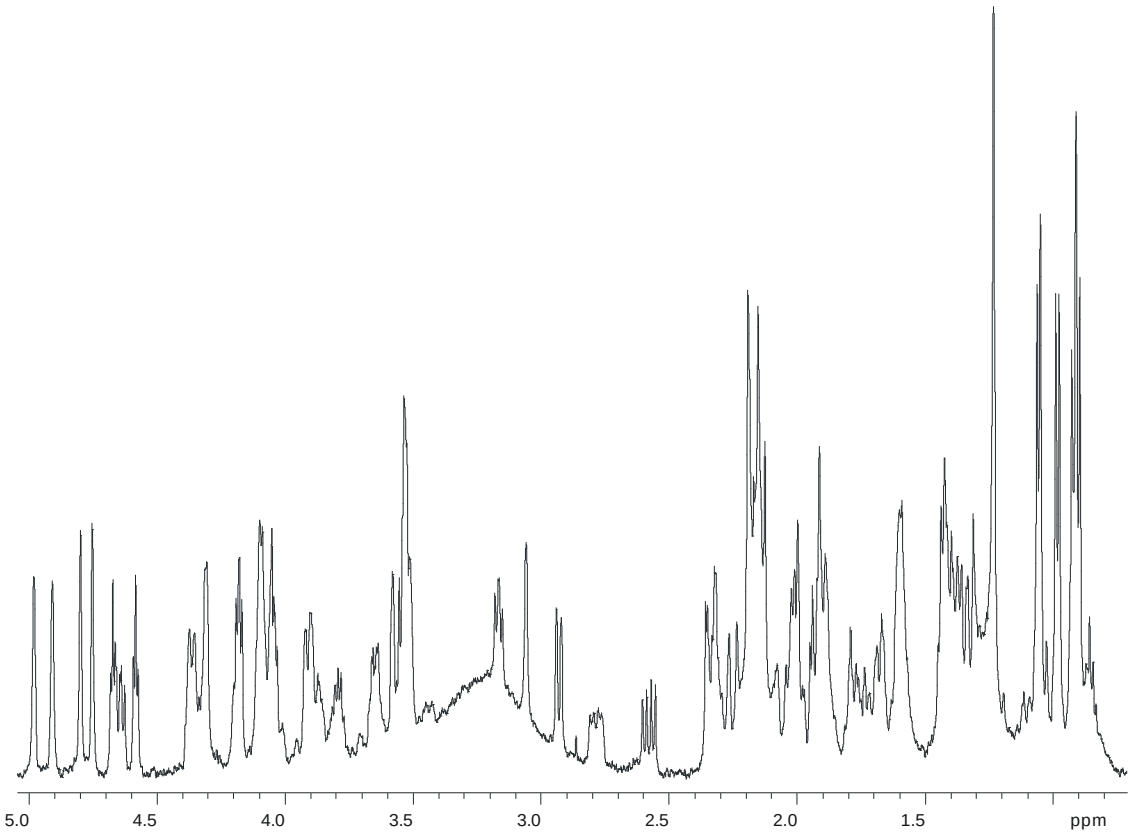

Figure 3.4.1 The ^{1}H NMR spectrum of SH3 116.4 (**3.14**)

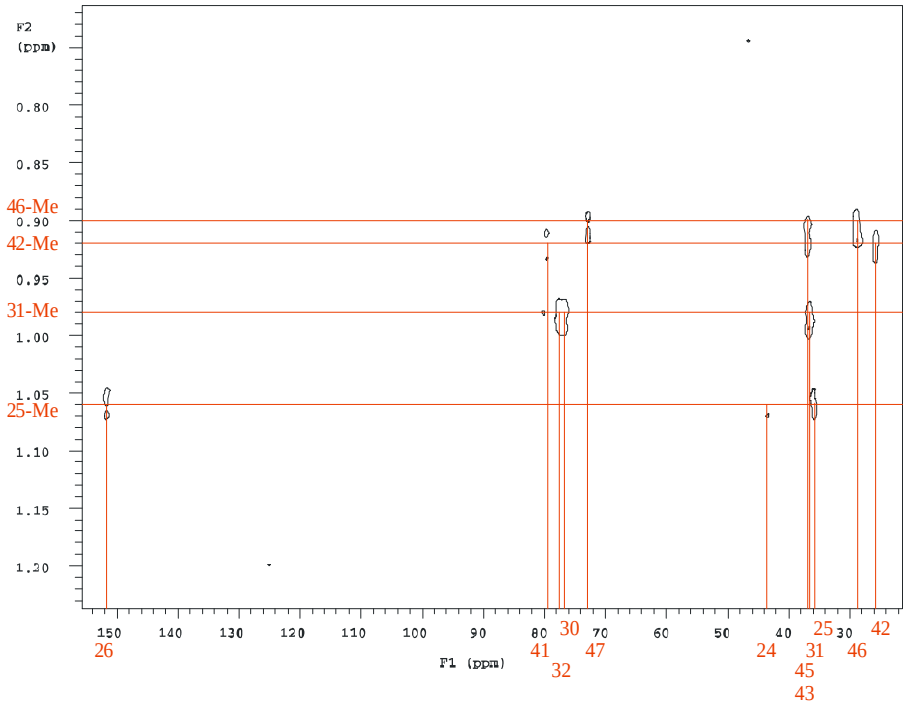

Figure 3.4.2 Part of the CIGAR NMR spectrum of SH3 116.4 (**3.14**)

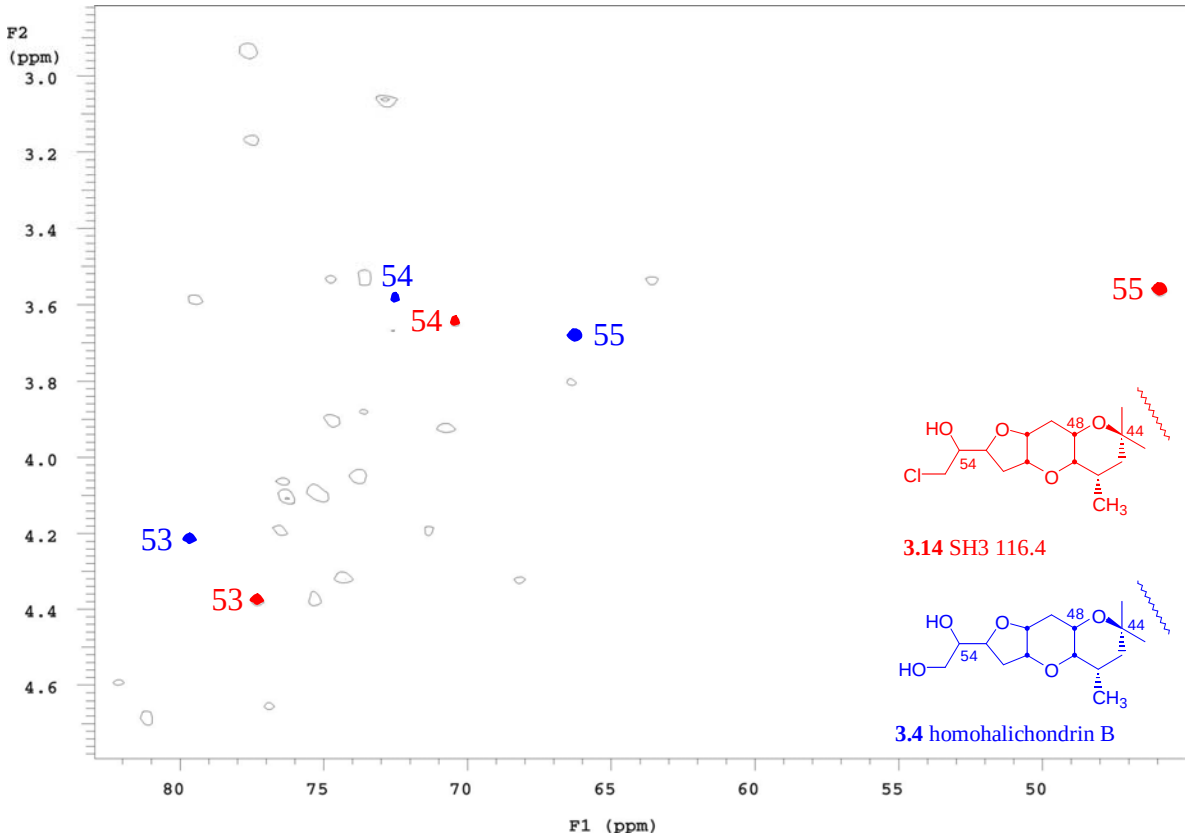

Figure 3.4.3 The overlaid HSQC NMR spectra for SH3 116.4 (**3.14**) and homohalichondrin B (**3.4**). Correlations in red are those observed for SH3 116.4 only, correlations in blue are those observed for homohalichondrin B only, and uncoloured correlations are identical for both molecules.

In order to confirm the presence of chlorine in the molecule, the isotope patterns in the HRLCMS spectra were investigated. A good match was obtained between the observed and predicted isotope patterns for both $[M + NH_4]^+$ and $[M + NH_4$ ï $HCl]^+$ (Fig. 3.4.4). Signals for $[M + Na$ ï $HCl]^+$ and $[M + K$ ï $HCl]^+$ were also observed.

The connectivity of the left hand end of the molecule was confirmed by gCOSY and TOCSY data, as described previously, and ROESY correlations confirmed the relative stereochemistry, which is consistent with that observed for homohalichondrin B (Fig. 3.4.5). An attempt to gain some insight into the stereochemistry at positions C53 and C54 from coupling constants derived from cross sections in the TOCSY experiment failed due to insufficient resolution.

A. $[M + NH_4]^+$ observed

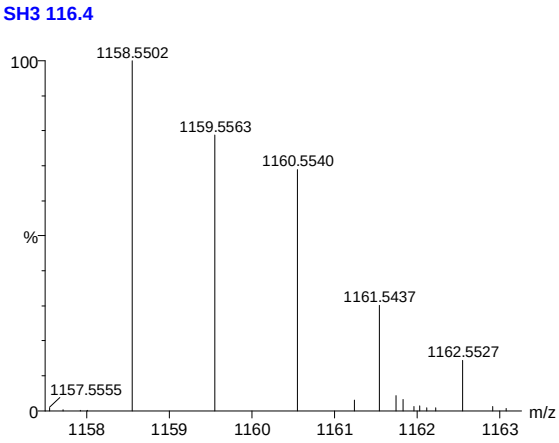

B. $[M + NH_4 - HCl]^+$ observed

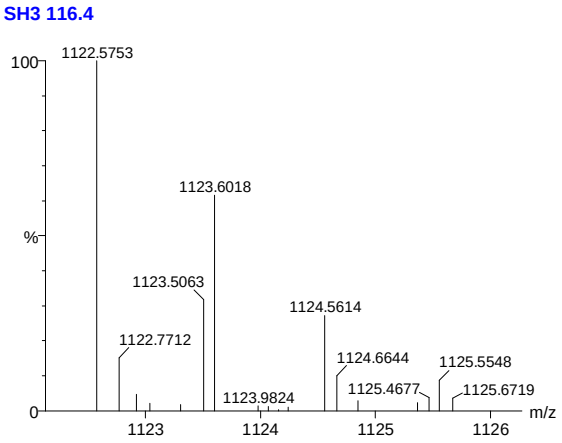

C. $[M + NH_4]^+$ predicted

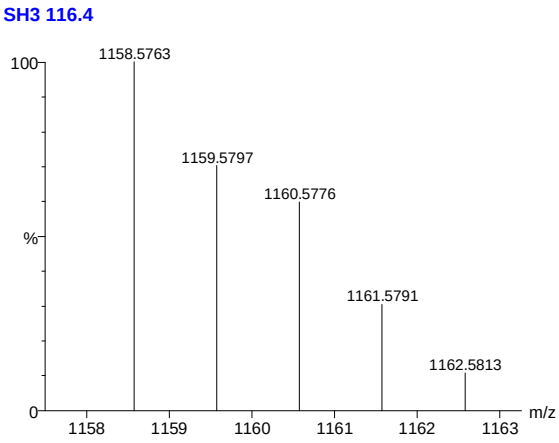

D. $[M + NH_4 - HCl]^+$ predicted

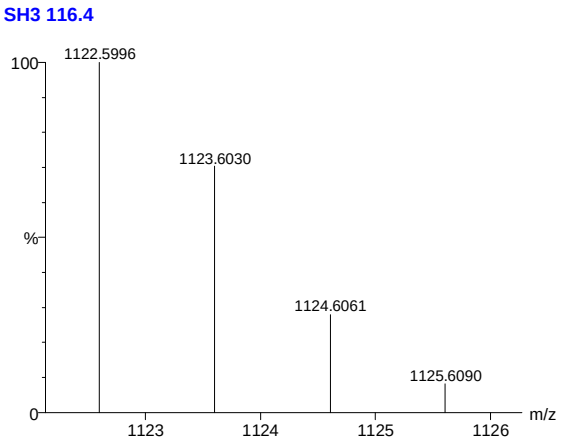

Figure 3.4.4 Observed (**A.** & **B.**) and predicted (**C.** & **D.**) isotope patterns for SH3 116.4 (**3.14**) $[M + NH_4]^+$ and [M + NH4 ï HCl]$^+$, respectively

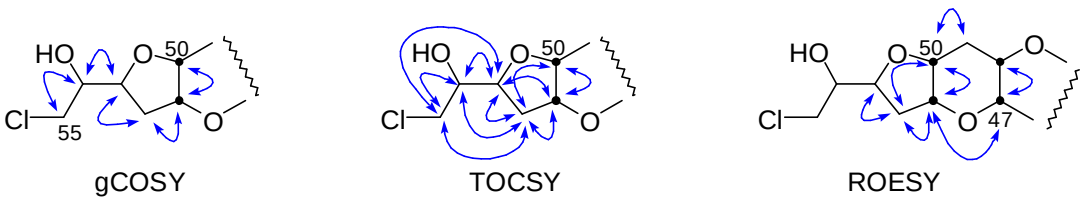

Figure 3.4.5 gCOSY and TOCSY for the C50-C55 region and selected ROESY correlations for the C47-C55 region of SH3 116.4 (**3.14**)

3.5 Structure elucidation of SH3 118.2 (3.15)

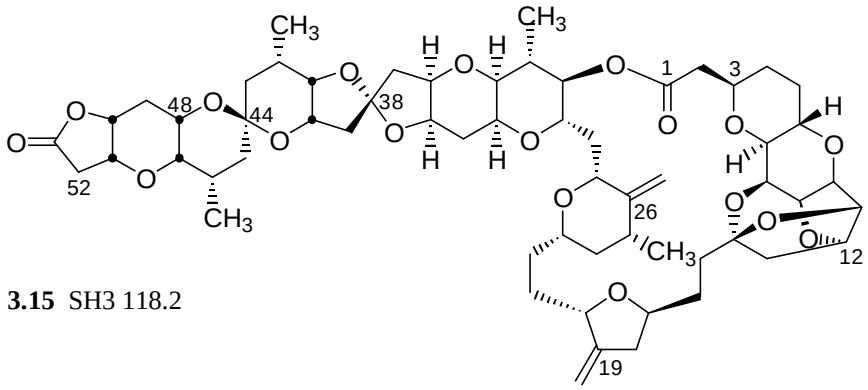

3.15 SH3 118.2

SH3 118.2 (**3.15**) was the most polar of the five new halichondrin derivatives (Fig. 3.3.1). High-resolution LCMS (*m/z* 1099.5171 $[M+Na]^+$, φ = -7.1 mmu), in combination with NMR data (Table 3.5.1), gave the molecular formula $C_{59}H_{80}O_{18}$ (20 double bond equivalents). This is 46 mass units less than that observed for homohalichondrin B (**3.4**), corresponding to the replacement of the terminal chain from carbon 54 in homohalichondrin B with a carboxyl moiety, thus converting the terminal ring to a ɔ-lactone. The NMR assignments were confirmed by gCOSY, TOCSY, ROESY, HSQC and CIGAR 2D experiments, in addition to comparisons with the known NMR shifts for homohalichondrin B. Due to the small sample size, no ^{13}C NMR spectrum was run. The ^{13}C data reported in Table 3.5.1 were obtained from the HSQC and CIGAR experiments. The ^{1}H NMR spectrum is shown in Figure 3.5.1.

Overlaying of the HSQC spectra with those of known halichondrins was again used to good effect in the structure elucidation of this molecule. The observed ^{1}H and ^{13}C NMR shifts for SH3 118.2 (**3.15**) showed excellent agreement with those of homohalichondrin B (**3.4**) up to position 46, and similar shifts for position 47 (Table 3.5.1). The ^{13}C NMR chemical shift for C47 (ŭ 73.2) was confirmed from the CIGAR experiment, leading to confirmation of the ^{1}H NMR chemical shift (ŭ 3.13) *via* the HSQC spectrum. This left three methines and two methylenes unassigned from the HSQC spectrum. The connectivity of this portion of the molecule was established *via* gCOSY and TOCSY data (Fig. 3.5.2). As was observed for C49 in SH3 116.2 (**3.13**), a large geminal coupling constant of 17 Hz for the methylene protons at C52 (ŭ 2.56, 2.65) is consistent with the attachment of a carboxyl moiety at C53.

Table 3.5.1 ^{1}H and ^{13}C NMR chemical shift data for homohalichondrin B (**3.4**) and SH3 118.2 (**3.15**)[a]

	homohalichondrin B		SH3 118.2	
position	C	H	C[b]	H
1	171.2		*c*	
2	40.4	2.34, 2.58	40.3	2.32, 2.57
3	73.6	3.88	73.7	3.87
4	30.7	1.34, 1.72	30.6	1.37, 1.73
5	30.0	1.38, 2.08	29.9	1.37, 2.07
6	68.2	4.34	68.2	4.30
7	77.7	2.94	77.7	2.92
8	74.3	4.32	74.4	4.30
9	73.8	4.04	73.8	4.03
10	76.5	4.20	76.5	4.17
11	82.1	4.58	82.2	4.57
12	81.1	4.68	81.1	4.66
13	48.3	1.94, 2.16	48.3	1.93, 2.14
14	110.1		*c*	
15	34.4	1.60, 2.16	34.4	1.61, 2.15
16	28.1	1.40, 2.16	28.1	1.41, 2.15
17	75.4	4.10	75.2	4.09
18	38.7	2.26, 2.79	38.6	2.26, 2.78
19	151.8		*c*	
19=CH2	104.5	4.91, 4.98	*c*	4.90, 4.97
20	75.0	4.38	75.3	4.37
21	29.0	1.44, 1.88	29.5	1.39, 1.88
22	32.0	1.60, 1.60	31.9	1.59, 1.59
23	74.8	3.52	74.7	3.52
24	43.4	1.05, 1.70	43.3	1.04, 1.67
25	35.9	2.20	35.9	2.19
25-Me	18.0	1.06	17.9	1.05
26	151.5		151.7	
26=CH2	104.2	4.75, 4.80	*c*	4.74, 4.79
27	73.5	3.54	73.6	3.50
28	36.9	1.94, 2.02	36.8	1.92, 2.02
29	71.2	4.20	71.3	4.19
30	76.6	4.65	77.0	4.65
31	36.8	2.04	36.3	2.01
31-Me	15.0	0.99	15.0	0.97
32	77.5	3.17	77.4	3.15
33	66.5	3.78	66.3	3.78
34	29.4	1.80, 2.14	29.1	1.77, 2.14
35	75.3	4.10	75.2	4.09
36	76.3	4.10	76.3	4.10
37	43.4	1.90, 2.35	43.4	1.88, 2.34
38	112.4		*c*	
39	42.5	2.21, 2.21	42.6	2.18, 2.18
40	70.8	3.92	70.9	3.89
41	79.4	3.60	79.3	3.57
42	25.8	2.32	25.6	2.26
42-Me	17.7	0.93	17.5	0.90
43	36.5	1.29,1.45	36.6	1.32-1.40
44	96.6		*c*	
45	36.8	1.42, 1.42	36.6	1.32-1.40
46	28.9	2.18	28.6	2.17
46-Me	17.1	0.90	16.9	0.88
47	72.8	3.06	73.2	3.13
48	63.6	3.53	62.7	3.59
49	31.4	1.79, 2.15	29.9	1.91, 2.37
50	74.7	3.90	75.2	4.31
51	76.3	4.04	72.8	4.18
52	37.2	2.02, 2.02	38.6	2.56, 2.65
53	79.8	4.25	*c*	
54	72.0	3.57		
55	65.6	3.69, 3.69		

[a] Values in ppm relative to C**H**Cl_3 (ŭ 7.25) and **C**DCl_3 (ŭ 77.0). [b] Values obtained from HSQC and CIGAR spectra. [c] Values not detected.

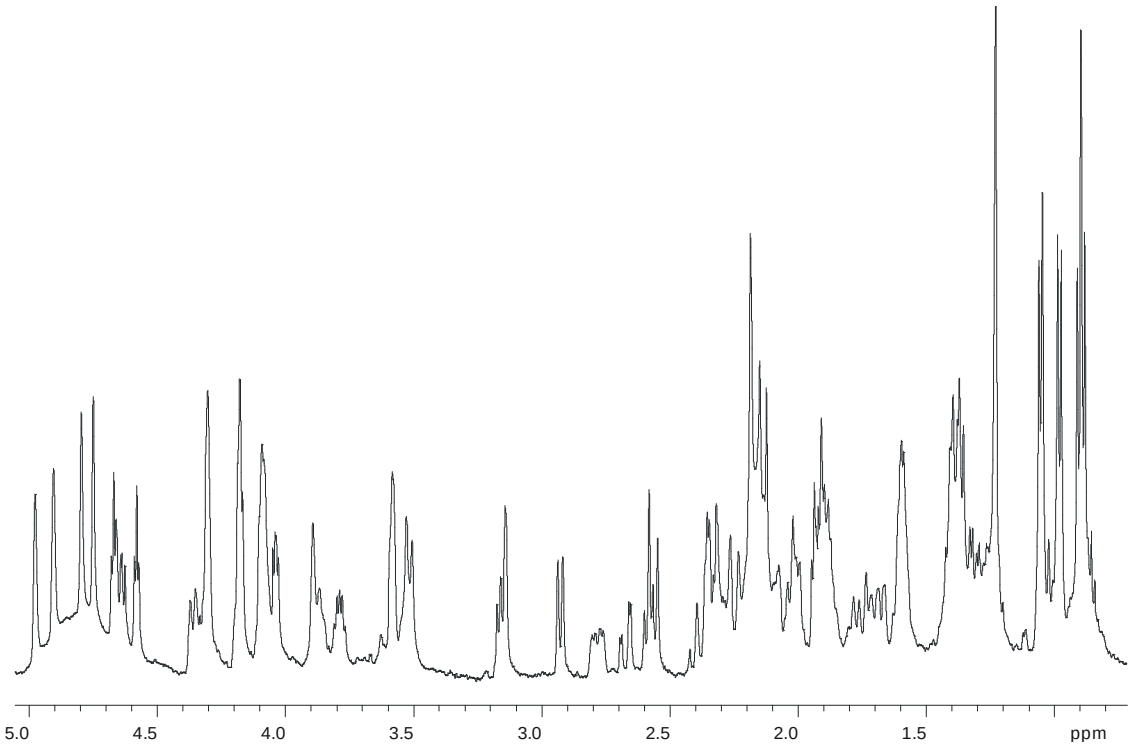

Figure 3.5.1 The ^{1}H NMR spectrum of SH3 118.2 (**3.15**)

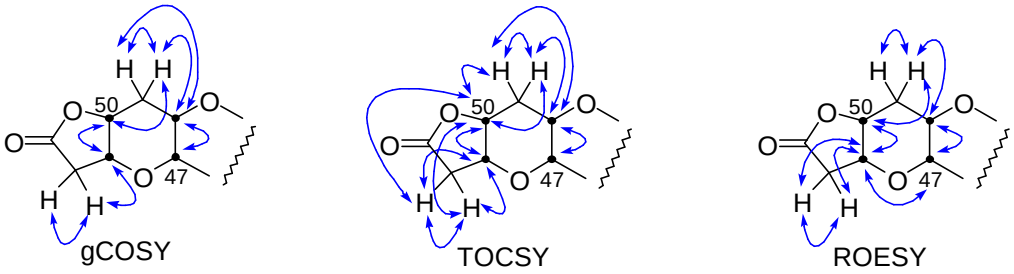

Figure 3.5.2 gCOSY, TOCSY and selected ROESY correlations for the C47-C52 region of SH3 118.2 (**3.15**)

Unfortunately, H51 (ŭ 4.18) was very close to H10 (ŭ 4.17) in the ^{1}H NMR spectrum, so it was not possible to confirm *cis* relative stereochemistry from the observance of a small coupling constant as was the case for SH3 116.2 (**3.13**). However, observed ROESY correlations (Fig. 3.5.2) indicated stereochemistry as shown above (**3.15**), which is consistent with that observed for homohalichondrin B (**3.2**).

3.6 Structure elucidation of SH3 118.3 (3.16)

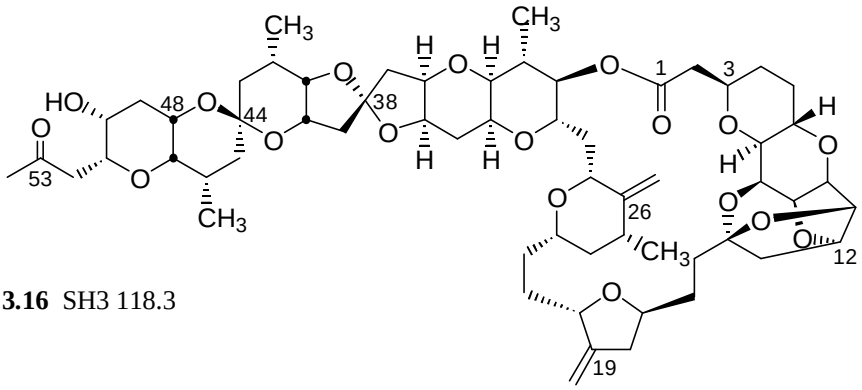

3.16 SH3 118.3

SH3 118.3 (**3.16**) was the third least polar of the five new halichondrin derivatives (Fig. 3.3.1). High-resolution LCMS (*m/z* 1115.5530 $[M+Na]^+$, φ = -2.5 mmu), in combination with NMR data (Table 3.6.1), gave the molecular formula $C_{60}H_{84}O_{18}$ (19 double bond equivalents). This is 30 mass units less than that observed for isohomohalichondrin B (**3.3**), corresponding to the loss of CH_2O from the side chain from carbon 55. The NMR assignments were confirmed by gCOSY, TOCSY, ROESY and HSQC 2D experiments, in addition to comparisons with the known NMR shifts for isohomohalichondrin B. Due to the small sample size, no ^{13}C NMR spectrum was obtained. The ^{13}C data reported in Table 3.6.1 were obtained from the HSQC experiment. The ^{1}H NMR spectrum is shown in Figure 3.6.1.

Again, overlaying of the HSQC spectra with those of known halichondrins was used in the structure elucidation of this molecule. The observed ^{1}H and ^{13}C NMR shifts for SH3 118.3 (**3.16**) showed excellent agreement with those of isohomohalichondrin B (**3.3**) up to position 50, and had similar chemical shifts at position 51 (Table 3.5.1). This left one methyl and one methylene unassigned from the HSQC spectrum. The connectivity of this portion of the molecule was established *via* gCOSY and TOCSY data, and the relative stereochemistry was confirmed to be the same as that observed for isohomohalichondrin B *via* ROESY correlations (Fig. 3.6.2).

Table 3.6.1 ^{1}H and ^{13}C NMR chemical shift data for isohomohalichondrin B (**3.3**) and SH3 118.3 (**3.16**)[a]

	isohomohalichondrin B		SH3 118.3	
position	C	H	C[b]	H
1	171.1		*c*	
2	40.4	2.36, 2.61	40.4	2.34, 2.59
3	73.6	3.89	73.6	3.87
4	30.6	1.38, 1.75	30.6	1.36, 1.74
5	30.0	1.41, 2.12	30.0	1.37, 2.08
6	68.2	4.35	68.2	4.32
7	77.6	2.95	77.6	2.93
8	74.3	4.33	74.3	4.31
9	73.8	4.06	73.8	4.04
10	76.5	4.22	76.5	4.18
11	82.1	4.60	82.2	4.58
12	81.0	4.70	81.1	4.66
13	48.3	1.95, 2.16	48.3	1.94, 2.15
14	110.0		*c*	
15	34.4	1.62, 2.18	34.4	1.61, 2.18
16	28.1	1.42, 2.18	28.0	1.42, 2.15
17	75.3	4.10	75.3	4.09
18	38.7	2.27, 2.80	38.7	2.25, 2.78
19	151.7		*c*	
19=CH2	104.4	4.93, 5.01	*c*	4.91, 4.98
20	75.3	4.39	75.3	4.36
21	29.3	1.42, 1.90	29.4	1.39, 1.86
22	32.0	1.62, 1.62	32.0	1.60, 1.60
23	74.8	3.55	74.8	3.53
24	43.3	1.05, 1.72	43.3	1.04, 1.70
25	35.9	2.23	35.9	2.21
25-Me	18.0	1.07	17.9	1.06
26	151.5		*c*	
26=CH2	104.1	4.78, 4.83	*c*	4.76, 4.80
27	73.5	3.56	73.6	3.53
28	36.9	1.95, 2.01	36.8	1.92, 2.01
29	71.1	4.22	71.2	4.19
30	77.2	4.66	76.9	4.64
31	36.5	2.03	36.5	2.02
31-Me	15.0	1.00	15.0	0.99
32	77.5	3.20	77.4	3.17
33	66.4	3.84	66.3	3.80
34	29.0	1.81, 2.16	29.0	1.80, 2.13
35	75.1	4.12	75.3	4.09
36	76.2	4.12	76.2	4.09
37	43.3	1.92, 2.37	43.5	1.90, 2.33
38	112.4		*c*	
39	42.5	2.22, 2.22	42.6	2.21, 2.21
40	71.2	3.94	71.1	3.91
41	79.0	3.64	79.1	3.61
42	25.7	2.29	25.7	2.28
42-Me	17.5	0.95	17.5	0.93
43	36.9	1.33, 1.55	36.9	1.33, 1.52
44	97.2		*c*	
45	37.2	1.49, 1.52	37.1	1.43, 1.48
46	28.6	2.18	28.6	2.15
46-Me	16.8	0.90	16.8	0.89
47	75.9	3.25	76.0	3.22
48	66.4	3.75	66.4	3.72
49	34.4	1.84, 2.13	34.4	1.83, 2.10
50	66.4	3.52	66.4	3.49
51	76.4	3.82	76.3	3.77
52	45.2	2.62, 2.93	45.7	2.59, 2.72
53	209.5		*c*	
54	46.1	2.74, 2.74	31.1	2.18
55	57.8	3.86, 3.86		

[a] Values in ppm relative to C**H**Cl_3 (ŭ 7.25) and **C**DCl_3 (ŭ 77.0). [b] Values obtained from HSQC spectrum. [c] Values not detected.

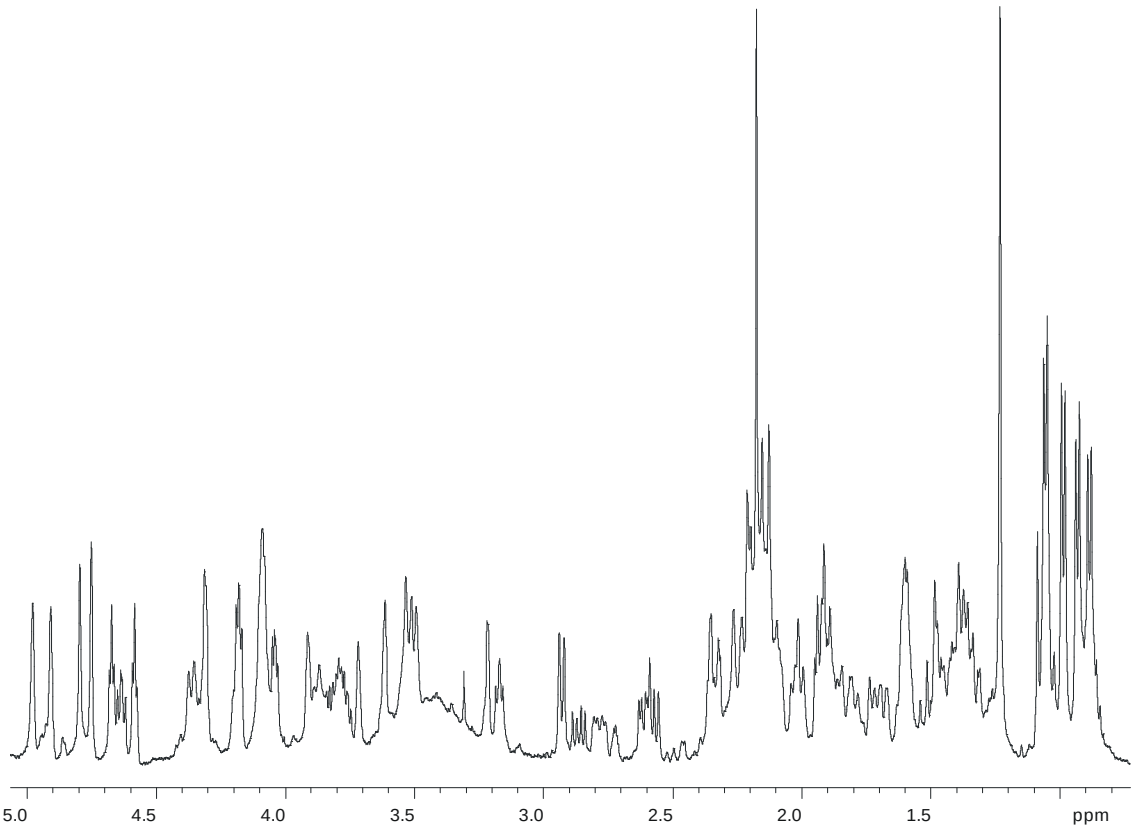

Figure 3.6.1 The ^{1}H NMR spectrum of SH3 118.3 (**3.16**)

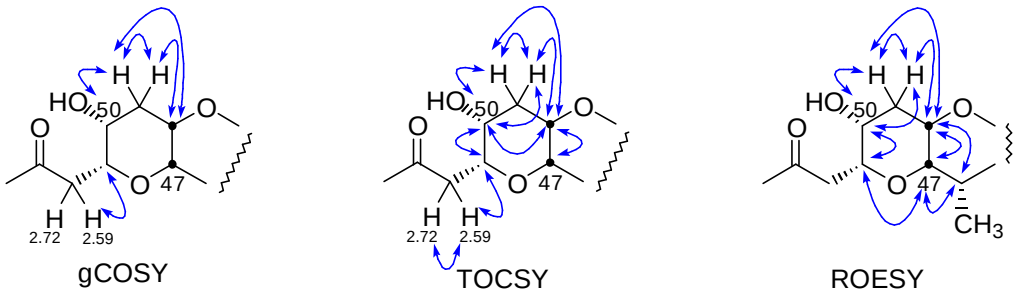

Figure 3.6.2 gCOSY, TOCSY correlations for the C47-C54 region and selected ROESY correlations for the C46-C54 region of SH3 118.3 (**3.16**)

3.7 Structure elucidation of SH3 118.4 (3.17)

The structure of SH3 118.4 has not yet been determined. SH3 118.4 (**3.17**) was the least polar of the five new halichondrin derivatives (Fig. 3.3.1). High-resolution LCMS gave the most likely molecular formulae as $C_{61}H_{86}O_{18}$ (19 double bond equivalents) or $C_{60}H_{82}O_{19}$ (20 double bond equivalents). gCOSY, TOCSY, ROESY, HSQC and CIGAR 2D NMR experiments were run. Due to the small sample size, no ^{13}C NMR spectrum was obtained. The ^{13}C data reported in Table 3.7.1 were obtained from the HSQC and CIGAR experiments. The ^{1}H NMR spectrum is shown in Figure 3.7.1.

The NMR data indicated a similarity to halichondrin B (**3.2**) up to C48 (Table 3.7.1), however the connectivity of the molecule beyond this position has yet to be established.

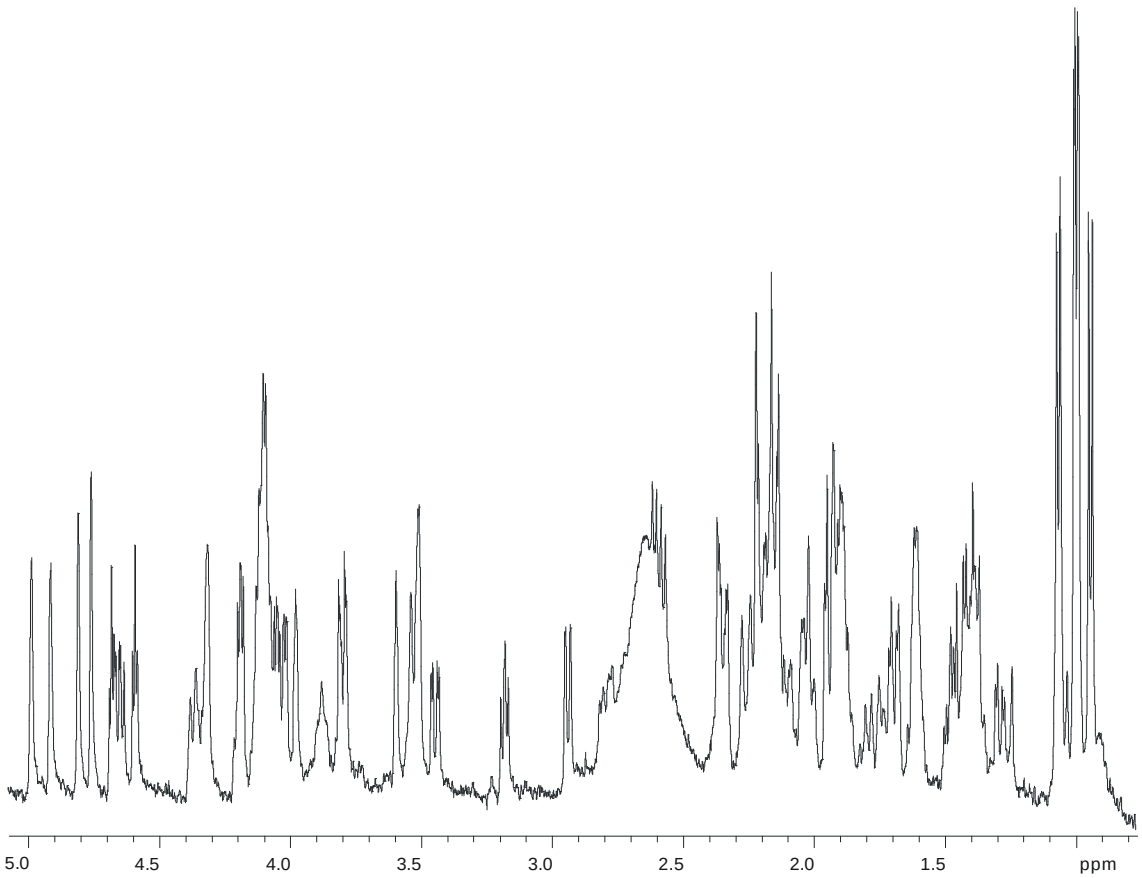

Figure 3.7.1 The ^{1}H NMR spectrum of SH3 118.4 (**3.17**)

Table 3.7.1 ^{1}H and ^{13}C NMR chemical shift data for halichondrin B (**3.2**) & SH3 118.4 (**3.17**) up to C48[a]

	halichondrin B		SH3 118.4	
position	C	H	C[b]	H
1	171.2		*c*	
2	40.4	2.35, 2.60	40.4	2.33, 2.59
3	73.7	3.86	73.8	3.88
4	30.7	1.37, 1.75	30.7	1.37, 1.72
5	30.0	1.35, 2.08	30.0	1.35, 2.09
6	68.2	4.34	68.2	4.32
7	77.7	2.94	77.7	2.94
8	74.3	4.33	74.3	4.32
9	73.8	4.04	73.8	4.04
10	76.5	4.20	76.5	4.19
11	82.1	4.60	82.2	4.59
12	81.1	4.68	81.0	4.68
13	48.3	1.94, 2.15	48.4	1.95, 2.14
14	110.1		*c*	
15	34.4	1.62, 2.18	34.5	1.57, 2.16
16	28.2	1.42, 2.16	28.2	1.42, 2.16
17	75.5	4.10	75.4	4.10
18	38.7	2.26, 2.80	38.6	2.25, 2.79
19	151.8		*c*	
19=CH2	104.4	4.92, 4.98	*c*	4.91, 4.99
20	75.4	4.37	75.4	4.37
21	29.5	1.40, 1.88	29.6	1.40, 1.87
22	32.0	1.60, 1.60	32.0	1.60, 1.60
23	74.9	3.53	74.9	3.54
24	43.4	1.04, 1.70	43.4	1.04, 1.67
25	35.9	2.20	36.0	2.20
25-Me	18.0	1.07	18.0	1.06
26	151.6		151.7	
26=CH2	104.2	4.77, 4.81	*c*	4.76, 4.81
27	73.5	3.54	73.6	3.52
28	36.9	1.94, 2.02	36.8	1.92, 2.00
29	71.2	4.21	71.2	4.19
30	76.9	4.63	77.0	4.65
31	36.6	2.04	36.3	2.04
31-Me	15.1	0.99	15.0	0.99
32	77.5	3.18	77.5	3.18
33	66.3	3.80	66.5	3.80
34	29.1	1.79, 2.13	29.0	1.78, 2.13
35	75.0	4.10	75.1	4.10
36	76.2	4.10	76.3	4.10
37	43.5	1.92, 2.35	43.5	1.92, 2.35
38	112.5		*c*	
39	42.7	2.24, 2.24	42.7	2.22, 2.22
40	71.7	4.00	71.3	3.98
41	79.0	3.63	79.2	3.59
42	25.6	2.23	25.7	2.24
42-Me	17.6	0.94	17.6	0.94
43	36.6	1.29, 1.52	36.8	1.29, 1.45
44	97.5		*c*	
45	36.9	1.42, 1.50	37.0	1.39, 1.48
46	25.7	2.35	25.4	2.36
46-Me	17.8	0.99	17.7	0.99
47	80.2	3.61	80.2	3.51
48	71.7	4.05	71.8	4.02
49	35.9	1.9, 2.32		
50	79.8	4.08		
51	73.0	3.80		
52	37.2	1.62, 1.79		
53	70.4	4.02		
54	66.9	3.54, 3.61		

[a] Values in ppm relative to C**H**Cl_3 (ŭ 7.25) and **C**DCl_3 (ŭ 77.0). [b] Values obtained from HSQC spectrum. [c] Values not detected.

3.8 Summary

The structures of four new halichondrins have been determined. All of these compounds are very similar to known B series halichondrins, with differences occurring only beyond carbon 48. As biological activity has been shown to be derived from the region of the molecule between carbons 1 and 30, they all retain good activity in the P388 assay as expected.

CHAPTER 4. Marine siderophores.

4.1 Introduction

Most micro-organisms require iron for growth,[86] yet iron is present at very low concentrations (0.02 ï 1 nM) throughout much of the worldôs surface ocean waters.[65,87] These low levels of iron have been shown to limit the growth of many micro-organisms.[88] In order to acquire iron, many aerobic bacteria produce siderophores, which are high-affinity iron(III)-binding ligands that facilitate Fe(III) transport into the bacterium.[89] While the structures of hundreds of terrestrial siderophores are known, relatively few structures of siderophores produced by marine bacteria have been elucidated.[65] A number of siderophores containing the 2,3-dihydroxybenzoate moiety, which functions in Fe(III) coordination, have been reported. However, until the recent discovery of petrobactin (**4.1**),[67,68] no examples with 3,4-dihydroxy substitution had been published. In contrast to a plethora of reported aliphatic sulfonates,[90] sulfonation of the aromatic groups is also rare in the natural product literature. The known sulfonated aromatic natural products are siderophores derived from either a terrestrial *Pseudomonad,*[91,92] or a marine *Psuedoalteromonad*[69] species (e.g. **1.20**).

Crude oil is one of the most significant organic pollutants in the marine environment. Many compounds in crude oil are, however, biodegradable, and this observation has led to the study of oil-degrading marine micro-organisms. *Marinobacter hydrocarbonoclasticus*, initially isolated from an oil slick on the French Mediterranean coast,[93,94] is an ubiquitous marine bacterium[95,96] that grows on a variety of hydrocarbons as its sole carbon source.

In this section of work, the structural characterisation of a new siderophore, petrobactin sulfonate (**4.2**),[97] isolated from the oil-degrading marine bacterium *Marinobacter hydrocarbonoclasticus* will be presented. Petrobactin sulfonate is, to our knowledge, the first marine-derived siderophore containing a sulfonated 3,4-dihydroxy aromatic ring. In addition, a revision of the NMR assignments of petrobactin will be discussed, along with the structural characterisation of the cyclic imide of petrobactin (**4.3**) and the two cyclic imides of petrobactin sulfonate (**4.4** and **4.5**). These compounds are summarised in Table 4.1.1.

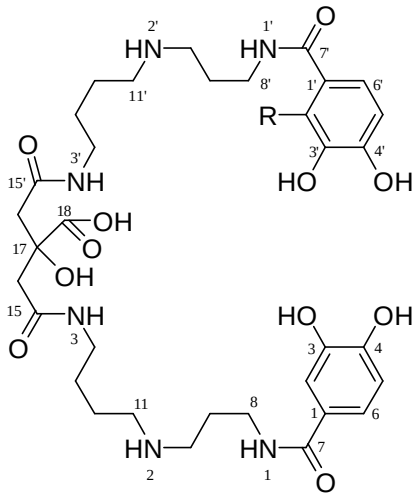

4.1 R = H petrobactin
4.2 R = SO_3H petrobactin sulfonate

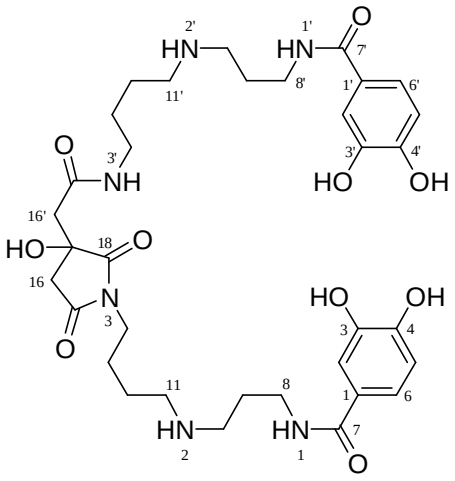

4.3 petrobactin cyclic imide

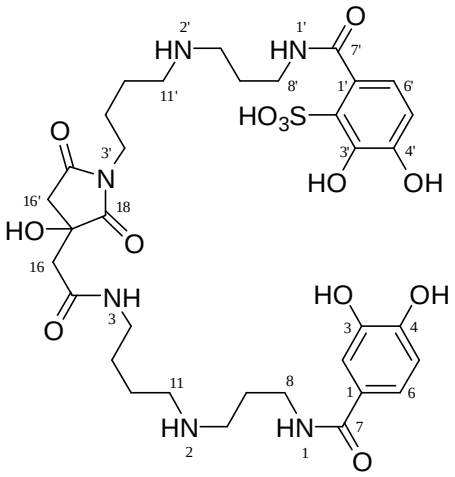

4.4 petrobactin sulfonate cyclic imide 1

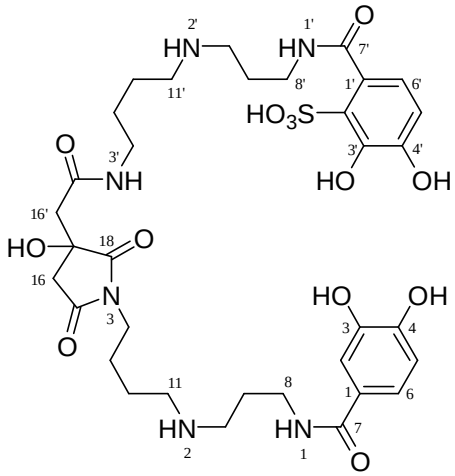

4.5 petrobactin sulfonate cyclic imide 2

Table 4.1.1 Molecular formulae and calculated masses of compounds **4.1 - 4.5**

Compound	**Number**	**Molecular formula**	**Calc. $[M + H]^+$**
petrobactin	**4.1**	$C_{34}H_{50}N_6O_{11}$	**719.3616**
petrobactin sulfonate	**4.2**	$C_{34}H_{50}N_6O_{14}S$	**799.3184**
petrobactin cyclic imide	**4.3**	$C_{34}H_{48}N_6O_{10}$	**701.3510**
petrobactin sulfonate cyclic imides	**4.4 / 4.5**	$C_{34}H_{48}N_6O_{13}S$	**781.3078**

4.2 Isolation and characterisation of petrobactin sulfonate (4.2)

The siderophores produced in the culture of *Marinobacter hydrocarbonoclasticus* were isolated by adsorption to Amberlite XAD-2 resin after acidifying the culture medium to pH 2.5-3 and removing the bacterial cells by centrifugation. Elution from the resin was achieved using 100% methanol. Preparative-scale reversed-phase HPLC of this methanol fraction resulted in the isolation of the known petrobactin (**4.1**)[67,68] and the new compound petrobactin sulfonate (**4.2**),[97] with typical yields of 1.2 mg and 0.55 mg per litre of culture medium, respectively. This culture and isolation work was done by Frithjof Küpper, a Post Doctoral research fellow in the Butler group at UCSB.

High resolution electrospray mass spectrometry (*m/z* 799.3199 $[M + H]^+$, φ = +1.5 mmu), in combination with ^1H and ^{13}C NMR data (Table 4.2.1, and Figures 4.2.1 and 4.2.2, respectively), gave the molecular formula $C_{34}H_{50}N_6O_{14}S$ (13 double bond equivalents). The presence of sulfur was confirmed by elemental analysis. More significantly, a mass difference of 80 Da from the $[M + H]^+$ molecular ion of petrobactin (HRFABMS *m/z* 719.3614)[67] suggested the addition of a sulfonate group. Further evidence supporting the presence of a sulfonate group was obtained from tandem ESI-MS in negative ion mode, considering the species at *m/z* 797.2. At a collision voltage of > 150 V, a peak of *m/z* 79.9, attributable to a sulfonate moiety, was observed.

The ^1H and ^{13}C NMR assignments for petrobactin sulfonate (**4.2**) were confirmed by gCOSY (Fig. 4.2.3), HSQC (Fig. 4.2.4), gHMBC (Fig. 4.2.5) and CIGAR (Fig. 4.2.6) 2D experiments (Table 4.2.1). The splitting patterns observed in the aromatic region of the ^1H NMR spectrum were indicative of the unusual 3,4-dihydroxybenzoyl moiety, a functionality unique to petrobactin (**4.1**) and petrobactin sulfonate (**4.2**) in the marine siderophore literature. The presence of a single correlation for one of the aromatic rings in the gCOSY experiment, from H5 (δ 6.76) to H6 (δ 7.18), also supported 3,4-disubstitution. It was not possible to see the equivalent correlation from the other aromatic ring in this experiment, due to the closeness in chemical shift of the H5' (δ 6.76) and H6' (δ 6.72) protons. All correlations observed in the gHMBC and CIGAR experiments in the aromatic region were consistent with the presence of two catechol rings, including two $^4J_{CH}$ correlations, from H6 (δ 7.18) to C3 (δ 144.9) and H6' (δ 6.72) to C3' (δ 142.3), in the CIGAR experiment. No evidence to differentiate the hydroxyl

protons at the 3, 4 and 4' positions was obtained (δ 9.12, 9.16 and 9.54, respectively), however the 3'-OH proton was able to be assigned at 11.23 ppm, due to observed correlations in the gHMBC and CIGAR experiments to C2' (δ 127.0), C3' (δ 142.3) and C4' (δ 147.2).

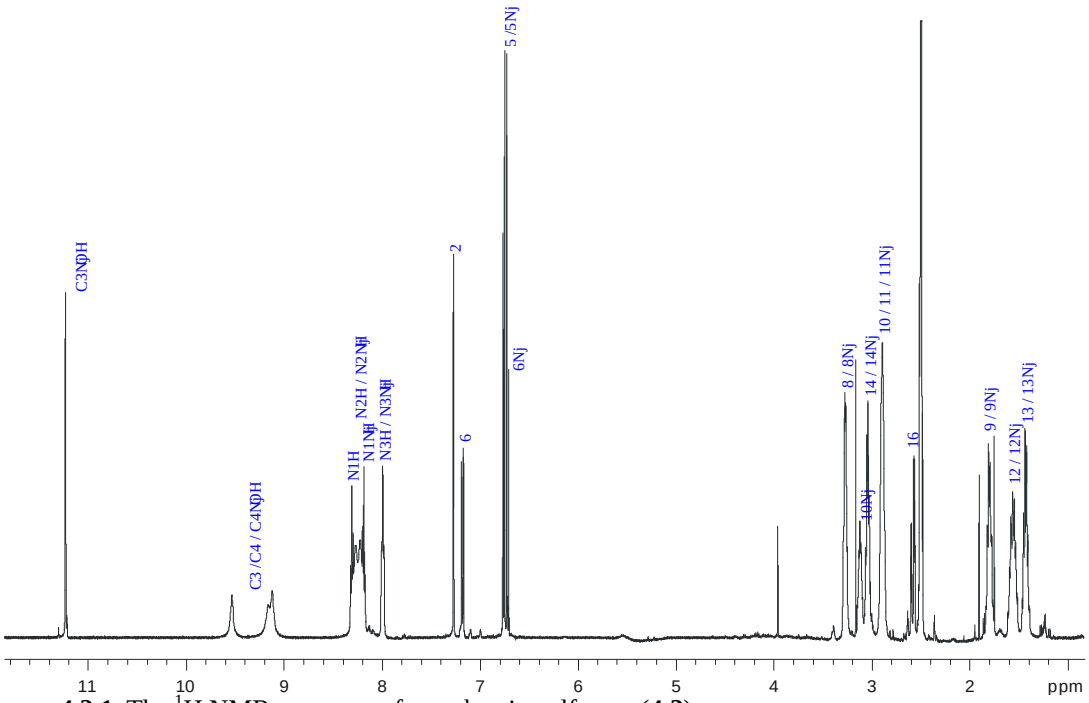

Figure 4.2.1 The ^{1}H NMR spectrum of petrobactin sulfonate (**4.2**)

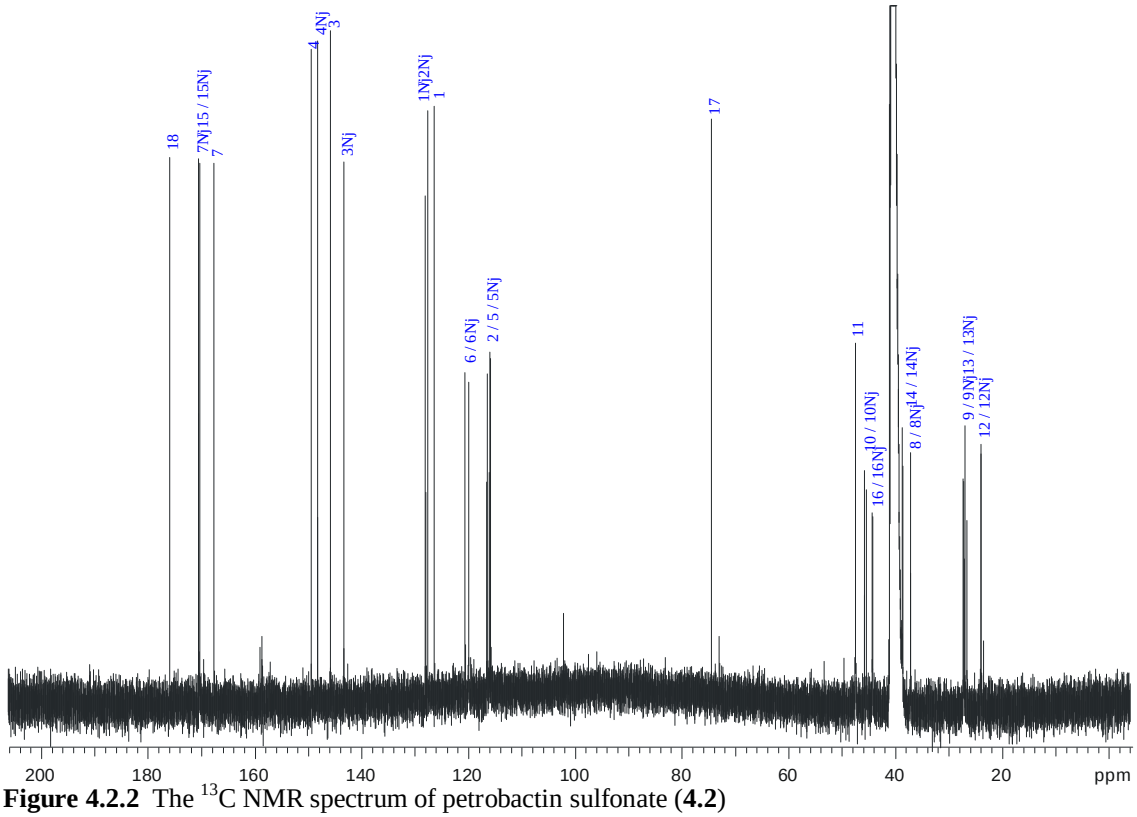

Figure 4.2.2 The ^{13}C NMR spectrum of petrobactin sulfonate (**4.2**)

Table 4.2.1 ^{1}H, ^{13}C and 2D NMR data for Petrobactin sulfonate (**4.2**)[a]

position	ŭ$_H$ mult (*J* in Hz)	ŭ$_C$	gCOSY	HSQC	gHMBC and CIGAR[b]
1	na	125.4			
1'	na	126.6			
2	7.27 d (2)	115.0		C2	C1 (wk), C3, C4, C6, C7
2'	na	127.0			
3	na	144.9			
3'	na	142.3			
4	na	148.5			
4'	na	147.2			
5	6.76 d (8.5)	114.8	H6	C5	C1, C2 (wk),[c] C3, C4, C7
5'	6.76 d (8.5)	115.5		C5'	C1', C3', C4', C7'[c]
6	7.18 dd (2, 8.5)	119.0	H5	C6	C2, C3 (wk),[c] C4 (wk),[c] C7
6'	6.72 d (8.5)	119.6		C6'	C2', C3', C4', C7'
7	na	166.6			
7'	na	169.3			
8 / 8'	3.27 m	36.1, 36.2	H9/H9', N1H/N1'H	C8 / C8'	C7/C7', C9/C9', C10/C10'
9	1.80 m	26.3	H8, H10	C9	C8, C10
9'	1.80 m	25.6	H8', H10'	C9'	C8', C10'
10	2.89 m	44.8	H9, N2H	C10	C8 (wk)[c]
10'	3.12 m	44.4	H9', N2'H	C10'	C8',[c] C9'[d]
11 / 11'	2.89 m	46.5	H12/H12', N2H/N2'H	C11/C11'	C13/C13' (wk)[c]
12 / 12'	1.56 m	23.0	H11/H11', H13/H13'	C12/C12'	C11/C11',[d] C13/C13',[d] C14/C14' (wk)
13 / 13'	1.43 m	26.0	H12/H12',H14/H14'	C13/C13'	C11/C11', C12/C12',[d] C14/C14'
14 / 14'	3.04 m	37.7	H13/H13', N3H/N3'H	C14/C14'	C12/C12', C13/C13', C15/C15'
15 / 15'	na	169.5			
16 / 16'	2.50 d (15), 2.58 d (15), 2.59 d (14.5)	43.3		C16/C16'	C15/C15', C16'/C16, C17, C18
17	na	73.5			
18	na	175.0			
N1H	8.31 t (6)	na	H8		C7, C8
N1'H	8.19 t (6)	na	H8'		C7', C8'
N2H	8.27 m	na	H10, H11		
N2'H	8.23 m	na	H10', H11'		
N3H/N3'H	7.99 t (5)	na	H14/H14'		C14/C14', C15/C15'
OH (C3')	11.23 s	na			C2', C3', C4'
OH (C3 / C4 / C4')	9.12, 9.16, 9.54 (all br s)				

[a] Values in ppm relative to $CD_3(C\mathbf{H}D_2)SO$ (ŭ 2.50) and $(\mathbf{C}D_3)_2SO$ (ŭ 39.6). [b] gHMBC and CIGAR experiments run with coupling constants optimised at 5 and 5-10 Hz, respectively. [c] Correlation only seen in the CIGAR experiment. [d] Weak correlation observed in the CIGAR experiment.

The aromatic splitting patterns in the ^{1}H NMR spectrum also indicated that the sulfonate group was attached to one of the catechol rings of the previously symmetrical petrobactin molecule. The H2 doublet (ŭ 7.27), H5 doublet (ŭ 6.76) and H6 doublet of doublets (ŭ 7.18) remained from the ^{1}H NMR spectrum of petrobactin, however these resonances integrated as one proton, two protons and one proton, respectively. Thus, the doublet at 6.76 ppm accounted for both H5 and H5'. The doublet of doublets at 7.18 ppm, assigned to H6 and due to the combination of H5 vicinal (ortho) coupling (8.5 Hz) and H2 meta coupling (2 Hz), was not seen for H6'. Instead, a 1-proton doublet, with H5' ortho coupling only (8.5 Hz), was observed for this proton (ŭ 6.72). The lack of meta coupling in this signal indicated substitution at the 2' position. In addition, no signal assignable to a proton attached to C2' was observed. Thus, it was inferred that the sulfonate was in the 2' position.

The connectivity of the molecule was determined *via* gCOSY (Fig. 4.2.3), gHMBC (Fig. 4.2.5) and CIGAR (Fig. 4.2.6) correlations (Table 4.2.1). The gCOSY experiment unequivocally established the connectivity of the two spermidinyl moieties in the molecule. In particular, gCOSY correlations from H11 (δ 2.89) and H13 (δ 1.43) to H12 (δ 1.56) and from H12 and H14 (δ 3.04) to H13 (along with the equivalent correlations to H12' and H13') required a reversal of the ^{1}H and ^{13}C assignments at the 12 and 13 positions from those previously reported for petrobactin (**4.1**).[67,68]

The attachment of each catechol ring to a spermidinyl group *via* a carbonyl group on both sides of the molecule was established through gHMBC and CIGAR correlations (Table 4.2.1, and Figures 4.2.5 and 4.2.6, respectively), including two $^{4}J_{CH}$ correlations, from H5 (δ 6.76) to C7 (δ 166.6) and H5' (δ 6.76) to C7' (δ 169.3), in the CIGAR experiment. These experiments also established the connectivity of the N3 / N3' ends of the spermidinyl groups to a single citryl moiety, as well as the connectivity of the citryl group itself.

It appears that the structure of petrobactin sulfonate (**4.2**) is in the form of a double zwitterion involving N2 and N2' and the sulfonate and carboxylate moieties. The strongest evidence for this lies in the observed chemical shifts for the N2 and N2' protons (δ 8.27 and 8.23, respectively), which are in the correct range for protons on a positively charged nitrogen in an alkyl chain (~ 6 ï 9 ppm) and significantly downfield from the expected chemical shift for protons on a neutral nitrogen atom in an alkyl chain (0.5 ï 4 ppm).[98] Further evidence is to be found in the observed proton and

carbon chemical shifts at the adjacent 10 / 10' and 11 / 11' positions (Table 4.2.1),[98,99] in the integrals of the protons attached to nitrogen in the ^{1}H NMR spectrum and in the splitting of H10' in the same spectrum (triplet of triplets, appearing as a ñquintetò).

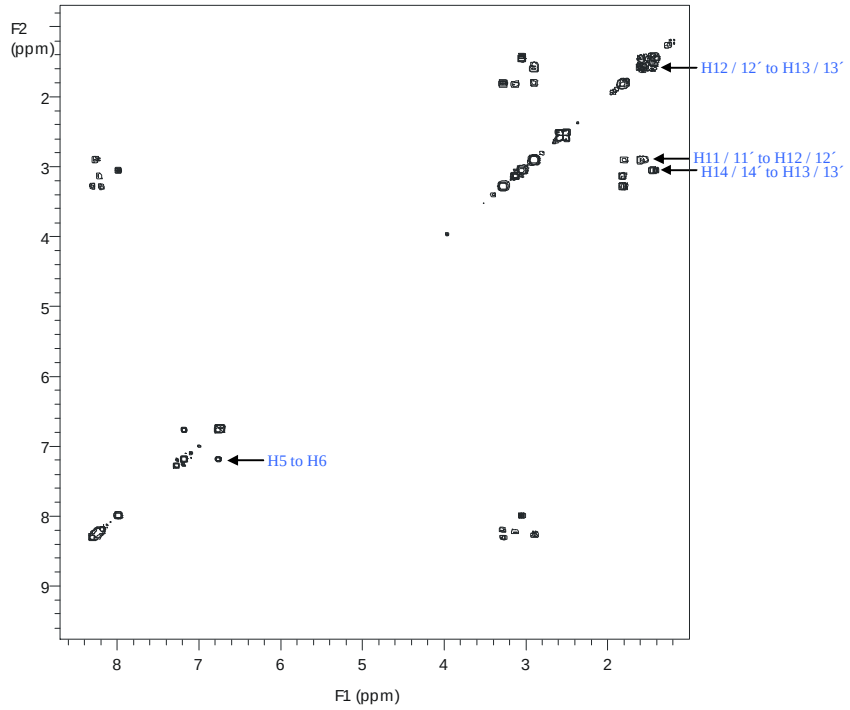

Figure 4.2.3 The gCOSY NMR spectrum of petrobactin sulfonate (**4.2**)

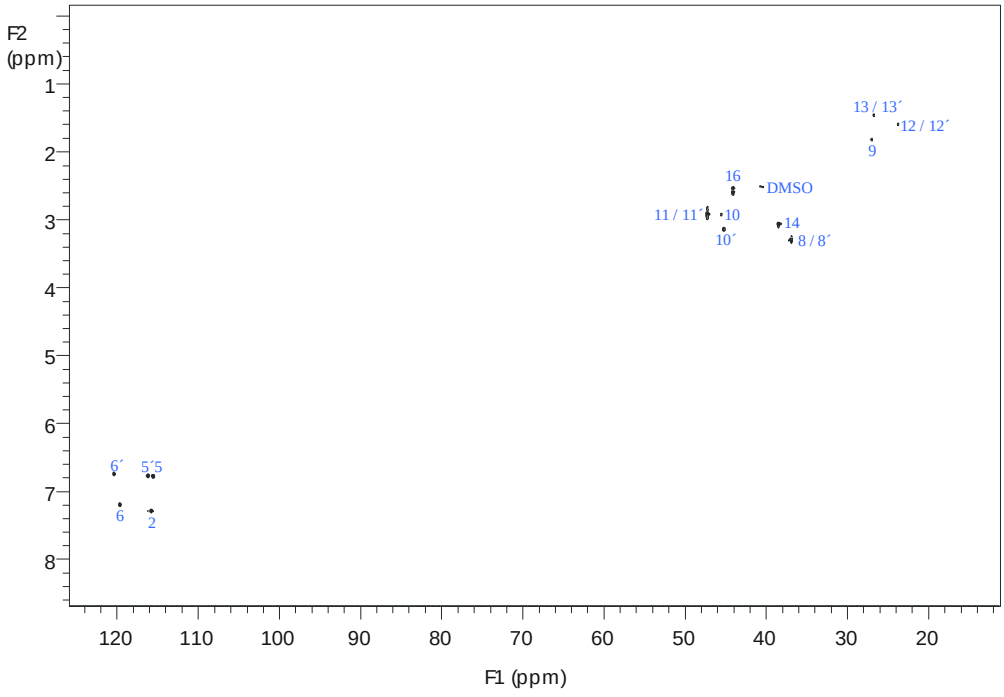

Figure 4.2.4 The HSQC NMR spectrum of petrobactin sulfonate (**4.2**)

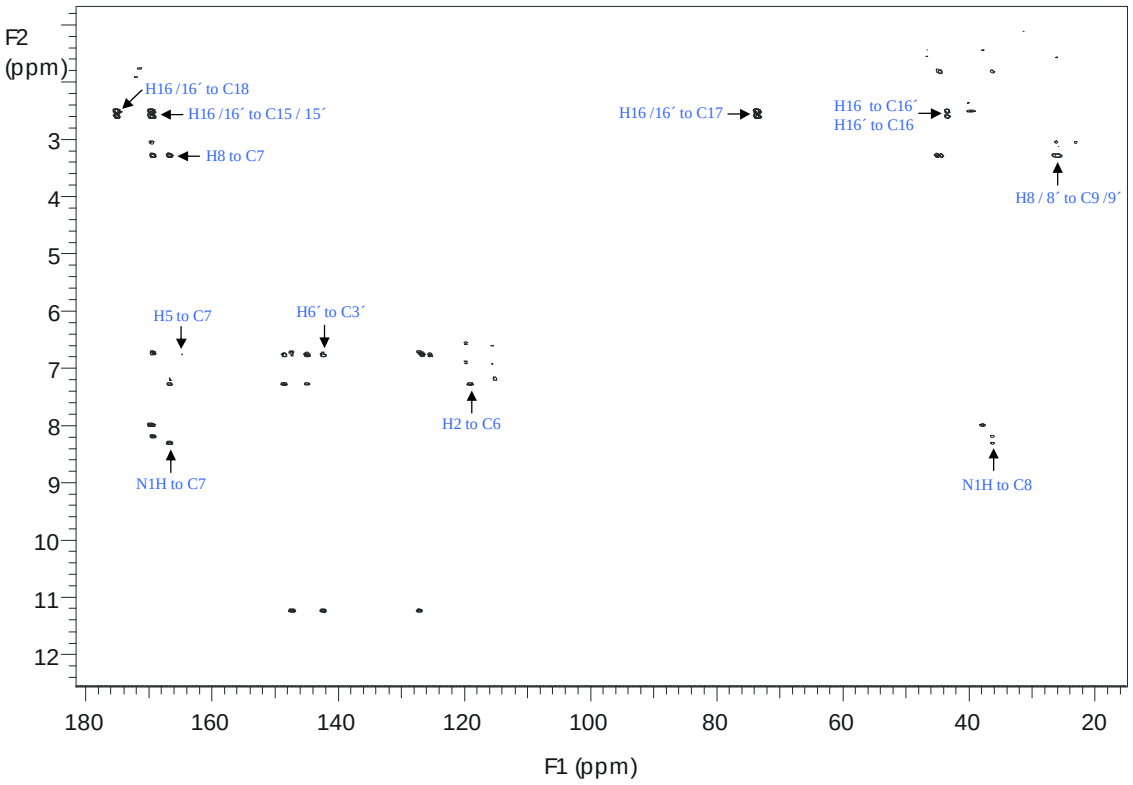

Figure 4.2.5 The gHMBC NMR spectrum of petrobactin sulfonate (**4.2**)

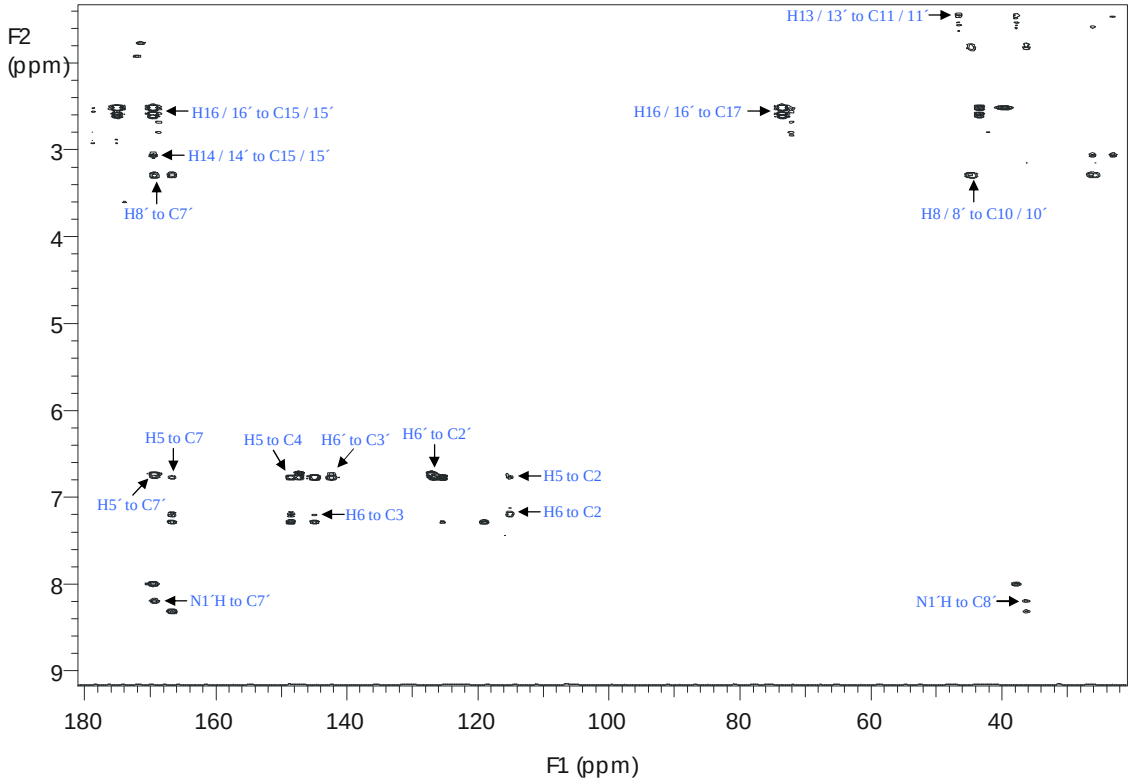

Figure 4.2.6 The CIGAR NMR spectrum of petrobactin sulfonate (**4.2**)

4.3 Revision of the NMR assignments of petrobactin (4.1)

In determining the structure of petrobactin sulfonate, observed gCOSY correlations from H11 (δ 2.89) and H13 (δ 1.43) to H12 (δ 1.56) and from H12 and H14 (δ 3.04) to H13 (along with the equivalent correlations to H12' and H13') required a reversal of the ^{1}H and ^{13}C assignments at the 12 and 13 positions from those previously reported for petrobactin (**4.1**).[67,68] In order to confirm that such a reversal should also apply in the case of petrobactin itself (see Fig. 4.3.1 for the ^{1}H NMR spectrum), a gCOSY experiment was run on a petrobactin sample (Fig. 4.3.2). In this experiment, correlations from H11 (δ 2.89) and H13 (δ 1.42) to H12 (δ 1.55) and from H12 and H14 (δ 3.04) to H13 confirmed that the previously reported ^{1}H and ^{13}C assignments at positions 12 and 13 in this molecule did in fact need to be interchanged.

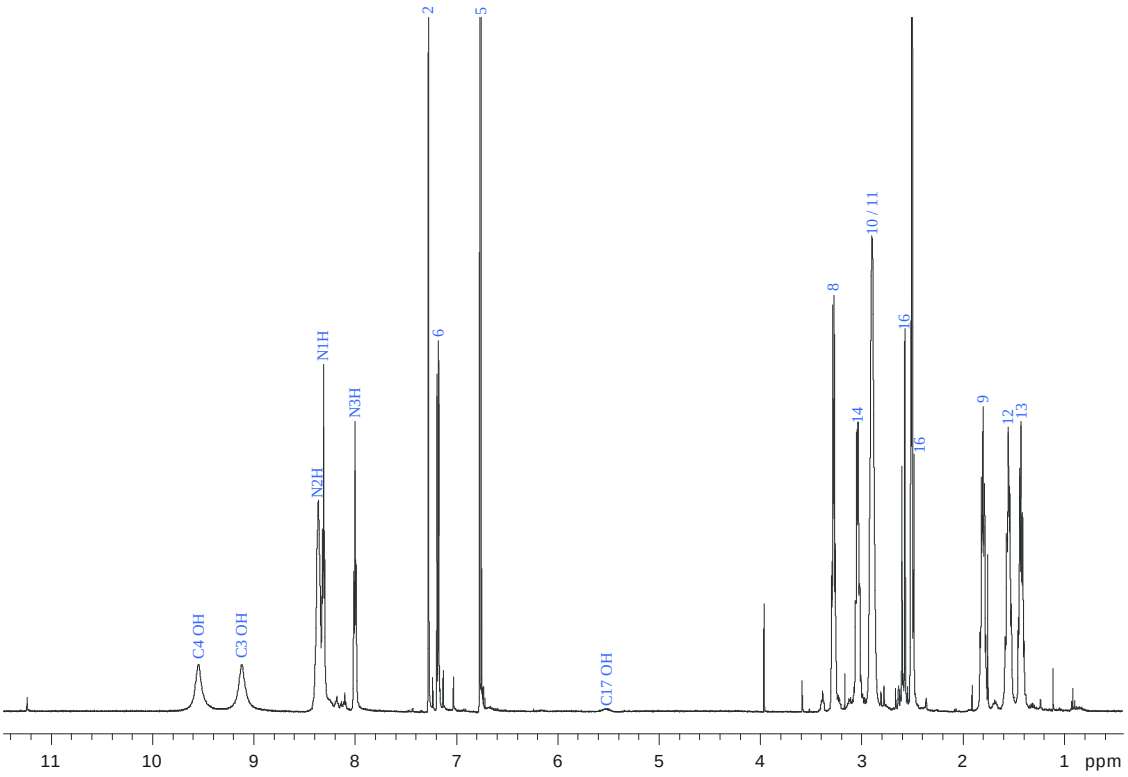

Figure 4.3.1 The ^{1}H NMR spectrum of petrobactin (**4.1**)

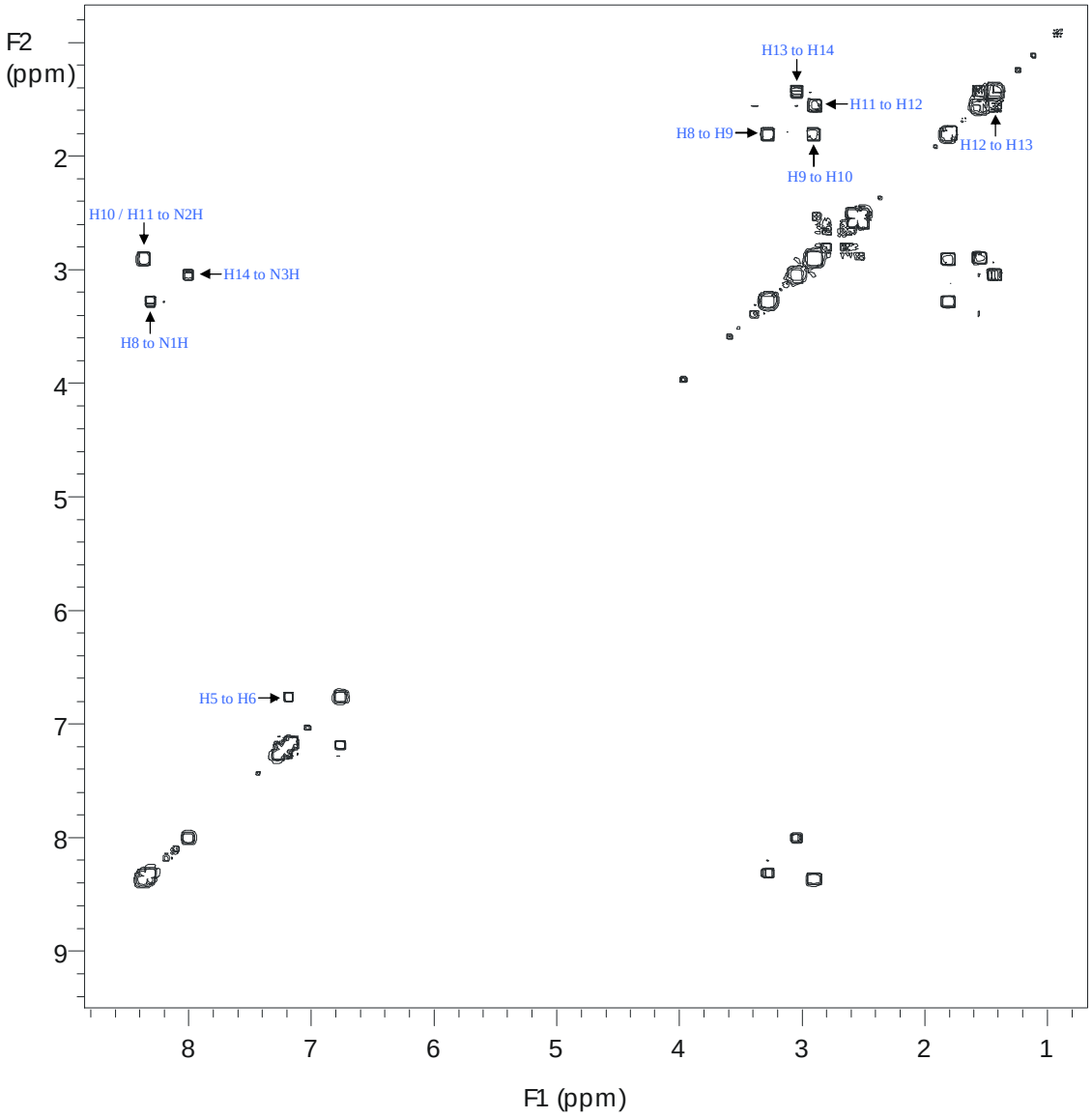

Figure 4.3.2 The gCOSY NMR spectrum of petrobactin (**4.1**)

4.4 The cyclic imide of petrobactin (4.3)

It was observed that a loss of 18 mass units occurred on exposure of petrobactin to acid. Reaction of petrobactin with 0.1% TFA gave ~10% of the dehydrated form after an hour. This compound has subsequently been established as the cyclic imide of petrobactin (**4.3**), and was isolated *via* preparative-scale reversed-phase HPLC. Analysing compound **4.3** *via* high-resolution ESIMS (*m/z* 701.3511 $[M + H]^+$, $\varphi = +0.1$ mmu), in combination with NMR data (Table 4.4.1), the molecular formula $C_{34}H_{48}N_6O_{10}$ (14 double bond equivalents) was obtained. This is 18 mass units less than that observed for petrobactin, corresponding to loss of water on formation of the cyclic imide. The NMR assignments were confirmed by gCOSY, HSQC and CIGAR 2D experiments, in addition to comparisons with the known NMR shifts for petrobactin and petrobactin sulfonate. The ^{1}H NMR spectrum is shown in Figure 4.4.1.

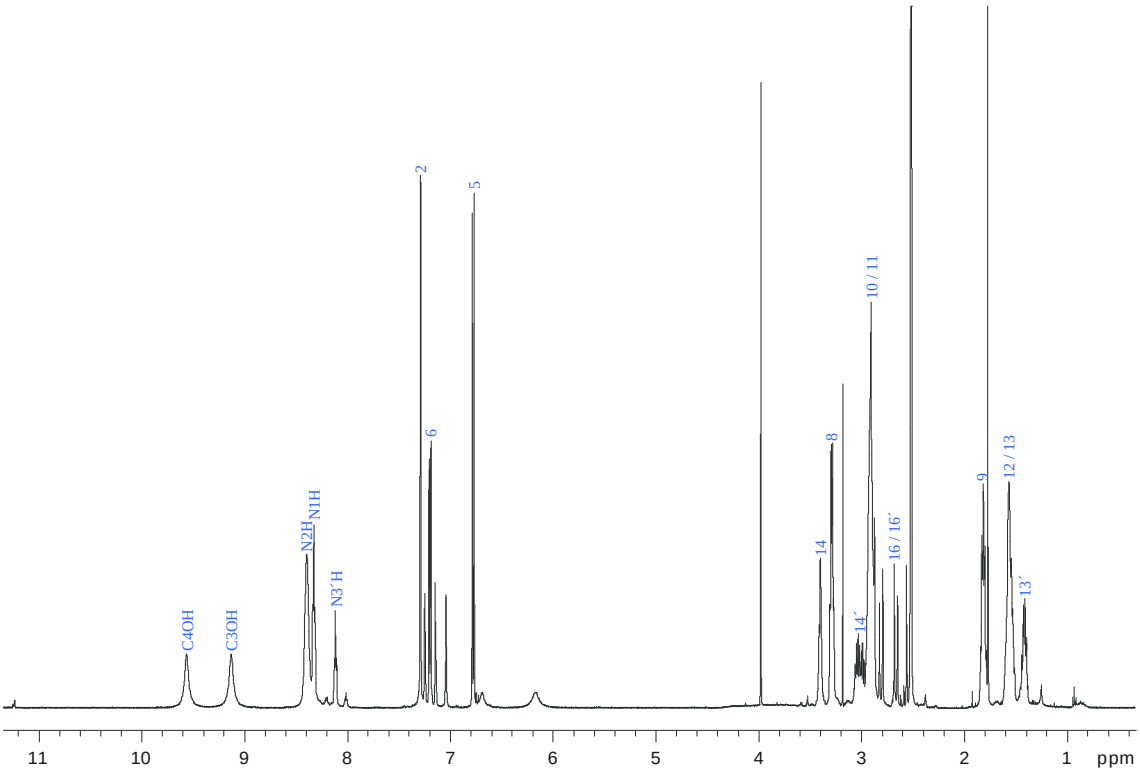

Figure 4.4.1 ^{1}H NMR spectrum of the cyclic imide of petrobactin (**4.3**)

Table 4.4.1 ^{1}H, ^{13}C and 2D NMR data for the cyclic imide of Petrobactin (**4.3**)[a]

position	ŭ$_H$ mult (*J* in Hz)	ŭ$_C$	gCOSY	HSQC	CIGAR[b]
1 / 1'	na	125.4			
2	7.27 d (2)	115.0		C2	C1, C3, C4, C6, C7
2'	7.27 d (2)	115.0		C2'	C1', C3', C4', C6', C7'
3 / 3'	na	144.9			
4 / 4'	na	148.5			
5	6.76 d (8.5)	114.8	H6	C5	C1, C3, C4, C7
5'	6.76 d (8.5)	114.8	H6'	C5'	C1', C3', C4', C7'
6	7.18 dd (2, 8.5)	119.0	H5	C6	C2, C3, C4, C5, C7
6'	7.18 dd (2, 8.5)	119.0	H5'	C6'	C2', C3', C4', C5', C7'
7 / 7'	na	166.7			
8 / 8'	3.27 m	36.1	H9/H9', N1H/N1'H	C8/C8'	C7/C7', C9/C9', C10/C10'
9 / 9'	1.80 m	26.2	H8/H8', H10/H10'	C9/C9'	C8/C8', C10/C10'
10 / 10'	2.89 m	44.8	H9/H9', N2H/N2'H	C10/C10'	
11 / 11'	2.89 m	46.3, 46.5	H12/H12', N2H/N2'H	C11/C11'	
12 / 12'	1.55 m	22.9, 23.1	H11/H11', H13'	C12/C12'	C11/C11'
13	1.55 m	24.2	H14	C13	C11
13'	1.39 m	26.0	H12', H14'	C13'	C11', C12', C14'
14	3.38 t (6.5)	37.2	H13	C14	C12, C13, C15, C18
14'	2.97 m	37.7	H13', N3'H	C14'	C12', C13', C15'
15	na	175.1			
15'	na	168.7			
16	2.53 d (15.5), 2.87 d (15.5)	42.0	H16	C16	C15, C16', C17, C18
16'	2.65 d (15.5), 2.79 d (15.5)		H16'	C16'	C15', C16, C17, C18
17	na	72.0			
18	na	178.7			
N1H	8.31 t (5)	na	H8		C7, C8
N1'H	8.31 t (5)	na	H8'		C7', C8'
N2H	8.38 m	na	H10, H11		
N2'H	8.38 m	na	H10', H11'		
N3'H	8.10 t (5.8)	na	H14'		C14', C15'
OH (C3, C3', C4, C4')	9.11, 9.55 (both br s)	na			

[a] Values in ppm relative to $CD_3(C\mathbf{H}D_2)SO$ (ŭ 2.50) and $(\mathbf{C}D_3)_2SO$ (ŭ 39.6). [b] CIGAR experiment run with coupling constants optimised at 5-10 Hz.

The observed ^{1}H NMR shifts for the cyclic imide of petrobactin (**4.3**) showed excellent agreement with those of petrobactin up to C12 / C12'. The connectivity of the remainder of the molecule was established *via* gCOSY and CIGAR data (Table 4.4.1). In the CIGAR experiment, $^{4}J_{CH}$ correlations were observed between H5 / H5' (δ 6.76) and C7 / C7' (δ 166.7), H5 / H5' (δ 6.76) and C2 / C2' (δ 7.27), and H6 / H6' (δ 7.18) & C3 / C3' (δ 144.9), as expected from the data discussed above for petrobactin sulfonate (Fig. 4.4.2). The CIGAR experiment was also used to confirm the chemical shifts of C15, C15', and C18. Correlations to C15 (δ 175.1) were observed from both H14 (δ 3.38) and H16 (δ 2.53, 2.87). Correlations to C15' (δ 168.4) were observed from both H14' (δ 2.97) and H16' (δ 2.65, 2.79). And correlations to C18 (δ 178.7) were observed from H14 (δ 3.38), H16 (δ 2.53, 2.87) and H16' (δ 2.65, 2.79). The correlation between H14 and C18 is of particular importance in corroborating the formation of the cyclic imide. The ^{1}H NMR signal for the N3' proton integrated as one proton, lending further support.

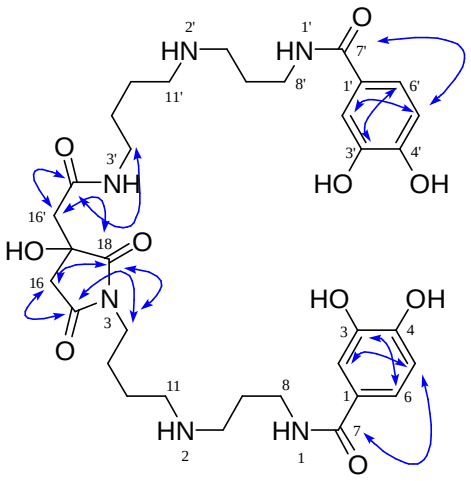

Figure 4.4.2 Selected CIGAR correlations for the cyclic imide of petrobactin (**4.3**)

The structure of the cyclic imide of petrobactin (**4.3**) appears to be in the form of a double zwitterion, as was found for petrobactin sulfonate. Again, evidence for this lies in the observed chemical shift for the N2 / N2' protons (δ 8.38), a signal which integrates as four protons, and in the observed proton and carbon chemical shifts at the adjacent 10 / 10' and 11 / 11' positions (Table 4.4.1). Unlike the situation for petrobactin sulfonate, however, all the H10 / H10' and H11 / H11' protons had the same chemical shift (δ 2.89), so no further evidence for the presence of a double zwitterion could be extracted from splitting patterns.

4.5 The cyclic imides of petrobactin sulfonate (4.4 and 4.5)

As petrobactin sulfonate is not a symmetrical molecule, exposure of this compound to acid resulted in the formation of two cyclic imides, compounds **4.4** and **4.5**. These cyclic imides were obtained by reacting petrobactin sulfonate with 0.5% formic acid for five days at 40 degrees Celsius (Fig. 4.5.1). The subsequent appearance of two later-eluting peaks was noted in the HPLC traces during this conversion (Fig. 4.5.1). These were hypothesised to be the acid derivatives **4.6** and **4.7** of the cyclic imides, but were not investigated further.

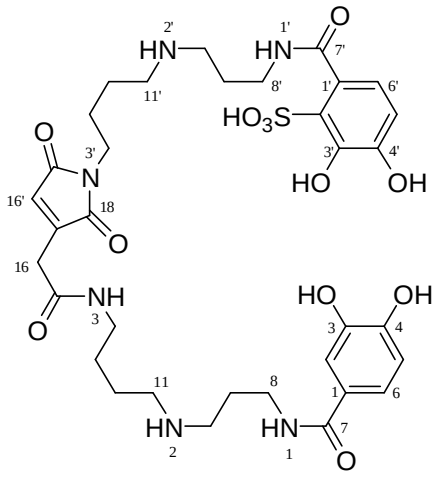

4.6 acid derivative of petrobactin sulfonate cyclic imide 1

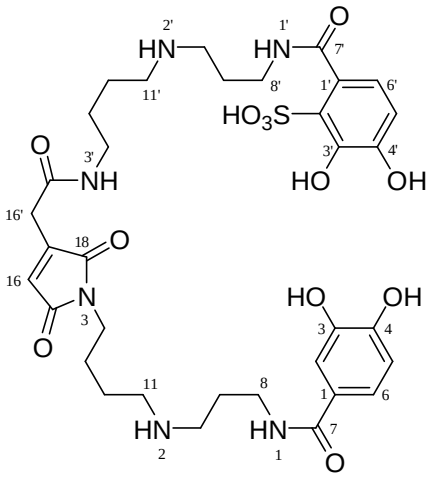

4.7 acid derivative of petrobactin sulfonate cyclic imide 2

Purification of the cyclic imides was achieved *via* preparative-scale reversed-phase HPLC. Analysing a mixture of compounds **4.4** and **4.5** *via* high-resolution ESIMS (*m/z* 781.3047 $[M + H]^+$, φ = -3.1 mmu), in combination with NMR data (Table 4.5.1), the molecular formula $C_{34}H_{48}N_6O_{13}S$ (14 double bond equivalents) was obtained. This is 18 mass units less than that observed for petrobactin sulfonate, again corresponding to loss of water on formation of the cyclic imide. The NMR assignments were confirmed by gCOSY, HSQC and CIGAR 2D experiments, in addition to comparisons with the known NMR shifts for petrobactin sulfonate. The ^{1}H NMR spectrum is shown in Figure 4.5.2. The data presented in Table 4.5.1 are reported for compound **4.5** only for the purpose of clarity.

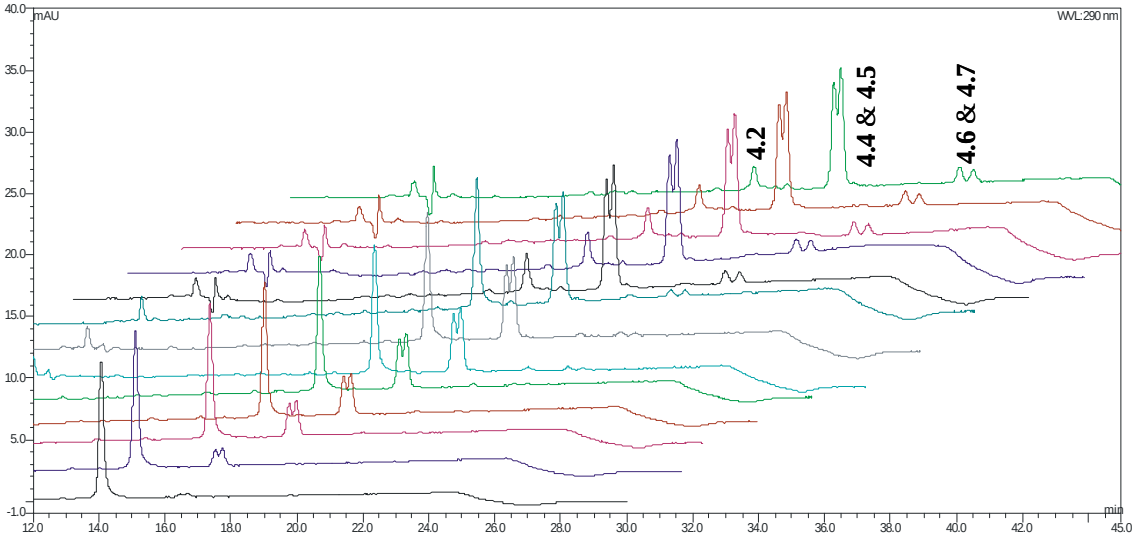

Figure 4.5.1 Stacked HPLC chromatograms recorded over eight days showing the conversion of petrobactin sulfonate (**4.2**) to its two cyclic imides (**4.4** and **4.5**), along with the subsequent conversion of the cyclic imides to their proposed acid derivatives (**4.6** and **4.7**), in the presence of acid at 40 °C. Peaks on the top trace are labelled.

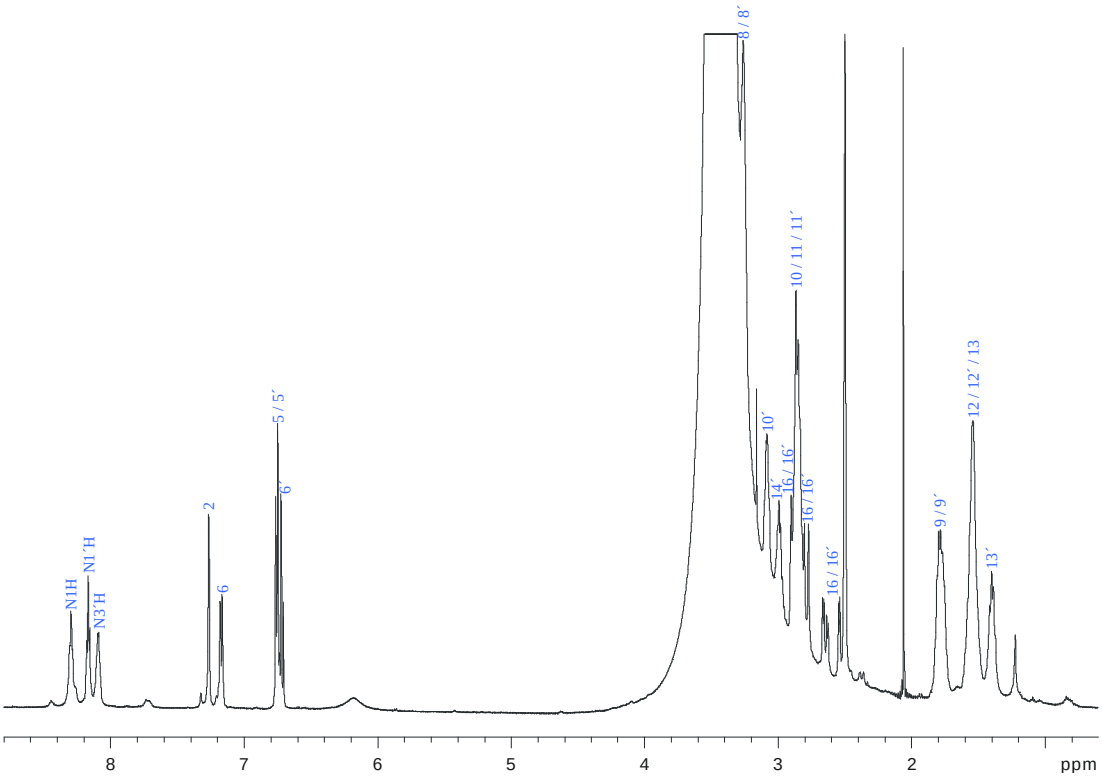

Figure 4.5.2 ^{1}H NMR spectrum of a mixture of the cyclic imides of petrobactin sulfonate (**4.4** and **4.5**)

Table 4.5.1 ^{1}H, ^{13}C and 2D NMR data for one of the cyclic imides of Petrobactin sulfonate (**4.5**)[a]

position	ŭ$_H$ mult (*J* in Hz)	ŭ$_C$	gCOSY	HSQC	CIGAR[b]
1	na	125.5			
1'	na	126.7			
2	7.26 br s	115.2		C2	C3, C4, C6, C7
2'	na	127.1		C2'	C1', C3', C4', C6', C7'
3	na	145.1			
3'	na	142.5			
4	na	148.6			
4'	na	147.4			
5	6.76 d (8)	115.0	H6	C5	C1, C3, C4
5'	6.76 d (8)	115.7		C5'	C1', C3', C4', C7'
6	7.17 br d (8.5)	119.1	H5	C6	C4, C5, C7
6'	6.71 d (8)	119.8		C6'	C2', C4', C7'
7	na	166.8			
7'	na	169.4[c]			
8 / 8'	3.26 m	36.4	H9/H9', N1H/N1'H	C8/C8'	C7/C7', C9/C9', C10/C10'
9	1.76[c] m	26.8[d]		C9	
9'	1.80[c] m	25.9[d]		C9'	
10	2.87 m	45.2[d]	H9/H9', N2H/N2'H	C10	
10'	3.08	44.7[d]		C10'	C9'
11 / 11'	2.87 m	46.7		C11/C11'	
12 / 12'	1.54 m	23.5		C12/C12'	
13	1.54 m	24.4[d]		C13	
13'	1.40 m	26.3		C13'	
14	3.39 br s	37.5[d]		C14	C13, C15, C18
14'	3.00 m	38.1		C14'	
15	na	175.2[c]			
15'	na	168.7[c]			
16	2.52 d (15), 2.53 d (15), 2.89 d (15)	42.3[d]	H16	C16	C15, C16', C17, C18
16'	2.64 d (15), 2.65 d (15), 2.79 d (15.5)	42.2[d]	H16'	C16'	C15', C16, C17, C18
17	na	72.2			
18	na	179.0			
N1H	8.30 t (5)	na	H8		C7
N1'H	8.17 t (5.5)	na	H8'		C7'
N2H/ N2'H	nd	na			
N3'H	8.10 t (4)	na	H14'		C15' (weak)

[a] Values in ppm relative to $CD_3(C\mathbf{H}D_2)SO$ (ŭ 2.50) and $(\mathbf{C}D_3)_2SO$ (ŭ 39.6). [b] CIGAR experiment run with coupling constants optimised at 5-10 Hz. [c] Chemical shift obtained from the CIGAR experiment. [d] Chemical shift obtained from the HSQC experiment.

The observed ^{1}H NMR shifts for the cyclic imides of petrobactin sulfonate (**4.4** and **4.5**) showed excellent agreement with those of petrobactin sulfonate up to C12 / C12'. The connectivity of the remainder of the molecule was established *via* gCOSY and CIGAR data (Table 4.4.2). Correlations in the CIGAR experiment to C15 (δ 175.2) were observed from both H14 (δ 3.39) and H16 (δ 2.52, 2.53, 2.89). Correlations to C15' (δ 168.4) were observed from H16' (δ 2.64, 2.65, 2.79), while correlations to C18 (δ 178.7) were observed from H14 (δ 3.39), H16 (δ 2.52, 2.53, 2.89) and H16' (δ 2.64, 2.65, 2.79). Again, the correlation between H14 and C18 is of particular importance in establishing the formation of the cyclic imide, and the ^{1}H NMR signal for the N3' proton integrated as one proton, lending further support.

As was the case for petrobactin sulfonate, due to the closeness in chemical shift it was not possible to confirm a correlation in the gCOSY experiment between the H5' (δ 6.76) and H6' (δ 6.71) protons. Although the N1 (δ 8.30), N1' (δ 8.17) and N3' (δ 8.10) protons were seen in the ^{1}H NMR spectrum, the N2 / N2' protons were not observed, presumably due to their more readily exchangeable nature.

Unfortunately, the quality of the proton and carbon spectra was not as high as that obtained for the other siderophores discussed above. This was due to a smaller sample size and possibly also that the analysis was done on a mixture of the two cyclic imides of petrobactin sulfonate, creating a slight ñblurringò effect. As a result of this, some of the ^{13}C NMR resonances were obtained from the HSQC and CIGAR experiments (Table 4.4.2). In addition, some of the splitting patterns observed for the other siderophores in the ^{1}H NMR spectra were not observed in this case. For example, a broad singlet was observed for the H2 proton (δ 7.26) instead of the expected doublet due to meta coupling across the ring, a broad doublet was observed for the H6 proton (δ 7.17) instead of the expected doublet of doublets, and a broad singlet was observed for the H14 proton (δ 3.39) instead of the expected triplet. This loss of detail carried over into the CIGAR experiment also, where only one of the previously observed $^{4}J_{CH}$ correlations was seen, between H5' (δ 6.76) and C7' (δ 166.7). However, the data obtained were still of sufficient quality to unequivocally characterise the compounds.

It is likely that these compounds are also in the form of a double zwitterion, although evidence for this lies solely in the observed proton and carbon chemical shifts at the 10 / 10' and 11 / 11' positions. As the N2 / N2' protons were not observed in the ^{1}H NMR spectrum, nothing can be deduced from an observed chemical shift or an integral.

Although a discrete signal was observed for the H10' proton (δ 3.08), downfield from the H10 / H11 / H11' resonances (δ 2.87), the splitting pattern was not clear, so nothing could be inferred about the number of protons attached to the adjacent nitrogen.

Purification of each of the petrobactin sulfonate cyclic imides was achieved *via* analytical HPLC on ODS-silica, using a CH_3CN/H_2O gradient (7% to 11%) over 20 minutes, with 0.5% formic acid and a column temperature of 26 degrees Celsius. These were stable for limited periods of time in the freezer, however unfortunately they re-equilibrated to a 1:1 mixture at room temperature (Fig. 4.5.3).

Due to the difficulty in maintaining pure samples of each of the cyclic imides of petrobactin sulfonate, a mixture of compounds **4.4** and **4.5** was analysed *via* LCMSMS in an attempt to distinguish them. The same HPLC conditions described above for the purification of the two cyclic imides were used. From an analysis of the fragmentation patterns of each peak observed in the HPLC chromatogram, it was determined that the first eluting peak was compound **4.4** and the second eluting peak was compound **4.5** (Fig. 4.5.4).

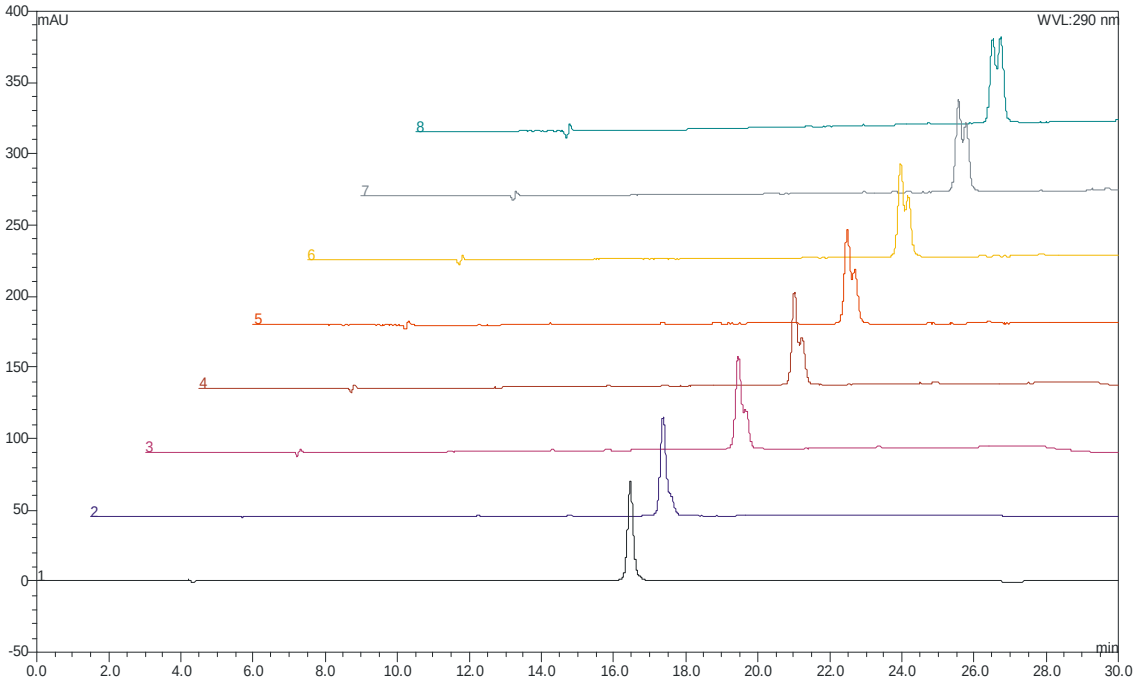

Figure 4.5.3 Stacked HPLC chromatograms recorded over seven days showing the re-equilibration of one of the petrobactin sulfonate cyclic imides (**4.4**) to a 1:1 mixture of the two cyclic imides (**4.4** and **4.5**) at 40 °C

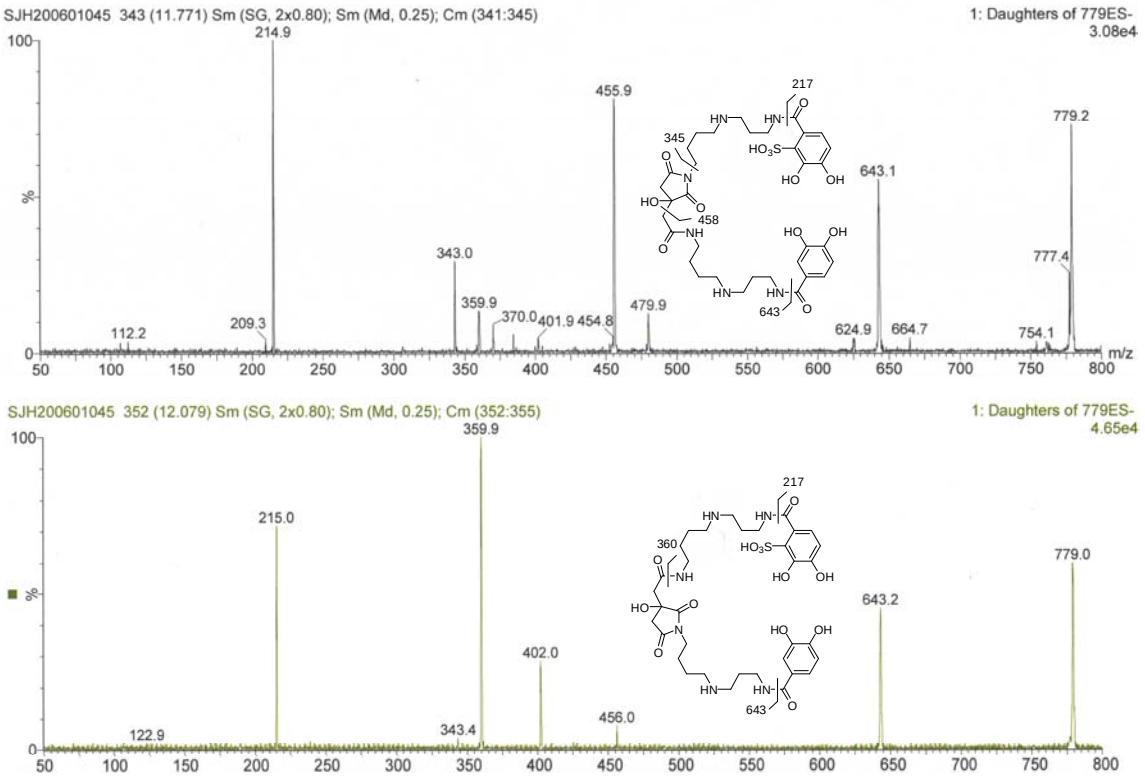

Figure 4.5.4 LCMSMS of the cyclic imides of petrobactin sulfonate (**4.4** and **4.5**), showing the fragmentation patterns that distinguished compounds **4.4** and **4.5.** The top trace is that of the first eluting cyclic imide (**4.4**) and the bottom trace that of the second eluting cyclic imide (**4.5**) on a C18 column

It is interesting to compare the signals for the H16 / H16' protons across the five siderophores discussed above. These were observed as two doublets for petrobactin, three doublets for petrobactin sulfonate, four doublets for the cyclic imide of petrobactin, and six doublets for the cyclic imides of petrobactin sulfonate. This was due to a lack of symmetry in the sulfonated siderophores.

4.6 Summary

A new sulfonated siderophore, petrobactin sulfonate (**4.2**),[97] has been isolated and characterised. Interestingly, only one of the two catecholate groups of the otherwise symmetrical molecule was sulfonated. This sulfonate functionality was unequivocally established to be vicinal to the two hydroxyl groups on one of the catecholate ring systems, as is the case for the sulfonated dihydropyoverdins.[91] The sulfonated form of petrobactin is more hydrophilic than petrobactin, which results in shorter retention times

in RP-HPLC and probably also in reduced membrane permeability. The altered physicochemical properties might also have a function in the particular environment of *Marinobacter hydrocarbonoclasticus* at the interface of seawater to oil hydrocarbons. In an analogous case, TRENCAM, a synthetic siderophore analogue containing the aromatic 2,3-dihydroxy catechol group, was rendered more water-soluble by sulfonation.[100]

In addition, a revision of the NMR assignments of petrobactin has been presented, along with the structural characterisation of the cyclic imide of petrobactin (**4.3**) and the two cyclic imides of petrobactin sulfonate (**4.4** and **4.5**). Compound **4.3** has been reported previously as an impurity in the synthesis of petrobactin.[68,101] Cyclic imide formation has also been observed in other siderophores.[102] Compounds **4.4** and **4.5** occur as a 1:1 mixture, and re-equilibrate to this from a pure sample of each. They were, however, successfully distinguished *via* tandem LCMS.

CHAPTER 5. Experimental.

5.1 General Methods

5.1.1 Nuclear Magnetic Resonance (NMR)

^{1}H, COSY, TOCSY, ROESY, HSQC, HMBC and CIGAR experiments were all recorded on a Varian INOVA 500 spectrometer at 23°C, operating at 500 MHz. The INOVA was equipped with a variable temperature and inverse-detection 5 mm probe, a triple-resonance indirect detection PFG probe for compounds **4.1**, **4.2** and **4.3,** or a 500 MHz Protasis Capillary NMR probe for spectra reported in Chapter 3. The ^{13}C NMR spectrum on the mixture of compounds **4.4** and **4.5** was recorded on a Varian UNITY 300 NMR spectrometer, at 23°C, operating at 75 MHz. The UNITY was equipped with a variable temperature direct broadband 5 mm probe. The ^{13}C NMR spectra for compounds **4.1**, **4.2** and **4.3** were recorded on a Varian INOVA 500 spectrometer at 23°C, operating at 125 MHz, using a 5mm variable temperature switchable PFG probe. Chemical shifts are expressed in parts per million (ppm) on the δ scale, and were referenced to the appropriate solvent peaks: $CDCl_3$ referenced to C**H**Cl_3 at δ_H 7.25 (^{1}H) and **C**HCl_3 at δ_C 77.0 (^{13}C); CD_3OD referenced to C**H**D_2OD at δ_H 3.31 (^{1}H) and **C**D_3OD at δ_C 49.3 (^{13}C); DMSO-d_6 referenced to CD_3(C**H**D_2)SO at δ_H 2.50 (^{1}H) and (**C**D_3)$_2$SO at δ_C 39.6 (^{13}C). The spectra in Chapter 3 were obtained in $CDCl_3$ with 0.1% C_5D_5N, in order to remove any traces of acid from the solvent.

5.1.2 Fast Atom Bombardment Mass Spectrometry

Low Resolution Fast Atom Bombardment Mass Spectrometry (LRFABMS) was recorded on a Kratos MS80 RFA Mass Spectrometer operated at 4000 V. An Ion Tech ZNIIFN ion gun was used, with Xe as the reagent gas, operating at 8 kV with an ion current of 2 mA, and using *m*-nitrobenzyl alcohol (NOBA) as the support matrix.

5.1.3 Liquid Chromatography Mass Spectrometry

High Resolution Liquid Chromatography Mass Spectra (HRLCMS) were recorded on a Waters 2790 HPLC system equipped with a Waters 996 photodiode array detector (PDA) coupled to a Micromass LCT spectrometer using a probe voltage of 3200V, an operating temperature of 150°C and a source temperature of 80°C. The carrier solvent

was 50:50 ACN/H_2O at 20 µL/minute (for direct inject mode). Typically, 10 µL of a 10 µg/mL solution was injected. Leucine enkephalin was used as the internal standard.

5.1.4 Electrospray Ionisation Mass Spectrometry

High Resolution Electrospray Ionisation Mass Spectra (HRESIMS) were recorded on a Micromass LCT spectrometer using a probe voltage of 3200V, an operating temperature of 150°C and a source temperature of 80°C. The carrier solvent was 50:50 ACN/H_2O at 20 µL/minute (for direct inject mode). Typically, 10 µL of a 10 µg/mL solution was injected. Leucine enkephalin was used as the internal standard. Electrosprayï ionization mass spectra (ESI-MS) reported in Chapter 4 were recorded in both the positive and negative modes on a Micromass (Manchester, UK) quadrupole time of flight (QTOF-2) mass spectrometer.

5.1.5 Tandem Liquid Chromatography Mass Spectrometry

Tandem Liquid Chromatography Mass Spectrometry (LCMSMS) used in the analysis of compounds **4.4** and **4.5** in Chapter 4 were performed on an LC ACQUITY UPLC® System with a Waters Quattro microÊ API mass spectrometer. An Agilent Zorbax SB-C18 column was used (5µm, 150 x 2.1 mm), with a 7 to 11% CH_3CN/H_2O gradient over 20 minutes, with 0.5% formic acid.

5.1.6 High Performance Liquid Chromatography (HPLC)

In most projects the Milli-Q® H_2O was acidified with 0.05% TFA. No TFA was used in the analyses reported in Chapter 3. All samples were filtered through 0.45 μm PTFE membrane filters immediately prior to injection.

Analytical HPLC was carried out on a Dionex liquid chromatograph equipped with a UVD 340U diode array detector, and connected to an Alltech ELSD 800. For reversed phase HPLC, a Phenomenex Prodigy C18 ODS3 column (5 µm, 250 x 4.6 mm) was used, apart from analyses in Chapter 3 where a reversed phase Brownlee Labs analytical ODS-224 SPHERI-5 column (5 µm, 220 x 4.6 mm) was used. A standard flow rate of 1 mL/min was used with stated concentrations of ACN (HPLC grade) in H_2O (Milli-Q®). Variable concentrations of ACN or MeOH (HPLC grade) in H_2O (Milli-Q®) were used for the mobile phase.

Preparative HPLC was performed on a Shimadzu LC-4A instrument equipped with a UV Spectrophotometric Detector SPD-2AS (wavelength λ=210 nm) and a Hewlett Packard 3390A integrator. Reversed phase HPLC was performed on a Phenomenex Luna C18, 10 x 250 mm, 5 μ column run at 5 mL/min. Variable concentrations of ACN or MeOH (HPLC grade) in H_2O (Milli-Q®) were used for the mobile phase.

5.1.7 Column chromatography

Column chromatography was performed with glass columns of stated dimensions or in pre-prepared cartridges as indicated. All solvents used for chromatography were of commercial grade and distilled once, except for MeOH, which was double distilled. Reversed phase C18 columns were run under pressure (0.5 kPa) with oxygen-free N_2 gas.

Reversed phase chromatography (RP) used Bakerbond (40μm) octadecyl (C18) packing. Samples were either dissolved in a minimal volume of solvent and loaded directly on to the column, or absorbed to fresh C18 or celite at a ratio of 1:50 using a minimum volume of solvent which was removed under vacuum prior to loading onto the column. Sephadex LH20 (Pharmacia Biotech AB) pre-soaked overnight in CH_2Cl_2 was used for gel permeation chromatography.

5.1.8 Thin Layer Chromatography (TLC)

DIOL analytical TLC was performed using Merck F_{254} glass-backed plates of 0.2 mm thickness. DIOL plates were eluted with 4 % MeOH/CH_2Cl_2. Merck RP-18 F_{254} TLC plates of 0.2 mm thickness were used for the analytical C18 TLC, eluting with stated CH_3CN/H_2O mixtures. TLC plates containing halichondrins were visualised using a phosphomolybdic acid (PMA) in ethanol (EtOH) spray (10% PMA in EtOH, *w/v*), followed by heating at ca 80 °C for 5 minutes to yield characteristic brown spots.

5.1.9 Scanning Electron Microscopy (SEM)

A Leica S440 scanning electron microscope was used, at accelerating voltages of 10-20 kV.

5.1.10 Transmission Electron Microscopy (TEM)

A JEOL JEM 1200-EX was used, at an accelerating voltage of 80 kV.

5.1.11 Optical rotation

Optical rotations were measured at 589 nm (Na_D) using a Perkin-Elmer 341 polarimeter.

5.1.12 P388 assay

This assay involved the use of the murine leukaemia cell line P388 (ATCC CCL 46, P388D1), and consisted of a serial dilution of the sample of interest followed by incubation for 72 hours with P388 cells. Cell viability was determined colorimetrically by the addition of a yellow dye, MTT tetrazolium. Unhealthy or dead cells cannot metabolise this dye, so a yellow colour remains. Healthy cells, however, are able to reduce the dye to MTT formazan, resulting in an intense purple colour (Figure 5.1.1).

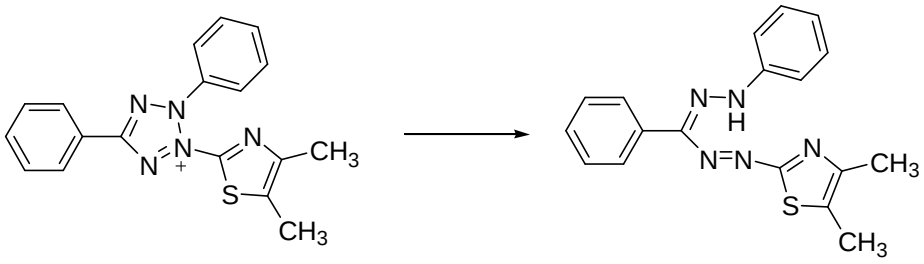

MTT tetrazolium salt (yellow) MTT formazan (purple)

Figure 5.1.1 Reduction of the yellow MTT tetrazolium salt to the purple MTT formazan by healthy P388 cells

The concentration of the sample required to reduce cell growth by 50%, when compared to a set of controls, is expressed as an IC_{50} in ng/mL.

5.1.13 Solvents

HPLC grade solvents, doubly deionized Nanopure water and Milli-Q® water were used where stated. Technical grade solvents were distilled prior to use. Methanol was distilled twice.

5.2 Work Described in Chapter Two

5.2.1 Calcium magnesium free artificial seawater

Calcium magnesium free artificial seawater (CMF-ASW) was prepared by combining the following two solutions, and adjusting the resultant solution to pH 8.2 using NaCl and HCl:

Solution 1: 27 g NaCl
1 g Na_2SO_4
0.8 g KCl
0.2 g $NaHCO_3$
500 mL deionised water

Solution 2: (0.2 M phosphate buffer)
2.76 g NaH_2PO_4
11.35g Na_2HPO_4
500 mL deionised water

5.2.2 Percoll® density gradient

A bent Pasteur pipette was used to layer 2 mL of each of 60, 45, 30, 15 and finally 5 % Percoll® solutions (in CMF-ASW) in a 15 mL polypropylene centrifuge tube, to make a 10 mL Percoll® density gradient. The dissociated cells were loaded on to the top of the gradient, and centrifuged at 600 rpm for 10 minutes. The resultant bands of cells were removed with a Pasteur pipette. Percoll® was from Sigma (P-1644, 65455-52-9).

5.2.3 Fixed *Lamellomorpha strongylata* samples

Six duplicate (twelve in total) samples of *Lamellomorpha strongylata* in fixative were used. In each set of six samples, three were diced sponge pieces and three were whole pieces of sponge. Fixative used were:

a. 2.5 % glutaraldehyde
0.05 M cacodylate, pH 8.0

b. 2.5 % glutaraldehyde
2.0 % formaldehyde
0.05 M cacodylate, pH 7.8

c. 2.0 % formaldehyde

0.05 M cacodylate, pH 8.0

d. 0.2 % glutaraldehyde in CMF-ASW, pH 8.3

Formaldehyde was used for fixing samples quickly, while glutaraldehyde was thought to be a better long-term fixative.

5.2.4 Fixed *Lissodendoryx* sp. samples

Samples were provided by NIWA in the following four fixatives:

a. Davidsons: 10 % glycerine
20 % formalin
30 % 95% EtOH
30 % deionised water
10 % glacial acetic acid

b. IG4F: 1 % glutaraldehyde
4 % stock buffered formaldehyde in 50 % filtered seawater

c. 10 % formaldehyde in CMF-ASW

d. 1.9 % formaldehyde, 1.5 % glutaraldehyde in CMF-ASW

5.2.5 Gram positive / Gram negative staining

1. Cell sample left to dry on a microscope slide, then passed through a flame.
2. Slide covered in crystal violet, and left for 30 seconds.
3. Slide washed with water, covered with Gramôs iodine, and left for 30 seconds.
4. Slide washed with water, followed by alcohol, then again with water.
5. Slide counterstained with safranin for 30 seconds.
6. Slide washed with water, and blotted dry with filter paper.

A dark purple colour indicates gram positive bacteria.
A pale pink colour indicates gram negative bacteria.

5.2.6 SEM sample preparation

1 g of fixed sponge material was washed three times in CMF-ASW, chopped in a Virtis blender for 10 minutes, and filtered through 75 µm mesh to give a dissociated cell sample. The filtrate was centrifuged at 1100 rpm for 5 minutes. The resultant pellet

was then sequentially suspended in 50, 70, 80, 90 and 95% ethanol/water followed by 100% ethanol for 1 hour each, centrifuging as above between each iteration. The pellet was then sequentially suspended in 20, 40, 60, 80 % ethanol/amyl acetate followed by 3 x 100% amyl acetate for 1 hour each, again centrifuging as above between each iteration. The pellet was re-suspended in amyl acetate, filtered onto Whatman filter paper, and critical point dried with liquid CO_2. A 1 cm circle of filter paper containing the cells was mounted onto an aluminium stub using a carbon tab, and sputter-coated with ca. 40 nm gold/palladium.

5.2.7 TEM sample preparation

Dissociated cells were prepared as follows:

1. Primary fixation: 2-3 hours in 3 % glutaraldehyde in 0.075 M PO_4 buffer.
2. Buffer wash: 3 changes of 0.075 M PO_4 buffer, 10 minutes per change.
3. Post fixation: 2-3 hours in 1 % osmium tetroxide in 0.075 M PO_4 buffer.
4. Dehydration: 10 minutes each in 20, 40, 60, 80 and 3 x 100 % acetone
5. Infiltration: 30 % Spurrôs resin in acetone for several hours, then 75 % resin overnight.
6. Embedding: 100 % Spurrôs resin, polymerised overnight at 70 °C in a beem capsule

Ultra-thin sections (50 ï 80 µm) were cut using an LKB2128 Ultramicrotome system. These sections were then stained with 5 % uranyl acetate for 30 minutes, washed with deionised water, stained with Satoôs lead stain for 20 minutes, and again washed thoroughly with deionised water. They were then dried for several hours.

The 0.075 M PO_4 buffer, pH 7.2, was prepared by combining 36 mL of stock solution A, 14 mL stock solution B and 83 mL deionised water.

Stock solution A: 17.805 g Na_2HPO_4Å2H_2O per 500 mL (0.2 M solution)

Stock solution B: 15.605 g NaH_2PO_4Å2H_2O per 500 mL (0.2 M solution)

5.2.8 Dissociation of sponge material

Each sponge sample was washed three times in CMF-ASW, blended for the times specified, and filtered through an appropriate sized mesh. This was repeated as required. Details of each procedure are given in Chapter 2.

5.3 Work Described in Chapter Three

5.3.1 Isolation of five new halichondrins

One tonne of *Lissodendoryx* sp. was collected in 1995 in order to supply halichondrin B (310 mg) and isohomohalichondrin B (~300 mg) for further trials. During the final purification of isohomohalichondrin B by preparative HPLC on ODS-silica (CH_3CN/H_2O, 7:3 or 9:1), twelve 2.5 L bottles of side cut residue were accumulated. The residue from each of these bottles was dried down individually, weighed, and analysed by ^1H NMR and analytical HPLC on ODS-silica (CH_3CN/H_2O, 7:3 and 9:1) (SH3 10.1-12). Signals in the ^1H NMR spectra characteristic of the halichondrins (for example, those between 4.7 and 5 ppm corresponding to the 19=CH_2 and 26=CH_2 exocyclic methylenes) were observed in the extracts of all twelve bottles. In the HPLC spectra, halichondrin-like peaks, which exhibit end absorption only, were also seen.

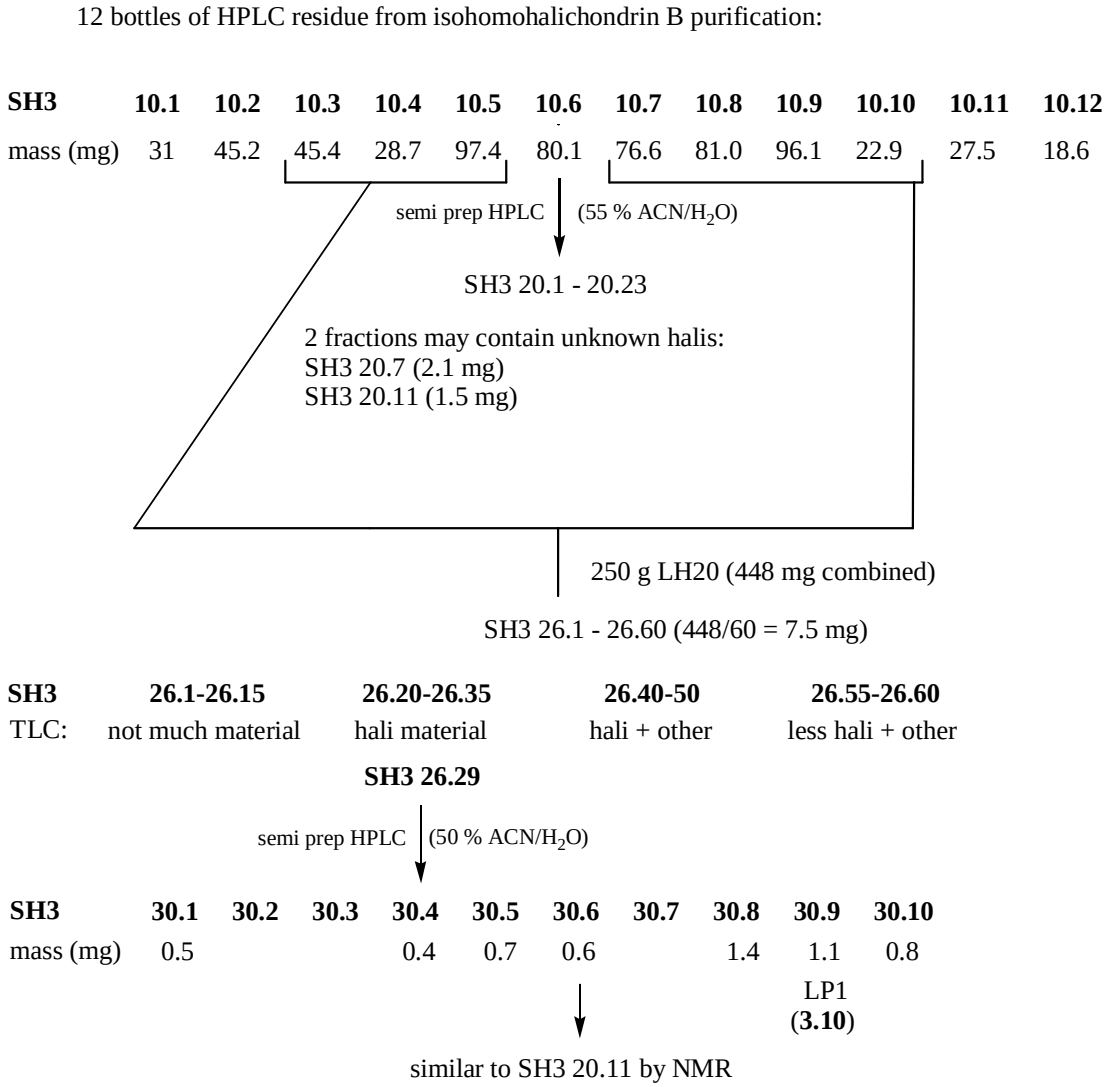

Figure 5.3.1 Extraction scheme used in isolation of the five new halichondrins

Bottle number six was processed on a preparative HPLC ODS-silica column, eluting with 55% CH_3CN/H_2O, to give 24 fractions. These fractions were analysed *via* ^1H NMR and analytical HPLC on ODS-silica (CH_3CN/H_2O, 7:3 and 9:1). Along with fractions containing known halichondrins, two fractions (SH3 20.7 and SH3 20.11) were found to contain unknown halichondrin material. From their HPLC spectra, fractions SH3 20.7 (2.1 mg) and SH3 20.11 (1.5 mg) were comprised of four and two components respectively. In the hope that only one component in each fraction was halichondrin-like and responsible for most of the mass of the sample, an attempt was made to separate the components of these two fractions on a 2 g LH-20 column (40 x 0.5 cm) eluting with CH_2Cl_2. However, all the components co-eluted off LH-20 in fractions 2 to 7, implying that they were all at the very least similar in size, if not all closely related halichondrins.

In order to obtain enough of the new halichondrin material for structural characterisation, material from bottles three to five and seven to ten were combined (~300 mg), and processed on a 250 g LH-20 column (57 x 4.3 cm, eluting with CH_2Cl_2) to give 60 fractions (SH3 26.1-60). Following DIOL TLC (4% $MeOH/CH_2Cl_2$), analytical HPLC on ODS-silica and ^1H NMR analysis, fraction 30 (SH3 26.30, 5.1 mg) was selected as the starting point for further chromatographic separation.

Fraction 30 was loaded onto a semi-preparative ODS-silica HPLC column *via* two 300 μL injections, eluting with 60% and 65% CH_3CN/H_2O, respectively. Peak separation was not sufficient in either case for collection of the individual components present, so all fractions were recombined. Fraction 29 (SH3 26.29, ~7 mg) was then loaded onto the same column, eluting with 50% CH_3CN/H_2O. Better peak separation was achieved using this solvent mix, and fractions 1-10 were collected (SH3 30.1-10). From its ^1H NMR spectrum, fraction SH3 30.6 (0.6 mg) was found to contain new halichondrin material. This was similar, but not identical to, material seen in bottle number six fraction 11, described above. Other fractions were found to contain known halichondrins. For example, fraction SH3 30.9 (1.1 mg) was identified as the known 53-methoxyneoisohomohalichondrin B (**3.10**) by ^1H NMR analysis.

Fractions SH3 20.7, SH3 20.11 and SH3 30.6 were processed by analytical HPLC on ODS-silica (CH_3CN/H_2O, 7:3) to give five pure fractions (**SH3 116.2**, **116.4**, **118.2**, **118.3** and **118.4**), which were identified as new halichondrins *via* analytical HPLC on ODS-silica (CH_3CN/H_2O, 7:3), ^1H NMR and LCMS. They were characterised by

HRLCMS and NMR. Quantification of the samples was achieved as reported in Chapter 3 (Table 3.2.2). All samples were active in the P388 assay (Table 3.2.2).

5.3.2 Spectroscopic assignment of SH3 116.2 (3.13)

White solid, estimated 50 μg sample, UV (CH_3CN/H_2O, 7:1) end absorption only; NMR data in Table 3.3.1; HRLCMS *m/z* 1038.5372 $[M + NH_4]^+$ (calcd for $C_{56}H_{80}O_{17}N$, 1038.5426).

5.3.3 Spectroscopic assignment of SH3 116.4 (3.13)

White solid, estimated 50 μg sample, UV (CH_3CN/H_2O, 7:1) end absorption only; NMR data in Table 3.4.1; HRLCMS *m/z* 1179.5001 $[M + K]^+$ (calcd for $C_{61}H_{85}O_{18}ClK$, 1179.5062).

5.3.4 Spectroscopic assignment of SH3 118.2 (3.13)

White solid, estimated 110 μg sample, UV (CH_3CN/H_2O, 7:1) end absorption only; NMR data in Table 3.5.1; HRLCMS *m/z* 1099.5171 $[M + Na]^+$ (calcd for $C_{59}H_{80}O_{18}Na$, 1099.5242).

5.3.5 Spectroscopic assignment of SH3 118.3 (3.13)

White solid, estimated 88 μg sample, UV (CH_3CN/H_2O, 7:1) end absorption only; NMR data in Table 3.6.1; HRLCMS *m/z* 1115.5530 $[M + Na]^+$ (calcd for $C_{60}H_{84}O_{18}Na$, 1115.5555).

5.3.6 Spectroscopic analysis of SH3 118.4 (3.13)

White solid, 50 μg sample, UV (CH_3CN/H_2O, 7:1) end absorption only; NMR data up to C48 in Table 3.7.1. Analysis incomplete.

5.4 Work Described in Chapter Four

5.4.1 General experimental procedures

The UV spectrum for compound **4.2** was measured on a Cary 300 spectrophotometer. The elemental analysis was carried out by Quantitative Technologies Inc. (QTI), Salem Industrial Park, Bldg 5, Whitehouse, NJ 08888, USA: Sample, petrobactin-SO_3, %C 40.46, %H 4.61, %N 6.86, %S 4.23.

5.4.2 Culture and isolation

M. hydrocarbonoclasticus (SP.17; ATCC 49840),[93,94] was cultured in a hypersaline medium (0.5 M / 29.22 g NaCl, 0.4 g $MgSO_4 \cdot 7H_2O$, 1.0 g NH_4Cl, 3.0 g K_2HPO_4, 0.15 g $CaCl_2 \cdot 2H_2O$ and 5.0 g sodium succinate / $Na_2C_4H_4O_4 \cdot 6H_2O$ per liter of Nanopure water) in order to optimize siderophore production. The cultures were typically grown as 2 L cultures in 4 L flasks on a rotary shaker (150 r.p.m.) for 7 days. At the time of harvesting, cultures were in stationary phase. After centrifugation of the culture medium (5000 r.p.m., 20 min), Amberlite XAD-2 resin (Supelco) was added to the decanted supernatant (ca. 100 g / L), and the resultant mixture was shaken for at least 4 hours at > 100 r.p.m.. The XAD was then loaded into a glass chromatography column (2 cm internal diameter), washed with one column volume of Nanopure water and eluted with 100 % methanol. Using the solution-phase Chrome Azurol S (CAS) assay with shuttle, [103] the methanol fraction was found to contain the siderophores. Since the culture medium remained CAS-positive, it was acidified to pH 2.5, re-extracted with XAD resin, and shaken at > 100 r.p.m. for at least 6 hours. The XAD was again recovered, washed and eluted as described above. The final purification of petrobactin and petrobactin sulfonate was achieved on the combined methanol fractions using preparative reversed-phase HPLC (Vydac C4 column (10 εm, 250 x 22 mm) using a CH_3CN/H_2O gradient (0% to 60%) over 35 minutes, with 0.1% trifluoroacetic acid). Acid was removed from the samples *via* repeated addition and evaporation of methanol during the drying process. This culture and isolation work was done by Frithjof Küpper, a Post Doctoral research fellow in the Butler group at UCSB.

The cyclic imides of petrobactin (**4.3**) and petrobactin sulfonate (**4.4** and **4.5**) were obtained by reacting petrobactin (**4.1**) and petrobactin sulfonate (**4.2**) with 0.1% TFA and 0.5% formic acid, respectively, in water at 40 °C for eight days. Purification was by reversed-phase HPLC as described above.

5.4.3 Spectroscopic assignment of petrobactin (4.1)

White solid, 12 mg sample, ^{1}H NMR and ^{13}C NMR reported previously,[67] HRMS *m/z* 719.3606 $[M + H]^+$ (calcd for $C_{34}H_{51}N_6O_{11}$, 719.3615).[68]

5.4.4 Spectroscopic assignment of petrobactin sulfonate (4.2)

White solid, 10 mg sample, $[\alpha]^{20}_{D}$ ï 2.5° (*c* 0.013, DMSO); UV (DMSO) ¬max (log Ů) 229 (3.95), 253 (3.83), 291 (3.74) nm; ^{1}H NMR (DMSO-d_6, 500 MHz) see Table 4.2.1; ^{13}C NMR (DMSO-d_6, 125 MHz) see Table 4.2.1; HRESIMS *m/z* 799.3199 $[M + H]^+$ (calcd for $C_{34}H_{51}N_6O_{14}S$, 799.3184).

5.4.5 Spectroscopic assignment of petrobactin cyclic imide (4.3)

White solid, 5.5 mg sample, ^{1}H NMR (DMSO-d_6, 500 MHz) see Table 4.4.1, ^{13}C NMR (DMSO-d_6, 125 MHz) see Table 4.4.1, HRESIMS *m/z* 701.3511 $[M + H]^+$ (calcd for $C_{34}H_{49}N_6O_{10}$, 701.3510).

5.4.6 Spectroscopic assignment of petrobactin sulfonate cyclic imides (4.4 and 4.5)

White solid, 2.4 mg sample, ^{1}H NMR (DMSO-d_6, 500 MHz) see Table 4.4.2, ^{13}C NMR (DMSO-d_6, 75 MHz) see Table 4.4.2, HRESIMS *m/z* 781.3047 $[M + H]^+$ (calcd for $C_{34}H_{49}N_6O_{13}S$, 781.3078).

1. Devries D.J. & Hall M.R. Marine biodiversity as a source of chemical diversity. *Drug Dev Res*, **1994**, *33*, 161-173.
2. Bakus G.J., Targett N.M. & Schulte B. Chemical ecology of marine organisms - an overview. *J Chem Ecol*, **1986**, *12*, 951-987.
3. Hay M.E. Marine chemical ecology: what's known and what's next? *J Exp Mar Biol Ecol*, **1996**, *200*, 103-134.
4. Cooksey C.J. Tyrian purple: 6,6'-dibromoindigo and related compounds. *Molecules*, **2001**, *6*, 736-769.
5. Hamann M.T., Otto C.S., Scheuer P.J. & Dunbar D.C. Kahalalides: bioactive peptide from a marine mollusk *Elysia rufescens* and its algal diet *Bryopsis* sp. *J Org Chem*, **1996**, *61*, 6594-6600.
6. Hamann M.T. & Scheuer P.J. Kahalalide F, a bioactive depsipeptide from the sacoglossan mollusk *Elysia rufescens* and the green alga *Bryopsis* sp. *J Am Chem Soc*, **1993**, *115*, 5825-5826.
7. Newman D.J. & Cragg G.M. Marine natural products and related compounds in clinical and advanced preclinical trials. *J Nat Prod*, **2004**, *67*, 1216-1238.
8. Rinehart K.L., Gloer J.B., Cook J.C., Mizsak S.A. & Scahill T.A. Structures of the didemnins, anti-viral and cytotoxic depsipeptides from a Caribbean tunicate. *J Am Chem Soc*, **1981**, *103*, 1857-1859.
9. Dilip de Silva E. & Scheuer P.J. Manoalide, an antibiotic sesterterpenoid from the marine sponge *Luffariella variabilis* (Polejaeff). *Tetrahedron Lett*, **1980**, *21*, 1611-1614.
10. Jacobs R.S. & Faulkner D.J. inventors, University of California, Berkeley assignee. Isolation and preparation of manoalide analogs as antiinflammatory, immunosuppresive and antiproliferative agents. U.S. patent 830994, **1986**.
11. Potts B.C.M., Capon R.J. & Faulkner D.J. Luffalactone and (4e,6e)-dehydromanoalide from the sponge *Luffariella variabilis*. *J Org Chem*, **1992**, *57*, 2965-2967.
12. Potts B.C.M., Faulkner D.J., Decarvalho M.S. & Jacobs R.S. Chemical mechanism of inactivation of bee venom phospholipase A2 by the marine natural-products manoalide, luffariellolide, and scalaradial. *J Am Chem Soc*, **1992**, *114*, 5093-5100.
13. Munro M.H.G., University of Canterbury, personal communication.
14. Rinehart K.L., Holt T.G., Fregeau N.L., Stroh J.G., Keifer P.A., Sun F., Li L.H. & Martin D.G. Ecteinascidin 729, ecteinascidin 743, ecteinascidin 745, ecteinascidin 759a, ecteinascidin 759b, and ecteinascidin 770 - potent antitumor agents from the Caribbean tunicate *Ecteinascidia turbinata*. *J Org Chem*, **1990**, *55*, 4512-4515.
15. Wright A.E., Forleo D.A., Gunawardana G.P., Gunasekera S.P., Koehn F.E. & McConnell O.J. Antitumor tetrahydroisoquinoline alkaloids from the colonial ascidian *Ecteinascidia turbinata*. *J Org Chem*, **1990**, *55*, 4508-4512.
16. Bergquist P.R., *Sponges*. 1st Edition ed. 1978, London: Hutchinson & Co. Ltd. p181.
17. Blunt J.W., Copp B.R., Munro M.H.G., Northcote P.T. & Prinsep M.R. Marine natural products. *Nat Prod Rep*, **2003**, *20*, 1-48.
18. Dumdei E.J., Blunt J.W., Munro M.H.G. & Pannell L.K. Isolation of calyculins, calyculinamides, and swinholide H from the New Zealand deep-water marine sponge *Lamellomorpha strongylata*. *J Org Chem*, **1997**, *62*, 2636-2639.
19. Li S.X., Dumdei E.J., Blunt J.W., Munro M.H.G., Robinson W.T. & Pannell L.K. Theonellapeptolide IIIe, a new cyclic peptolide from the New Zealand deep water sponge, *Lamellomorpha strongylata*. *J Nat Prod*, **1998**, *61*, 724-728.

20. Kato Y., Fusetani N., Matsunaga S., Hashimoto K., Fujita S. & Furuya T. The bioactive marine metabolites. 16. Calyculin A, a novel antitumor metabolite from the marine sponge *Discodermia calyx. J Am Chem Soc*, **1986**, *108*, 2780-2781.
21. Kato Y., Fusetani N., Matsunaga S., Hashimoto K. & Koseki K. Isolation and structure elucidation of calyculin B, calyculin C, and calyculin D, novel antitumor metabolites, from the marine sponge *Discodermia calyx. J Org Chem*, **1988**, *53*, 3930-3932.
22. Carmely S. & Kashman Y. Structure of swinholide A, a new macrolide from the marine sponge *Theonella swinhoei. Tetrahedron Lett*, **1985**, *26*, 511-514.
23. Carmely S., Rotem M. & Kashman Y. Swinholide A, a new marine macrolide - complete assignment of H-1 and C-13 spectra by 2D NMR techniques. *Magn Reson Chem*, **1986**, *24*, 343-349.
24. Kobayashi M., Tanaka J., Katori T., Matsuura M. & Kitagawa I. Structure of swinholide A - a potent cytotoxic macrolide from the Okinawan marine sponge *Theonella swinhoei. Tetrahedron Lett*, **1989**, *30*, 2963-2966.
25. Bewley C.A., Holland N.D. & Faulkner D.J. Two classes of metabolites from *Theonella swinhoei* are localized in distinct populations of bacterial symbionts. *Experientia*, **1996**, *52*, 716-722.
26. Andrianasolo E.H., Gross H., Goeger D., Musafija-Girt M., McPhail K.P., Leal R.M., Mooberry S.L. & Gerwick W.H. Isolation of swinholide A and related glycosylated derivatives from two field collections of marine cyanobacteria. *Org Lett*, **2005**, *7*, 1375-1378.
27. Youssef D.T.A. & Mooberry S.L. Hurghadolide A and swinholide I, potent actin-microfilament disrupters from the Red Sea sponge *Theonella swinhoei. J Nat Prod*, **2006**, *69*, 154-157.
28. Kitagawa I., Kobayashi M., Lee N.K., Shibuya H., Kawata Y. & Sakiyama F. Structure of theonellapeptolide Id, a new bioactive peptolide from an Okinawan marine sponge, *Theonella* sp. (Theonelliae). *Chem Pharm Bull*, **1986**, *34*, 2664-2667.
29. Kitagawa I., Lee N.K., Kobayashi M. & Shibuya H. Structure of theonellapeptolide Ie, a new tridecapeptide lactone from an Okinawan marine sponge, *Theonella* sp. (Theonellidae). *Chem Pharm Bull*, **1987**, *35*, 2129-2132.
30. Kitagawa I., Ohashi K., Kawanishi H., Shibuya H., Shinkai K. & Akedo H. Ionophoretic activities of oligopeptide lactones and resin-glycosides in human-erythrocytes. *Chem Pharm Bull*, **1989**, *37*, 1679-1681.
31. Kobayashi M., Lee N.K., Shibuya H., Momose T. & Kitagawa I. Marine natural-products. 26. Biologically-active tridecapeptide lactones from the Okinawan marine sponge *Theonella swinhoei* (Theonellidae). 2. Structures of theonellapeptolide Ia, theonellapeptolide Ib, theonellapeptolide Ic and theonellapeptolide Ie. *Chem Pharm Bull*, **1991**, *39*, 1177-1184.
32. Uemura D., Takahashi K., Yamamoto T., Katayama C., Tanaka J., Okumura Y. & Hirata Y. Norhalichondrin A, an antitumor polyether macrolide from a marine sponge. *J Am Chem Soc*, **1985**, *107*, 4796-4798.
33. Hirata Y. & Uemura D. Halichondrins - antitumor polyether macrolides. *Pure Appl Chem*, **1986**, *58*, 701-710.
34. Pettit G.R., Tan R., Gao F., Williams M.D., Doubek D.L., Boyd M.R., Schmidt J.M., Chapuis J.C., Hamel E., Bai R., Hooper J.N.A. & Tackett L.P. Isolation and structure of halistatin I from the eastern Indian Ocean marine sponge *Phakellia carteri. J Org Chem*, **1993**, *58*, 2538-2543.
35. Pettit G.R., Herald C.L., Boyd M.R., Leet J.E., Dufresne C., Doubek D.L., Schmidt J.M., Cerny R.L., Hooper J.N.A. & Rutzler K.C. Antineoplastic agents.

219. Isolation and structure of the cell-growth inhibitory constituents from the Western Pacific marine sponge *Axinella* sp. *J Med Chem*, **1991**, *34*, 3339-3340.
36. Aicher T.D., Buszek K.R., Fang F.G., Forsyth C.J., Jung S.H., Kishi Y., Matelich M.C., Scola P.M., Spero D.M. & Yoon S.K. Total synthesis of halichondrin B and norhalichondrin B. *J Am Chem Soc*, **1992**, *114*, 3162-3164.
37. Yu M.J., Littlefield B.A., Fang F.G., Orr J., Wong N., Lewis M.D., Silberman S.L. & Kishi Y. Discovery of E7389: chemistry strategy and material supply challenges. *AACR Educ Book*, **2006**, *2006*, 225-229.
38. Dabydeen D.A., Burnett J.C., Bai R.L., Verdier-Pinard P., Hickford S.J.H., Pettit G.R., Blunt J.W., Munro M.H.G., Gussio R. & Hamel E. Comparison of the activities of the truncated halichondrin B analog NSC 707389 (E7389) with those of the parent compound and a proposed binding site on tubulin. *Mol Pharmacol*, **2006**, *70*, 1866-1875.
39. Garcia-Rocha M., Garcia-Gravalos M.D. & Avila J. Characterisation of antimitotic products from marine organisms that disorganise the microtubule network: ecteinascidin 743, isohomohalichondrin-B and LL-15. *Br J Cancer*, **1996**, *73*, 875-883.
40. Bai R., Paull K.D., Herald C.L., Malspeis L., Pettit G.R. & Hamel E. Halichondrin B and homohalichondrin B, marine natural-products binding in the vinca domain of tubulin. Discovery of tubulin-based mechanism of action by analysis of differential cytotoxicity data. *J Biol Chem*, **1991**, *266*, 15882-15889.
41. Bergamaschi D., Ronzoni S., Taverna S., Faretta M., De Feudis P., Faircloth G., Jimeno J., Erba E. & D'Incalci M. Cell cycle perturbations and apoptosis induced by isohomohalichondrin B (IHB), a natural marine compound. *Br J Cancer*, **1999**, *79*, 267-277.
42. Jordan A., Hadfield J.A., Lawrence N.J. & McGown A.T. Tubulin as a target for anticancer drugs: agents which interact with the mitotic spindle. *Med Res Rev*, **1998**, *18*, 259-296.
43. Hung D.T., Jamison T.F. & Schreiber S.L. Understanding and controlling the cell cycle with natural products. *Chem Biol*, **1996**, *3*, 623-639.
44. Wilson L. & Jordan M.A. Microtubule dynamics - taking aim at a moving target. *Chem Biol*, **1995**, *2*, 569-573.
45. Avila J. The use of microtubule poisons on tumor cells. *Cancer J*, **1997**, *10*, 315-318.
46. Sorger P.K., Dobles M., Tournebize R. & Hyman A.A. Coupling cell division and cell death to microtubule dynamics. *Curr Opin Chem Biol*, **1997**, *9*, 807-814.
47. Hamel E. Antimitotic natural products and their interactions with tubulin. *Med Res Rev*, **1996**, *16*, 207-231.
48. Hamel E. Natural products which interact with tubulin in the vinca domain - maytansine, rhizoxin, phomopsin A, dolastatin 10 and dolastatin 15 and halichondrin B. *Pharmacol Ther*, **1992**, *55*, 31-51.
49. Nogales E., Wolf S.G. & Downing K.H. Structure of the alpha beta tubulin dimer by electron crystallography. *Nature*, **1998**, *391*, 199-203.
50. Nogales E., Wolf S.G. & Downing K.H. Structure of the alpha beta tubulin dimer by electron crystallography. *Nature*, **1998**, *393*, 191-191.
51. Dumontet C. & Sikic B.I. Mechanisms of action of and resistance to antitubulin agents: microtubule dynamics, drug transport, and cell death. *J Clin Oncol*, **1999**, *17*, 1061-1070.
52. Shi Q., Chen K., Morris-Natschke S.L. & Lee K.H. Recent progress in the development of tubulin inhibitors as antimitotic antitumor agents. *Curr Pharm Des*, **1998**, *4*, 219-248.

53. Margolis R.L. & Wilson L. Addition of colchicine-tubulin complex to microtubule ends - mechanism of substoichiometric colchicine poisoning. *Proc Natl Acad Sci USA*, **1977**, *74*, 3466-3470.
54. Rai S.S. & Wolff J. Localization of the vinblastine-binding site on beta-tubulin. *J Biol Chem*, **1996**, *271*, 14707-14711.
55. Van Belle S.J.P., Distelmans W., Vandebroek J., Bruynseels J., Vanginckel R.V. & Storme G.A. Phase I trial of Erbulozole (R55104). *Anticancer Research*, **1993**, *13*, 2389-2391.
56. Stierle A., Strobel G. & Stierle D. Taxol and taxane production by *Taxomyces andreanae*, an endophytic fungus of Pacific Yew. *Science*, **1993**, *260*, 214-216.
57. Schiff P.B., Fant J. & Horwitz S.B. Promotion of microtubule assembly *in vitro* by Taxol. *Nature*, **1979**, *277*, 665-667.
58. Bellamy W.T. P-glycoproteins and multidrug resistance. *Annu Rev Pharmacol Toxicol*, **1996**, *36*, 161-183.
59. Sikic B.I., Fisher G.A., Lum B.L., Halsey J., BeketicOreskovic L. & Chen G. Modulation and prevention of multidrug resistance by inhibitors of P-glycoprotein. *Cancer Chemother Pharmacol*, **1997**, *40*, S13-S19.
60. Cutler C.S., Lewis J.S. & Anderson C.J. Utilization of metabolic, transport and receptor-mediated processes to deliver agents for cancer diagnosis. *Adv Drug Deliv Rev*, **1999**, *37*, 189-211.
61. Giannakakou P., Sackett D.L., Kang Y.K., Zhan Z.R., Buters J.T.M., Fojo T. & Poruchynsky M.S. Paclitaxel-resistant human ovarian cancer cells have mutant beta-tubulins that exhibit impaired paclitaxel-driven polymerization. *J Biol Chem*, **1997**, *272*, 17118-17125.
62. Zhang K., Mack P. & Wong K.P. Glutathione-related mechanisms in cellular resistance to anticancer drugs. *Int J Oncol*, **1998**, *12*, 871-882.
63. Lehne G., Elonen E., Baekelandt M., Skovsgaard T. & Peterson C. Challenging drug resistance in cancer therapy - review of the first Nordic conference on chemoresistance in cancer treatment, October 9th and 10th, 1997. *Acta Oncol*, **1998**, *37*, 431-439.
64. St'astny M., Strohalm J., Plocova D., Ulbrich K. & Rihova B. A possibility to overcome P-glycoprotein (PGP)-mediated multidrug resistance by antibody-targeted drugs conjugated to N-(2-hydroxypropyl)methacrylamide (HPMA) copolymer carrier. *Eur J Cancer*, **1999**, *35*, 459-466.
65. Butler A. Acquisition and utilization of transition metal ions by marine organisms. *Science*, **1998**, *281*, 207-210.
66. Haygood M.G., Holt P.D. & Butler A. Aerobactin production by a planktonic marine *Vibrio* sp. *Limnol Oceanogr*, **1993**, *38*, 1091-1097.
67. Barbeau K., Zhang G.P., Live D.H. & Butler A. Petrobactin, a photoreactive siderophore produced by the oil-degrading marine bacterium *Marinobacter hydrocarbonoclasticus*. *J Am Chem Soc*, **2002**, *124*, 378-379.
68. Bergeron R.J., Huang G.F., Smith R.E., Bharti N., McManis J.S. & Butler A. Total synthesis and structure revision of petrobactin. *Tetrahedron*, **2003**, *59*, 2007-2014.
69. Kanoh K., Kamino K., Leleo G., Adachi K. & Shizuri Y. Pseudoalterobactin A and B, new siderophores excreted by marine bacterium *Pseudoalteromonas* sp. KP20-4. *J Antibiot*, **2003**, *56*, 871-875.
70. Abergel R.J., Wilson M.K., Arceneaux J.E.L., Hoette T.M., Strong R.K., Byers B.R. & Raymond K.N. Anthrax pathogen evades the mammalian immune system through stealth siderophore production. *Proc Natl Acad Sci USA*, **2006**, *103*, 18499-18503.

71. Pfleger B.F., Lee J.Y., Somu R.V., Aldrich C.C., Hanna P.C. & Sherman D.H. Characterization and analysis of early enzymes for petrobactin biosynthesis in *Bacillus anthracis*. *Biochemistry*, **2007**, *46*, 4147-4157.
72. Kitagawa I., Kobayashi M., Katori T., Yamashita M., Tanaka J., Doi M. & Ishida T. Absolute stereostructure of swinholide A, a potent cytotoxic macrolide from the Okinawan marine sponge *Theonella swinhoei*. *J Am Chem Soc*, **1990**, *112*, 3710-3712.
73. Piel J. Bacterial symbionts: prospects for the sustainable production of invertebrate-derived pharmaceuticals. *Curr Med Chem*, **2006**, *13*, 39-50.
74. Phillips A.J., University of Colorado at Boulder, personal communication.
75. Battershill C.N., Australian Institute of Marine Science, personal communication.
76. Litaudon M., Hickford S.J.H., Lill R.E., Lake R.J., Blunt J.W. & Munro M.H.G. Antitumor polyether macrolides: new and hemisynthetic halichondrins from the New Zealand deep-water sponge *Lissodendoryx* sp. *J Org Chem*, **1997**, *62*, 1868-1871.
77. Kishi Y., Fang F.G., Forsyth C.J., Scola P.M. & Yoon S.K. inventors, Harvard College, USA assignee. Halichondrins and related compounds. U.S. patent 5436238, **1995**.
78. Stamos D.P., Chen S.S. & Kishi Y. New synthetic route to the C14-C38 segment of halichondrins. *J Org Chem*, **1997**, *62*, 7552-7553.
79. Wang Y., Habgood G.J., Christ W.J., Kishi Y., Littlefield B.A. & Yu M.J. Structure-activity relationships of halichondrin B analogues: modifications at C30-C38. *Bioorg Med Chem Lett*, **2000**, *10*, 1029-32.
80. Littlefield B.A., Palme M.H., Seletsky B.M., Towle M.J., Yu M.J. & Zheng W. inventors, Eisai Co., Ltd. assignee. Macrocyclic analogs and methods of their use and preparation. U.S. patent 6,214,865, **2001**.
81. Seletsky B.M., Wang Y., Hawkins L.D., Palme M.H., Habgood G.J., DiPietro L.V., Towle M.J., Salvato K.A., Wels B.F., Aalfs K.K., Kishi Y., Littlefield B.A. & Yu M.J. Structurally simplified macrolactone analogues of halichondrin B. *Bioorg Med Chem Lett*, **2004**, *14*, 5547-5550.
82. Zheng W., Seletsky B.M., Palme M.H., Lydon P.J., Singer L.A., Chase C.E., Lemelin C.A., Shen Y., Davis H., Tremblay L., Towle M.J., Salvato K.A., Wels B.F., Aalfs K.K., Kishi Y., Littlefield B.A. & Yu M.J. Macrocyclic ketone analogues of halichondrin B. *Bioorg Med Chem Lett*, **2004**, *14*, 5551-5554.
83. Littlefield B.A. & Towle M.J. inventors, Eisai Co., Ltd. assignee. Methods and compositions comprising a halichondrin B analog for use in treating cancer. U.S. patent 6653341, **2006**.
84. Pretsch E., Buhlmann P. & Affolter C., *Structure determination of organic compounds*. Third ed. 2000, Berlin: Springer-Verlag. page 223.
85. Hadden C.E., Martin G.E. & Krishnamurthy V.V. Constant time inverse-detection gradient accordion rescaled heteronuclear multiple bond correlation spectroscopy: CIGAR-HMBC. *Magn Reson Chem*, **2000**, *38*, 143-147.
86. Lankford C.E. Bacterial assimilation of iron. *CRC Crit Rev Microbiol*, **1973**, *2*, 273-331.
87. Morel F.M.M. & Price N.M. The biogeochemical cycles of trace metals in the oceans. *Science*, **2003**, *300*, 944-947.
88. Coale K.H., Johnson K.S., Chavez F.P., Buesseler K.O., Barber R.T., Brzezinski M.A., Cochlan W.P., Millero F.J., Falkowski P.G., Bauer J.E., Wanninkhof R.H., Kudela R.M., Altabet M.A., Hales B.E., Takahashi T., Landry M.R., Bidigare R.R., Wang X.J., Chase Z., Strutton P.G., Friederich G.E., Gorbunov M.Y., Lance V.P., Hilting A.K., Hiscock M.R., Demarest M., Hiscock W.T.,

Sullivan K.F., Tanner S.J., Gordon R.M., Hunter C.N., Elrod V.A., Fitzwater S.E., Jones J.L., Tozzi S., Koblizek M., Roberts A.E., Herndon J., Brewster J., Ladizinsky N., Smith G., Cooper D., Timothy D., Brown S.L., Selph K.E., Sheridan C.C., Twining B.S. & Johnson Z.I. Southern ocean iron enrichment experiment: carbon cycling in high- and low-Si waters. *Science*, **2004**, *304*, 408-414.

89. Albrecht-Gary A.M. & Crumbliss A.L., *Coordination chemistry of siderophores: thermodynamics and kinetics of iron chelation and release*, in *Metal Ions in Biological Systems, Vol 35*. 1998. p. 239-327.
90. Cook A.M. & Denger K. Dissimilation of the C-2 sulfonates. *Arch Microbiol*, **2002**, *179*, 1-6.
91. Budzikiewicz H., Fuchs R. & Taraz K. Dihydropyoverdin-7-sulfonic acids - unusual bacterial metabolites. *Nat Prod Lett*, **1998**, *12*, 125-130.
92. Schroder H., Adam J., Taraz K. & Budzikiewicz H. Dihydropyoverdin sulfonic-acids - intermediates in the biogenesis. *Z Naturforsch C: Biosci*, **1995**, *50*, 616-621.
93. Al-Mallah M., Goutx M., Mille G. & Bertrand J.-C. Production of emulsifying agents during growth of a marine *Alteromonas* in sea water with eicosane as carbon source, a solid hydrocarbon. *Oil Chem Pollut*, **1990**, *6*, 289-305.
94. Gauthier M.J., Lafay B., Christen R., Fernandez L., Acquaviva M., Bonin P. & Bertrand J.C. *Marinobacter hydrocarbonoclasticus* gen. nov., sp. nov., a new, extremely halotolerant, hydrocarbon-degrading marine bacterium. *Int J Syst Bacteriol*, **1992**, *42*, 568-576.
95. Huu N.B., Denner E.B.M., Ha D.T.C., Wanner G. & Stan-Lotter H. *Marinobacter aquaeolei* sp. nov., a halophilic bacterium isolated from a Vietnamese oil-producing well. *Int J Syst Bacteriol*, **1999**, *49*, 367-375.
96. Sproer C., Lang E., Hobeck P., Burghardt J., Stackebrandt E. & Tindall B.J. Transfer of *Pseudomonas nautica* to *Marinobacter hydrocarbonoclasticus*. *Int J Syst Bacteriol*, **1998**, *48*, 1445-1448.
97. Hickford S.J.H., Küpper F.C., Zhang G.P., Carrano C.J., Blunt J.W. & Butler A. Petrobactin sulfonate, a new siderophore produced by the marine bacterium *Marinobacter hydrocarbonoclasticus*. *J Nat Prod*, **2004**, *67*, 1897-1899.
98. Pretsch E., Clerc T., Seibl J. & Simon W., *Tables of spectral data for structure determination of organic compounds*. 2nd ed. 1989, New York: Springer-Verlag.
99. Sarneski J.E., Surprenant H.L., Molen F.K. & Reilley C.N. Chemical shifts and protonation shifts in C13 Nuclear Magnetic-Resonance studies of aqueous amines. *Anal Chem*, **1975**, *47*, 2116-2124.
100. Thomas F., Beguin C., Pierre J.L. & Serratrice G. Thermodynamic and kinetic studies of the sulfonated derivative of the iron chelator TRENCAM, an analog of enterobactin. *Inorg Chim Acta*, **1999**, *291*, 148-157.
101. Gardner R.A., Kinkade R., Wang C.J. & Phanstiel O. Total synthesis of petrobactin and its homologues as potential growth stimuli for *Marinobacter hydrocarbonoclasticus*, an oil-degrading bacteria. *J Org Chem*, **2004**, *69*, 3530-3537.
102. Wang Q.X.H. & Phanstiel O. Total synthesis of acinetoferrin. *J Org Chem*, **1998**, *63*, 1491-1495.
103. Schwyn B. & Neilands J.B. Universal chemical assay for the detection and determination of siderophores. *Anal Biochem*, **1987**, *160*, 47-56.

J. Nat. Prod. **2004,** *67,* 1897−1899 **1897**

Petrobactin Sulfonate, a New Siderophore Produced by the Marine Bacterium *Marinobacter hydrocarbonoclasticus*

Sarah J. H. Hickford,[†,‡] Frithjof C. Küpper,[†] Guangping Zhang,[†] Carl J. Carrano,[§] John W. Blunt,[‡] and Alison Butler*[,†]

Department of Chemistry and Biochemistry, University of California, Santa Barbara, California 93106-9510, Department of Chemistry, University of Canterbury, Private Bag 4800, Christchurch, New Zealand, and Department of Chemistry, San Diego State University, San Diego, California 92182

Received May 25, 2004

Culture of the oil-degrading marine bacterium *Marinobacter hydrocarbonoclasticus* gave the known siderophore petrobactin (**1**) and the new metabolite petrobactin sulfonate (**2**), the first marine siderophore containing a sulfonated 3,4-dihydroxy aromatic ring. The structure of petrobactin sulfonate was elucidated from spectral data, resulting in a revision of the NMR assignments of petrobactin.

Crude oil is one of the most significant organic pollutants to the marine environment. Many compounds in crude oil are biodegradable, and this observation has fueled investigations on oil-degrading marine microorganisms. *Marinobacter hydrocarbonoclasticus* is a ubiquitous marine bacterium,[1,2] which grows on a variety of hydrocarbons as its sole carbon source. Iron is essential to the growth of the vast majority of microorganisms,[3] yet iron is present at very low concentrations (0.02−1 nM) throughout much of the world's surface ocean waters.[4−6] These low levels of iron have been shown to limit growth of many microorganisms.[4] In response to low iron environments, aerobic bacteria often produce siderophores, which are high-affinity iron(III)-binding compounds that facilitate Fe(III) transport into the bacterium.[7] While the structures of hundreds of terrestrial siderophores are known, relatively few structures of siderophores produced by marine bacteria have been elucidated.[5] A number of siderophores contain the 2,3-dihydroxybenzoate moiety, which functions in Fe(III) coordination; however, until the recent discovery of petrobactin (**1**),[8,9] no example with 3,4-dihydroxy substitution had been published. In contrast to a plethora of reported aliphatic sulfonates,[10] sulfonation of the aromatic groups is rather rare in the natural product literature. Interestingly, the known sulfonated aromatic natural products are siderophores derived from either terrestrial *Pseudomonad*[11,12] or marine *Pseudoalteromonad*[13] species. We report herein the structural characterization of a new siderophore, petrobactin sulfonate (**2**), isolated from the oil-degrading marine bacterium *Marinobacter hydrocarbonoclasticus*.

The siderophores produced in the culture of *M. hydrocarbonoclasticus* were isolated by adsorption to Amberlite XAD-2 resin after removing the bacterial cells by centrifugation and acidifying the culture medium to pH 2.5−3. The siderophores were eluted with methanol. Preparative-scale reversed-phase HPLC of this methanol fraction resulted in the isolation of the known petrobactin (**1**)[8,9] and the new compound petrobactin sulfonate (**2**), with typical yields of 1.2 and 0.55 mg per liter of culture medium, respectively.

High-resolution electrospray mass spectrometry (*m/z* 799.3199 $[M + H]^+$, $\Delta = +1.5$ mmu), in combination with ^1H and ^{13}C NMR data (Table 1), gave the molecular formula $C_{34}H_{50}N_6O_{14}S$ (13 double-bond equivalents). The presence of sulfur was confirmed by elemental analysis. More significantly, a mass difference of 80 Da from the $[M + H]^+$ molecular ion of petrobactin (HRFABMS *m/z* 719.3614)[8] suggested the addition of a sulfonate group. Further evidence supporting the presence of a sulfonate group was obtained from tandem ESI-MS in negative ion mode, considering the species at *m/z* 797.2. At a collision voltage of >150 V, a peak of *m/z* 79.9, attributable to a sulfonate moiety, was observed.

The ^1H and ^{13}C NMR assignments for petrobactin sulfonate (**2**) were confirmed by gCOSY, HSQC, gHMBC, and CIGAR[14] 2D experiments (Table 1). The splitting patterns observed in the aromatic region of the ^1H NMR spectrum were indicative of the unusual 3,4-dihydroxybenzoyl moiety, a functionality unique to petrobactin (**1**) and petrobactin sulfonate (**2**) in the marine siderophore literature. The presence of a single correlation for one of the aromatic rings in the gCOSY experiment, from H-5 (δ 6.76) to H-6 (δ 7.18), also supported 3,4-disubstitution. It was not possible to see the equivalent correlation from the other aromatic ring in this experiment, due to the closeness in chemical shift of the H-5′ (δ 6.76) and H-6′ (δ 6.72) protons. All correlations observed in the gHMBC and CIGAR experiments in the aromatic region were consistent with the presence of two catechol rings, including two $^4J_{CH}$ correlations, from H-6 (δ 7.18) to C-3 (δ 144.9) and H-6′ (δ 6.72) to C-3′ (δ 142.3), in the CIGAR experiment. No evidence to differentiate the hydroxyl protons at the 3, 4, and 4′ positions was obtained (δ 9.12, 9.16, and 9.54, respectively); however, the 3′-OH proton was able to be assigned at 11.23 ppm, due to observed correlations in the gHMBC and CIGAR experiments to C-2′ (δ 127.0), C-3′ (δ 142.3), and C-4′ (δ 147.2).

The aromatic splitting patterns in the ^1H NMR spectrum also indicated that the sulfonate group was attached to one of the catechol rings of the previously symmetrical petrobactin molecule. The H-2 doublet (δ 7.27), H-5 doublet (δ 6.76), and H-6 doublet of doublets (δ 7.18) remained from the ^1H NMR spectrum of petrobactin; however these resonances integrated as one proton, two protons, and one proton, respectively. Thus, the doublet at 6.76 ppm accounted for both H-5 and H-5′. The doublet of doublets at 7.18 ppm, assigned to H-6 and due to the combination of H-5 vicinal (ortho) coupling (8.5 Hz) and H-2 meta coupling (2 Hz), was not seen for H-6′. Instead, a one-proton doublet,

* To whom correspondence should be addressed. Tel: 805-893-8178. Fax: 805-893-4120. E-mail: butler@chem.ucsb.edu.
† University of California.
‡ University of Canterbury.
§ San Diego State University.

10.1021/np049823i CCC: $27.50
Published on Web 10/08/2004

Table 1. ^{1}H, ^{13}C, and 2D NMR Data for Petrobactin Sulfonate (**2**)

position	δ_H mult (*J* in Hz)	δ_C	gCOSY	HSQC	gHMBC and CIGAR[a]
1	na	125.4			
1′	na	126.6			
2	7.27 d (2)	115.0		C-2	C-1 (wk), C-3, C-4, C-6, C-7
2′	na	127.0			
3	na	144.9			
3′	na	142.3			
4	na	148.5			
4′	na	147.2			
5	6.76 d (8.5)	114.8	H-6	C-5	C-1, C-2 (wk),[b] C-3, C-4, C-7
5′	6.76 d (8.5)	115.5		C-5′	C-1′, C-3′, C-4′, C-7′ [b]
6	7.18 dd (2, 8.5)	119.0	H-5	C-6	C-2, C-3 (wk),[b] C-4 (wk),[b] C-7
6′	6.72 d (8.5)	119.6		C-6′	C-2′, C-3′, C-4′, C-7′
7	na	166.6			
7′	na	169.3			
8/8′	3.27 m	36.1, 36.2	H-9/H-9′, N-1H/N-1′H	C-8/C-8′	C-7/C-7′, C-9/C-9′, C-10/C-10′
9	1.80 m	26.3	H-8, H-10	C-9	C-8, C-10
9′	1.80 m	25.6	H-8′, H-10′	C-9′	C-8′, C-10′
10	2.89 m	44.8	H-9, N-2H	C-10	C-8 (wk)[b]
10′	3.12 m	44.4	H-9′, N-2′H	C-10′	C-8′,[c] C-9′[c]
11/11′	2.89 m	46.5	H-12/H-12′, N-2H/N-2′H	C-11/C-11′	C-13/C-13′ (wk)[b]
12/12′	1.56 m	23.0	H-11/H-11′, H-13/H-13′	C-12/C-12′	C-11/C-11′,[c] C-13/C-13′,[c] C-14 /C-14′ (wk)
13/13′	1.43 m	26.0	H-12/H-12′, H-14/H-14′	C-13/C-13′	C-11/C-11′, C-12 /C-12′,[c] C-14 /C-14′
14/14′	3.04 m	37.7	H-13/H-13′, N-3H/N-3′H	C-14/C-14′	C-12/C-12′, C-13 /C-13′, C-15 /C-15′
15/15′	na	169.5			
16/16′	2.50 d (15) 2.58 dd (4, 15)	43.3		C-16/C-16′	C-15 /C-15′, C-16′ /C-16, C-17, C-18
17	na	73.5			
18	na	175.0			
N-1H	8.31 t (6)	na	H-8		C-7, C-8
N-1′H	8.19 t (6)	na	H-8′		C-7′, C-8′
N-2H	8.27 m	na	H-10, H-11		
N-2′H	8.23 m	na	H-10′, H-11′		
N-3H/N-3′H	7.99 t (5)	na	H-14/H-14′		C-14 /C-14′, C-15 /C-15′
OH (C-3′)	11.23 s	na			C-2′, C-3′, C-4′
OH (C-3/C-4 /C-4′)	9.12, 9.16, 9.54 (all br s)	na			

[a] gHMBC and CIGAR experiments run with coupling constants optimized at 5 and 5−10 Hz, respectively. [b] Correlation only seen in the CIGAR experiment. [c] Weak correlation observed in the CIGAR experiment.

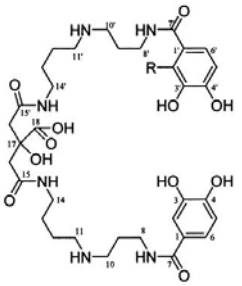

1: R = H
2: R = SO_3H

with H-5′ ortho coupling only (8.5 Hz), was observed for this proton (δ 6.72). The lack of meta coupling in this signal indicated substitution at the 2′ position. In addition, no signal assignable to a proton attached to C-2′ was observed. Thus, it was inferred that the sulfonate was in the 2′ position.

The connectivity of the molecule was determined via gCOSY, gHMBC, and CIGAR correlations (Table 1). The gCOSY experiment unequivocally established the connectivity of the two spermidinyl moieties in the molecule. In particular, gCOSY correlations from H-11 (δ 2.89) and H-13 (δ 1.43) to H-12 (δ 1.56) and from H-12 and H-14 (δ 3.04) to H-13 (along with the equivalent correlations to H-12′ and H-13′) required a reversal of the ^{1}H and ^{13}C assignments at the 12 and 13 positions from those previously reported for petrobactin (**1**).[8,9] To confirm that such a reversal should also apply in the case of petrobactin itself, a gCOSY experiment was run on a petrobactin sample. In this experiment, correlations from H-11 (δ 2.89) and H-13 (δ 1.42) to H-12 (δ 1.55) and from H-12 and H-14 (δ 3.04) to H13 confirmed that the previously reported ^{1}H and ^{13}C assignments at positions 12 and 13 in this molecule did in fact need to be interchanged.

The attachment of each catechol ring to a spermidinyl group via a carbonyl group on both sides of the molecule was established through gHMBC and CIGAR correlations (see Table 1), including two $^{4}J_{CH}$ correlations, from H-5 (δ 6.76) to C-7 (δ 166.6) and H-5′ (δ 6.76) to C-7′ (δ 169.3), in the CIGAR experiment. These experiments also established the connectivity of the N3/N3′ ends of the spermidinyl groups to a single citryl moiety, as well as the connectivity of the citryl group itself.

It appears that the structure of petrobactin sulfonate (**2**) is in the form of a double zwitterion involving N-2 and N-2′ and the sulfonate and carboxylate moieties. The strongest evidence for this lies in the observed chemical shifts for the N-2 and N-2′ protons (δ 8.27 and 8.23, respectively), which are in the correct range for protons on a positively charged nitrogen in an alkyl chain (~6−9 ppm) and significantly downfield from the expected chemical shift for protons on a neutral nitrogen atom in an alkyl chain (0.5−4 ppm).[15] Further evidence is to be found in the observed proton and carbon chemical shifts at the adjacent 10/10′

and 11/11′ positions (Table 1),[15,16] in the integrals of the protons attached to nitrogen in the ^{1}H NMR spectrum, and in the splitting of H-10′ in the same spectrum (triplet of triplets, appearing as a "quintet").

In conclusion, we report a new sulfonated siderophore, petrobactin sulfonate (**2**). Interestingly, only one of the two catecholate groups of the otherwise symmetrical molecule was sulfonated; thus C-17 is a stereogenic center in petrobactin sulfonate ($[\alpha]^{20}_D$ −2.5° (*c* 0.013, DMSO)), but not in petrobactin. A possible functional significance in the outer membrane recognition process has not yet been investigated. The sulfonate functionality was unequivocally established to be vicinal to the two hydroxyl groups on one of the catecholate ring systems, as is the case for the sulfonated dihydropyoverdins.[12] The sulfonated form of petrobactin is more hydrophilic than petrobactin, which results in shorter retention times in RP-HPLC and possibly also in reduced membrane permeability. The altered physicochemical properties might also have a function in the particular environment of *M. hydrocarbonoclasticus* at the interface of seawater to oil hydrocarbons. In an analogous case, TRENCAM, a synthetic siderophore analogue containing the aromatic 2,3-dihydroxy catechol group, was rendered more water-soluble by sulfonation.[17] Future studies of the metabolism of petrobactin sulfonate may provide new insight into the biosynthetic and biodegradative pathways of aromatic sulfonates.

Experimental Section

General Experimental Procedures. The optical rotation was measured at 589 nm (Na_D) using a Perkin-Elmer 341 polarimeter. The UV spectrum was measured on a Cary 300 spectrophotometer. ^{1}H, ^{13}C, and 2D NMR (^{1}H−^{1}H gCOSY, ^{1}H−^{13}C HSQC, ^{1}H−^{13}C gHMBC, and ^{1}H−^{13}C CIGAR) spectra were recorded on a Varian INOVA 500 MHz spectrometer. Electrospray-ionization mass spectra (ESI-MS) were recorded in both the positive and negative modes on a Micromass (Manchester, UK) quadrupole time-of-flight (QTOF-2) mass spectrometer. The elemental analysis was carried out by Quantitative Technologies Inc. (QTI). HPLC grade solvents and doubly deionized Nanopure water were used throughout.

Culture and Isolation. *M. hydrocarbonoclasticus* (SP.17; ATCC 49840)[18,19] was cultured in a hypersaline medium (0.5 M/29.22 g NaCl, 0.4 g $MgSO_4 \cdot 7H_2O$, 1.0 g NH_4Cl, 3.0 g K_2HPO_4, 0.15 g $CaCl_2 \cdot 2H_2O$, and 5.0 g sodium succinate/$Na_2C_4H_4O_4 \cdot 6H_2O$ per liter of Nanopure water) in order to optimize siderophore production. The cultures were typically grown as 2 L cultures in 4 L flasks on a rotary shaker (150 rpm) for 7 days. At the time of harvesting, cultures were in stationary phase. After centrifugation of the culture medium (5000 rpm, 20 min), Amberlite XAD-2 resin (Supelco) was added to the decanted supernatant (ca. 100 g/L), and the resultant mixture was shaken for at least 4 h at >100 rpm. The XAD was then loaded into a glass chromatography column (2 cm internal diameter), washed with one column volume of Nanopure water, and eluted with 100% methanol. Using the solution-phase Chrome Azurol S (CAS) assay with shuttle,[20] the methanol fraction was found to contain the siderophores. Since the culture medium remained CAS-positive, it was acidified to pH 2.5, re-extracted with XAD resin, and shaken at >100 rpm for at least 6 h. The XAD was again recovered, washed, and eluted as described above. The final purification was achieved on the combined methanol fractions using preparative reversed-phase HPLC (Vydac C4 column (10 μm, 22 mm i.d. × 250 mm) using a CH_3CN/H_2O gradient (0% to 60%) over 35 min, with 0.1% trifluoroacetic acid). Acid was removed from the samples via repeated addition and evaporation of methanol during the drying process.

Petrobactin sulfonate (2): white solid; $[\alpha]^{20}_D$ −2.5° (*c* 0.013, DMSO); UV (DMSO) λ_{max} (log ϵ) 229 (3.95), 253 (3.83), 291 (3.74) nm; ^{1}H NMR (DMSO-d_6, 500 MHz) see Table 1; ^{13}C NMR (DMSO-d_6, 125 MHz), see Table 1; ESI-MS *m/z* 799.3199 $[M + H]^+$ (calcd for $C_{34}H_{51}N_6O_{14}S$, 799.3184).

Acknowledgment. Funding from NIH GM38130 and The Center for Environmental BioInorganic Chemistry (CEBIC), an NSF Environmental Molecular Science Institute (CHE-0221978), is gratefully acknowledged. We thank J. Pavlovich (mass spectrometry) and A. Shirazi (NMR) for technical assistance, and A. M. Cook (Department of Biology, University of Konstanz) for useful discussions.

Supporting Information Available: ^{1}H NMR, ^{13}C NMR, gCOSY, HSQC, gHMBC, and CIGAR spectra of petrobactin sulfonate. ^{1}H NMR and gCOSY spectra of petrobactin. This material is available free of charge via the Internet at http://pubs.acs.org.

References and Notes

(1) Spoer, C.; Lanf, E.; Hobeck, P.; Burghardt, J.; Stackebrandt, E.; Tindall, B. J. *Int. J. Syst. Bacteriol.* **1998**, *48*, 1445−1448.
(2) Huu, N. D.; Denner, E. B. M.; Ha, D. T. C.; Wanner, G.; Stan-Lotter, H. *Int. J. Syst. Bacteriol.* **1999**, *49*, 367−375.
(3) Lankford, C. E. *CRC Crit. Rev. Microbiol.* **1973**, *2*, 273−331.
(4) Coale, K. H.; Johnson, K. S.; Chavez, F. P.; Buesseler, K. O.; Barber, R. T.; Brzezinski, M. A.; Cochlan, W. P.; Millero, F. J.; Falkowski, P. G.; Bauer, J. E.; Wanninkhof, R. H.; Kudela, R. M.; Altabet, M. A.; Hales, B. E.; Takahashi, T.; Landry, M. R.; Bidigare, R. R.; Wang, X.; Chase, Z.; Strutton, P. G.; Friederich, G. E.; Gorbunov, M. Y.; Lance, V. P.; Hilting, A. K.; Hiscock, M. R.; Demarest, M.; Hiscock, W. T.; Sullivan, K. F.; Tanner, S. J.; Gordon, R. M.; Hunter, C. N.; Elrod, V. A.; Fitzwater, S. E.; Jones, J. L.; Tozzi, S.; Koblizek, M.; Roberts, A. E., Herndon, J., Brewster, J., Ladizinsky, N., Smith, G., Cooper, D.; Timothy, D.; Brown, S. L.; Selph, K. E.; Sheridan, C. C.; Twining, B. S.; Johnson, Z. I. *Science* **2004**, *304*, 408−414, and references therein.
(5) Butler, A. *Science* **1998**, *281*, 207−210, and references therein.
(6) Morel, F. M. M.; Price, N. M. *Science* **2003**, *300*, 944−947, and references therein.
(7) Albrecht-Gary, A.-M.; Crumbliss, A. L. *Metal Ions Biol. Syst.* **1998**, *35*, 239−327
(8) Barbeau, K.; Zhang, G.; Live, D. H.; Butler, A. *J. Am. Chem. Soc.* **2002**, *124*, 378−379.
(9) Bergeron, R. J.; Huang, G.; Smith, R. E.; Bharti, N.; McManis, J. S.; Butler, A. *Tetrahedron* **2003**, *59*, 2007−2014.
(10) Cook, A. M.; Denger, K. *Arch. Microbiol.* **2002**, *179*, 1−6.
(11) Schröder, H.; Adam, J.; Taraz, K.; Budzikiewicz, H. Z. *Naturforsch.* **1995**, *50c*, 616−621.
(12) Budzikiewicz, H.; Fuchs, R.; Taraz, K.; Marek-Kozaczuk, M.; Skorupska, A. *Nat. Prod. Lett.* **1998**, *12*, 125−130.
(13) Kanoh, K.; Kamino, K.; Laleo, G.; Adachi, K.; Shizuri, Y. *J. Antibiot.* **2003**, *56*, 871−875.
(14) Hadden, C. E.; Martin, G. E.; Krishnamurthy, V. V. *Magn. Reson. Chem.* **2000**, *38*, 143−147.
(15) Pretsch, E.; Clerc, T.; Seibl, J.; Simon, W. *Tables of Spectral Data for Structure Determination of Organic Compounds*, 2nd ed.; Springer-Verlag: New York, 1989; pp C174−175 and H75.
(16) Sarneski, J. E.; Surprenant, H. L.; Molen, F. K.; Reilley, C. N. *Anal. Chem.* **1975**, *47*, 2116−2124.
(17) Thomas, F.; Beguin, C.; Pierre, J.-L.; Serratrice, G. *Inorg. Chim. Acta* **1999**, *291*, 148−157.
(18) Gauthier, M. J.; Lafay, B.; Christen, R.; Fernandez, L.; Acquaviva, M.; Bonin, P.; Bertrand, J.-C. *Int. J. Syst. Bacteriol.* **1992**, *42*, 568−576.
(19) Al-Mallah, M.; Goutx, M.; Mille, G.; Bertrand, J.-C. *Oil Chem. Pollut.* **1990**, *6*, 289−305.
(20) Schwyn, B.; Neilands, J. B. *Anal. Biochem.* **1987**, *160*, 47−56.

NP049823I

Current Organic Chemistry, 2000, *4*, 765-807 765

Bioactive Marine Alkaloids

S. Urban, S. J. H. Hickford, J. W. Blunt and M. H. G. Munro*

Department of Chemistry, University of Canterbury, Christchurch, New Zealand

with a contribution on the chemotaxonomy of Latrunculiidae from M. Kelly

National Institute of Water & Atmospheric Research Ltd, Auckland, New Zealand

Abstract: The structures, origins, biogenesis, synthesis and bioactivity of a selection of N-heterocyclic marine alkaloids are reviewed. The emphasis is on compounds poised as potential anticancer drugs: lamellarins (pyrroles), cephalostatins/ritterazines (pyrazines) and ecteinascidins (isoquinolines). Also discussed are examples of bioactive marine alkaloids that have emerged as novel leads. These include manzamines (β-carbolines), variolins (pyridopyrrolopyrimidines) and the pyrroloquinoline family. This review emphasises the role of marine alkaloids as an important source of leads for drug discovery.

INTRODUCTION

Mention of marine natural products conjures up visions of structures of bewildering complexity, an array of new structural types and inevitably expectations of biomedical potential. Structural complexity is confirmed by the likes of maitotoxin [1], and the rapid growth of this field is displayed graphically in Fig. (**1**) [2]. There was initial optimism in marine-derived pharmaceuticals due to the early discovery of the arabinoside nucleosides [3] and the subsequent development of successful nucleoside-based drugs such as Ara-C, acyclovir and AZT. This was followed in the 1970's by the discovery of 1-methylisoguanosine, a compound with a wide range of potent pharmacological properties [4]. Add to these early discoveries arguments based on biodiversity, and this initial optimism was well justified. We are all aware that "when it comes to diversity, nature comes out

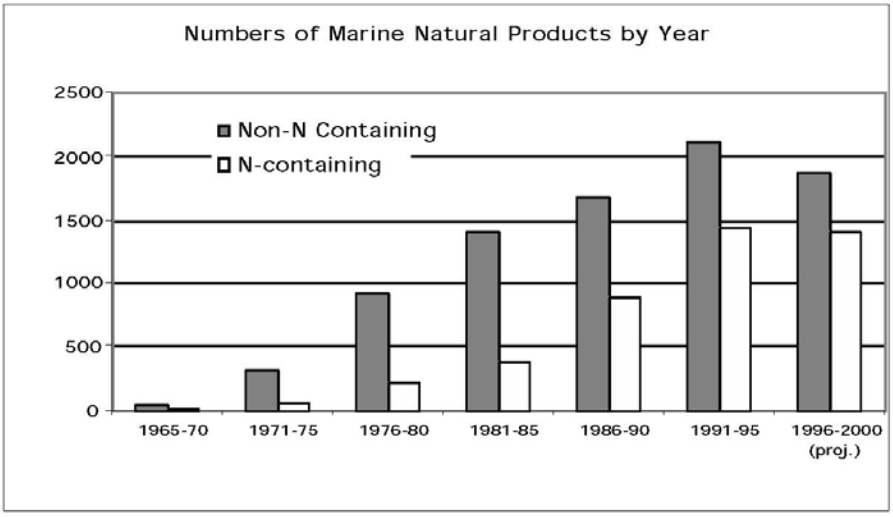

Fig. (1). Evolution of the field of marine natural products, 1965-2000.

*Address correspondence to this author at the Department of Chemistry, University of Canterbury, Christchurch, New Zealand

1385-2728/00 $19.00+.00

ahead" [5]. It has, however, taken some 50 years to reach the current situation where there are now compounds in clinical trials in the area of anticancer drugs and drugs to deal with the problem of intractable pain [6]. Over the next decade, the rate of discovery should increase. The past 25 years has seen a shift in emphasis from the curiosity-driven search for new metabolites to a more pragmatic, target-driven approach based on the application of an ever increasing number of pharmacologically-relevant assays to the evaluation of extracts and the bioassay-guided separation of active metabolites.

Since 1950, over 5,000 papers have been published reporting the structures of some 12,000 marine metabolites [2]. Over this period every marine phylum has been investigated, but more attention has been lavished on certain phyla. This is shown graphically in Fig. (**2**), where it is notable that phyla such as Porifera, Cnidaria and Rhodophycota have attracted a disproportionate amount of attention from researchers. To a certain extent, this reflects fads from the past, as in the case of the heavy emphasis on the collection of Rhodophycota in the 1970's. This trend can also be construed in terms of ease of collection of certain phyla, or the targeted collection of certain phyla such as Porifera, Chordata and Bryozoa based on the analysis of bioassay data from earlier collections [e.g. 7]. The best analysis of data to date has been that compiled by Murphy from National Cancer Institute (NCI) data which clearly showed that the incidence of bioactivity was higher in the Porifera, Chordata and Bryozoa [8].

Bioactivity has been associated traditionally with nitrogenous compounds, but until the 1970's there was a relative dearth of N-containing metabolites isolated from marine sources. In a 1977 review by Faulkner, covering the period 1974-1976, commentary is provided on a selection of 304 compounds, of which just 32 contained N (10.5%) [9]. The total structures published in that period numbered some 553, of which 79 contained at least one N [2]. Ireland *et al.* were among the first to analyse the distribution of marine metabolites [10], and for the period 1977-85, of the 1706 metabolites, 332 (19.5%) contained at least one N. As isolation

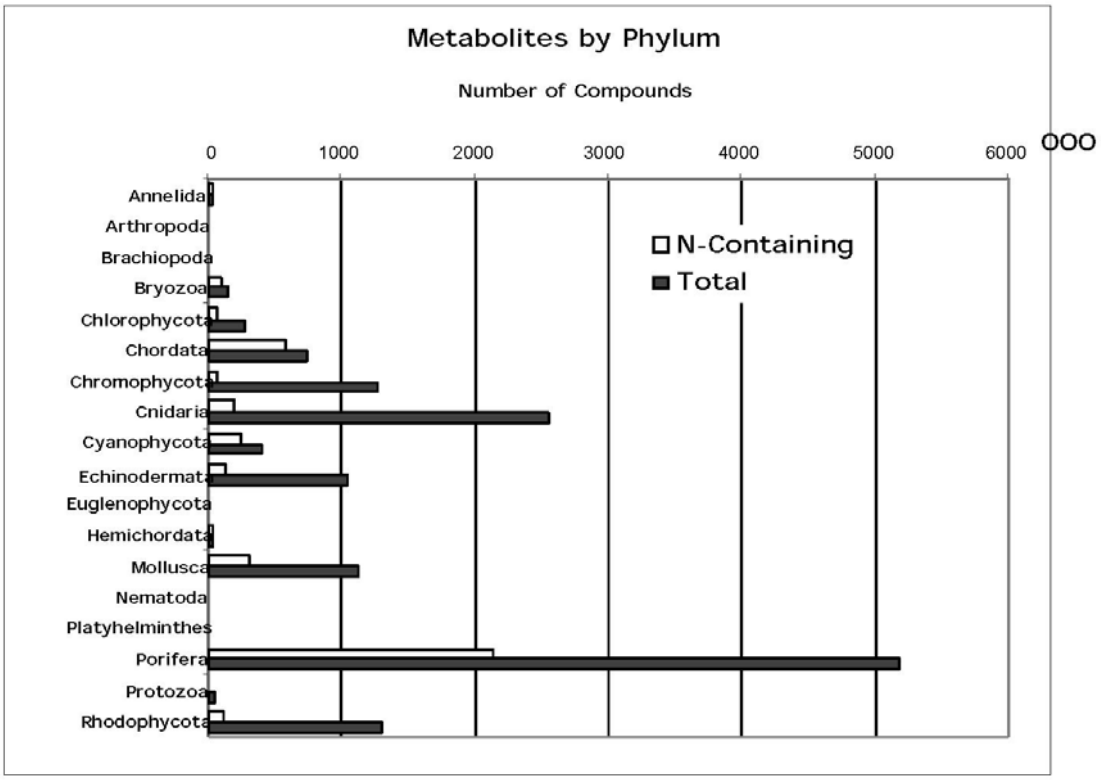

Fig. (2). Distribution of metabolites among the marine phyla.

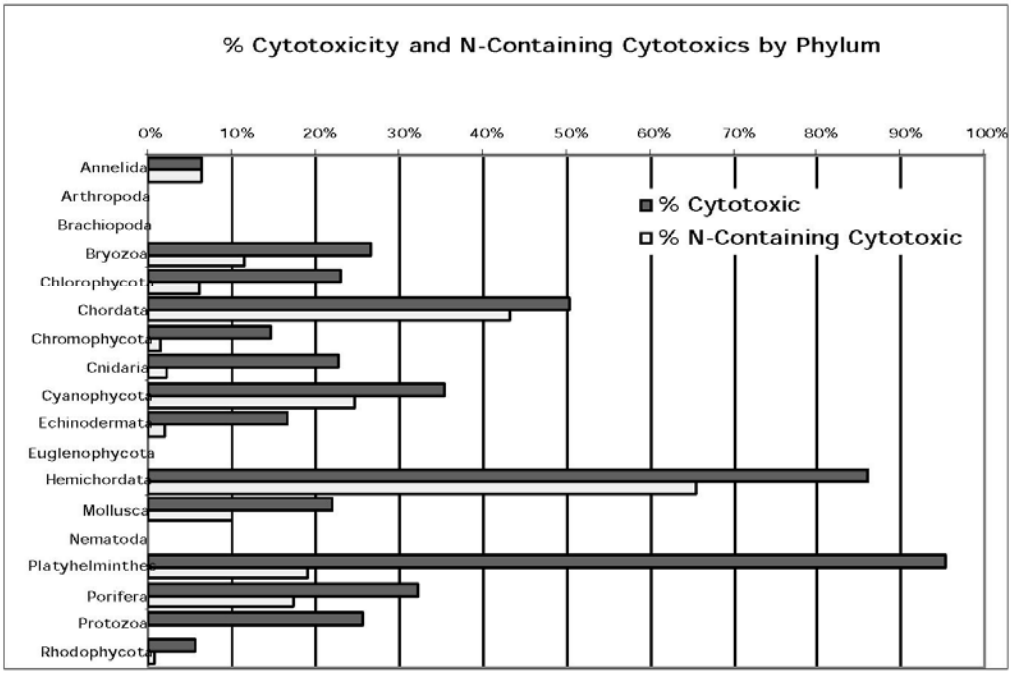

Fig. (3). Relative cytotoxicity among the marine phyla.

techniques became more sophisticated (HPLC) or better able to cope with the isolation of polar, water soluble compounds [11, 12], and bioassay-guided isolation more prevalent, this situation rapidly changed. Out of the 11,964 structures of marine origin logged in MarinLit, 3,564 (29.8%) contain at least one N [2]. In fact, 22.8% of the total metabolites contain two or more N. The changing picture over the years is shown graphically in Fig. (**1**). If the trend continues, it will not be too many years before a greater number of N-containing than non-N containing metabolites will be isolated. In Fig. (**2**), the relative proportions of N-containing metabolites is given as a function of phylum of origin. Finally, in Fig. (**3**), the relative probability of finding cytotoxic compounds from the marine environment is presented on a phylum basis. For comparison purposes, the N-containing cytotoxic compounds are compared on the same graph. A high correlation between cytotoxicity and N-containing compounds is evident in certain phyla such as Annelida, Chordata, Hemichordata or Cyanophycota, while in other phyla the correlation is not so high as in, for example, the Porifera and Bryozoa. When the range of compounds isolated from the Chordata is examined, this correlation of N with cytotoxicity is not surprising, as the reported chemistry of the phylum Chordata is dominated by that of cyclic peptides, β-carbolines, pyridoacridones etc. [2]. In contrast, the chemistry of the phylum Cnidaria is dominated by isoprenoid chemistry [2].

A selection of compounds of marine origin that are poised as potential anticancer drugs are listed in Table 1. Several of these are polyethers (spongistatins/altohyrtins/cinachyrolide, halichondrin B, isohomohalichondrin B), of peptidic origin (aplidine, dolastatin 10, cryptophycin, kahalalide, thiocoraline), macrolides (aplyronine, bryostatin 1), polyketides (discodermolide), or mixed terpenoids (eleutherobin, sarcodictyins). Nitrogen heterocycles are well represented within this selected group, encompassing the cephalostatins/ritterazines (pyrazines), ecteinascidins (isoquinolines), lamellarins (pyrroles), manzamines (β-carbolines) and eleutherobins/sarcodictyins (imidazoles).

In this review, we shall explore the origins and availability of a selection of N-heterocyclic systems that are associated with compounds of high biological activity. In each case the isolation, comments pertaining to the structural elucidation, distribution, biogenesis, synthesis and bioactivity are presented. The successful synthesis of bioactive marine natural products is particularly important, as

Table 1. Bioactive Marine Metabolites at Advanced Levels of Testing as Anticancer Drugs

Organism	Source	Activity
Aplidine	ascidian	protein synthesis inhibitor
Aplyronine	sea hare	actin
Bryostatin 1	bryozoan	-
Cephalostatin/Ritterazines	tube worm/ascidian	-
Cryptophycins	blue green alga	antimitotic
Discodermolide	sponge	antimitotic
Dolastatin 10	sea hare	antimitotic
Ecteinascidin 743	ascidian	antimitotic
Eleutherobins	soft coral	antimitotic
Halichondrin B	sponge	antimitotic
Isohomohalichondrin B	sponge	antimitotic
Kahalalide F	mollusc	-
Lamellarin N	mollusc/ascidian/sponge	antimitotic
Sarcodictyins	soft coral	antimitotic
Spongistatins/Altohyrtins/Cinachyrolide	sponges	antimitotic
Thiocoraline	marine microorganism	RNA inhibition

the ability to establish the supply of a potential drug is second only to its discovery. Too often, development of a potential drug from a marine macroorganism has been compromised by the lack of material for a full pharmaceutical evaluation.

PYRROLE ALKALOIDS

DOPA-Derived Pyrrole Alkaloids

The pyrrole ring system, found frequently in marine alkaloids, is derived either from the amino acid DOPA (2-amino-3-(3',4'-dihydroxyphenyl) propionic acid) or from tyrosine.

Isolation, Structure Determination and Distribution

The Lamellarins

The lamellarins, first reported by Faulkner's group in 1985 with the isolation of lamellarins A-D (**1-4**) from the Palauan mollusc *Lamellaria* sp. [13], represent an interesting class of natural products, as they have been isolated from various marine organisms including ascidians, sponges and molluscs. The structure of lamellarin A (**1**), determined by an X-ray crystallographic study, was found to exist in solution as a 1:1 mixture of two geometrical isomers, due to restricted rotation about the C1-C11 bond [13]. In contrast, lamellarins E-H (**5-8**) were described in 1988 from the colonial ascidian *Didemnum chartaceum* collected from the Indian Ocean [14], suggesting that lamellarins A-D (**1-4**), isolated from *Lamellaria* sp., were most likely sequestered from an ascidian in the mollusc's diet [14]. In 1993, lamellarins I-M (**9-13**) and the triacetate of lamellarin N (**14**), along with lamellarins A-D (**1-4**), were reported from the colonial ascidian *Didemnum* sp. collected in North Queensland, Australia [15], lending further support to the idea that the mollusc *Lamellaria* sp. sequesters the compounds from a didemnid ascidian food source.

Lamellarins O (**15**) and P (**16**) were the first examples of the lamellarin structure class isolated from a marine sponge, *Dendrilla cactos*, collected from Bass Strait, Australia [16]. In the case of these

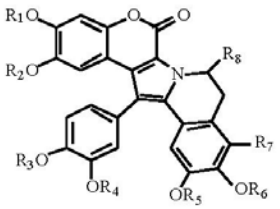

	R_1	R_2	R_3	R_4	R_5	R_6	R_7	R_8
1	H	CH_3	H	CH_3	CH_3	CH_3	OCH_3	OH
3	H	CH_3	H	CH_3	CH_3	CH_3	OCH_3	H
5	H	CH_3	CH_3	H	CH_3	CH_3	OH	H
6	H	CH_3	CH_3	CH_3	CH_3	CH_3	OH	H
7	CH_3	H	CH_3	H	CH_3	H	H	H
9	H	CH_3	CH_3	CH_3	CH_3	CH_3	OCH_3	H
10	H	CH_3	CH_3	CH_3	CH_3	H	H	H
11	H	CH_3	H	CH_3	CH_3	CH_3	OH	H
12	H	CH_3	CH_3	H	CH_3	H	H	H
19	H	H	H	H	CH_3	H	H	H
20	SO_3Na	CH_3	CH_3	H	CH_3	CH_3	OCH_3	H
21	SO_3Na	CH_3	CH_3	H	CH_3	CH_3	H	H
22	SO_3Na	CH_3	CH_3	H	CH_3	CH_3	OCH_3	OH
23	SO_3Na	CH_3	CH_3	H	H	CH_3	H	H
24	H	CH_3	CH_3	H	CH_3	CH_3	OCH_3	H
25	H	CH_3	CH_3	H	CH_3	CH_3	H	H
26	H	CH_3	CH_3	H	CH_3	CH_3	OCH_3	OH
31	SO_3^-	CH_3	H	CH_3	CH_3	CH_3	OCH_3	H
32	SO_3^-	CH_3	CH_3	H	CH_3	H	H	H
33	CH_3	H	CH_3	H	CH_3	SO_3^-	H	H
34	CH_3	H	H	H	CH_3	H	H	H

lamellarins, the pyrrole ring system is not fused to adjacent aromatic rings. From another specimen of *Dendrilla cactos*, collected off the coast of New South Wales, Australia, lamellarins Q (**17**) and R (**18**) were isolated [17]. In 1996, lamellarin S (**19**), from an Australian ascidian *Didemnum* sp., was the only example of a lamellarin that demonstrated atropisomerism [18]. Lamellarin S (**19**) displayed a positive optical rotation, indicating it to be at the very least enantiomerically enriched [18]. Repeated optical rotation measurements of lamellarin S (**19**) over several months suggested slow racemisation, with a half-life calculated to be *ca.* 90 days [18]. Molecular modeling indicated that the lowest energy barrier to rotation for lamellarin S (**19**) was 84 kJ/mol, with both atropisomers being of comparable energy [18]. Nine further lamellarin analogues were reported from an unidentified ascidian from the Arabian Sea [19]. These included the first report of four sulfated lamellarins, namely the 20-sulfated derivatives of lamellarins T, U, V and Y (**20-23**), and lamellarins T to X (**24-28**), as well as the isolation of lamellarin N (**29**) [19]. Five further lamellarin-class alkaloids were reported in 1999 from the Australian ascidian *Didemnum chartaceum*, collected from the Great Barrier Reef [20]. These included the 20-sulfated derivatives of lamellarins B, C and L (**30-32**), the 8-sulfated derivative of lamellarin G (**33**) and one non-sulfated compound, lamellarin Z (**33**) [20]. Lamellarin G 8-sulfate (**33**) is the first example of a lamellarin with a sulfate substituent at the C8 position, while lamellarin Z (**34**) is the first example of a demethoxylated lamellarin [20]. Finally, the most recent lamellarin isolated is lamellarin α 20-sulfate (**35**), which was isolated from the same ascidian collected from the Arabian Sea described above [19, 21]. Lamellarin α 20-sulfate (**35**) is of particular interest as it is active against both pre-integration complexes *in vitro* and the HIV-1 virus in cell culture [21].

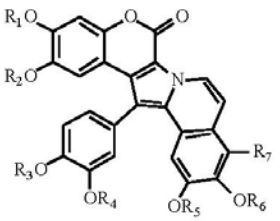

	R_1	R_2	R_3	R_4	R_5	R_6	R_7
2	H	CH_3	H	CH_3	CH_3	CH_3	OCH_3
4	H	CH_3	H	CH_3	CH_3	H	H
8	H	H	H	H	H	H	H
13	H	CH_3	H	CH_3	CH_3	CH_3	OH
14	Ac	CH_3	CH_3	Ac	CH_3	Ac	H
27	H	CH_3	CH_3	H	CH_3	CH_3	OCH_3
28	H	CH_3	CH_3	H	CH_3	CH_3	OH
29	H	CH_3	CH_3	H	CH_3	H	H
30	SO_3^-	CH_3	H	CH_3	CH_3	CH_3	OCH_3
35	SO_3Na	CH_3	H	CH_3	CH_3	CH_3	H

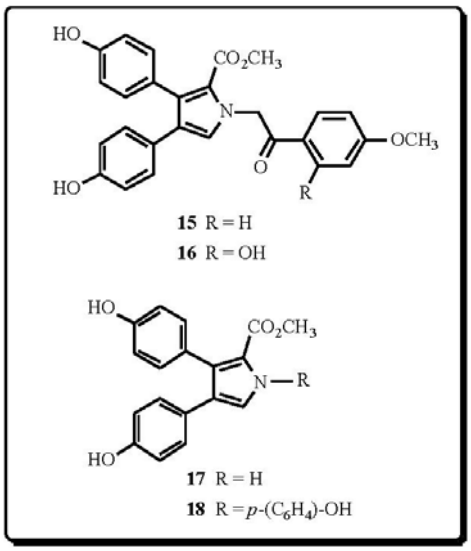

The Ningalins

Ningalins A-D (**36-39**) were reported in 1997 from a Western Australian ascidian of the genus *Didemnum* [22]. These aromatic alkaloids possess new carbon skeletons, and are composed of C18, C25, C32 and C40 condensed aromatic systems, respectively, with the common feature being that all appear to be derived from the condensation of two, three, four and five DOPA precursors, respectively [22]. These highly condensed alkaloids experience much steric crowding, thereby forcing several catechol rings into twisted configurations.

The Lukianols

In 1992, two cytotoxic triphenylpyrrolo-oxazinones, lukianol A (**40**) and lukianol B (**41**), were isolated from an encrusting ascidian collected in a lagoon in the Palmyra atoll [23]. A structural relationship exists between the lukianols and the lamellarins.

The Polycitones and Polycitrins

In 1994, three compounds, polycitone A (**42**) and polycitrins A (**43**) and B (**44**), were reported from the marine ascidian *Polycitor* sp. collected in Sodwana Bay, South Africa [24]. These compounds represent novel marine alkaloids with unprecedented

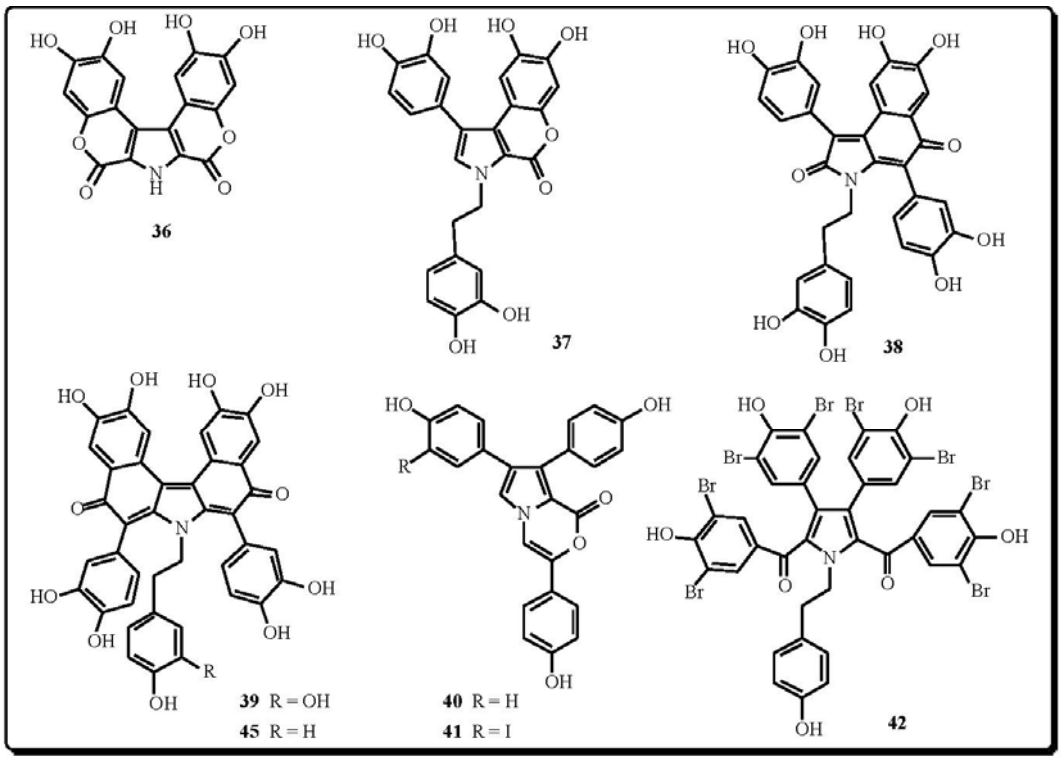

carbon skeletons, with polycitrins A and B being fluorescent.

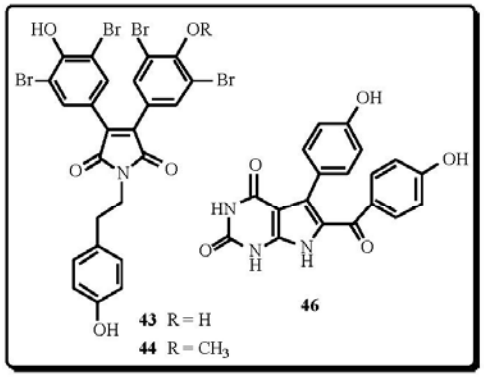

Purpurone

In 1993, a purple compound named purpurone (**45**) was reported from the marine sponge *Iotrochota* sp. collected in Palau [25]. As the pure compound could not be isolated until the extract had been subjected to mild acid hydrolysis, it was speculated that the more lipophilic compound came from precursors that were either sugar or protein conjugates [25].

Tyrosine-Derived Pyrrole Alkaloids

Rigidin

Rigidin (**46**), one of the first tyrosine-derived pyrrole alkaloids, was isolated in 1990 from the Okinawan marine ascidian *Eudistoma* cf. *rigida* [26]. Rigidin was isolated as a purple compound, and reported to display potent calmodulin antagonistic activity [26].

The Storniamides

In 1996, four novel peptide alkaloids, storniamides A-D (**47**-**50**), were described from the sponge *Cliona* sp. collected near San Antonio Oeste, Argentina [27]. It was noted that the storniamides are derived from tyrosine units. Structural resemblance to other marinemetabolites, such as the lukianols A (**40**) and B (**41**), polycitone A (**42**) and polycitrins A (**43**) and B (**44**) (which all lack the two enamide functionalities found in the storniamides), and the sponge metabolite purpurone (**45**), as well as the lamellarins (which possess additional rings), has also been noted.

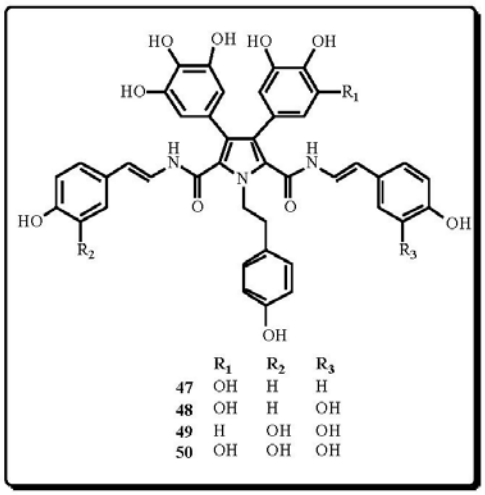

SYNTHESIS

DOPA-Derived Pyrrole Alkaloids

There has been intense interest in the lamellarins from synthetic chemists, probably due to their very interesting biological properties. In 1995, the first synthesis of lukianol A (**40**) and lamellarin O dimethyl ether (**51**) was reported by Fürstner and co-workers, using a titanium-mediated approach [28]. As this synthesis passes through the formation of lamellarin O dimethyl ether (**51**), the close chemical relationship between these natural products, isolated from distinctly different marine organisms, was noted [28]. In 1997, total syntheses of lamellarin D (**4**) and lamellarin H (**8**) were reported by Ishibashi *et al.* [29]. The pentacyclic lamellarin ring system was constructed by *N*-ylide mediated pyrrole ring formation and subsequent lactonisation of the intermediate obtained by an assembly of a known benzylisoquinoline, benzoate and ethyl bromoacetate [29]. A biomimetic three step one-pot synthesis of lamellarin G trimethyl ether (**52**) was reported in 1997 [30]. Following Pharma Mar's report on the efficacy of lamellarin K (**11**) in the treatment of multidrug resistant tumours [31], a convergent total synthesis of lamellarin K (**11**) was reported by Banwell *et al.* [32], and later patented [33]. The pivotal step in the approach to the lamellarin ring system involved construction of the central pyrrole ring moiety *via* an intramolecular [3+2] cycloaddition of an isoquinoline-based azomethine ylide to give a suitably tethered tolan [32, 33]. Very recently, the core unit associated with lamellarins K (**11**) and N (**35**) was formed from a 1,2,4-trisubstituted pyrrole,

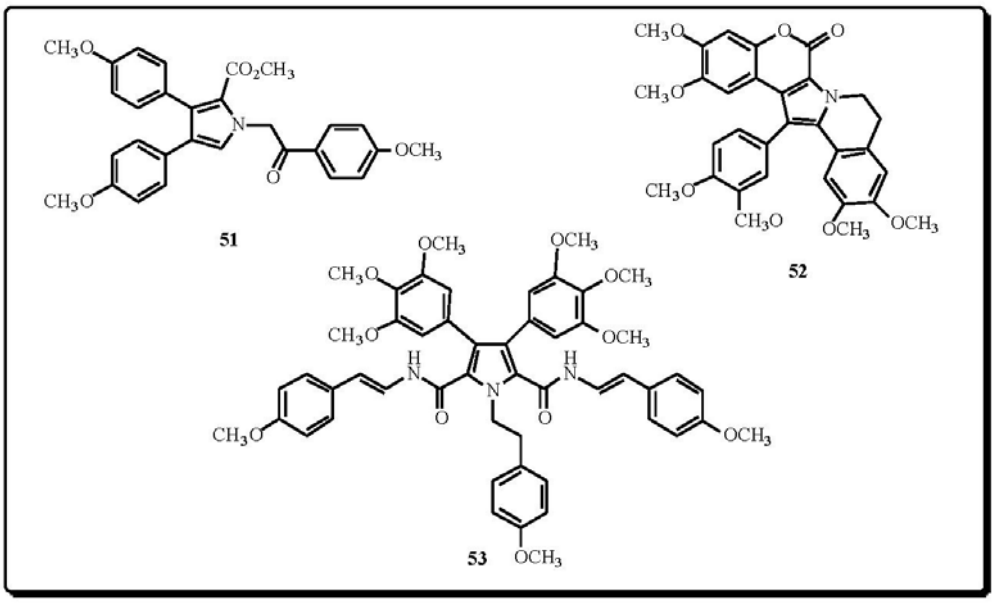

which underwent a double-barrelled Heck cyclisation [33]. The approach here involved construction of the pyrrole core first, and then construction of the lamellarin framework around this core using Negishi and double-barrelled Heck-type reactions to establish key carbon-carbon bonds [34]. Lamellarin O (**15**), lamellarin Q (**17**) and lukianol A (**40**), as well as some more highly oxygenated congeners, have been synthesised by Banwell *et al.*, using Stille, Suzuki or Negishi cross-coupling reactions as the key step [35]. These syntheses represent rare examples of the use of palladium-catalysed cross-coupling chemistry for the introduction of carbon-based substituents onto the pyrrole nucleus [35]. The latest convergent synthesis of the lamellarins involves a one-pot reaction of a 3,4-dihydro-1-benzylisoquinoline and a 3-bromocoumarin [36]. The key steps include an intermolecular Michael-type addition, followed by an intramolecular S_N2 reaction [36]. Ningalin A (**36**), lamellarin O (**15**), lukianol A (**40**) and permethyl storniamide A (**53**) were recently synthesised by Boger *et al.* [37]. This concise, non-obvious approach employed a heteroaromatic azadiene Diels-Alder reaction to assemble the substituents onto a six-membered 1,2-diazine core. This was followed by a reductive ring contraction reaction to provide the corresponding pyrrole, an entity not normally assembled by a [4+2] cycloaddition reaction [37].

In 1995, the biomimetic total synthesis of polycitrin A (**43**) was described [38]. It was formed in six steps from 3-(4-methoxyphenyl)-pyruvic acid, and is based on the formation of 3,4-bisarylpyrrole-2,5-dicarboxylic acids from 3-arylpyruvic acids by oxidative coupling and sequential pyrrole ring formation [38]. The pyrrole dicarboxylic acids are then converted into 3,4-bisaryl maleimides by treatment with hypochlorite [38]. Bromination and introduction of the *N*-alkyl substituent completed the synthesis [38].

Tyrosine-Derived Pyrrole Alkaloids

An efficient nine-step synthesis of rigidin (**46**) was first reported in 1993, from 6-chlorouracil and ethyl (2,4-dimethoxybenzyl)-glycinate [39]. A key feature of the synthetic route revealed a new method for the annulation of pyrrole rings onto pyrimidine rings. In 1994, a second total synthesis of rigidin (**46**) was reported by Sakamoto and co-workers [40]. In this case, rigidin (**46**) was synthesised in six steps by the combination of acylation *via* lithiation and arylation by a palladium-catalysed reaction starting from 2,4-dimethoxypyrrolo[2,3-*d*]pyrimidine [40]. A third synthesis of rigidin (**46**) was reported in 1995, starting from 2,4-dimethoxy-7-phenylsulfonylpyrrolo[2,3,-*d*]pyrimidine [41]. A recent synthesis of rigidin (**46**) featured a new method for the annulation of pyrrole rings onto a pyrimidine ring, which was achieved in nine steps [42].

A concise three step synthesis of storniamide A nonamethyl ether (**53**) was achieved from 3-(3,4,5-

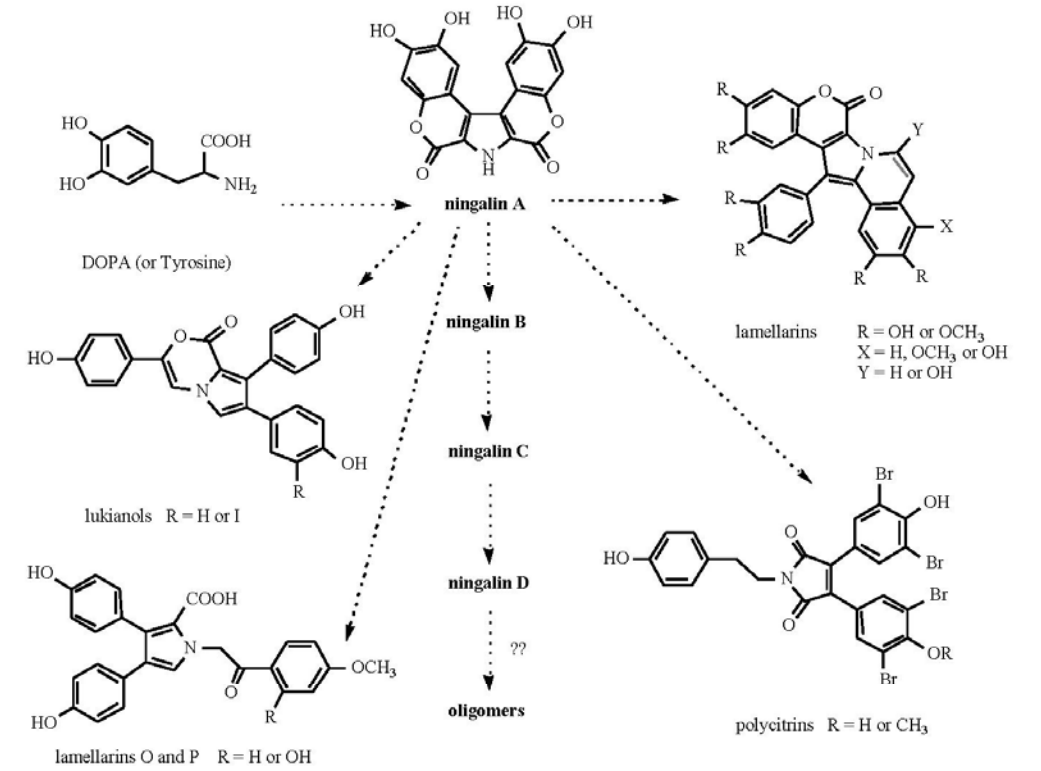

Fig. (4). Postulated biogenetic pathway for the alkaloids thought to be DOPA-derived.

trimethoxyphenyl)-pyruvic acid and 2-(4-hydroxyphenyl)-ethylamine [43].

Biogenesis

The biogenesis of this group of pyrrole compounds is suggested to proceed *via* the condensation of two, three, four and five DOPA precursors, respectively (Fig. (**4**)) [22], leading to the lamellarins, polycitrins and lukianols by way of the ningalins. In addition, the close analogy between purpurone (**45**) and ningalin D (**39**) indicates that DOPA condensation chemistry is biologically more widespread than previously thought [22].

The polyaromatic lamellarin alkaloids were proposed to be derived from three tyrosine residues [15]. However, the isolation of lamellarin R (**18**) represented a curious departure from the common structural features of the lamellarins. The *N*-substituent to lamellarin R (**18**) appears not to be derived from tyrosine [17].

As mentioned previously, a structural relationship exists between the lukianols and the lamellarins. Cleavage of the bond between C5 of the pyrrole and its phenyl substituent in lamellarin A (**1**), followed by opening and re-closing the lactone ring with the *N*-alkyl chain, results in the generation of a lukianol [23]. This idea was supported by the isolation of lamellarin O (**15**), which was proposed to be a ring-opened analogue of lukianol A (**40**).

A possible biogenetic relationship between the lamellarins and polycitone A (**42**) and polycitrins A (**43**) and B (**44**) was put forward by Kashman *et al.* in 1994 [24]. Purpurone (**45**) is a 40-carbon metabolite which bears some similarity to polycitone A (**42**), despite having a different skeleton and ring system.

Given the occurrence of lamellarins in molluscs, ascidians and sponges, the question of the biosynthetic origin of the lamellarins and the potential role of symbiotic organisms must be considered.

Bioactivity of the Lamellarins

Undoubtedly, the outstanding activity of some of the lamellarin alkaloids is responsible for the many synthetic efforts and patent applications on this structure class. The syntheses of some of the lamellarins have allowed the biological activity of these natural products to be further investigated. For instance, lamellarin O (**15**) and lukianol A (**40**) were shown to exhibit modest cytotoxic activity against both wild-type and multidrug resistant (MDR) tumour cell lines, with the former compound exhibiting activity at a micromolar level, suggesting it may serve as a new lead for the development of antitumour agents insensitive to MDR [37]. In addition, a new class of agents, including permethyl storniamide (**53**) and its precursor (**54**), which lack inherent cytotoxic activity, reverse the multidrug resistant phenotype, re-sensitising a human colon cancer cell line (HCT116/VM46) to vinblastine and doxorubicin at lower doses than the prototypical agent verapamil [37].

Lamellarin α 20-sulfate (**35**) has been found to be an inhibitor of HIV-1 integrase, and is active against the HIV-1 virus in cell culture [21]. While sulfated molecules have been identified as integrase inhibitors, lamellarin α 20-sulfate (**35**) is of particular interest as it represents a compound which is active against pre-integration complexes as well as a purified integrase protein and virus [21]. Lamellarin α 20-sulfate (**35**) inhibited the integrase terminal cleavage activity, with an IC_{50} of 16 μM, and the strand transfer activity, with an IC_{50} of 22 μM [21]. The toxicity of the lamellarin sulfates was tested using the MTT cytotoxicity assay, with lamellarin α 20-sulfate (**35**) displaying the least toxicity (LD_{50} 274 μM) [21]. The antiviral IC_{50}'s for lamellarin α 20-sulfate (**35**), using a variety of HIV assays, had a range of 8-62 μM [21]. These findings provide a new class of compound for potential development of clinically useful integrase inhibitors [21].

Studies of the resistance modifier activity of different lamellarins at non-toxic concentrations were carried out in cells exhibiting multidrug resistance (MDR). Lamellarin I (**9**) exhibited the highest chemosensitising activity [31]. At non-toxic doses, verapamil and lamellarin I (**9**) effectively increased the cytotoxicity of doxorubicin, vinblastine and daunorubicin in a concentration-dependent manner in MDR cells, but the potency of lamellarin I (**9**) as a MDR modulator was 9- to 16-fold higher than that of verapamil [31]. It has been suggested that lamellarin I (**9**) reverses MDR by directly inhibiting the P-glycoprotein-mediated drug efflux. These results highlighted the possibility of using these marine-derived compounds as anti-MDR drugs and as non-toxic modulators of the MDR phenotype [31].

All lamellarins display some level of cytotoxicity, however lamellarin D triacetate (**55**), lamellarin K (**11**), lamellarin K triacetate (**56**), lamellarin M (**13**) and lamellarin N triacetate (**14**) exhibited the highest cytotoxic activity against all the cell lines tested [31]. The results of this study suggested that lamellarins may be useful in the treatment of MDR tumours by means of two independent mechanisms of action: cytotoxicity against cancer cells and enhancement of the cytotoxicity of doxorubicin against MDR cells, restoring in them the levels of sensitivity to those of the parental cells [31]. Although a clear correlation between structure and cytotoxic activity of the lamellarins tested could not be established, it was suggested that an increase in the number of methylations and/or methoxylations caused a decrease in the antitumour activity of the compounds [31]. After determination of cytotoxicity, the different lamellarins were tested for chemosensitisation at non-toxic concentrations [31]. Lamellarin I (**9**) was the most potent of all the lamellarins tested for both chemosensitisation to doxorubicin-mediated inhibition of P388/Schabel cell growth, and restoration of the retention of rhodamine 123 in Lo Vo/Dx cells [31]. In 1997,

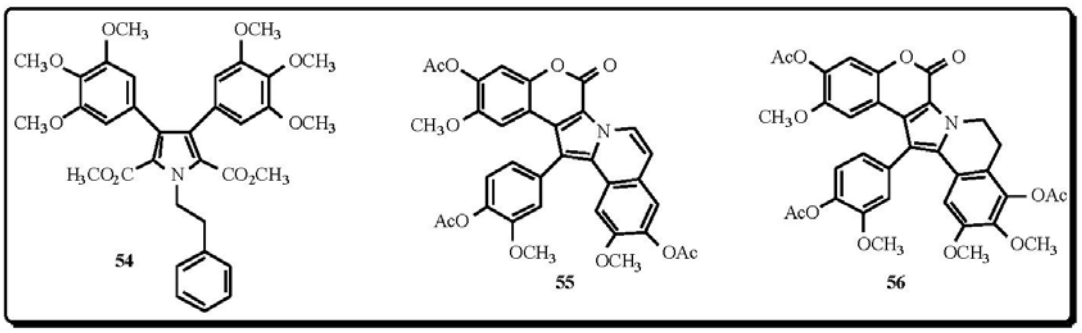

Pharma Mar patented the use of the lamellarins for the treatment of MDR tumours [44].

PYRAZINE ALKALOIDS

Isolation, Structure Determination and Distribution

The dimeric steroid pyrazine marine alkaloids, which include the cephalostatins and theritterazines, are remarkable natural products. There are now 45 trisdecacyclic pyrazines, which have been exclusively isolated and characterised by the Pettit and Fusetani groups [45-49]. As with many other compounds of marine origin, the structures of the cephalostatins and ritterazines were unprecedented in both the marine and terrestrial environments.

The cephalostatins were isolated from the marine tube worm *Cephalodiscus gilchristi* collected off East Africa, while the ritterazines were isolated from the Japanese ascidian *Ritterella tokioka* [45-49]. The presence of these compounds in two disparate phyla suggests the involvement of a symbiotic microorganism. As there have been several reviews on these compounds, covering isolation, structure elucidation, biological activity and synthetic efforts to 1995 [45-49], only significant details published after 1995 will be discussed.

The Cephalostatins

There have been a total of 19 cephalostatins isolated by Pettit *et al.* from various collections of the East African marine tube worm *Cephalodiscus gilchristi* [50-61]. The first collection of *C. gilchristi* was made in 1972 [50], but due to the low yield of the cephalostatins (0.0008%) and the complexity and unprecedented nature of their structures, cephalostatin 1 (**57**) was not reported until 1988 [50]. This structure, a tridecacyclic compound, is quite unusual as it consists of nine fused rings formed by the coupling of two highly functionalised steroid units, linked to a pyrazine ring at their 2,3-positions. In addition, two spiroketal rings terminate each end of the fused ring system, generating a total of thirteen rings. In the ten years from 1988 to 1998, a further eighteen cephalostatins were reported by the Pettit group [51-61]. The cephalostatins exhibit extraordinarily strong cytotostatic activity, with their most potent member, cephalostatin 1 (**57**), being 400-fold more active *in vitro* than taxol, and one of the most powerful cytostatics ever to be tested by the NCI [62 and references therein]. Quite recently, the newest members of the cephalostatin family of compounds, namely cephalostatins 18 (**58**) and 19 (**59**), were reported as "the last currently detectable" cephalostatins from a 1990 re-collection of *C. gilchristi* [61]. Structure activity information on this series has grown significantly because of the isolation of new cephalostatins, the isolation of the ritterazines and the enormous concurrent synthetic efforts [45].

The Ritterazines

There have now been a total of 26 ritterazines isolated by Fusetani *et al.*, all from the ascidian *Ritterella tokioka* [63-69]. The ritterazines and cephalostatins share common structural features. The cephalostatins have the more oxygenated Northern hemispheres, while the Southern hemispheres are more oxygenated in the ritterazines. Fusetani *et al.* went on to employ the use of ^{15}N-HMBC NMR techniques to determine the orientation of the two steroidal units about the pyrazine ring in ritterazine A (**60**) [65]. With the isolation of ritterazines B (**61**) and C (**62**), they were able to determine the absolute configuration by application of the modified Mosher method [66, 68]. Prior to this, Pettit had speculated about the absolute configuration of cephalostatins from X-ray data [50].

The isolation of ritterazines D-M in 1995 [64] has been reviewed [45, 48]. In 1997, Fusetani *et al.* reported the isolation of ritterazines N-Z (**63-75**) [63]. Ritterazines N to S (**63-68**), having two nonpolar steroidal units, were much less active than ritterazine B (**61**). Ritterazines T to Y (**69-74**) are related to ritterazine A (**60**) and B (**61**), being composed of polar and nonpolar steroidal units, but lacking the C7' and C17' hydroxyl groups. Ritterazine V (**72**) is the only ritterazine in which a polar steroidal unit is rearranged. Chemical transformations of ritterazine B (**61**) (the most active of the ritterazines) led to eight further synthetic ritterazines (**76-83**), and gave information as to the structural features of the ritterazines important for cytotoxic activity [63].

Although ritterazines T to X (**69-73**) are only marginally active, ritterazine Y (**74**) is a potent cytotoxin [63]. However, it is 30 times less potent than ritterazine B (**61**). The modification of ritterazine Y (**74**), i.e. rearrangement of the steroid skeleton(s) and isomerisation of the 5/6 spiroketal to the 5/5 spiroketal, significantly diminished the cytotoxic activity. Ritterazine Z (**75**) is the only isomer that forms an oxygen bridge between C18 and C22. Weak cytotoxic activity of this compound is probably due to the presence of the rearranged nonpolar unit in the Northern hemisphere [63]. A

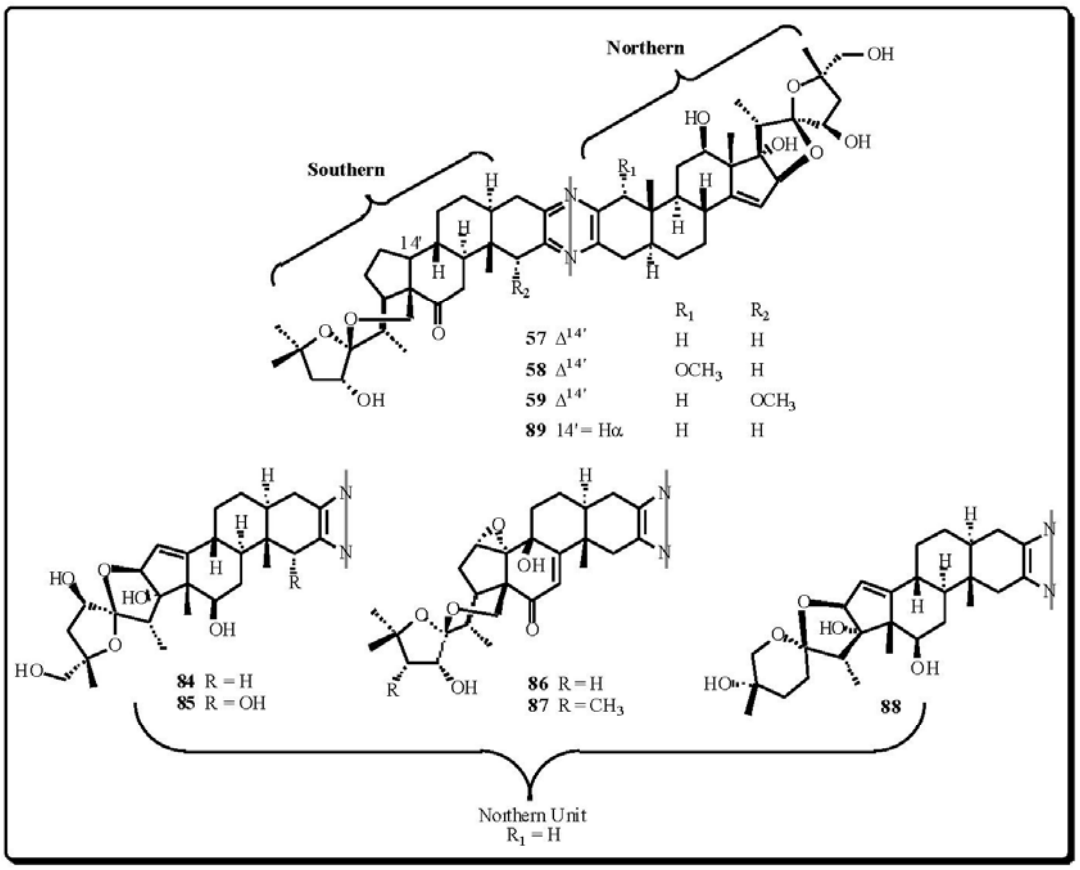

significant contribution of the terminal 5/6 spiroketal to cytotoxicity is evident by comparing the activities of ritterazines B (**61**) and C (**62**). It was suggested that the spatial arrangement of the 5/6 spiroketal with respect to the rest of the skeleton is of importance for the potent cytotoxic activity. The presence of the 5/6 spiroketal on the right hand side of the polar steroid unit is necessary, but is not sufficient to account for the potent cytotoxic activity. Symmetric, or nearly symmetric, ritterazines (ritterazines J to M, having two polar steroidal units with a 5/6 spiroketal) are 100 times less active than ritterazine B (**61**) [63]. For full descriptions of the ritterazines, the reader is referred to Fusetani's work [63].

Bioactivity

Cephalostatin 1 (**57**) is an extremely potent *in vivo* cytotoxic agent, and a powerful inhibitor of cell growth (PS cell line ED_{50} 10^{-7}-10^{-9} μg/mL) [51]. The mode of action of cephalostatin 1 (**57**) is unknown. However, given their steroidal nature and the ubiquitous presence of sterols in eukaryotic cell membranes, it has been suggested that the cephalostatins may well be acting at this level [51]. The dimeric nature of cephalostatin 1 (**57**), with its molecular dimensions of 30 Å x 9 Å x 5 Å, led to the suggestion that the dimer may be able to span the lipid bilayer and perturb the eukaryotic cell membrane [48]. The presence of two hydrophilic ends, the result of oxygenation in the steroidal side chain and the C-D rings, would facilitate such a role [51]. Another suggested role is that of enzyme inhibitors that form hydrogen bonds with a specific target [48,70]. More recently, Fuchs has suggested a process that involves protonation or epoxidation of the D-ring double bond to generate reactive electrophilic intermediates [48, 71].

Between 1989 and 1994, Pettit *et al.* patented the isolation, structure elucidation and use of cephalostatins 1 through 9 as antitumour agents [72-75].

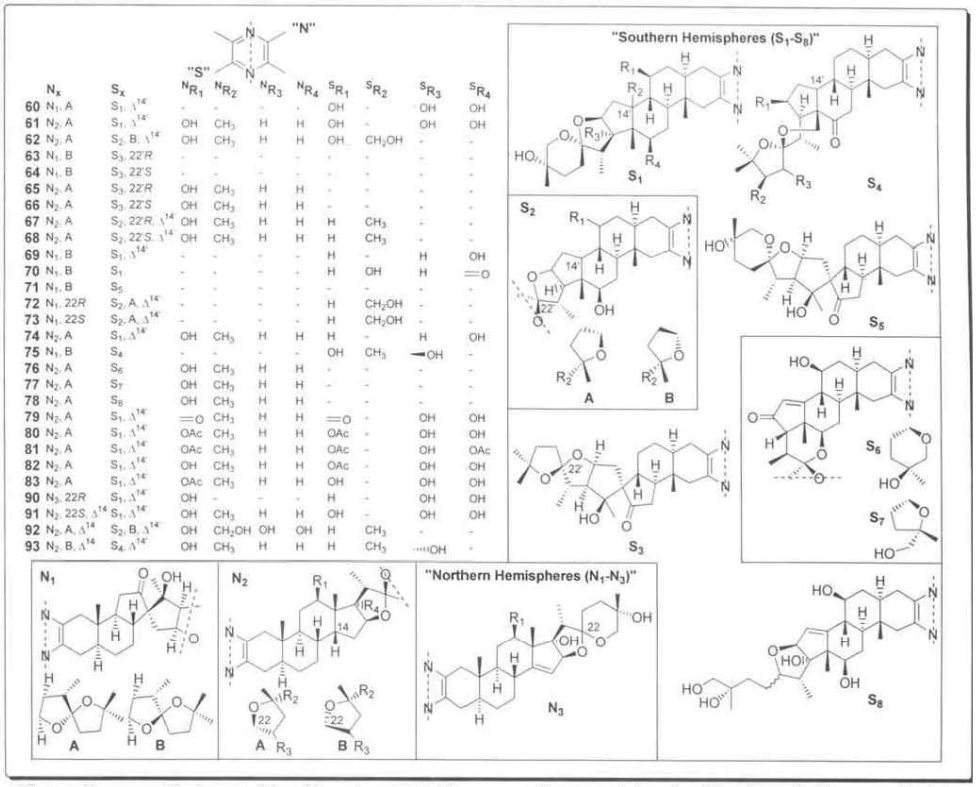

	N_x	S_x	$^NR_1$	$^NR_2$	$^NR_3$	$^NR_4$	$^SR_1$	$^SR_2$	$^SR_3$	$^SR_4$
60	N_1, A	S_1, Δ^{14}	-	-	-	-	OH	-	OH	OH
61	N_2, A	S_1, Δ^{14}	OH	CH_3	H	H	OH	-	OH	OH
62	N_2, A	S_2, B, Δ^{14}	OH	CH_3	H	H	OH	CH_2OH	-	-
63	N_1, B	S_3, 22*R*	-	-	-	-	-	-	-	-
64	N_1, B	S_3, 22*S*	-	-	-	-	-	-	-	-
65	N_2, A	S_3, 22*R*	OH	CH_3	H	H	-	-	-	-
66	N_2, A	S_3, 22*S*	OH	CH_3	H	H	-	-	-	-
67	N_2, A	S_2, 22*R*, Δ^{14}	OH	CH_3	H	H	H	CH_3	-	-
68	N_2, A	S_2, 22*S*, Δ^{14}	OH	CH_3	H	H	H	CH_3	-	-
69	N_1, B	S_1, Δ^{14}	-	-	-	-	H	-	H	OH
70	N_1, B	S_1	-	-	-	-	H	OH	H	=O
71	N_1, B	S_5	-	-	-	-	-	-	-	-
72	N_1, 22*R*	S_2, A, Δ^{14}	-	-	-	-	H	CH_2OH	-	-
73	N_1, 22*S*	S_2, A, Δ^{14}	-	-	-	-	H	CH_2OH	-	-
74	N_2, A	S_1, Δ^{14}	OH	CH_3	H	H	H	-	H	OH
75	N_1, B	S_4	-	-	-	-	OH	CH_3	OH	-
76	N_2, A	S_6	OH	CH_3	H	H	-	-	-	-
77	N_2, A	S_7	OH	CH_3	H	H	-	-	-	-
78	N_2, A	S_8	OH	CH_3	H	H	-	-	-	-
79	N_2, A	S_1, Δ^{14}	=O	CH_3	H	H	=O	-	OH	OH
80	N_2, A	S_1, Δ^{14}	OAc	CH_3	H	H	OAc	-	OH	OH
81	N_2, A	S_1, Δ^{14}	OAc	CH_3	H	H	OAc	-	OH	OAc
82	N_2, A	S_1, Δ^{14}	OH	CH_3	H	H	OAc	-	OH	OH
83	N_2, A	S_1, Δ^{14}	OAc	CH_3	H	H	OH	-	OH	OH
90	N_3, 22*R*	S_1, Δ^{14}	OH	-	-	-	H	-	OH	OH
91	N_2, 22*S*, Δ^{14}	S_1, Δ^{14}	OH	CH_3	H	H	OH	-	OH	OH
92	N_2, A, Δ^{14}	S_2, B, Δ^{14}	OH	CH_2OH	OH	OH	H	CH_3	-	-
93	N_2, B, Δ^{14}	S_4, Δ^{14}	OH	CH_3	H	H	H	CH_3	OH	-

Nature has provided a wealth of structure activity relationships in the form of the 45 variations on the pyrazine structural theme, although a number of questions remain [76 and references therein]. One of these relates to subtle variations of stereochemistry and substitution observed on the six basic steroid units, which generate marked effects on bioactivity. The 19 cephalostatins exhibit some of the most extreme examples of differential cytotoxicity yet encountered in the NCI screen [57]. The variation in sensitivity among the different lines spans as much as 1,000 to 10,000-fold [57]. A comparable pattern is seen with the cytostatic activities of ritterazines A-Z and the eight synthetic analogues [63-69]. Interestingly, the cephalostatins are very much more cytotoxic against P388 murine leukaemia cells (ED_{50} values in the range 10^{-4}-10^{-7} ng/mL) than the ritterazines (IC_{50} 10^{-3}-10^{-2} ng/mL) [68].

In summary, the SAR's in the cephalostatin series suggests that aromatisation of the C'-ring markedly diminishes the potency [56]. In addition, an increased level of hydroxylation resulted in a decrease in human cancer cell growth inhibition, as in the cases of cephalostatin 12 (**84**) and cephalostatin 13 (**85**) compared to cephalostatin 1 (**57**) [58]. With the isolation of cephalostatins 14 (**86**) and 15 (**87**), it was found that modification of the left-side moiety by introduction of the 8β-hydroxy-11-ene-12-one and/or the 14,15α-epoxy system resulted in a reduction of the *in vitro* activity [59]. Recent SAR studies on cephalostatins and their analogues revealed that the Northern part is not only the most common unit in the cephalostatin family but is also strongly associated with the most potent antitumour activity [76, 77].

In the ritterazine series, A (**60**), B (**61**), D-M and Y (**74**) were highly cytotoxic to P388 leukaemia cells, whereas N (**63**), O-S (**64-68**), W (**72**), X (**73**) and Z (**75**), having no 5/6 spiroketal, were only marginally active [67]. It is noteworthy that by synthesis a whole new range of bioactive pyrazine analogues have become available (see next section).

Synthesis

Clinical trials of cephalostatins 1 (**57**) and 7 (**88**) stalled because of severe difficulties in harvesting these rare materials. Just 100 mg and < 60 mg, respectively, were obtained from 450 kg of worm collected by SCUBA operations at the extreme depths of 60-80 m. Supply by synthesis is non-trivial due to the complexity of their steroidal substructures. However, just four years after the isolation of cephalostatin 1 (**57**), the first synthetic studies in this area were reported by Fuchs *et al.* [70]. The outstanding cytostatic activity of the cephaplostatins, together with their structural novelty and rarity, had immediately led to synthetic activities in various laboratories, but with different goals. Either the focus was on the total synthesis of the cephalostatins, or on the synthesis and biological evaluation of appropriate analogues in an attempt to determine essential biological substructures. The synthetic efforts have been undertaken by Fuchs [70-71, 76-93], Winterfeldt [62, 94-97] and Heathcock [98-101], with one other report in 1997 [102]. The syntheses and methodologies reported up to 1995 have been reviewed by Ganesan [45]. Since 1995, there has been continued success in the synthesis of cephalostatin and ritterazine analogues.

Examination of the analogues prepared by synthesis disclosed the importance of the $\Delta^{14,15}$ double bond and the nonsymmetric structure of the cephalostatins for activity [45, 71]. In 1996, dihydrocephalostatin 1 (**89**), which has a C/D-*trans* junction in one steroid unit, was synthesised by Fuchs *et al.* [78] and reported to be as potent as cephalostatin 1 (**57**) [78]. So, contrary to earlier presumptions about the need for the Southern D-ring olefin moiety for the biological activity of cephalostatin 1 (**57**), this entity is clearly not a prerequisite for high activity. In 1996, Winterfeldt *et al.* were successful in preparing easily accessible, biologically active cephalostatin analogues, and in developing a novel method for the directed and flexible synthesis of nonsymmetrical *bis*-steroidal pyrazines [94]. This group set out to determine the essential biological substructures of the cephalostatins by synthesis and biological evaluation of appropriate analogues. In 1998, they described the synthesis of cephalostatin analogues by symmetrical and non-symmetrical routes [62]. In the symmetrical route, the aim was the straightforward synthesis of symmetrical *bis*-steroidal pyrazines by dimerisation of an α-amino ketone precursor such as an enamino ketone. The C_2-symmetrical pyrazines of type **A** (Fig. (**5**)) obtained in this manner then had to be desymmetrised and further functionalised at a later stage of the synthesis. The aim of the non-symmetrical route was the direct synthesis of non-symmetrical *bis*-steroidal pyrazines of type **B** (Fig. (**5**)) by chemo- and regioselectively controlled coupling of two different steroids [62].

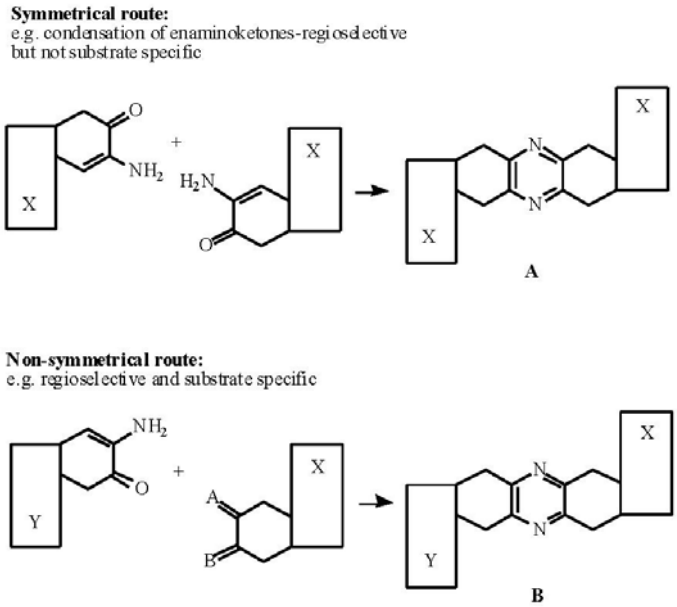

Fig. (5). Synthetic strategies leading to steroidal pyrazines.

Interestingly, several of the ritterazines exhibit cytotoxicities approaching the same nanomolar range as the most active of the cephalostatins, although the ritterazines are far less oxygenated. Their relative simplicity promises greater synthetic accessibility with probable retention of significant bioactivity [76].

A synthesis of (+)-cephalostatin 7 (**88**), (+)-cephalostatin 12 (**84**) and (+)-ritterazine K (**90**) was recently achieved by Fuchs [92]. This group then published a further two papers detailing improvements in synthetic methodologies [83, 84], as well as the synthesis of the Northern unit of the cephalostatin family [79]. The Northern part of the cephalostatins is not only the most common unit in the cephalostatin family, but is also strongly associated with the most potent antitumour activity [76, 77].

It was in 1998 that Fuchs *et al.* completed the first total synthesis of cephalostatin 1 (**57**), along with the construction of hybrids composed of ritterazine and cephalostatin steroidal subunits [76]. The authors described the first synthesis of the Northern hemisphere of ritterazine G (**91**) *via* a formal isomerisation of the spiroketal group of hecogenin acetate, extension of an optimised photolysis/Prins protocol to install the Δ^{14} functionality, and use of the protocol to deliver the same moiety into the Southern hemisphere of cephalostatin 1 (**57**) from an advanced saturated intermediate. Application of this unsymmetrical pyrazine formation method provided the first total synthesis of cephalostatin 1 (**57**), along with the hybrid analogues ritterostatin G_N1_N (**92**) and ritterostatin G_N1_S (**93**) [76].

The synthetic compound ritterostatin G_N1_N (**92**) was exceptionally potent in the NCI's *in vitro* human cancer cell panel [76]. In fact, it is more potent than cephalostatin 1 (**57**) for the leukaemia K-562 cell line, equipotent for ovarian OVCAR-8, renal SN12C and breast MCF7/ADR-RES cell lines, and nearly so for several others [76]. Ritterostatin G_N1_N (**92**) possesses a mean tumour inhibiting activity approaching that of taxol, superior to that of cephalostatin 7 (**88**) in all categories of cancer cell lines tested, and superior to that of all standard chemotherapeutics, including adriamycin, cisplatin, 5-fluorouracil and cyclophosphamide [76]. Ritterostatin G_N1_S (**93**) was significantly less active than ritterostatin G_N1_N (**92**), affecting only 10 of 60 cell lines at 900 nM concentration [76]. However, its activity level remains high, although with diminished scope [76]. This was expected, due to the lack of a 17α-hydroxyl group, a feature present in at least one hemisphere of all the most active ritterazines and cephalostatins [76].

Biogenesis

The cephalostatins and ritterazines represent rare examples of steroidal alkaloids with a nitrogen functionality at C-2. Biogenetically, the novel pyrazine ring might be formed from two 2,3-dioxo steroids through the addition of an ammonia equivalent and subsequent condensation [51]. For example, the central pyrazine ring may result from a biosynthetic condensation of 2-amino-3-oxo steroid units. There are distinct elements of overlap between the ritterazine and the cephalostatin structures. On examining ritterazine K (**90**) it is clear that it contains the Southern-half of cephalostatin 7 (**88**). Interestingly, Fuchs *et al.* suggested that similar statistical coupling as that employed by his group in the total synthesis of cephalostatin 7 (**88**), cephalostatin 12 (**84**) and ritterazine K (**90**) occurs in nature, which implies that ritterazine K (**90**) might also be produced by *C. gilchristi* [48, 93]. The Pettit group then examined residual material, and were able to identify a compound, in microgram quantities, with the same chromatographic profile as that of ritterazine K (**90**) [48].

In summary, the biosynthesis of these compounds seems to occur in two phases - coupling of two steroids *via* a pyrazine linker followed by oxidation at various positions [45].

β-CARBOLINE/ISOQUINOLINE ALKALOIDS

In addition to being among the most commonly encountered alkaloid frameworks in the terrestrial environment, the β-carboline and isoquinoline ring systems occur in compounds derived from a wide variety of marine phyla, encompassing Porifera, Chordata, Cnidaria, Bryozoa and microalgae [103]. Harman (1-methyl-β-carboline) and nor-harman (β-carboline) were the first marine-derived β-carbolines to be reported in 1980, from the bioluminescent marine dinoflagellate *Noctiluca miliaris* [104]. The first isolation of a β-carboline of sponge origin came with the report of the potent cytotoxic compound manzamine A in 1986, from *Haliclona* sp. [105]. However, the most pharmacologically promising family of compounds with the isoquinoline skeleton isolated to date are the ecteinascidins, first reported in 1990 from the colonial marine ascidian *Ecteinascidia turbinata* [106, 107].

ECTEINASCIDINS

Isolation, Structure Determination and Distribution

The ecteinascidins are a family of marine isoquinolines reported by Rinehart *et al.* and Wright *et al.* in consecutive papers [106, 107]. These compounds were obtained as trace components of the ascidian *Ecteinascidia turbinata* (Order Enterogona, Family Perophoridae) collected in the Caribbean and the Florida Keys, respectively, each in yields of 10^{-4} to 10^{-6}%. *E. turbinata* is a colonial ascidian which is observed to grow preferentially on mangrove roots at depths of 1-3 m [108]. In 1969, *E. turbinata* was reported to contain a potent antitumour agent [109], but the compounds responsible for this activity resisted isolation for over fifteen years. It was not until the development of countercurrent chromatography, TLC bioautography on tissue culture plates, fast atom bombardment mass spectrometry and long-range heteronuclear correlation techniques in NMR spectroscopy that the isolation and structure elucidation of the ecteinascidins became possible. The ecteinascidins have been coded by numbers based on the highest mass of the ions originally observed for each compound (which corresponded to the ion obtained following the loss of the C21 OH group).

The first of these compounds to be reported were ecteinascidin (Et) 729 (**94**), Et 743 (**95**), Et 745, Et 759A, Et 759B and Et 770 [106, 107]. Structure confirmation and assignment of the relative stereochemistry of Et 729 and Et 743 was achieved *via* X-ray crystallography [110]. The absolute stereochemistry was assumed to be the same as in safracin A, and this was later confirmed by a study using chiral GC and 2D NMR spectroscopy [111]. The ecteinascidins are structurally related to microbial antibiotics, the safracins and saframycins, which has led to speculation that these compounds may be derived from a symbiotic microorganism [107, 112].

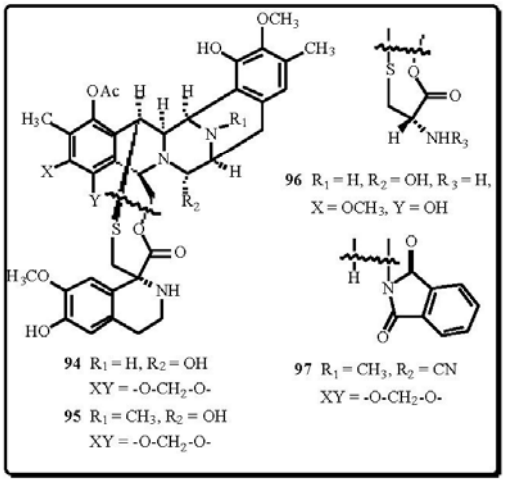

Et 729 (**94**) was found to have the most potent antitumour activity (IC_{50} 0.93 ng/mL *vs* P388 murine leukaemia; T/C 246 at 10 μg/kg *vs* B16 melanoma), and so was selected by the NCI for initial pre-clinical trials. However, Et 743 (**95**) also demonstrated very strong antitumour activity (IC_{50} 0.5 ng/mL *vs* L1210 leukaemia cells and 1.3 ng/mL *vs* P388 murine leukaemia cells), with similar potency, tumour selectivity and *in vivo* activity against murine and human tumour models to that observed for Et 729. As Et 743 was also the most abundant ecteinascidin, with a yield of 1 x 10^{-4}% from the source organism, it replaced Et 729 in subsequent trials. Et 743 has been shown to be 200 times more potent than taxol [113].

Rinehart's group have subsequently reported, in 1992, the isolation of Et 722 and Et 736 [110], which contain a tetrahydro-β-carboline instead of a tetrahydroisoquinoline ring [108]. In 1996, the same group also reported the isolation of the putative biosynthetic precursors of the previously reported ecteinascidins, Et 583 (**96**), Et 597, Et 594 and Et 596 [111]. These finds were followed in 1998 by the nucleophile-substituted ecteinascidins Et 760, Et 788, Et 802, Et 815 and Et 858 and the *N*-oxide ecteinascidins Et 717, Et 775 and Et 789, which demonstrated exceedingly potent cytotoxicity against L1210 murine leukaemia cells [114].

Synthesis and Supply

Following initial reports of partial syntheses of ecteinascidin 743 (**95**) [115, 116] the enantio- and stereocontrolled, convergent and short total synthesis was reported by Corey *et al.* in 1996 [117]. Alternative approaches have been postulated subsequently, but have not yet been achieved [118, 119]. In 1999, Corey's group reported the synthesis of an Et 743 analogue, phthalascidin (**97**), which has comparable *in vitro* potency and mode of action to Et 743, but is easier to synthesise and is considerably more stable in solution [120].

Supply of the source organism is always a major concern once a drug is selected for further investigation. *E. turbinata* is collected from its mangrove root habitat whilst leaving the stolon (root) behind, thus allowing it to regrow, and

reproduce sexually [121]. The colony has been observed to regenerate in 6-9 weeks after partial removal of a cluster, thus allowing the limited supply of the ecteinascidins for drug development studies *via* natural recollection, with no environmental impact on the ecological conditions of the surrounding region [122]. The aquaculture of the organism has also been investigated with much success, both in controlled aquaria conditions and more recently in the wild by CalBioMarine [123] and Pharma Mar [113].

Biogenesis

A biogenetic scheme for the formation of the ecteinascidins has been proposed by Rinehart [111]. This involves the formation of the A-B units *via* condensation of two DOPA-derived building blocks, where the tetrahydroisoquinoline ring in unit B is closed by condensation (Pictet-Spengler) with a serine- (or glycine-) derived aldehyde, as observed for the related saframycins. *S*-Adenosylmethionine is thought to be the most likely source of the methyl groups at C6, O7, C16, O17 and N12 ((Fig. (**6**)) [111].

Bioactivity

The mechanism of action of the ecteinascidins has attracted considerable attention in the last few years. Many studies have been undertaken in order to provide insight into the molecular basis for the antitumour activity of Et 743 (**95**). However, the exact mechanism of action still remains to be determined. Et 743 has been shown to covalently bind to the exocyclic 2-amino group (N2) of guanine located in the DNA minor groove [124, 125, 126]. The rigid *bis*-(tetrahydroisoquinoline)A-B units are thought to be the principal sites of interaction with DNA bases [127, 128]. These units are proposed to generate parallel networks of drug-DNA hydrogen bonds, which stabilise the pre-alkylation binding complex and thus govern sequence recognition and reactivity [129]. However, the C-subunit has also been shown to be important, as its modification affects the potency and antitumour selectivity of Et 743 [111]. Recent work has also shown Et 743 to induce DNA-topoisomerase I cross-linking, although it seems that this is not the primary mode of action as high doses are required in order to produce the effect [130, 120]. Et 743 has also been shown to bend DNA towards the major groove, a unique feature

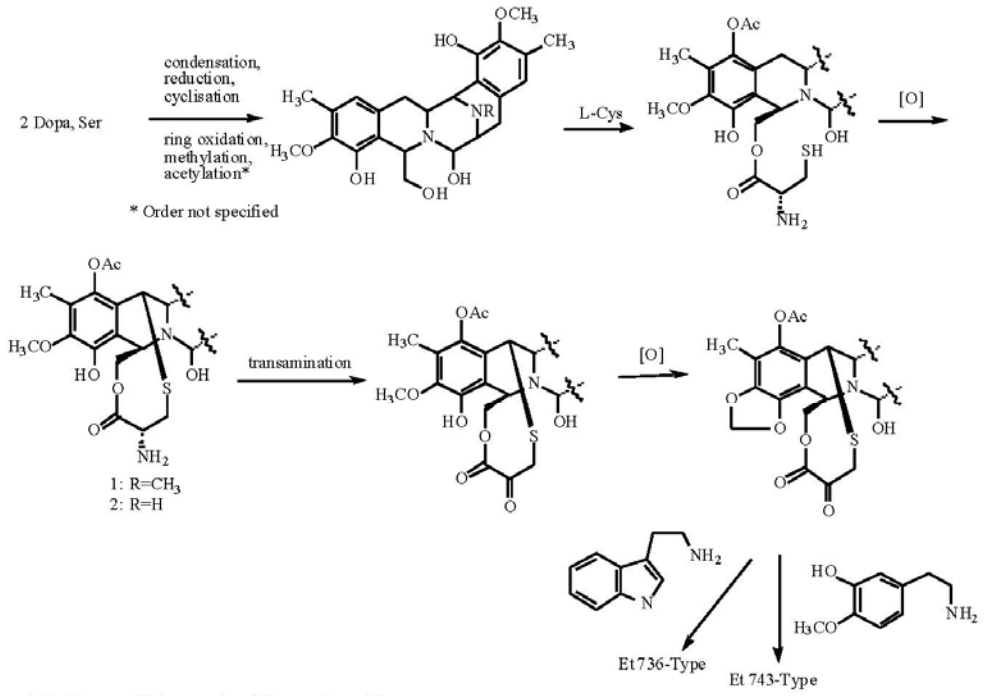

Fig. (6). Proposed biogenesis of the ecteinascidins.

among DNA-interactive agents that occupy the minor groove [131].

Long-term exposure of tumours to Et 743 (**95**) has been shown to be the most effective form of treatment [132]. This raised concerns as to the myelotoxicity (bone marrow toxicity) of the drug. However, it has been established that Et 743 does not demonstrate selective myelotoxicity, and that therapeutically active doses can be reached with tolerable bone marrow toxicity [133]. It earlier appeared that hepatotoxicity may be one of the drug's dose-limiting side effects, although encouraging results have since been obtained on the toxicological profile of Et 743 in monkeys and in Phase I and II clinical trials [122].

Et 743 (**95**) also interacts with the microtubule network, and blocks the cell cycle progression at late S G2/M phases [122, 132]. However, the drug does not appear to have a direct effect on tubulin. It seems instead to prevent the attachment of assembled microtubules to the centrozome. The resultant disorganised microtubule fibres are then observed to aggregate around the outside of the cell nucleus, thus preventing the formation of the mitotic spindle and halting mitosis. The microtubules are also observed to adopt a curved appearance, forming a circle around the cell nucleus instead of being arranged in a line from the centrosome to the cell membrane [134, 135]. This mechanism of action appears to be different from those previously reported for microtubule inhibitors.

MANZAMINES AND RELATED COMPOUNDS

Isolation, Structure Determination, Distribution and Bioactivity

The manzamines are β-carboline alkaloids substituted at C1, generally by intricate nitrogen-containing polycyclic systems. Manzamine A (**98**) (P388 murine leukaemia cell line IC_{50} 0.07 μg/mL) was first reported by Higa's group in 1986 as the major cytotoxic component of the Okinawan marine sponge *Haliclona* sp. (Order Haplosclerida, Family Chalinidae). The absolute configuration was established *via* X-ray crystallography [105]. The same structure was reported in 1987 by Nakamura's group as keramamine A, this time derived from the Okinawan marine sponge *Pellina* sp. (Order Nepheliospongida, Family Oceanapiidae), along with keramamine B (**99**) [136]. Keramamine A and B exhibitedantimicrobial activity against *Staphylococcus aureus* (MIC 6.3 and 25 μg/mL, respectively). Keramamine B was later to have its structure revised to that reported for manzamine F (**100**) [137]. Manzamine A has been found to be active against human colon tumour cells, lung carcinoma cells and breast cancer cells (0.5 μg/mL) [138]. A wide variety of manzamines, and other compounds thought to be their biogenetic precursors, have been reported from a total of nine different marine sponge genera from seven families and four orders. This has led to speculation that production of these compounds may be due to the biosynthetic participation of common microorganisms [136, 137, 139]. To date, manzamine A has shown the most potent biological activity.

Minor components of *Haliclona* sp., manzamines B (**101**) (P388 IC_{50} 6 μg/mL), C (**102**) (P388 IC_{50} 3 μg/mL), and D (**103**) (P388 IC_{50} 0.5 μg/mL), were subsequently reported by Higa's group [140, 141], followed by manzamines E (**104**) (P388 IC_{50} 5 μg/mL) and F (**100**) (P388 IC_{50} 5 μg/mL) from the Okinawan marine sponge *Xestospongia* sp. (Order Petrosida, Family Petrosiidae) [137]. 8-Hydroxymanzamine A (**105**) (manzamine G) (KB human epidermoid carcinoma cell line IC_{50} 0.03 μg/mL) was obtained from the Indonesian marine sponge *Pachypellina* sp. (Order Petrosida, Family Oceanapiidae) by Scheuer's group [142].

A clue as to the biosynthetic origins of the manzamines came in 1992 with the isolation, along with previously reported manzamines, of ircinals A (**106**) and B (**107**) together with manzamines H (**108**) and J (**109**), again by Higa's group, from the Okinawan marine sponge *Ircinia* sp. (Order Dictyoceratida, Family Thorectidae) [143]. These compounds exhibited cytotoxicity against L1210 murine leukaemia cells, with IC_{50} values of 1.4, 1.9, 1.3 and 2.6 μg/mL, respectively, and against KB human epidermoid carcinoma cells, with IC_{50} values of 4.8, 3.5, 4.6 and >10 μg/mL, respectively. Reaction of ircinals A and B with tryptamine followed by DDQ oxidation gave manzamines A (**98**) and J (**109**), respectively.

A variety of new manzamines were reported in 1994. Crews *et al.* reported two new 8-hydroxymanzamines, 1,2,3,4-tetrahydo-2-*N*-methyl-8-hydroxymanzamine A (**110**) (P388 ED_{50} 0.8 μg/mL) andl,2,3,4-tetrahydo-8-hydroxymanzamine A (**111**), which were both isolated from the Papua New Guinea marine sponges *Petrosia contignata* (Order Petrosida, Family Petrosiidae) and *Cribrochalina* sp. (Order Haplosclerida, Family Niphatidae) [144]. These new manzamines have structures similar to that of manzamine G (**105**), and

represent further intermediates in the Baldwin/Whitehead manzamine biosynthetic path (*vide infra*).

Seven new manzamines, or manzamine precursors, were reported by Kobayashi's group in 1994, from the Okinawan marine sponge *Amphimedon* sp. (Order Haplosclerida, Family Niphatidae). These were 6-hydroxymanzamine A (**112**) (manzamine Y), 3,4-dihydromanzamine A (**113**), keramaphidins B (**114**) and C (**115**), keramamine C (**116**) and ircinols A (**117**) and B (**118**), along with the known manzamine A (**98**) [145, 146, 147]. The first two of these compounds were found to be cytotoxic against L1210 murine leukaemia cells (IC_{50} 1.5 and 0.48 μg/mL, respectively) and KB human epidermoid carcinoma cells (IC_{50} 2.5 and 0.61 μg/mL,respectively),while keramaphidin B is cytotoxic against P388 murine leukaemia and KB human epidermoid carcinoma cells (IC_{50} 0.28 and 0.3 μg/mL, respectively).

An X-ray diffraction analysis of keramaphidin B (**114**), which possesses four asymmetric centres, revealed it to be a naturally occurring racemate [148]. The separation, *via* chiral HPLC, of the two enantiomers was reported in 1996 by Kobayashi's group [149]. Analyses of the crystals and the mother liquor gave ratios of the (+)- and (-)- forms of keramaphidin B as ca. 1:1 and 20:1, respectively. The absolute stereochemistry of (+)-keramaphidin B, established *via* Mosher's method, was also reported in 1996 by Kobayashi's group [150]. Interestingly, the major components of the sponge *Amphimedon* sp., manzamines A (**98**) and B (**101**) and ircinals A (**106**) and B (**107**), have the same absolute configuration as the minor enantiomer, (-)-keramaphidin B, while the minor components, ircinols A (**117**) and B (**118**), have the same absolute configuration as the major enantiomer, (+)-keramaphidin B. The ingamines and ingenamines (*vide infra*) also have the same absolute configuration as the major enantiomer.

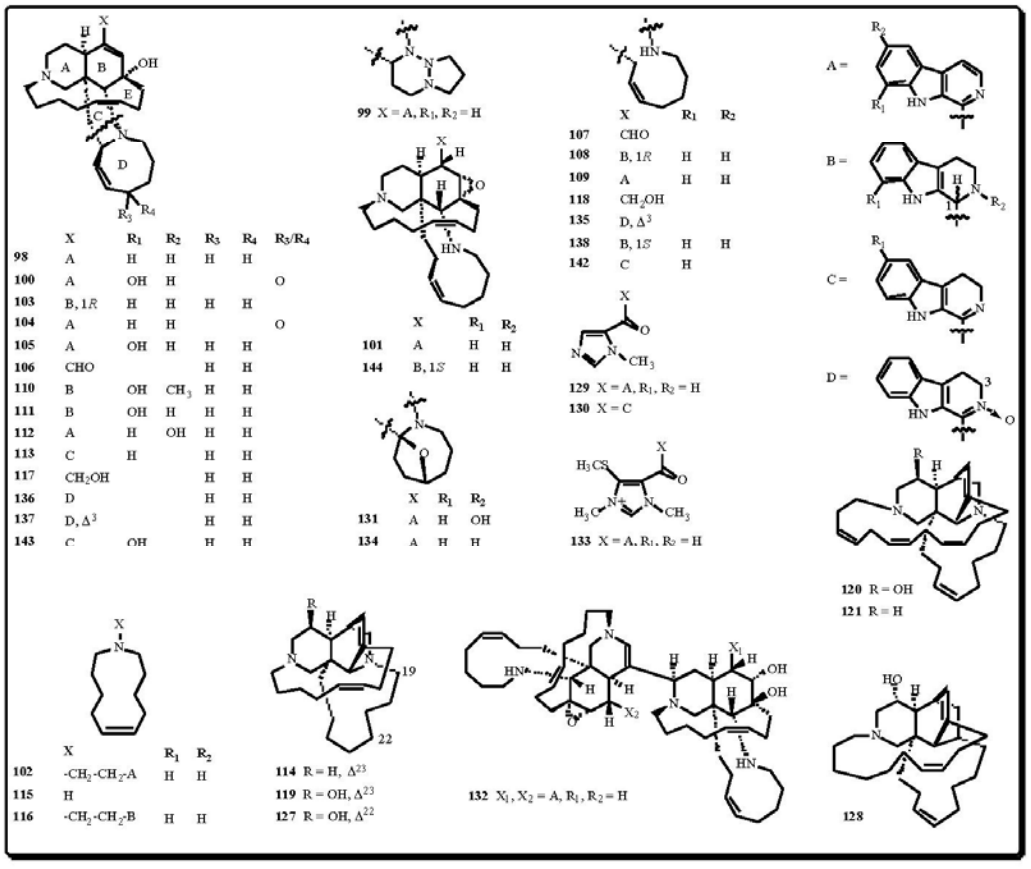

Ircinols A (**117**) and B (**118**) represent the first occurrence of compounds which display the opposite absolute configurations to those of the manzamine alkaloids, and are a rare example of both enantiomeric forms being isolated from the same organism. They are cytotoxic against L1210 murine leukaemia cells (IC_{50} 2.4 and 7.7 μg/mL, respectively) and KB human epidermoid carcinoma cells (IC_{50} 6.1 and 9.4 μg/mL, respectively).

Again in 1994, Andersen's group reported the isolation of ingenamine (**119**) (P388 ED_{50} 1 μg/mL), an hydroxy derivative of keramaphidin B, from the Papua New Guinea marine sponge *Xestospongia ingens* [151]. Two additional structures related to ingenamine, ingamines A (**120**) and B (**121**), were subsequently reported by this group from the same sponge in the same year [152]. Both compounds were cytotoxic against the P388 murine leukaemia cell line, with ED_{50} values of 1.5 μg/mL. In 1995, five new ingenamines, ingenamines B-F (**122-126**), were reported from the same sponge by the same group [153]. In addition, the absolute configurations, obtained *via* Mosher's method, of the ingenamines and ingamines were discovered to be antipodal to those reported for manzamines A (**98**) and B (**101**) and ircinals A (**106**) and B (**107**), but identical to those for ircinols A (**117**) and B (**118**).

Xestocyclamine A was first reported in 1993 by the Crews group, again from the Papua New Guinea marine sponge *Xestospongia ingens* [154]. Its structure was revised in the following year (**127**), when the isolation of xestocyclamine B (**128**) was reported [155]. Xestocyclamine A is moderately potent against PKC (IC_{50} 4 μg/mL).

The structures of xestomanzamines A (**129**) and B (**130**) and manzamines X (**131**) and Y (**112**) were reported by the Kobayashi group in 1995 [139]. Xestomanzamines A and B and manzamine X were isolated from the Okinawan marine sponge *Xestospongia* sp., along with manzamines A (**98**), E (**104**) and F (**100**). Manzamine Y was isolated from the Okinawan marine sponge *Haliclona* sp., in addition to manzamines A, B (**101**) and C (**102**). Manzamines X and Y and xestomanzamine B exhibited weak cytotoxicities against KB human epidermoid carcinoma cells (IC_{50} 7.9, 7.3 and 14.0 μg/mL, respectively).

Also in 1995, Scheuer's group reported the isolation of kauluamine (**132**), an unsymmetrical

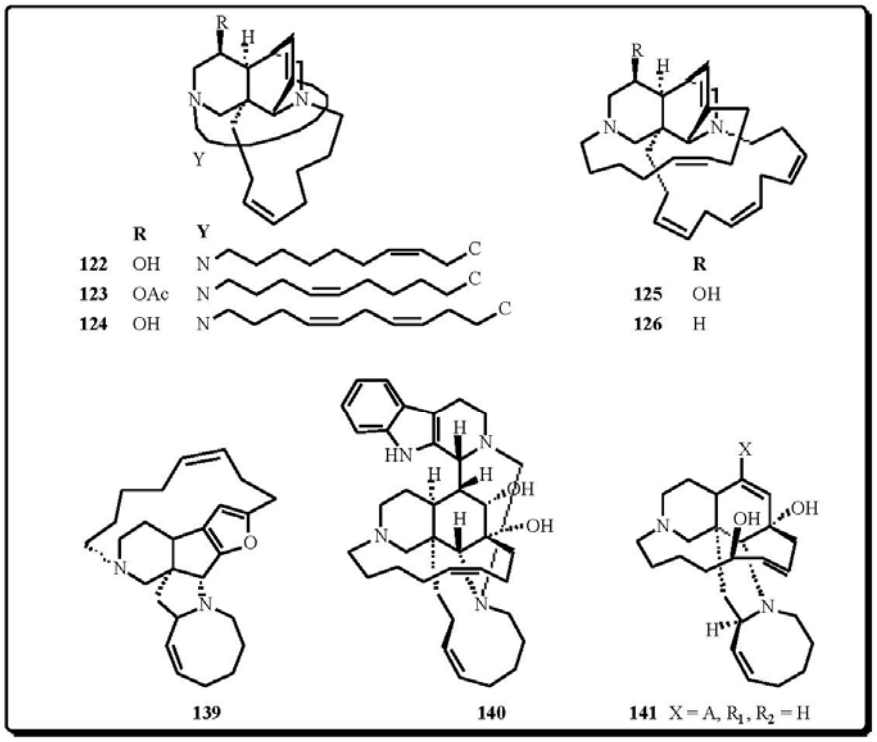

manzamine dimer, from the Indonesian marine sponge *Prianos* sp. (Order Halichondrida, Family Halichondriidae) [156]. Kauluamine showed moderate immunosuppressive activity in the mixed lymphoma reaction, but was not found to exhibit cytotoxic or antiviral activity.

Yet another sponge entered the equation in 1996, with the isolation by Guyot's group of hyrtiomanzamine (**133**) from the Red Sea sponge *Hyrtios erecta* (Order Dictyoceratida, Family Irciniidae) [157]. This compound displayed immunosuppressive activity in the B lymphocytes reaction assay (EC_{50} 2 μg/mL), but no cytotoxicity against the KB human epidermoid carcinoma cell line. Hyrtiomanzamine is structurally very similar to xestomanzamine A (**129**).

Four new manzamines were reported by Proksch's group from the Philippine marine sponge *Xestospongia ashmorica* in 1996. These were the 6-deoxy derivative of manzamine X (**134**), and the *N*-oxides of manzamine J (**135**), 3,4-dihydromanzamine A (**136**) and manzamine A (**137**), respectively [158]. These compounds were cytotoxic against the L5178 murine lymphoma cell line (ED_{50} 1.8, 3.2, 1.6 and 1.6 μg/mL, respectively).

The most recently reported research in this area has been undertaken by Kobayashi's group, and has focussed on the Okinawan marine sponge *Amphimedon* sp. In 1996, the structure of manzamine L (**138**) was reported [149]. Manzamine L exhibited cytotoxicity against L1210 murine lymphoma cells and KB human epidermoid carcinoma cells (IC_{50} 3.7 and 11.8 μg/mL, respectively). In 1997, the structure of nakadomarin A (**139**) was reported, which contained an unprecedented 8/5/5/5/15/6 ring system [159], followed in 1998 by ma'eganedin A (**140**), a new tetrahydro-β-carboline alkaloid with a methylene carbon bridge between N2 and N27 [160]. These two compounds are thought to be biogenetically derived from ircinals A (**106**) and B (**107**), respectively, and both demonstrate cytotoxicity against L1210 murine lymphoma cells (IC_{50} 1.3 and 4.4 μg/mL, respectively). In addition, nakadomarin A showed inhibitory activity against cyclin dependent kinase 4 (IC_{50} 9.9 μg/mL) and antimicrobial activity against the fungus *Trichophyton mentagrophytes* (MIC 23 μg/mL) and a gram-positive bacterium *Corynebacterium xerosis* (MIC 11 μg/mL). Ma'eganedin A also exhibited anti-bacterial activity against *Corynebacterium xerosis*, along with *Sarcina lutea* and *Bacillus subtilis* (MIC 5.7, 2.8 and 2.8 μg/mL, respectively).

Still from the same Okinawan marine sponge, *Amphimedon* sp., Kobayashi's group reported the structures of the new compounds manzamine M (**141**), 3,4-dihydromanzamine J (**142**) and 3,4-dihydro-6-hydroxymanzamine A (**143**) in 1998, followed by that of 1,2,3,4-tetrahydromanzamine B (**144**) in 1999 [161, 162]. Manzamine M is the first manzamine congener with an hydroxyl group on the C13–C20 chain. All four compounds exhibited cytotoxicity against L1210 murine leukaemia cells (IC_{50} 1.4, 0.5, 0.3 and 0.3 μg/mL, respectively). In addition, the first three compounds showed antibacterial activity against *Sarcina lutea* (MIC 2.3, 12.5 and 6.3 μg/mL, respectively) and *Corynebacterium xerosis* (MIC 5.7, 12.5 and 3.1 μg/mL, respectively). 1,2,3,4-tetrahydromanzamine B also demonstrated cytotoxicity against KB human epidermoid carcinoma cells (IC_{50} 1.2 μg/mL).

Biogenesis and Synthesis

With the co-isolation of ircinals A (**106**) and B (**107**) with a variety of manzamines in 1992, from the Okinawan marine sponge *Ircinia* sp., came some indication as to the biosynthetic origins of the manzamines. In the same year, Baldwin and Whitehead proposed an elegant biogenetic pathway for the formation of the tetracyclic ring system of the more complex manzamines. This involved an intramolecular Diels-Alder reaction of a tricyclic ring system (*bis*-3-alkyldihydropyridine) (**A**) containing a dihydropyridine (the diene) and a conjugated iminium ion (the dienophile), followed by disproportionation and hydrolysis of the intermediate iminium ion (**B**) to give a tetracyclic aldehyde (**D**) (reminiscent of ircinal B) which was subsequently reacted with tryptophan to yield manzamine B (**101**), followed by manzamine A (**98**) (Fig. (7)) [163]. Ircinal B has the overall skeleton and aldehyde functionality present in the tetracyclic intermediate of this biogenetic scheme.

Baldwin and Whitehead have subsequently achieved the key cycloaddition step on a model system [164], the synthesis of the *bis*-3-alkyldihydropyridinium species from a C10 symmetrical dialdehyde unit, propenal and ammonia [165, 166], the synthesis of an advanced intermediateto keramaphidin which could feasibly be converted to keramaphidin B (**114**) *via* ring-closing metathesis [167], and the biomimetic synthesis of keramaphidin B [166]. Keramaphidin

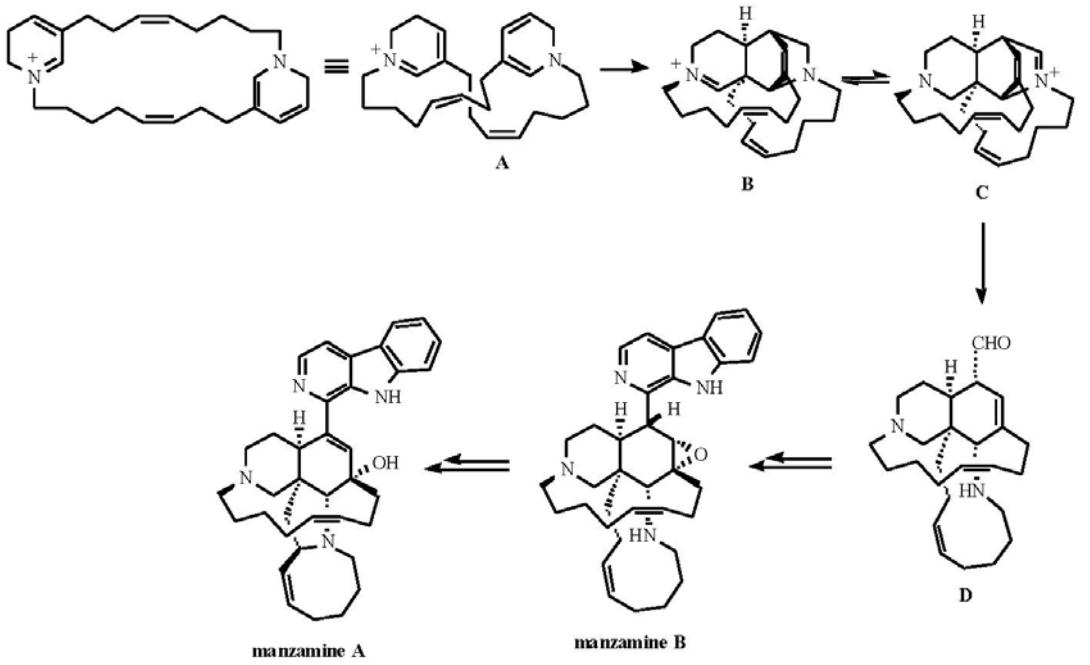

Fig. (7). Proposed Baldwin/Whitehead biogenetic scheme.

B is simply the reduced form of the proposed cycloadduct **B** (Fig. (7)).

Based on the Baldwin/Whitehead biogenetic scheme, keramaphidin B (**114**) is thought to be a precursor of the ircinals, while keramaphidin C (**115**) and keramamine C (**116**) are plausible biogenetic precursors to manzamine C (**102**), which may be generated from keramamine C obtained by the coupling of keramaphidin C with tryptamine and a C3 moiety [146, 148]. The isolation of ingenamine (**119**), an hydroxy derivative of keramaphidin B, by Andersen's group lends further support to this scheme [151].

Das *et al.* have reported a model synthesis for keramaphidin B (**114**) which is similar to that reported by Baldwin and Whitehead, mainly differing in terms of the conditions used for the cycloaddition step [168]. This group subsequently proposed an alternative pathway for the formation of a macrocycle (**145**), similar to **A**, *via* condensation of malondialdehyde, ammonia and an unsaturated dialdehyde. Two routes from this macrocycle to manzamine A (**98**) are then postulated, one adapted from the Baldwin/Whitehead model, and the other involving direct cyclisation of the macrocycle followed by reduction of the resultant imine and cyclisation to

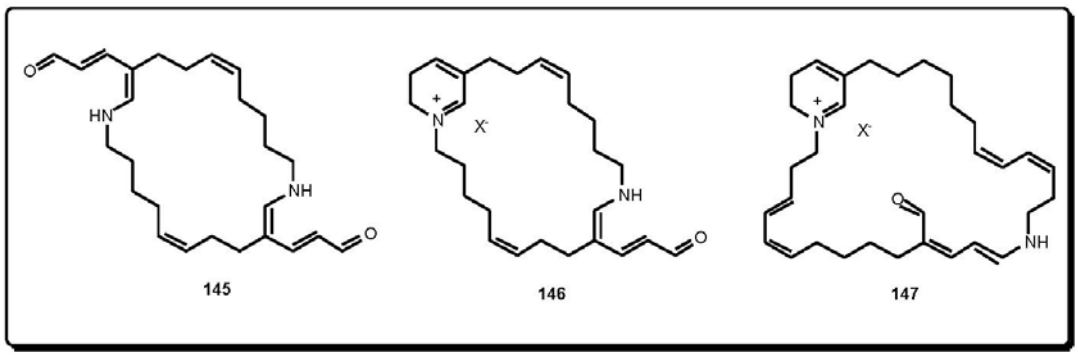

the enamine [169]. A further modification of the Baldwin/Whitehead model was proposed by Das *et al.* in 1999, where the biogenesis of manzamine A/keramaphidin B and halicyclamine A was postulated to derive from two further macrocycles (**146**, **147**) [170].

A biogenetic pathway deriving manzamine Y (**112**) and subsequently X (**131**) from manzamine A (**98**) has been proposed by Kobayashi *et al.* [139]. The xestomanzamines were reported in the same paper, and are postulated to be biosynthesised from the combination of an *N*-methyl histidine and a tryptamine unit. In addition, following the report of manzamine L (**138**) in 1996 by the same group, its biogenesis *via* the ircinals was proposed [149].

Xestocyclamine A (**127**), like ingenamine (**119**) and keramaphidin B (**114**), has a skeleton which is identical to that of the proposed pentacyclic intermediate in the Baldwin/Whitehead biogenetic scheme. It was isolated by Crews *et al.* from the Papua New Guinea marine sponge *Xestospongia ingens* [154]. The ingamines and ingenamines were reported from the same sponge by Andersen's group [151, 152, 153, 171]. Interestingly, their absolute configurations were discovered to be antipodal to those reported for manzamines A (**98**) and B (**101**) and ircinals A (**106**) and B (**107**), but identical to those for ircinols A (**117**) and B (**118**). Thus, it is clear that there are two antipodal series of alkaloids formed *via* the Baldwin/Whitehead biogenetic scheme from keramaphidin B (Fig. (7)).

Extensive reviews have recently been published on the syntheses of the manzamines [172, 173]. These cover the two total syntheses of manzamine C (**102**) [174, 175, 176], along with a variety of approaches toward the total synthesis of manzamine A (**98**), encompassing biomimetic, radical, photochemical, ionic, intermolecular Diels-Alder and intramolecular Diels-Alder cyclisations. The syntheses of a variety of related compounds are also incorporated. Since this time, however, the total synthesis of manzamine A has been achieved [177].

The first total syntheses of manzamines A (**98**) and D (**103**), along with those of ircinal A (**106**) and ircinol A (**117**), were reported in 1998 by Winkler *et al.*, featuring a highly stereoselective tandem intramolecular vinylogous amide photoaddition/retro-Mannich fragmentation/ Mannich cyclisation sequence as the key step [177]. The enantioselective total synthesis of ircinal A was reported in the following year by Martin *et al.*, using a novel domino Stille/Diels-Alder reaction followed by two sequential ring-closing metathesis reactions [178]. In addition, the synthesis of the manzamine dimer kauluamine (**132**), reported by Scheuer's group in 1995, has been achieved [179]. New approaches towards the total synthesis of manzamine A continue to be put forward [180, 181, 182].

PYRIDOPYRROLOPYRIMIDINE ALKALOIDS

The pyridopyrrolopyrimidine skeleton is rare, with only synthetic derivatives having been reported prior to 1994 [183 and references therein]. The isolation of the variolins from an Antarctic marine sponge represented the first examples of natural products containing this moiety [183]. This made the variolins an interesting class of alkaloid from both structural and biogenetic points of view. The variolins were isolated from the Antarctic sponge *Kirkpatrickia varialosa* in 1994 [183, 184]. The compounds isolated included variolin A (**148**), variolin B (**149**), *N*(3')-methyl tetrahydrovariolin B (**150**) and variolin D (**151**), the latter of which was reported to be an artifact of the extraction process produced by aerial oxidation of the major compounds [183, 184]. The structures of the variolins were assigned by spectroscopic techniques and X-ray crystallography [183, 184].

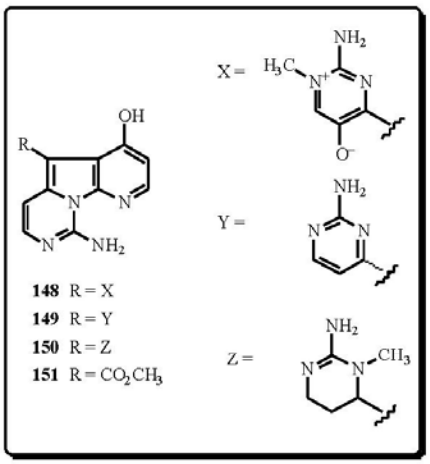

There was an order of magnitude variation in the cytotoxicity of the two major variolins against the P388 cell line, with an IC_{50} of 3.8 μg/mL for variolin A to an IC_{50} of 210 ng/mL for variolin B (**149**). Variolin B (**149**) was also more effective against *Herpes simplex* than the *Polio* virus by a factor of four times, but was inactive against a range

of other microorganisms [183]. *N*-(3')-methyl tetrahydrovariolin B (**150**) inhibited the growth of *Saccharomyces cerevisiae* (36 mm zone at 2 mg/mL) and showed *in vitro* activity against the HCT 116 cell line (IC_{50} 0.48 μg/mL), but only modest *in vivo* activity against the P388 cell line (T/C 125% at 10 mg/kg) [184]. Variolin D (**151**) was inactive in all the assays, and this led to the conclusion that the substitution on the pyridopyrrolopyrimidine ring system with 2-aminopyrimidine is necessary for the biological activity [183]. It was also suggested that variolin B (**149**) may belong to the same class of DNA-intercalating compounds as ellipticine and its analogues [183].

There has been considerable interest in the synthesis of the variolins, due to the novelty of the structure and biological properties. Recent reports include the synthesis of 1,2-dihydropyyrolo[1,2-*c*]pyrimidin-1-ones, thereby establishing a versatile procedure for the introduction of substituents into the pyrrolopyrimidones at defined positions [185]. Later work from this same group reports on the synthesis of 1-protected-3-trimethylstannyl-7-azaindoles and their coupling with aryl and heteroaryl halides [186]. Further progress on the synthesis of the variolins was presented at the 2nd Euroconference on Marine Natural Products (Santiago de Compostela, September, 1999), where three synthetic strategies, which differ in the formation of either the A, B or C ring as late steps, were detailed [187].

Recent work at the University of Canterbury has resulted in a rapid three-step synthesis of the variolin core, starting from commercially available 4-chloro-2-thiomethylpyrimidine as shown in Fig. (**8**) [J. Morris, University of Canterbury, personal communication].

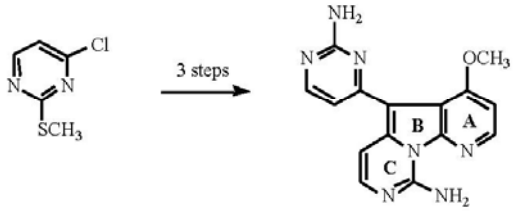

Fig. (8). Synthetic approach to the variolin skeleton.

PYRROLOQUINOLINE ALKALOIDS

Pyrroloquinolines, or more correctly representatives of the 1,3,4,5-tetrahydro-pyrrolo[4,3,2-*de*]quinoline ring system, were first recognised as a naturally occurring system in 1961, with the structural elucidation of the toad poison dehydrobufotenine [188]. The first report of this ring system from the marine environment was in 1986, with the structural elucidation of discorhabdin C (**152**) [189] from the New Zealand sponge *Latrunculia* cf. *bocagei*. Discorhabdin C is an example of a fully substituted iminoquinone unit (**153**). In the decade that followed, many further examples of trisubstituted (**154**) and fully substituted iminoquinones (**155**) were isolated, based primarily on their outstanding biological properties. These have included further discorhabdins [190-201], prianosins [202-205], batzellines [206], isobatzellines [207], damirones [208], makaluvamines [209-214] and more recently epinardins [215], tsitsikammamines [216] and wakayin [217] classes, as well as veiutamine [218].

Isolation and Structure Determination

Discorhabdins, Prianosins and Epinardins

A search for bioactivity attracted researchers to the various species of the *Latrunculia* genus of sponge from both the New Zealand mainland, and from Antarctica. The extracts from these species invariably exhibited very strong activity against the P388 leukaemia cell line *in vitro*. Discorhabdin C (**152**), the least complex member of the family, was isolated by bioassay-guided fractionation of extracts of the sponge *Latrunculia* cf. *bocagei*, and the structure determined by single-crystal X-ray crystallography along with other spectroscopic techniques [189]. The structures of discorhabdins A (**156**), B (**157**) and D (**158**) were assigned using 2D NMR spectroscopic analysis [190, 191]. The genus *Latrunculia* (Order Hadromerida, Family Latrunculiidae) in New Zealand has at least three recognisable species: *Latrunculia brevis, L.* sp. B and *L.* cf. *bocagei*. In Antarctica, at least 2 species have been described: *L. apicalis* and *L. biformis*. A feature of the genus is the characteristic discorhabd microscleres, from which the discorhabdins were originally named. Discorhabdins A, B and C were each the major component in *Latrunculia brevis*, *L.* sp. B and *L.* cf. *bocagei*, respectively. The New Zealand *L. brevis* also contained heptacyclic members of the discorhabdin family. These are discorhabdin D (**158**) and 2-hydroxydiscorhabdin D (**159**).

In 1987, prianosin A, identical to discorhabdin A (**156**) in structure and absolute configuration, was isolated from the Japanese sponge *Prianos melanos* [202]. The absolute stereochemistry of the

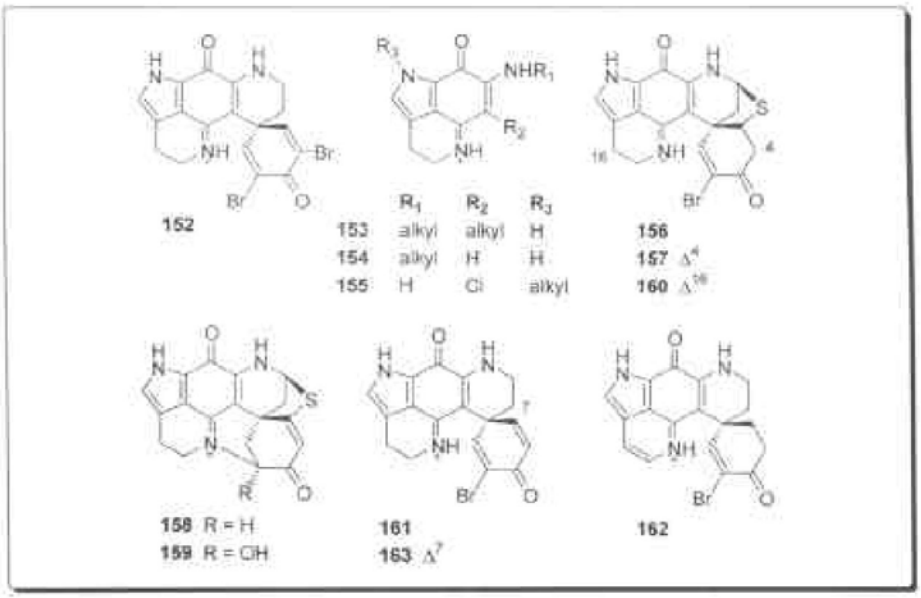

discorhabdin family is based on the configuration established for prianosin A by X-ray crystallography. This research was followed a year later by structures for the prianosins B, C and D [203]. Prianosin B is Δ^{16}-discorhabdin A (**160**), and although aminophenol structures had been suggested originally for prianosins C and D, these were later corrected to those corresponding to discorhabdin D and 2-hydroxydiscorhabdin D [204].

Discorhabdin E (**161**) [195], a minor component from *L.* cf. *bocagei*, and discorhabdin F (**162**), from the Antarctic species *L. biformis* [196], were subsequently isolated, as was discorhabdin G (**163**), the first Δ^7 derivative in the discorhabdin series. Discorhabdin G was found in the Antarctic species *L. apicalis* [198, 199], in addition to the more abundant discorhabdin C (**152**).

There was clear evidence from HPLC and TLC analysis of the New Zealand species of *Latrunculia* that in addition to the major components present, there were also other minor discorhabdin-like components. Standard isolation methodology was used, with particular emphasis on reverse phase flash chromatography and medium-pressure chromatography on Lobar C18 columns, or use of LH-20 gel permeation chromatography. By these means, discorhabdins I, J, K, L, M, N and O (**164-170**) were isolated. These latter discorhabdins have previously been reported [197], but are as yet unpublished. The structural assignments were based on similarity of 1D and 2D NMR spectra to those of the known discorhabdins, and the use of MS techniques to establish molecular formulae. Some of the new discorhabdins were relatively minor variants on the central theme. However, one surprising departure was the finding of several new discorhabdins with a thiohistidine group attached at C1. These compounds arise presumably *via* Michael-type addition to the Δ^1-enone system. 1-Methyl-4-mercaptohistidine, or ovothiol A, had previously been reported from the ovarian tissue of the starfish *Evasterias troschelii* [219], and imbricatine, a benzyltetrahydro-isoquinoline alkaloid from the asteriod *Dermasterias imbricata* [220], contains a mercaptohistidine moiety linked *via* a thioether bond that resembles that found in discorhabdins J, K and M [197]. A variation on the thiohistidine theme was the finding of a glycine moiety attached at the same position (discorhabdin N). Paucity of sample leaves an element of uncertainty with the structure of this discorhabdin.

The most recently isolated members of the direct discorhabdin family are discorhabdins P (**171**) [200] and Q (**172**) [201]. Discorhabdin P, formally *N*-methyldiscorhabdin C, was isolated from a deep water Caribbean *Batzella* sp. and for two reasons is an important find. It is the first *N*-methylated discorhabdin, and isolation from a *Batzella* sp. adds credence to the putative biosynthetic pathway suggested for these pyrroloquinoline alkaloids (*vide*

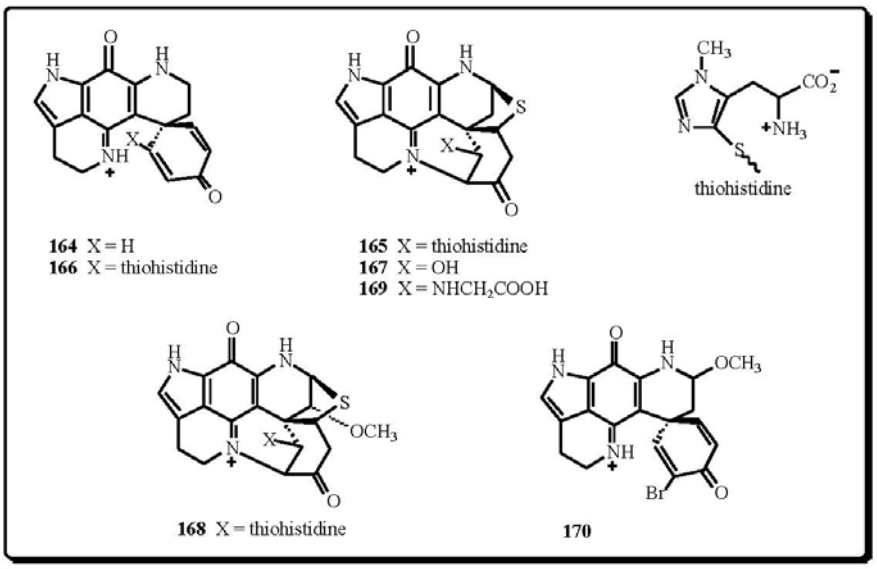

infra). Discorhabdin Q, Δ^{16}-discorhabdin B, was isolated from two genera of sponge, *Latrunculia purpurea* from Wessell Island, Australia, and numerous species of *Zyzzya massalis* and *Z. fuliginosa,* where it was noted as the most prevalent or the only discernable discorhabdin present.

The epinardins A to D (**173**-**176**), from an unidentified deep-water (-115 m) Demospongia species [215], reveal yet another aspect of the chemistry of this group of compounds. They contain an allylic alcohol system rather than the usual unsaturated ketone. The Δ^7 and the 8-OCH_3 features of the epinardins C (**175**) and D (**176**) have also been observed in discorhabdins G (**163**) and O (**170**). The allylic alcohol theme is present in one of the two 14-bromodiscorhabdin C analogues (**177**) and (**178**) isolated from a previously undescribed

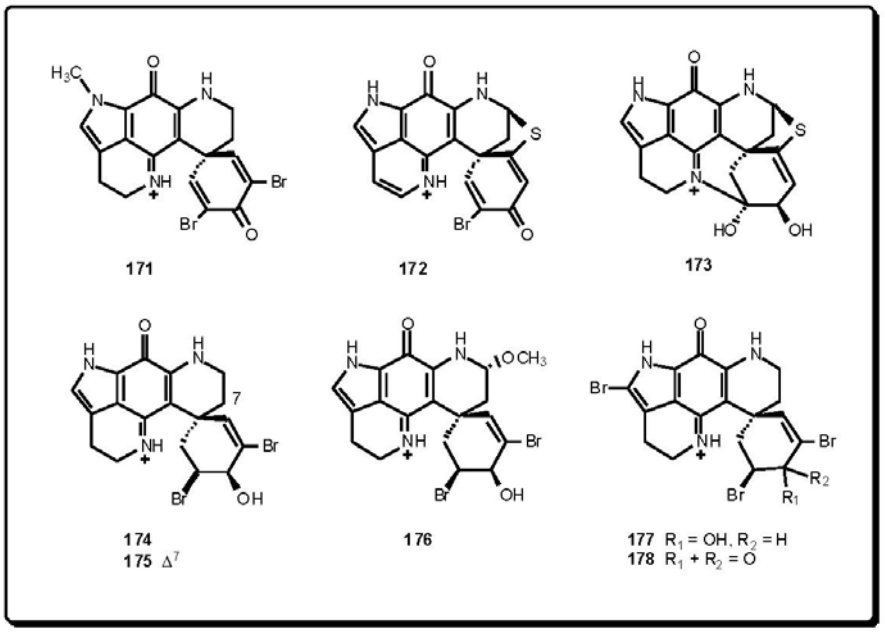

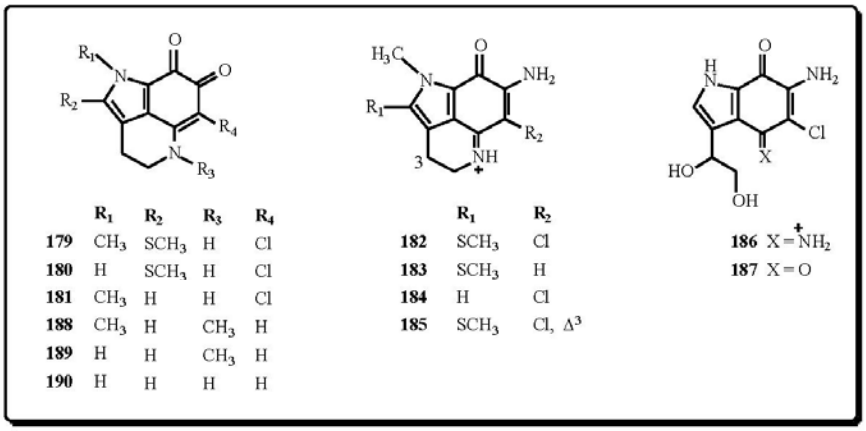

	R_1	R_2	R_3	R_4
179	CH_3	SCH_3	H	Cl
180	H	SCH_3	H	Cl
181	CH_3	H	H	Cl
188	CH_3	H	CH_3	H
189	H	H	CH_3	H
190	H	H	H	H

	R_1	R_2
182	SCH_3	Cl
183	SCH_3	H
184	H	Cl
185	SCH_3	Cl, Δ^3

186 X = $\overset{+}{N}H_2$

187 X = O

Latrunculid sponge found in the Tsitsikamma Marine Reserve off the south-eastern coast of South Africa [216].

Batzellines, Isobatzellines and Damirones

The batzellines A-C (**179-181**) [206] and isobatzellines A-D (**182-185**) [207] were discovered as an outcome of a search for herbicidal agents from marine organisms. They were isolated from a deep-water (-120 m) Bahamian sponge of the genus *Batzella*. These were typical of compounds of the pyrroloquinoline class, being reddish brown/black solids. The two groups of compounds are closely related, containing general structural features of an *S*-CH_3 group on the pyrrolo ring, an *N*-CH_3 and a chloro group. The principal difference between the two series is that the batzellines are aminoquinones, while the isobatzellines are aminoiminoquinones. The structures of the batzellines were secured by X-ray crystallography, NMR analysis and chemical interconversion. The isobatzelline structures were assigned based on NMR spectral comparisons with the batzellines and chemical interconversions. The batzellines and isobatzellines had been detected using cytotoxicity and antifungal assays. Interestingly, a structural variant, the secobatzellines A (**186**) and B (**187**) [221], were also identified from a deep-water Bahamian *Batzella* species, using an enzyme-based assay screening for inhibitors of calcineurin. The structures were assigned by NMR analysis and correlation with the batzelline/isobatzelline data. However, it was suggested that secobatzelline B is a likely artifact of isolation.

Two pyrroloquinolines related to the batzellines were isolated from a Palauan sponge initially identified as belonging to the genus *Damiria* [208] and named damirones A (**188**) and B (**189**). The structural assignments were made on the basis of spectroscopic arguments and similarity to the batzellines. As noted in the paper, the close chemotaxonomic relationship between the damirones and the batzellines had implications for the taxonomy of the sponges, as both genera are classified on the basis of negative characters. Further consideration of the taxonomy of the *Damiria* sponge led to taxonomic revision of the Palauan *Damiria* sp. and its subsequent reassignment as *Zyzzya fuliginosa* [211] . A third damirone, C (**190**), lacking the *N*-methyl group of damirones A and B, was subsequently isolated from a Micronesian sample of *Zyzzya fuliginosa*, along with a series of makaluvamines [211].

Makaluvamines

The initial members of the makaluvamine family were isolated from samples of a Fijian sponge collected from Makaluva Island [209]. The sponge was initially assigned as *Zyzzya* cf. *massalis*, but has since been reassigned as *Zyzzya fuliginosa* [211-213, 222]. The makaluvamines A-F (**191-196**) resulted from a continuing search by the Ireland group for potential antineoplastic agents from marine sources. The structures of the makaluvamines were based on extensive spectroscopic analysis (NMR, UV) and comparison with data from the isobatzelline series [207]. Makaluvamines A-C are closely related to the isobatzellines, but lack the thiomethyl and chloro groupings. In contrast, the makaluvamines D-F represented a new structural class, clearly linking the simpler members of the pyrroloquinolines (damirones, batzellines, isobatzellines and makaluvamines A-C) with the discorhabdin family of compounds. The co-occurrence of discorhabdin

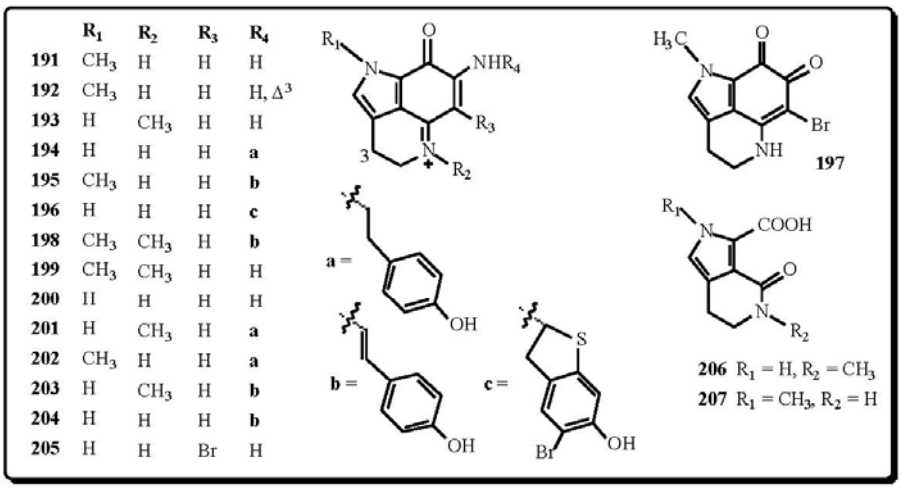

A (**156**) and damirone B (**189**) and another related pyrroloquinoline, makaluvone (**197**), with makaluvamines A-F was strongly supportive of the biosynthetic relationships between the pyrroloquinoline group of compounds (*vide infra*), as was the isolation of makaluvamine D and F from a *Latrunculia* sp. [197].

Further members of the makaluvamine class have since been reported. Makaluvamine G (**198**) was reported as the major component from an Indonesian sponge *Histodermella* sp. [210], now considered to be *Zyzzya fuliginosa* [211, 213, 222]. Makaluvamines A and C and damirones A and B were found co-occurring with makaluvamine G. From a Pohnpeian species of *Z. fuliginosa*, Faulkner has reported the isolation of makaluvamines H to M (**199-204**) [211], along with makaluvamines C, D, G and damirone C. An investigation of a Western Australian species of *Z. fuliginosa* reported the isolation of makaluvamines E, G and H and damirones A and B [214]. The final member of the series reported to date, makaluvamine N (**205**) [212], is a simple pyrroloquinoline comparable in structure to the isobatzellines with a halogen at the 6 position (R_3), but lacking a thiomethyl group.

Also reported from *Z. fuliginosa* are the makaluvic acids A (**206**) and B (**204**) [213], which can be considered as oxidation products of batzellines, isobatzellines or makaluvamines. Credence is given to this suggestion by the co-occurrence of 4-hydroxybenzoic acid, which can also be considered as an oxidation product of the tyramine portion of makaluvamines E or K which were found as co-occurring compounds. The structures of the makaluvic acids were based on NMR and MS arguments and X-ray crystallography.

Wakayin, Tsitsikammamine and Veiutamine

This group of compounds represents alternative structural motifs within the pyrroloquinolines. The isolation of wakayin (**208**), a new structural type of pyrroloquinoline from a *Clavelina* sp. ascidian found in shallow reef water off Wakaya Island in the Fiji Group, represents a real departure from the chemotaxonomic picture of the pyrroloquinolines

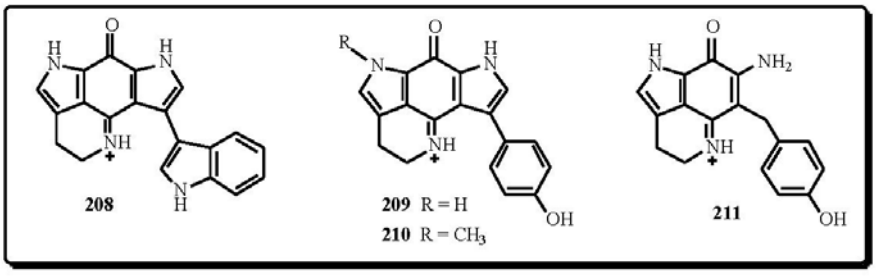

up to that point [217]. Hitherto, this structural group had only been found in the Porifera. The structure of wakayin, a topoisomerase II inhibitor, resulted from an extensive NMR analysis. A second group of bispyrroloquinolines, the tsitsikammamines A (**209**) and B (**210**), were isolated in 1996 from a South African Latrunculid sponge [216], and are a cross between the makaluvamine and discorhabdin skeletal types.

The final member in this grouping, veiutamine (**211**), is yet another pyrroloquinoline skeleton from a Fijian (Suva Harbour) *Zyzzya fuliginosa*, and not unexpectedly co-occurred with several makaluvamines (A, C, D and E) [218].

Discorhabdin Analogues

In addition to the isolation of naturally occurring pyrroloquinolines, a limited amount of chemistry has been carried out on discorhabdin C to generate a series of discorhabdin analogues based on the *spiro*-dienone system [195]. Discorhabdin C (**152**) was remarkably stable in acid, and required exposure to concentrated sulfuric acid to generate the phenol (**212**) by a dienone/phenol rearrangement. Following hydride reduction and aerial oxidation, the benzene derivative (**213**) was generated from the dienol (**214**). The stability of the pyrroloquinoline system was again confirmed by nitration of discorhabdin C phenol to give a nitro derivative (**215**) and a dienone (**216**). The various derivatives originating from this study formed the basis of a structure/activity study.

Distribution of the Pyrroloquinolines (Contributed by M. Kelly)

Following a thorough taxonomic re-evaluation of the various genera in which the pyrroloquinolines have been located to date, and of other compounds which have been attributed to the latrunculid genera [223], it is possible to draw definitive chemotaxonomic conclusions. Kelly-Borges and Vacelet's recent revision of the Latrunculiidae based on morphological characteristics has led to the transfer of latrunculin-producing species, previously identified as *Latrunculia*, e.g. *L. magnifica* Keller from the Red Sea, into the genus *Negombata*. *Negombata* spp. differ from *Latrunculia* spp. in fundamental taxonomic features such as the skeletal architecture and spicule complement, yet have been erroneously and hastily identified as *Latrunculia* spp. due to the presence of spined microscleres that only superficially resemble *Latrunculia*'s

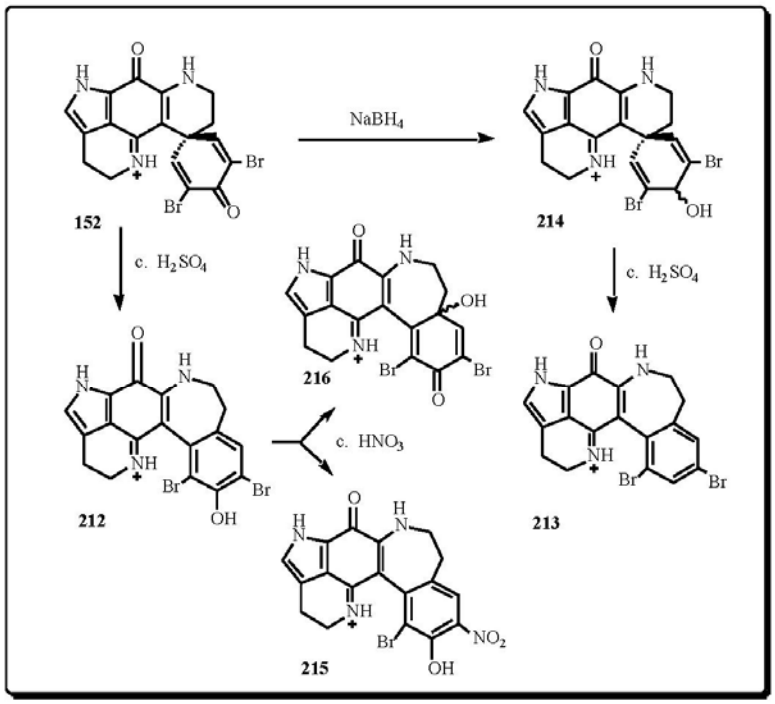

characteristic aniso acanthodiscorhabd microscleres. *Negombata* is also only found in tropical waters, whereas the distribution of *Latrunculia* spp. is in the southern hemisphere (southern ocean).

Similarly, the norsesterterpene peroxides are now considered to be a strong chemotaxonomic marker for the genera *Diacarnus* and *Sigmosceptrella*, into which many of the specimens identified as *Latrunculia* spp. from Australia and the Indo-Pacific have now been transferred. These genera are similar to *Negombata* in that they contain spined microscleres (spinulate microrhabds), a strongly plumose skeletal architecture, and are confined to the tropical latitudes [223].

Norsesterterpene peroxides have also been attributed to several undescribed species of *Prianos*, a genus which in the strict taxonomic sense belongs to the Haplosclerid family Chalinidae, and which contains surprisingly few described "true" species. This genus has unfortunately become a taxonomic "dustbin" for any sponge that has strongyles alone, due to the lack of additional differentiating characteristics. The Red Sea "*Prianos* sp." that produces the norsesterterpene peroxides, the muqubilins [224], is a species of *Diacarnus* with a reduced or totally absent microsclerecomplement, and vestigial strongyloxeas which resemble strongyles [223]. The observation of only strongyle-like spicules in this specimen superficially matches the generic diagnosis of *Prianos*.

The discorhabdins originate primarily from the genuine Southern Ocean *Latrunculia* species from South Africa and New Zealand [e.g. 195]. The notable exception to this is the isolation of prianosins (discorhabdins) from a sponge identified as *Prianos melanos* from shallow water in Okinawa [202]. Again, this identification is based on the erroneous observation of "strongyles-only" as the basis for assignment to the genus *Prianos*, and the black-green colour as the basis for assignment to the species *melanos*. In this case, *"Prianos" melanos* from Okinawa is similar to the latrunculid genus *Strongylodesma* known only from South Africa and New Caledonia (M. Kelly and T. Samaai, unpublished data). This genus lacks the characteristic microscleres of *Latrunculia*, and possesses "strongyles-only", but is similar to *Latrunculia* in all other morphological characteristics. Species of *Strongylodesma* are also known to produce a range of discorhabdins [M. Davies-Coleman, personal communication]. The issue is confused further as *Prianos melanos* de Laubenfels is only questionably a genuine species of *Prianos*.

The chemotaxonomic links between *Latrunculia* and *Zyzzya* are well established, with discorhabdins being isolated along with makaluvamines in *Zyzzya* species [e.g. 209] and makaluvamines occurring as minor components from *Latrunculia* species [197]. A new genus of South African Latrunculiidae morphologically intermediate to these two genera is of great significance, as it is linked by both morphology and the presence of the 14-bromodiscorhabdins (**177**) and (**178**) and the tsitsikammamines (**209**) and (**210**) ("hybrid" makaluvamines/discorhabdins) [216].

Another particularly important link is the discovery of discorhabdin P (**171**) in a deep-water Caribbean sponge identified as *Batzella* sp. [200], effectively establishing a chemotaxonomic link between this sponge, *Zyzzya* and *Latrunculia*. *N*-methylation is a feature of the pyrroloquinolines found in *"Batzella"*, and discorhabdin P is the only *N*-methyl discorhabdin isolated to date. The genus *Batzella* has also become a "taxonomic dustbin" for sponges containing only strongyle-like tornotes. It is hypothesised that this Caribbean deep-water sponge is also related taxonomically to the *Zyzzya*-

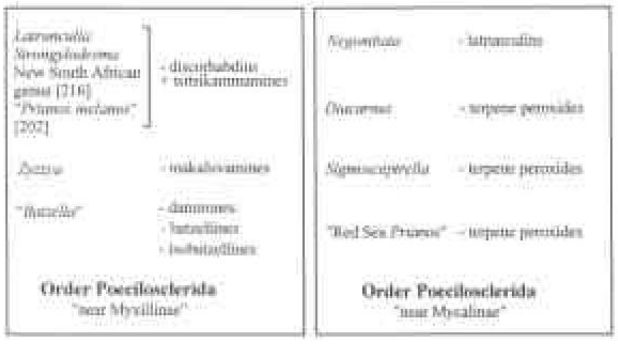

Fig. (9). A suggested taxonomy for the Latrunculiidae.

Latrunculia-Strongylodesma group, but that it is not a species of *Batzella* in the strict sense. *Batzella sensu strictu* is currently recognised within the Poecilosclerid family Phoriospongiidae.

Future taxonomic studies based on morphological examination of all relevant voucher specimens and molecular systematics should shed further light on the taxonomic relationships between *Zyzzya, Latrunculia* and related taxa *Negombata, Diacarnus* and *Sigmosceptrella*. It is hypothesised that all of the above genera are more closely related to Poecilosclerid sponges than to the order Hadromerida, where they are currently recognised [223], and that the latter group may comprise a new family closely allied with members of the subfamily Mycalinae. *Latrunculia* and *Strongylodesma*, the new South African Latrunculid genus [216], are similar in many characteristics to *Zyzzya* in the Poecilosclerid family Iophonidae, but are also sufficiently different to potentially constitute a new family.

Current indicators of phylogenetic affinity are summarised in Fig. (**9**).

Biogenesis

In 1995, a putative biogenesis of the discorhabdins was advanced [225] based on the perceived chemotaxonomic relationships between the various groups of pyrroloquinolines. This biogenetic proposal was supported by the observed modest incorporation (0.3%) of U-^{14}C-phenylalanine into discorhabdin B (**157**). No degradation studies were undertaken. In the biogenesis, it is suggested that the parent pyrroloquinoline (**A**) is formed from tryptophan as indicated in Fig. (**10**). From this parent pyrroloquinoline (**A**) the range of damirones, batzellines, isobatzellines and simple makaluvamines could be generated.

The parent pyrroloquinoline (**A**) is also invoked for the biogenesis of the more complex makaluvamines, discorhabdins, discorhabdin analogues and alternative skeletons such as wakayin and tsitsikammamines (Fig. (**11**)). The biogenetic pathway suggested by Munro [225] has been advanced by Heathcock, based on his successful biomimetic synthesis of discorhabdin C (**152**) and the first synthesis of dethiadiscorhabdin D [226]. Heathcock postulates that cyclisation of an appropriate makaluvamine takes place by an intramolecular Michael addition of the tyramine phenoxide, followed by auto-oxidation back to the quinone (outlined in Fig. (**11**)) leading to the discorhabdin C skeleton.

In examining the possibilities for formation of the discorhabdin D skeleton, Heathcock examined two possibilities. The first is the reduction of the quinoneimine to an aminophenol, followed by a 1,5-hydride shift and 1,6-addition of the enolate to the N of the quinoneimine (Fig. (**12**)). The alternative route suggests that the C2-N18 bond is formed by nucleophilic displacement of a C2 bromide, following reduction of the Δ^2-double bond of

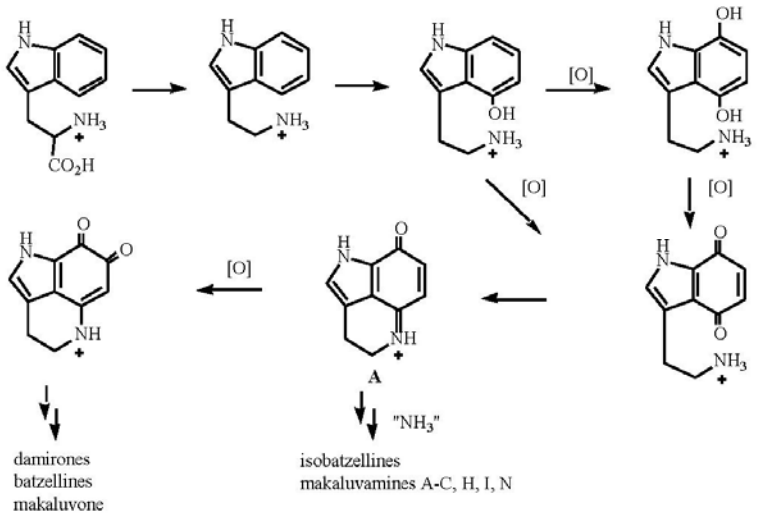

Fig. (10). Biogenetic proposal for the formation of the pyrroloquinoline skeleton.

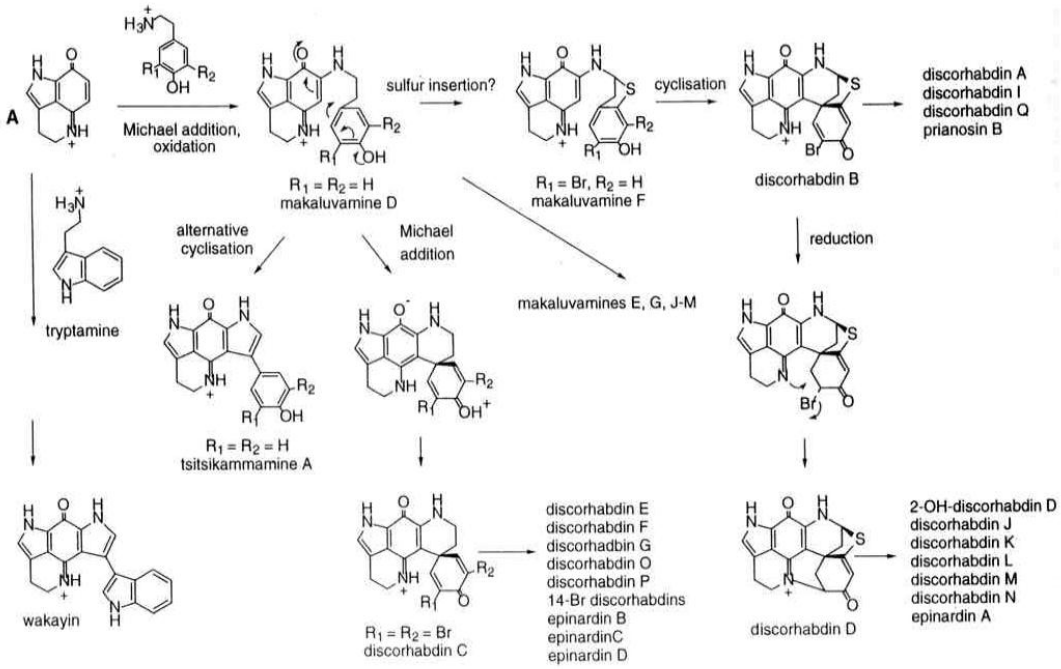

Fig. (11). Biogenetic proposal for the formation of the discorhabdins.

discorhabdin B, perhaps by the 1,5-hydride addition route. This second route is attractive as Heathcock has established that protonation of the enol is an intramolecular process with delivery of hydrogen from the protonated imine to generate an equatorial hydrogen. This intramolecular enol protonation would ensure that a C2 bromide would have the correct orientation for nucleophilic displacement, and indeed was used in the successful synthesis of dethiadiscorhabdin D [226]. From the discorhabdin B, C and D skeletons, the whole suite of known discorhabdins could be generated as suggested in Fig. (**11**).

An alternative cyclisation of makaluvamine D could lead to the tsitsikammamine skeleton, or by substituting tryptamine for a tyramine derivative, the wakayin skeleton could be generated (Fig. (**11**)).

Bioactivity

The incidence of bioactivity across the pyrroloquinoline series is high. It has stimulated

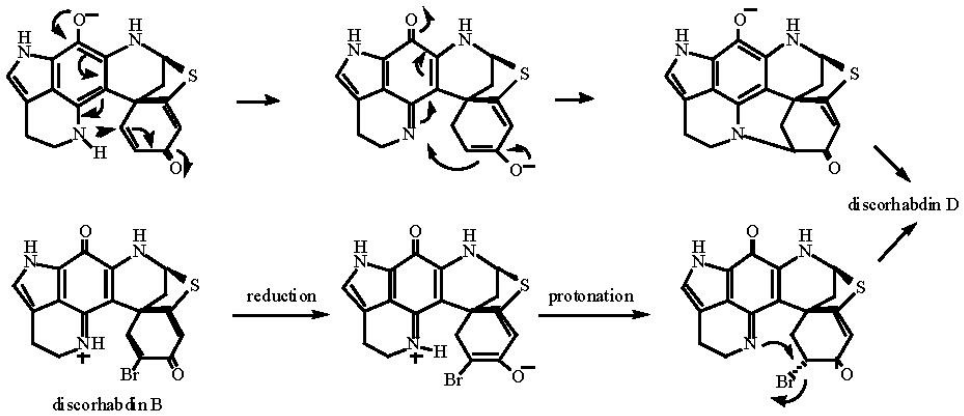

Fig. (12). Approaches to discorhabdin D.

great interest in discovery of further pyrroloquinoline representatives, and has resulted in the initiation of structure activity studies.

Discorhabdins

The discorhabdin series is characterised by a range of biological activity against a variety of assays, but especially noteworthy are the high levels of *in vitro* cytotoxicity against a variety of cell lines (P388, L1210, L5178, HCT-116 and KB) [189-193]. In the subsequent *in vivo* testing, only discorhabdin D (**158**) (T/C 132%) showed results that could be classified as significant (> 120%) [191]. With a wide range of discorhabdins and derivatives available, the structure/activity relationships (SAR's) are revealing (Table 2). From these data, it can be concluded that generation of the hepatacyclic system (e.g. discorhabdin D) leads to a significant drop in cytotoxicity (cf. discorhabdin I/D), as does substitution at C1 (cf. discorhabdin I/K or discorhabdin D/J, L, M, N). It can also be concluded that an intact dienone system is necessary (discorhabdin C/C dienol), and that formation of the 1**H**-azepine leads to significant loss of activity (discorhabdin C/C phenol). This suggestion is supported by the observation that on restoration of a dienone system, there is a recovery of activity (discorhabdin C dienone). This behaviour is suggestive that at least some element of the cytotoxicity of the discorhabdin skeleton is due to the propensity of the α-bromo-αβ-unsaturated ketone systems to act as Michael acceptors.[227].

Discorhabdin C (**152**), C dienol (**214**), C phenol (**212**) and C benzene (**213**) have been studied more extensively in the NCI's human tumour disease-oriented *in vitro* screen. Only discorhabdin C and the dienol met the criteria for further evaluation [195] by exhibiting differential cytotoxicity, but did not proceed further. Discorhabdin Q (**172**) was also examined the NCI's screen, and exhibited moderate generalised cytotoxicity (mean GI_{50} 0.5 μg/ml), but without a differential pattern of cytotoxicity [201].

Table 2. Structure Activity Relationships (SAR's) in the Discorhabdin Series

Discorhabdin	IC_{50} P388 (ng/mL)	Discorhabdin	IC_{50} P388 (ng/mL)
A [156]	10	L [167]	5200
B [157]	18	M [168]	>12500
C [152]	40	N [169]	>1250
D [158]	1150	O [170]	340
E [161]	200	C dienol [214]	525
G [163]	200	C phenol [212]	3000
I [164]	55	C benzene [213]	1700
J [165]	6600	C nitrophenol [215]	8500
K [166]	2500	C dienone [216]	385

In other assays, the discorhabdins and analogues have generally been noted as antimicrobial, with activities reported against various gram +ve and –ve bacilli, and antifungal activity against *Candida albicans*. In a more specific assay, discorhabdins A (**156**) and D (**158**) have been reported to be ten times as potent as caffeine in a Ca^{2+} assay, but this effect was not observed for prianosins B (**160**) and C (**159**) [202, 203, 205].

In mechanism-based assays, discorhabdin P (**171**) was found to be an inhibitor of two key peptidases, calcineurin and CPP32 (a member of the caspase family), at levels that were considered to be highly significant (0.55 and 0.37 μg/mL, respectively). Interestingly, discorhabdin P is *N*-methyldiscorhabdin C and in distinct contrast, discorhabdin C showed no activity against either enzyme [200].

Damirones, Batzellines, Isobatzellines and Makaluvamines

The damirones and batzellines have no reported biological activity. In contrast, the isobatzellines and secobatzellines, which contain the iminoquinone system, are cytotoxic. The isobatzellines A to D (**182-185**) are moderately active against the murine leukaemia P388 cell line (IC_{50} values 0.42–20 μg/mL), with isobatzelline A being the most active. The activity against the P388 cell line was accompanied, not unexpectedly, by antifungal activity against *Candida albicans* [207, 228]. Secobatzelline A (**186**) retains the iminoquinone system, but secobatzelline B (**187**) is the quinone. Secobatzelline A is particularly active against both the P388 and A-549 cell lines (IC_{50} 0.04 and 0.06 μg/mL, respectively), as well as being an effective inhibitor of calcineurin and CPP32 (IC_{50} 0.55 and 0.02 μg/mL, respectively) [221].

The bioactivity of the makaluvamines has been reviewed recently [229], and so will only be commented on briefly in this article. Using specifically mutated Chinese hamster cell lines, Ireland and Barrows developed a mechanism-based screen capable of detecting agents that act on DNA directly, or induce topoisomerase II to cleave DNA

through cleavable complexes [230]. This assay was used to establish that the likely mode of action of makaluvamines A to F **[191-196]** was by inhibition of topoisomerase II, although this suggestion was not fully supported by later papers [210-211]. In an extended study reported recently, using a wider range of makaluvamines, it was established that the makaluvamines have the ability to induce dose-dependent DNA cleavage *via* topoisomerase II [232]. Makaluvamines H (**199**) and I (**200**) are the most effective *in vitro*, and this is supported by *in vivo* results [214, 231, 232]. Exceptional activity was noted for makaluvamine H. The ability of the makaluvamines to promote topoisomerase II cleavage *in vitro* is quite possibly the activity that contributes to the high cytotoxicity of several of the makaluvamines in the HCT-116, P388, A549, HT-29, KB and MCF-7 cell lines [232].

Wakayin

Both makaluvamines and wakayin are DNA intercalators, but differ in their inhibition of the topoisomerases. Wakayin (**208**) induces topoisomerase I cleavage complexes, while the makaluvamines do not have appreciable topoisomerase I activity [233]. Wakayin is a new class of topoisomerase I inhibitor, and as such offers considerable potential as a new class of anticancer agent. The close structural relationship between the makaluvamines and wakayin offers hope that insights may come in time to establish the structural requirements for specific topoisomerase I or II inhibitors.

Synthesis

The high biological activity of the pyrroloquinoline skeleton and the structural novelty have ensured that there has been considerable synthetic activity over the past decade devoted to this target. Some of these approaches to the synthesis of the pyrroloquinoline skeleton have already been reviewed [229, 234]. Essentially, two synthetic approaches have been utilised in the construction of the pyrroloquinolines. The majority

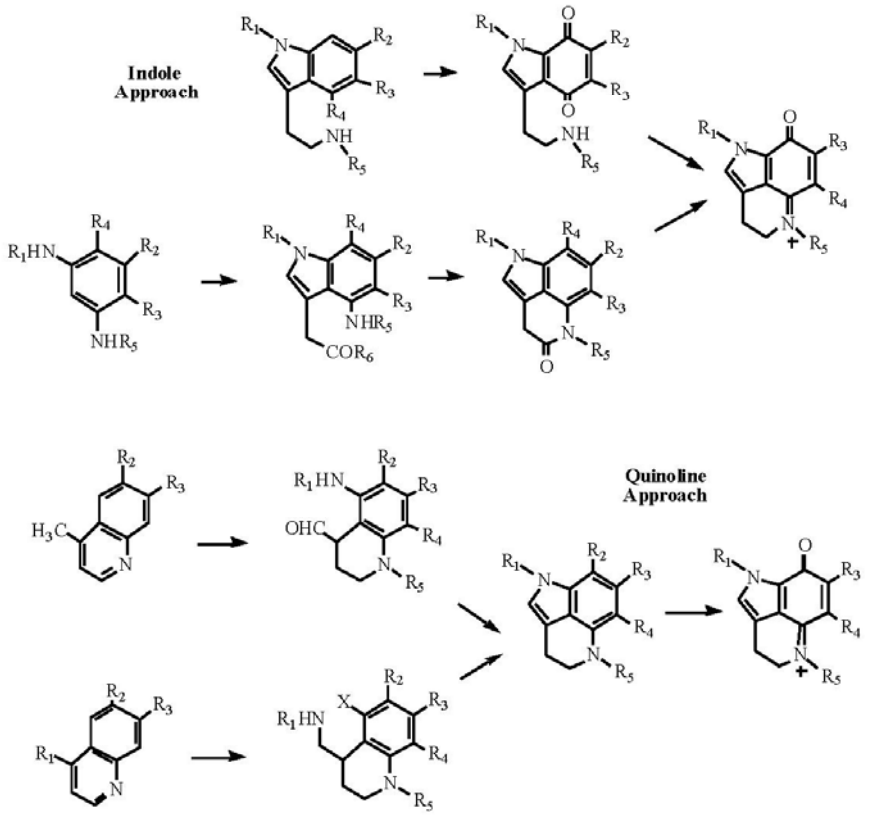

Fig. (13). Approaches to pyrroloquinolines.

of the synthetic effort has proceeded *via* a pre-existing indole nucleus, or invoked an indolic skeleton. The tricyclic core of the pyrroloquinoline has then been elaborated by generating the required six–membered ring by condensation of a tryptamine quinone, or by cyclisation of a 4-aminoindole carrying a two-carbon chain at the 3-position. These indole-based strategies are outlined in Fig. (**13**). By this strategy, successful syntheses of the damirones [235-237], makaluvamines [236, 238-245], batzellines and isobatzelline [236, 246] have been reported.

The alternative approach, based on a quinoline nucleus, requires a nitrogen substituent at the 5-position, or insertion of a N at the 5-position, and is also summarised in Fig. (**13**). The team of Joule and Alverez have been the main exponents of this route, and they and others have reported the successful synthesis or formal synthesis of the major pyrroloquinoline skeletons [247-256]. An interesting variant is the sequential generation of a quinolone followed by cyclisation to form the pyrroloquinoline system [257].

The major synthetic challenge *beyond* genesis of the pyrroloquinoline skeleton has been the generation of the discorhabdin skeleton. Several successful syntheses of discorhabdin C have now been published. To generate the *spiro*-dienone system, the coupling has been carried out using a hypervalent iodine reagent [241, 258-260], electrochemical oxidation [261-263], or by Michael addition [226]. Other approaches to disorhabdin C have also included phenolate alkylation [264] and iron-mediated spiroannulation [265].

No reports have yet appeared (to December, 1999) on the synthesis of any of the sulfur-containing discorhabdins, but Heathcock *et al.* have been successful in generation of the *spiro*-dienone by an intramolecular Michael addition followed by the Cu^{2+}-catalysed re-oxidation of the resultant aminophenol [226]. The formation of the C2-N18 bond is critical to the formation of the discorhabdin D skeleton. In the synthetic sequence, this was achieved by the stereoselective bromination of the ketone. The stereoselectivity arose as a consequence of the protonation of the enolate by the iminium ion to generate the C-Br bond in an axial configuration, set up for displacement by N18 (see Fig. (**12**)) to generate dethiadiscorhabdin D.

Veiutamine (**211**) has been synthesised by the direct lithiation of an appropriate *N*-BOC protected pyrroloquinoline nucleus [266], as has an aza analogue of damirone B [267]. Despite the synthesis of model compounds [268-269], wakayin is yet to be synthesised.

CONCLUSION

In examining bioactive natural products based on the pyrrole, pyrazine, isoquinoline, β-carboline and pyrroloquinoline motifs, the molecular biodiversity and biomedical potential offered by the marine environment is obvious. Several of the compounds reviewed are in clinical trials, or are being assessed in pre-clinical trials. A review of this type invariably brings up the vexed question of what role should natural products play in drug discovery. Currently, much of drug discovery is focused on the molecular approach and is dominated by the random screening of "chemical diversity". The viewpoint that genomics and combinatorial chemistry, in concert with high-throughput screening technologies, would supplant natural products is not an uncommon opinion. Indeed, the resources that pharmaceutical companies once focused on natural products research, are now re-directed towards combinatorial chemistry [5]. However, as several recent articles have pointed out, natural products play a unique role both in drug discovery and from the perspective of providing new types of structural diversity [5, 270-271]. The discovery of the variolin and the cephalostatin skeletons are good examples of novel structural types arising from random screening programmes. Whether or not synthetic chemists will replace natural products chemists is not the issue. The alternative approaches are each valuable and valid. The comprehensive statistical evaluation, undertaken by Henkel *et al.* [271], showed that there is a clear difference in the balance of structural properties (features) between natural products and synthetic compounds. As long as a difference remains between these two main sources for the biological screening effort, there will be a vital role for natural products, and in particular, marine natural products.

ACKNOWLEDGMENTS

The authors are grateful to the Cancer Society of New Zealand, Canterbury-West Coast Division Inc., for a Postgraduate Scholarship in Cancer Research (SJHH) and to Pharma Mar SA for providing funding for a Postdoctoral Fellowship (SU).

ABBREVIATIONS

1D & 2D NMR= One and two dimensional Nuclear Magnetic Resonance spectroscopy

A549 = Human lung carcinoma cell line

ATP = Adenosine triphosphate

AZT = 3'-Azido-3'-deoxythymidine

BOC = *N-tert*-Butoxycarbonyl

Calcineurin = Serine/threonine protein phosphatase

Caspase = Cysteine proteases

CPP32 = A cysteine protease

DDQ = 2,3-Dichloro-5,6-dicyano-1,4-benzoquinone

DNA = Deoxyribose nucleic acid

DOPA = [2-Amino-3-(3', 4'-dihydroxy-phenyl) propionic acid]

EC_{50} = Effective concentration (50%)

ED_{50} = Effective dose (50%)

Et = Ecteinascidin

G2-phase = The second gap-phase in cell cycle

GC = Gas liquid chromatography

HCT116 = Human colon cancer cell line

HCT116/VM46 = Multidrug resistant version of human colon cancer cell line; over-expression of P-glycoprotein

Hep G2 = Human hepatocellular carcinoma cell line

HIV = Human Immunodeficiency Virus

HPLC = High Performance Liquid Chromatography

IC_{50} = Inhibitory concentration (50%)

K-562 = Human chronic myelogenous leukaemia cell line

KB = Human oral epidermoid carcinoma cell line

L1210 = Lymphocytic murine leukaemia cell line

L5178 = Mouse lymphoma

LD_{50} = Lethal dose (50%)

LH-20 = Sephadex LH-20 gel permeation chromatography

Lo Vo/Dx = Human colon adenocarcinoma

M-phase = Mitotic phase of cell cycle

MCF7/ADR-RES = Human breast adenocarcinoma cell line

MDR = Multidrug resistant

MIC = Minimum inhibitory concentration

MS = Mass spectrometry

MTT = 3-(4,5-Dimethylthiazol-2-yl)-2,5-diphenyl-2*H*-tetrazolium bromide

^{15}N HMBC = Nitrogen Heteronuclear Multiple Bond Coherence (in NMR)

NCI = National Cancer Institute

OVCAR-8 = Ovarian cell line

P388 = Lymphoid murine leukaemia cell line

PKC = Protein kinase C

PP-1 = Protein phosphatase 1

PP-2A = Protein phosphatase 2A

PS system = NCI murine lymphocytic leukaemia

S-phase = Synthesis phase of cell cycle

SAR = Structural activity relationships

SK-MEL-5 = Human malignant melanoma cell line

SN12C = Renal cell line

SV40 = Transformed fibroblast cells

TLC = Thin layer chromatography

UACC-62 = Melanoma cell line

UV = Ultra-Violet spectrophotometry

REFERENCES

[1] Murata, M.; Naoki, H.; Matsunaga, S.; Satake, M.; Yasumoto, T. *J. Am. Chem. Soc.* **1994**, *116*, 7098.

[2] MarinLit, a database of marine natural product literature maintained by Blunt, J.W. and Munro, M.H.G.

[3] Bergman, W.; Feeney, R.J. *J. Org. Chem.* **1951**, *16*, 981.

[4] Quinn, R.J.; Gregson, R.P.; Cook, A.F.; Bartlett, R.T. *Tetrahedron Lett.* **1980**, *21*, 567.

[5] Zurer, P. *Chem. and Eng. News* **1999**, *March 29*, 28.

[6] Olivera, B.M. In Book of Abstracts, *The 9th NAITO Conference on Bioactive Natural Products and their Modes of Action*, Kanagawa, Japan **1997**, October 15-18, p. 30.

[7] Rinehart, K.L. Jr; Shaw, P.D.; Shield, L.S.; Gloer, J.B.; Harbour, G.C.; Koker, M.E.S.; Samain, D.; Schwartz, R.E.; Tymiak, A.A.; Weller, D.L.; Carter, G.T.; Munro, M.H.G.; Hughes, R.G. Jr; Renis, H.E.; Swynenberg, E.B.; Stringfellow, D.A.; Vavra, J.J.; Coats, J.H.; Zurenko, G.E.; Kuentzel, S.L.; Li, L.H.; Bakus, G.J.; Brusca, R.C.; Craft, L.L.; Young, D.N.; Connor, J.L. *Pure and Applied Chem.* **1981**, *53*, 795.

[8] Garson, M.J. In *Sponges in Time and Space*; van Soest, R.W.M.; van Kempen, Th.M.G.; Braekman, J.C., Ed.; Balkema, Rotterdam, **1994**; pp. 427-440.

[9] Faulkner, D.J. *Tetrahedron* **1977**, *33*, 1421.

[10] Ireland, C.; Roll, D.; Molinski, T.; McKee, T.; Zabriskie, M.; Swersey, C. *Memoirs Calif. Acad. Sci.* **1988**, *13*, 41.

[11] Blunt, J.W.; Calder, V.L.; Fenwick, G.D.; Lake, R.J.; McCombs, J.D.; Munro, M.H.G.; Perry, N.B. *J. Nat. Prod* **1987**, *50*, 290.

[12] Daloze, D.; Braekmann. In *Sponges in Time and Space*, van Soest, R.W.M.; van Kempen, Th.M.G.; Braekman, J.C., Ed.; Balkema, Rotterdam, **1994**; pp. 441-452.

[13] Andersen, R.J.; Faulkner, D.J.; Cun-Heng, H.; Van Duyne, G.D.; Clardy, J. *J. Am. Chem. Soc.* **1985**, *107*, 5492.

[14] Lindquist, N.; Fenical, W.; Van Duyne, G.D.; Clardy, J. *J. Org. Chem.* **1988**, *53*, 4570.

[15] Carroll, A.R.; Bowden, B.F.; Coll, J.C. *Aust. J. Chem.* **1993**, *46*, 489.

[16] Urban, S.; Butler, M.S.; Capon, R.J. *Aust. J. Chem.* **1994**, *47*, 1919.

[17] Urban, S.; Hobbs, L.; Hooper, J.N.A.; Capon, R.J. *Aust. J. Chem.* **1995**, *48*, 1491.

[18] Urban, S.; Capon, R.J. *Aust. J. Chem.* **1996**, *49*, 711.

[19] Venkata, M.; Reddy, M.V.R.; Faulkner, D.J.; Venkateswarlu, Y.; Rao, M.R. *Tetrahedron* **1997**, *53*, 3457.

[20] Davis, R.A.; Carroll, A.R.; Pierens, G.K.; Quinn, R.J. *J. Nat. Prod* **1999**, *62*, 419.

[21] Reddy, M.V.R.; Rao, M.R.; Rhodes, D.; Hansen, M.S.T.; Rubins, K.; Bushman, F.D.; Venkateswarlu, Y.; Faulkner, D.J. *J. Med. Chem.* **1999**, *42*, 1901.

[22] Kang, H.; Fenical, W. *J. Org. Chem.* **1997**, *62*, 3254.

[23] Yoshida, W.Y.; Lee, K.K.; Carroll, A.R.; Scheuer, P.J. *Helv. Chim. Acta* **1992**, *75*, 1721.

[24] Rudi, A.; Goldberg, I.; Stein, Z.; Frolow, F.; Benayahu, Y.; Schleyer, M.; Kashman, Y. *J. Org. Chem.* **1994**, *59*, 999.

[25] Chan, G.W.; Francis, T.; Thureen, D.R.; Offen, P.H.; Pierce, N.J.; Westley, J.W.; Johnson, R.K.; Faulkner, D.J. *J. Org. Chem.* **1993**, *58*, 2544.

[26] Kobayashi, J.; Cheng, J.; Kikuchi, Y.; Ishibashi, M.; Yamamura, S.; Ohizumi, Y.; Ohta, T.; Nozoe, S. *Tetrahedron Lett.* **1990**, *31*, 4617.

[27] Palermo, J.A.; Brasco, M.F.R.; Seldes, A.M. *Tetrahedron* **1996**, *52*, 2727.

[28] Furstner, A.; Weintritt, H.; Hupperts, A. *J. Org. Chem.* **1995**, *60*, 6637.

[29] Ishibashi, F.; Miyazaki, Y.; Iwao, M. *Tetrahedron* **1997**, *53*, 5951.

[30] Heim, A.; Terpin, A.; Steglich, W. *Angew. Chem. Int. Ed. Eng.* **1997**, *36*, 155.

[31] Fernández, J.L.; Garcia Gravalos, D.;Rodriquez Quesada, A. *PCT Int. Appl.* (patent) **1997**, 24 pp.

[32] Banwell, M.; Flynn, B.; Hockless, D. *Chem. Commun.* **1997**, 2259.

[33] Banwell, M.G.; Flynn, B.L.; CA130:3974; WO 9850365, A1 19981112, *PCT Int. Appl.* (patent) **1998**, 75 pp.

[34] Banwell, M.G.; Flynn, B.L.; Hockless, D.C.R.; Longmore, R.W.; Rae, A.D. *Aust. J. Chem.* **1998**, *52*, 755.

[35] Banwell, M.G.; Flynn, B.L.; Hamel, E.; Hockless, D.C.R. *Chem. Commun.* **1997**, 207.

[36] Díaz, M.T.; Guitián, E.; Castedo, L. In *Book of Abstracts, 2nd Euroconference on Marine Natural Products*, Spain **1999**, p. 188.

[37] Boger, D.L.; Boyce, C.W.; Labroli, M.A.; Sehon, C.A.; Jin, Q. *J. Am. Chem. Soc.* **1999**, *121*, 54.

[38] Terpin, A.; Polborn, K.; Steglich, W. *Tetrahedron* **1995**, *51*, 9941.

[39] Edstrom, E.D.; Wei, Y. *J. Org. Chem.* **1993**, *58*, 403.

[40] Sakamoto, T.; Kondo, Y.; Sato, S.; Yamanaka, H. *Tetrahedron Lett.* **1994**, *35*, 2919.

[41] Sakamoto, T.; Kondo, Y.; Sato, S.; Yamanaka, H. *J. Chem. Soc. Perkin Trans. 1* **1996**, 459.

[42] Wei, Y. *Diss. Abstr. Int. B* **1996**, *56*, 4894.

[43] Ebel, H.; Terpin, A.; Steglich, W. *TetrahedronLett.* **1998**, *39*, 9165.

[44] Quesada, A.R.; Gravalos, M.D.G.; Fernández, J.L. *Br. J. Cancer* **1996**, *74*, 677.

[45] Ganesan, A. *Stud. Nat. Prod. Chem.* **1996**, *18*, 875.

[46] Atta-ur-Rahman; Choudhary, M. I. *Alkaloids* **1999**, *52*, 233.

[47] Jacobs, M.F.; Kitching, W. *Curr. Org. Chem.* **1998**, *2*, 395.

[48] Ganesan, A. *Angew. Chem. Int. Ed. Eng.* **1996**, *35*, 611.

[49] Atta-ur-Rahman; Choudhary, M.I. *Nat. Prod. Rep.* **1997**, *14*, 191.

[50] Pettit, G.R.; Inoue, M.; Kamano, Y.; Herald, D.L.; Arm, C.; Dufresne, C.; Christie, N.D.; Schmidt, J.M.; Doubek, D.L.; Krupa, T.S. *J. Am. Chem. Soc.* **1988**, *110*, 2006.

[51] Ganesan, A.; Heathcock, C.H. *Chemtracts: Org. Chem.* **1988**, *1*, 311.

[52] Pettit, G.R.; Inoue, M.; Kamano, Y.; Dufresne, C.; Christie, N.; Niven, M.L.; Herald, D.L. *J. Chem. Soc. Chem. Commun.* **1988**, 1440.

[53] Pettit, G.R.; Inoue, M.; Kamano, Y.; Dufresne, C.; Christie, N.; Niven, M.L.; Herald, D.L. *J. Chem. Soc. Chem. Commun.* **1988**, 865.

[54] Pettit, G.R.; Kamano, Y.; Dufresne, C.; Inoue, M.; Christie, N.; Schmidt, J.M.; Doubek, D.L. *Can. J. Chem.* **1989**, *67*, 1509.

[55] Kamano, Y.; Inoue, M.; Pettit, G.R.; Dufresne, C.; Herald, D.L.; Christie, N.D. *Tennen Yuki Kagobutsu Toronkai Koen Yoshishu* **1988**, *30*, 220.

[56] Pettit, G.R.; Kamano, Y.; Inoue, M.; Dufresne, C.; Boyd, M.R.; Herald, C.L.; Schmidt, J.M.; Doubek, D.L.; Christie, N.D. *J. Org. Chem.* **1992**, *57*, 429.

[57] Pettit, G.R.; Xu, J.-P.; Williams, M.D.; Christie, N.D.; Doubek, D.L.; Schmidt, J.M.; Boyd, M.R. *J. Nat. Prod.* **1994**, *57*, 52.

[58] Pettit, G.R.; Ichihara, Y.; Xu, J.; Boyd, M.R.; Williams, M.D. *Bioorg. Med. Chem. Lett.* **1994**, *4*, 1507.

[59] Pettit, G.R.; Xu, J.P.; Ichihara, Y.; Williams, M.D.; Boyd, M.R. *Can. J. Chem.* **1994**, *72*, 2260.

[60] Pettit, G.R.; Xu, J.P.; Schmidt, J.M. *Bioorg. Med. Chem. Lett.* **1995**, *5*, 2027.

[61] Pettit, G.R.; Tan, R.; Xu, J.; Ichihara, Y.; Williams, M.D.; Boyd, M.R. *J. Nat. Prod.* **1998**, *61*, 955.

[62] Drögemüller, M.; Flessner, T.; Jautelat, R.; Scholz, U.; Winterfeldt, E. *Eur. J. Org. Chem.* **1998**, 2811.

[63] Fukuzawa, S.; Matsunaga, S.; Fusetani, N. *J. Org. Chem.* **1997**, *62*, 4484.

[64] Fukuzawa, S.; Matsunaga, S.; Fusetani, N. *Tetrahedron* **1995**, *51*, 6707.

[65] Fukuzawa, S.; Matsunaga, S.; Fusetani, N. *Tetrahedron Lett.* **1996**, *37*, 1447.

[66] Fukuzawa, S.; Matsunaga, S.; Fusetani, N. *Tennen Yuki Kagobutsu Toronkai Koen Yoshishu* **1994**, *36*, 81.

[67] Fukuzawa, S.; Matsunaga, S.; Fusetani, N. *Tennen Yuki Kagobutsu Toronkai Koen Yoshishu* **1996**, *38*, 73.

[68] Fukuzawa, S.; Matsunaga, S.; Fusetani, N. *J. Org. Chem.* **1995**, *60*, 608.

[69] Fukuzawa, S.; Matsunaga, S.; Fusetani, N. *J. Org. Chem.* **1994**, *59*, 6164.

[70] Pan, Y.; Merriman, R.L.; Tanzer, L.R.; Fuchs, P.L. *Bioorg. Med. Chem. Lett.* **1992**, *2*, 967.

[71] Bhandaru, S.; Fuchs, P.L. *TetrahedronLett.* **1995**, *36*, 8347.

[72] Pettit, G.R.; Kamano, Y.; CA115:248095; US 5047532 A; 19910910, *US Pat. Appl.* (patent) **1991**, 8 pp.

[73] Pettit, G.R.; Kamano, Y.; CA121:221984; EP 608109 A1; 19940727, *Eur. Pat. Appl.* (patent) **1994**, 19 pp.

[74] Pettit, G.R.; Kamano, Y.; CA113:84818; WO 89-US927; 19890307, *PCT Int. Appl.* (patent) **1989**, 29 pp.

[75] Pettit, G.R.; Kamano, Y.; CA112:62611; US 4873245 A; 19891010, *US Pat. Appl.* (patent) **1989**, 14 pp.

[76] LaCour, T.G.; Guo, C.; Bhandaru, S.; Boyd, M.R.; Fuchs, P.L. *J. Am. Chem. Soc.* **1998**, *120*, 692.

[77] Guo, C.; LaCour, T.G.; Fuchs, P.L. *Bioorg. Med. Chem. Lett.* **1999**, *9*, 419.

[78] Guo, C.; Bhandaru, S.; Fuchs, P.L. *J. Am. Chem. Soc.* **1996**, *118*, 10672.

[79] Kim, S.; Sutton, S.C.; Guo, C.; LaCour, T.G.; Fuchs, P.L. *J. Am. Chem. Soc.* **1999**, *121*, 2056.

[80] Jeong, J.U.; Fuchs, P.L. *J. Am. Chem. Soc.* **1994**, *116*, 773.

[81] Kim, S.; Fuchs, P.L. *Tetrahedron Lett.* **1994**, *35*, 7163.

[82] Jeong, J.U.; Fuchs, P.L. *Tetrahedron Lett.* **1994**, *35*, 5385.

[83] LaCour, T.G.; Fuchs, P.L. *TetrahedronLett.* **1999**, *40*, 4655.

[84] Guo, C.; Fuchs, P.L. *Diss. Abstr. Int. B* **1998**, *59*, 4114.

[85] Kim, S.; Fuchs, P.L. *Diss. Abstr. Int. B* **1995**, *56*, 827.

[86] Lee, S.W.; Fuchs, P.L. *Diss. Abstr. Int. B* **1994**, *54*, 4676.

[87] Jeong, J.U.; Fuchs, P.L. *Diss. Abstr. Int. B* **1997**, *57*, 4398.

[88] Bhandaru, S.; Fuchs, P.L. *Diss. Abstr. Int. B* **1997**, *58*, 1286.

[89] Bhandaru, S.; Fuchs, P.L. *Tetrahedron Lett.* **1995**, *36*, 8351.

[90] Kim, S.; Sutton, S.C.; Fuchs, P.L. *Tetrahedron Lett.* **1995**, *36*, 2427.

[91] Jeong, J.U.; Fuchs, P.L. *Tetrahedron Lett.* **1995**, *36*, 2431.

[92] Jeong, J.U.; Guo, C.; Fuchs, P.L. *J. Am. Chem. Soc.* **1999**, *121*, 2071.

[93] Jeong, J.U.; Sutton, S.C.; Kim, S.; Fuchs, P.L. *J. Am. Chem. Soc.* **1995**, *117*, 10157.

[94] Drögemüller, M.; Jautelat, R.; Winterfeldt, E. *Angew. Chem. Int. Ed. Engl.* **1996**, *35*, 1572.

[95] Kramer, A.; Ullmann, U.; Winterfeldt, E. *J. Chem. Soc. Perkin Trans. 1* **1993**, 2865.

[96] Jautelat, R.; Winterfeldt, E.; Kramer, A.; CA128:23056; DE 19620146 A1; 19971113, *Ger. Offen.* (patent) **1997**, 9 pp.

[97] Winterfeldt, E.; Kramer, A.; Ullmann, U; Laurent, H.; CA122:265778; DE 4318924 A1; 19941208, *Ger. Offen.* (patent) **1994**, 13 pp.

[98] Smith, S.C.; Heathcock, C.H. *J. Org. Chem.* **1992**, *57*, 6379.

[99] Heathcock, C.H.; Smith, S.C. *J. Org. Chem.* **1995**, *60*, 6641.

[100] Heathcock, C.H.; Smith, S.C. *J. Org. Chem.* **1994**, *59*, 6828.

[101] Kemp, S.J.; Fuchs, P.L. *Diss. Abstr. Int. B* **1996**, *57*, 1799.

[102] Maheswaran, S.; Fuchs, P.L. *Diss. Abstr. Int. B* **1997**, *58*, 1888.

[103] Baker, B.J. In *Alkaloids: Chemical and Biological Perspectives*; Pelletier W, Ed.; Pergamon: Oxford, **1996**; Vol. *10*, pp. 357-407.

[104] Inoue, S.; Okada, K.; Tanino, H.; Kakio, H.; Goto, T. *Chem. Lett.* **1980**, 297.

[105] Sakai, R.; Higa, T.; Jefford, C.W.; Bernardinelli, G. *J. Am. Chem. Soc.* **1986**, *108*, 6404.

[106] Rinehart, K.L.; Holt, T.G.; Fregeau, N.L.; Stroh, J.G.; Keifer, P.A.; Sun, F.; Li, L.H.; Martin, D.G. *J. Org. Chem.* **1990**, *55*, 4512.

[107] Wright, A.E.; Forleo, D.A.; Gunawardana, G.P.; Gunasekera, S.P.; Koehn, F.E.; McConnell, O. J. *J. Org. Chem.* **1990**, *55*, 4508.

[108] Rinehart, K.L. In *Med. Chem.: Today Tomorrow, Proc. AFMC Int. Med. Chem. Symp.*; Yamazaki M., Ed.; Blackwell: Oxford, UK, **1995**; pp. 7-14.

[109] Sigel, M.M.; Wellham, W.; Lichter, W.; Dudeck, L.E.; Gargus, J.L.; Lucas, A.H. In *Food-Drugs from the Sea Proceedings*, Youngken, H.W., Ed.; Marine Technology Society: Washington D.C., **1970**; pp. 281-294.

[110] Sakai, R.; Rinehart, K.L.; Guan, Y.; Wang, A.H. *J. Proc. Natl. Acad. Sci. USA* **1992**, *89*, 11456.

[111] Sakai, R.; Jares-Erijman, E.A.; Manzanares, I.; Elipe, M.V.S.; Rinehart, K.L. *J. Am. Chem. Soc.* **1996**, *118*, 9017.

[112] Fenical, W. *Oceanography* **1996**, *9*, 23.

[113] Robinson, A. *Business Week* **1999**, *Sept. 13*, 22.

[114] Rinehart, K.L.; Zhou, T. *PCT Int. Appl.* (patent) **1998**, WO 98-US7340 19980414, 27 pp.

[115] Jow, C.K. *Diss. Abstr. Int. B* **1995**, *56*, 6747.

[116] Corey, E.J.; Gin, D.Y. *TetrahedronLett.* **1996**, *37*, 7163.

[117] Corey, E.J.; Gin, D.Y.; Kania, R.S. *J. Am. Chem. Soc.* **1996**, *118*, 9202.

[118] Saito, N.; Tashiro, K.; Maru, Y.; Yamaguchi, K.; Kubo, A. *J. Chem. Soc. Perkin Trans. 1* **1997**, 53.

[119] Endo, A.; Kann, T.; Fukuyama, T. *Synlett* **1999**, 1103.

[120] Martinez, E.J.; Owa, T.; Schreiber, S.L.; Corey, E. *J. Proc. Natl. Acad. Sci. USA* **1999**, *96*, 3496.

[121] Jaspars, M. In *Advances in Drug Discovery Techniques*; Harvey, A.L., Ed.; Wiley, **1998**, pp. 65-84.

[122] Jimeno, J.M.; Faircloth, G.; Cameron, L.; Meely, K.; Vega, E.; Gömez, A.; Fernández, J.M.; Rinehart, K.L. *Drugs Fut.* **1996**, *21*, 1155.

[123] Jaspars, M. *Chem. Ind.* **1999**, 51.

[124] Pommier, Y.; Kohlhagen, G.; Bailly, C.; Waring, M.; Mazumder, A.; Kohn, K.W. *Biochemistry* **1996**, *35*, 13303.

[125] Moore, B.M.; Seaman, F.C.; Hurley, L.H. *J. Am. Chem. Soc.* **1997**, *119*, 5475.

[126] Moore, B.M.; Seaman, F.C.; Wheelhouse, R.T.; Hurley, L.H. *J. Am. Chem. Soc.* **1998**, *120*, 2490.

[127] Guan, Y.; Sakai, R.; Rinehart, K.L.; Wang, A.H.J. *J. Biomol. Struct. Dyn.* **1993**, *10*, 793.

[128] Moore, B.M.; Seaman, F.C.; Hurley, L.H. In *Ernst Schering Res. Found. Workshop*; Diederich, F.; Künzer, H., Eds; Springer: Berlin, New York, **1998**; pp. 81-95.

[129] Seaman, F.C.; Hurley, L.H. *J. Am. Chem. Soc.* **1998**, *120*, 13028.

[130] Takebayashi, Y.; Pourquier, P.; Yoshida, A.; Kohlhagen, G.; Pommier, Y. *Proc. Natl. Acad. Sci. USA* **1999**, *96*, 7196.

[131] Zewail-Foote, M.; Hurley, L.H. *J. Med. Chem.* **1999**, *42*, 2493.

[132] Izbicka, E.; Lawrence, R.; Raymond, E.; Eckhardt, G.; Faircloth, G.; Jimeno, J.; Clark, G.; Von Hoff, D.D. *Ann. Oncol.* **1998**, *9*, 981.

[133] Dincalci, M. *Ann. Oncol.* **1998**, *9*, 937.

[134] Jordan, A.; Hadfield, J.A.; Lawrence, N.J.; McGown, A.T. *Medicinal Research Reviews* **1998**, *18*, 259.

[135] García-Rocha, M.; García-Gravalos, M.D.; Avila, J. *Br. J. Cancer* **1996**, *73*, 875.

[136] Nakamura, H.; Deng, S.; Kobayashi, J.; Ohizumi, Y.; Tomotake, Y.; Matsuzaki, T.; Hirata, Y. *Tetrahedron Lett.* **1987**, 28, 621.

[137] Ichiba, T.; Sakai, R.; Kohmoto, S.; Saucy, G.; Higa, T. *Tetrahedron Lett.* **1988**, *29*, 3083.

[138] Higa, T.; Sakai, R. *PCT Int. Appl.* (patent) **1988**, WO 88/198 A1, 27 pp.

[139] Kobayashi, M.; Chen, Y.J.; Aoki, S.; In, Y.; Ishida, T.; Kitagawa, I. *Tetrahedron* **1995**, *51*, 3727.

[140] Sakai, R.; Kohmoto, S.; Higa, T.; Jefford, C.W.; Bernardinelli, G. *Tetrahedron Lett.* **1987**, *28*, 5493.

[141] Higa, T. In *Studies in Natural Products Chemistry*; Atta-ur-Rahman, Ed.; Elsevier: Amsterdam, **1989**; pp. 341-376.

[142] Ichiba, T.; Corgiat, J.M.; Scheuer, P.J.; Kelly-Borges, M. *J. Nat. Prod.* **1994**, *57*, 168.

[143] Kondo, K.; Shigemori, H.; Kikuchi, Y.; Ishibashi, M.; Sasaki, T.; Kobayashi, J. *J. Org. Chem.* **1992**, *57*, 2480.

[144] Crews, P.; Cheng, X.C.; Adamczeski, M.; Rodriguez, J.; Jaspars, M.; Schmitz, F.J.; Traeger, S.C.; Pordesimo, E.O. *Tetrahedron* **1994**, *50*, 13567.

[145] Kobayashi, J.; Tsuda, M.; Kawasaki, N.; Sasaki, T.; Mikami, Y. *J. Nat. Prod.* **1994**, *57*, 1737.

[146] Tsuda, M.; Kawasaki, N.; Kobayashi, J. *Tetrahedron Lett.* **1994**, *35*, 4387.

[147] Tsuda, M.; Kawasaki, N.; Kobayashi, J. *Tetrahedron* **1994**, *50*, 7957.

[148] Kobayashi, J.; Tsuda, M.; Kawasaki, N.; Matsumoto, K.; Adachi, T. *Tetrahedron Lett.* **1994**, *35*, 4383.

[149] Tsuda, M.; Inaba, K.; Kawasaki, N.; Honma, K.; Kobayashi, J. *Tetrahedron* **1996**, *52*, 2319.

[150] Kobayashi, J.; Kawasaki, N.; Tsuda, M. *Tetrahedron Lett.* **1996**, *37*, 8203.

[151] Kong, F.; Andersen, R.J.; Allen, T.M. *Tetrahedron Lett.* **1994**, *35*, 1643.

[152] Kong, F.M.; Andersen, R.J.; Allen, T.M. *Tetrahedron* **1994**, *50*, 6137.

[153] Kong, F.M.; Andersen, R.J. *Tetrahedron* **1995**, *51*, 2895.

[154] Rodriguez, J.; Peters, B.M.; Kurz, L.; Schatzman, R.C.; McCarley, D.; Lou, L.; Crews, P. *J. Am. Chem. Soc.* **1993**, *115*, 10436.

[155] Rodriguez, J.; Crews, P. *Tetrahedron Lett.* **1994**, *35*, 4719.

[156] Ohtani, I.I.; Ichiba, T.; Isobe, M.; Kelly-Borges, M.; Scheuer, P.J. *J. Am. Chem. Soc.* **1995**, *117*, 10743.

[157] Bourguet-Kondracki, M.L.; Martin, M.T.; Guyot, M. *Tetrahedron Lett.* **1996**, *37*, 3457.

[158] Edrada, R.A.; Proksch, P.; Wray, V.; Witte, L.; Muller, W.E.G.; van Soest, R.W.M. *J. Nat. Prod.* **1996**, *59*, 1056.

[159] Kobayashi, J.; Watanabe, D.; Kawasaki, N.; Tsuda, M. *J. Org. Chem.* **1997**, *62*, 9236.

[160] Tsuda, M.; Watanabe, D.; Kobayashi, J. *Tetrahedron Lett.* **1998**, *39*, 1207.

[161] Watanabe, D.; Tsuda, M.; Kobayashi, J. *J. Nat. Prod.* **1998**, *61*, 689.

[162] Tsuda, M.; Watanabe, D.; Kobayashi, J. *Heterocycles* **1999**, *50*, 485.

[163] Baldwin, J.E.; Whitehead, R.C. *Tetrahedron Lett.* **1992**, *33*, 2059.

[164] Baldwin, J.E.; Claridge, T.D.W.; Heupel, F.A.; Whitehead, R.C. *Tetrahedron Lett.* **1994**, *35*, 7829.

[165] Baldwin, J.E.; Claridge, T.D.W.; Culshaw, A.J.; Heupel, F.A.; Smrckova, S.; Whitehead, R.C. *Tetrahedron Lett.* **1996**, *37*, 6919.

[166] Baldwin, J.E.; Claridge, T.D.W.; Culshaw, A.J.; Heupel, F.A.; Lee, V.; Spring, D.R.; Whitehead, R.C., Boughtflower R.J.; Mutton, I.M.; Upton R.J. *Angew. Chem. Int. Ed. Eng.* **1998**, 37, 2661.

[167] Baldwin, J.E.; Bischoff, L.; Claridge, D.W.; Heupel, F.A.; Spring, D.R.; Whitehead, R.C. *Tetrahedron* **1997**, *53*, 2271.

[168] Gil, L.; Baucherel, X.; Martin, M.T.; Marazano, C.; Das, B.C. *Tetrahedron Lett.* **1995**, *36*, 6231.

[169] Kaiser, A.; Billot, X.; Gateauolesker, A.; Marazano, C.; Das, B.C. *J. Am. Chem. Soc.* **1998**, *120*, 8026.

[170] Jakubowicz, K.; Abdeljelil, K.B.; Herdemann, M.; Martin, M.T.; Gateau-Olesker, A.; Mourabit, A.A.; Marazano, C.; Das, B.C. *J. Org. Chem.* **1999**, *64*, 7381.

[171] Kong, F. *Diss. Abstr. Int. B* **1996**, *57*, 1812.

[172] Magnier, E.; Langlois, Y. *Tetrahedron* **1998**, *54*, 6201.

[173] Matzanke, N.; Gregg, R.J.; Weinreb, S.M. *Org. Prep. Proced. Int.* **1998**, *30*, 1.

[174] Torisawa, Y.; Hashimoto, A.; Nakagawa, M.; Hino, T. *Tetrahedron Lett.* **1989**, *30*, 6549.

[175] Torisawa, Y.; Hashimoto, A.; Nakagawa, M.; Seki, H.; Hara, R.; Hino, T. *Tetrahedron* **1991**, *47*, 8067.

[176] Nowak, W.; Gerlach, H. *Liebigs Ann. Chem.* **1993**, 153.

[177] Winkler, J.D.; Axten, J.M. *J. Am. Chem. Soc.* **1998**, *120*, 6425.

[178] Martin, S.F.; Humphrey, J.M.; Ali, A.; Hillier, M.C. *J. Am. Chem. Soc.* **1999**, *121*, 866.

[179] Ohtani, I.I.; Ichiba, T.; Isobe, M.; Kelly-Borges, M.; Scheuer, P.J. *Tennen Yuki Kagobutsu Toronkai Koen Yoshishu* **1995**, *37*, 236.

[180] Coldham, I.; Coles, S.J.; Crapnell, K.M.; Fernàndez, J.C.; Haxell, T.F.N.; Hursthouse, M.B.; Moseley, J.D.; Treacy, A.B. *Chem. Commun.* **1999**, 1757.

[181] Pandit, U.K.; Overkleeft, H.S.; Borer, B.C.; Bieräugel, H. *Eur. J. Org. Chem.* **1999**, 959.

[182] Bland, D.; Chambournier, G.; Dragon, V.; Hart, D.J. *Tetrahedron* **1999**, *55*, 8953.

[183] Perry, N.B.; Ettouati, L.; Litaudon, M.; Blunt, J.W.; Munro, M.H.G. *Tetrahedron* **1994**, *50*, 3987.

[184] Trimurtulu, G.; Faulkner, D.J.; Perry, N.B.; Ettouati, L.; Litaudon, M.; Blunt, J.W.; Munro, M.H.G.; Jameson, G.B. *Tetrahedron* **1994**, *50*, 3993.

[185] Alvarez, M.; Fernández, D.; Joule, J.A. *J. Chem. Soc. Perkin Trans. 1* **1999**, 249.

[186] Alvarez, M.; Fernández, D.; Joule, J.A. *Synthesis* **1999**, 615.

[187] Alvarez, M.; Fernández, D.; Meigh, J.P.K.; Joule, J.A. In *Book of Abstracts, 2nd Euroconference on Marine Natural Products*, Spain **1999**, p. 155.

[188] Märki, F.; Robertson, A.V.; Witkop, B. *J. Am. Chem. Soc.* **1961**, *83*, 3341.

[189] Perry, N.B.; Blunt, J.W.; McCombs, J.D.; Munro, M.H.G. *J. Org. Chem.* **1986**, *51*, 5476.

[190] Perry, N.B.; Blunt, J.W.; Munro, M.H.G. *Tetrahedron* **1988**, *44*, 1727.

[191] Perry, N.B.; Blunt, J.W.; Munro, M.H.G.; Higa, T.; Sakai, R. *J. Org. Chem.* **1988**, *53*, 4127.

[192] Munro, M.H.G.; Perry, N.B.; Blunt, J.W.; CA110:54771; WO 8800946, A1 19880211, *PCT Int. Appl.* (patent) **1988**, 34 pp.

[193] Munro, M.H.G.; Perry, N.B.; Blunt, J.W; CA112:112067; US 89294394, A 19890109, *US Pat. Appl.* (patent) **1989**, 3 pp.

[194] Munro, M.H.G.; Blunt, J.W.; Barns, G.; Battershill, C.N.; Lake, R.J.; Perry, N.B. *Pure Appl. Chem.* **1989**, *61*, 529.

[195] Copp, B.R.; Fulton, K.F.; Perry, N.B.; Blunt, J.W.; Munro, M.H.G. *J. Org. Chem.* **1994**, *59*, 8233.

[196] Blunt, J.W.; Munro, M.H.G.; Battershill, C.N.; Copp, B.R.; McCombs, J.D.; Perry, N.B.; Prinsep, M.; Thompson, A.M. *New J. Chem.* **1990**, *14*, 761.

[197] Perry, N.B.; McCombs, J.D.; Copp, B.R.; Rea, J.; Lill, R.; Major, D.A; Andrew, C.; Fulton, K.; Bringans, S.D.; Blunt, J.W.; Munro, M.H.G. In *Book of Abstracts, The 37th Annual Meeting of the American Society of Pharmacognosy,* University of California, Santa Cruz, CA, July 27-31, 1996, p. 28.

[198] Yang, A.; Baker, B.J.; Grimwade, J.; Leonard, A.; McClintock, J.B. *J. Nat. Prod.* **1995**, *58*, 1596.

[199] McClintock, J.B.; Baker, B. *J. Am. Zool.* **1997**, *37*, 329.

[200] Gunasekera, S.P.; McCarthy, P.J.; Longley, R.E.; Pomponi, S.A.; Wright, A.E.; Lobkovsky, E.; Clardy, J. *J. Nat. Prod* **1999**, *62*, 173.

[201] Dijoux, M.G.; Gamble, W.R.; Hallock, Y.F.; Cardellina, J.H.; van Soest, R.; Boyd, M.R. *J. Nat. Prod.* **1999**, *62*, 636.

[202] Kobayashi, J.; Cheng, J.; Ishibashi, M.; Nakamura, H.; Ohizumi, Y.; Hirata, Y.; Sasaki, T.; Lu, H.; Clardy, J. *Tetrahedron Lett.* **1987**, *28*, 4939.

[203] Cheng, J.; Ohizumi, Y.; Wälchli, M.R.; Nakamura, H.; Hirata, Y.; Sasaki, T.; Kobayashi, J. *J. Org. Chem.* **1988**, *53*, 4621.

[204] Kobayashi, J.; Cheng, J-F.; Yamamura, S.; Ishibashi, M. *Tetrahedron Lett.* **1991**, *32*, 1227.

[205] Kobayashi, J.; Oizumi, Y.; CA112:185776; JP 8883190, A2 *19880406 Jpn. Kokai Tokkyo Koho* (patent) **1989**, 4 pp.

[206] Sakemi, S.; Sun, H.H.; Jefford, C.W.; Bernardinelli, G. *Tetrahedron Lett.* **1989**, *30*, 2517.

[207] Sun, H.H.; Sakemi, S.; Burres, N.; McCarthy, P. *J. Org. Chem.* **1990**, *55*, 4964.

[208] Stierle, D.B.; Faulkner, D.J. *J. Nat. Prod.* **1991**, *54*, 1131.

[209] Radisky, D.C.; Radisky, E.S.; Barrows, L.R.; Copp, B.R.; Kramer, R.A.; Ireland, C.M. *J. Am. Chem. Soc.* **1993**, *115*, 1632.

[210] Carney, J.R.; Scheuer, P.J.; Kelly-Borges, M. *Tetrahedron* **1993**, *49*, 8483.

[211] Schmidt, E.W.; Harper, M.K.; Faulkner, D.J. *J. Nat. Prod.* **1995**, *58*, 1861.

[212] Venables, D.A.; Concepcion, G.P.; Matsumoto, S.S.; Barrows, L.R.; Ireland, C.M. *J. Nat. Prod.* **1997**, *60*, 408.

[213] Fu, X.; Ng, P.L.; Schmitz, F.J.; Hossain, M.B.; Vanderhelm, D.; Kelly-Borges, M. *J. Nat. Prod.* **1996**, *59*, 1104.

[214] Popov, A.M.; Utkina, N.K. *Khim. Farm. Zh.* **1998**, *32*, 12.

[215] D'Ambrosio, M.; Guerriero, A.; Chiasera, G.; Pietra, F. *Tetrahedron* **1996**, *52*, 8899.

[216] Hooper, G.J.; Davies-Coleman, M.T.; Kelly-Borges, M.; Coetzee, P.S. *Tetrahedron Lett.* **1996**, *37*, 7135.

[217] Copp, B.R.; Ireland, C.M.; Barrows, L.R. *J. Org. Chem.* **1991**, *56*, 4596.

[218] Venables, D.A.; Barrows, L.R.; Lassota, P.; Ireland, C.M. *Tetrahedron Lett.* **1997**, 38, 721.

[219] Turner, E.; Klevit, R.; Hopkins, P.B.; Shapiro, B.M. *J. Biol. Chem.* **1986**, *261*, 13056.

[220] Pathirana, C.; Andersen, R.J. *J. Am. Chem. Soc.* **1986**, *108*, 8288.

[221] Gunasekara, S.P.; McCarthy, P.J.; Longley, R.E.; Pomponi, S.A.; Wright, A.E. *J. Nat. Prod.* **1999**, *62*, 1208.

[222] van Soest, R.W.M; Braekman, J.C; Faulkner, D.J; Hajdu, E.Z; Harper, M.K; Vacelet, J. *Biologie* **1996**, *6*, 1.

[223] Kelly-Borges, M.; Vacelet, J. *Mem. Queensl. Mus.* **1995**, *38*, 477.

[224] Kashman, Y.; Rotem, M. *Tetrahedron Lett.* **1979**, 1707.

[225] Lill, R.E.; Major, D.A.; Blunt, J.W.; Munro, M.H.G.; Battershill, C.N.; McLean, M.G.; Baxter, R.L. *J. Nat. Prod.* **1995**, *58*, 306.

[226] Aubart, K.M.; Heathcock, C.H. *J. Org. Chem.* **1999**, *64*, 16.

[227] Hanson, R.L.; Lardy, H.A.; Kupchan, S.M. *Science* **1970**, *168*, 378.

[228] Sun, H.H.; Sakemi, S.; CA116:15810; US 5028613, A, 19910702, *US Pat. Appl.* (patent) **1991**, 7 pp.

[229] Ding, Q.Z.; Chichak, K.; Lown, J.W. *Curr. Med. Chem.* **1999**, *6*, 1.

[230] Swaffar, D.S.; Ireland, C.M.; Barrows, L.R. *Anti-Cancer Drugs* **1994**, *5*, 15.

[231] Barrows, L.R.; Radisky, D.C.; Copp, B.R.; Swaffar, D.S.; Kramer, R.A.; Warters, R.L.; Ireland, C.M. *Anti-Cancer Drug Des.* **1993**, *8*, 333.

[232] Matsumoto, S.S.; Haughey, H.M.; Schmehl, D.M.; Venables, D.A.; Ireland, C.M.; Holden, J.A.; Barrows, L.R. *Anti-Cancer Drugs* **1999**, *10*, 39.

[233] Kokoshka, J.M.; Capson, T.L.; Holden, J.A.; Ireland, C.M.; Barrows, L.R. *Anti-Cancer Drugs* **1996**, *7*, 758.

[234] Ozturk, T. In *Alkaloids;* Academic Press, New York, **1997**; Vol. 49, pp. 79.

[235] Sadanandan, E.V.; Cava, M.P. *Tetrahedron Lett.* **1993**, *34*, 2405.

[236] Yamada, F.; Hamabuchi, S.; Shimizu, A.; Somei, M. *Heterocycles* **1995**, *41*, 1905.

[237] Roue, N.; Barret, R. *J. Pharm. Belg.* **1995**, *50*, 94.

[238] Izawa, T.; Nishiyama, S.; Yamamura, S. *Tetrahedron Lett.* **1994**, *35*, 917.

[239] White, J.D.; Yager, K.M.; Yakura, T. *J. Am. Chem. Soc.* **1994**, *116,* 1831.

[240] Izawa, T.; Nishiyama, S.; Yamamura, S. *Tetrahedron* **1994**, *50,* 13593.

[241] Sadanandan, E.V.; Pillai, S.K.; Lakshmikantham, M.V.; Billimoria, A.D.; Culpepper, J.S.; Cava, M.P. *J. Org. Chem.* **1995**, *60,* 1800.

[242] Zhao, R.L.; Lown, J.W. *Synth. Commun.* **1997**, *27,* 2103.

[243] Iwao, M.; Motoi, O.; Fukuda, T.; Ishibashi, F. *Tetrahedron* **1998**, *54,* 8999.

[244] Kita, Y.; Egi, M.; Tohma, H. *Chem. Commun.* 1999, 143.

[245] Kita, Y.; Egi, M.; Takada, T.; Tohma, H. *Synthesis* **1999**, 885.

[246] Tao, X.L.; Nishiyama, S.; Yamamura, S. *Chem. Lett.* 1991, *10,* 1785.

[247] Roberts, D.; Venemalm, L.; Alvarez, M.; Joule, J.A. *Tetrahedron Lett.* **1994**, *35,* 7857.

[248] Roberts, D.; Alvarez, M.; Joule, J.A. *Tetrahedron Lett.* **1996**, *37,* 1509.

[249] Kraus, G.A.; Selvakumar, N. *Synlett* **1998**, 845.

[250] Kraus, G.A.; Selvakumar, N. *J. Org. Chem.* **1998**, *63,* 9846.

[251] Venemalm, L.; Estéves, C.; Alvarez, M.; Joule, J.A. *Tetrahedron Lett.* **1993**, *34,* 5495.

[252] Alvarez, M.; Bros, M. A.; Joule, J.A. *Tetrahedron Lett.* **1998**, *39,* 679.

[253] Roberts, D.; Joule, J.A.; Bros, M.A.; Alvarez, M. *J. Org. Chem.* **1997**, *62,* 568.

[254] Alvarez, M.; Bros, M.A.; Gras, G.; Ajana, W.; Joule, J.A. *Eur. J. Org. Chem.* **1999**, 1173.

[255] Peat, A.J.; Buchwald, S.L. *J. Am. Chem. Soc.* **1996**, *118,* 1028.

[256] Alvarez, M.; Ajana, W.; Balczewski, P.; Bros, M.A.; Roberts, D.; Venemalm, L.; Joule, J.A. In *Book of Abstracts, 2nd Euroconference on Marine Natural Products,* Spain **1999**, pp. 37-38.

[257] Makosza, M.; Stalewski, J.; Maslennikova, O.S. *Synthesis* **1997**, 1131.

[258] Kita, Y.; Yakura, T.; Tohma, H.; Kikuchi, K.; Tamura. T. *Tetrahedron Lett.* **1989**, *30,* 1119.

[259] Kita, Y.; Tohma, H.; Inagaki, M.; Hatanaka, K.; Kikuchi, K.; Yakura, T. *Tetrahedron Lett.* **1991**, *32,* 2035.

[260] Kita, Y.; Tohma, H.; Inagaki, M.; Hatanaka, K.; Yakura, T. *J. Am. Chem. Soc.* **1992**, *114,* 2175.

[261] Cheng, J-F.; Nishiyama, S.; Yamamura, S. *Chem. Lett.* **1990**, 1591.

[262] Tao, X.L.; Cheng, J-F.; Nishiyama, S.; Yamamura, S. *Tetrahedron* **1994**, *50,* 2017.

[263] Nishiyama, S.; Cheng, J-F.; Tao, X. L.; Yamamura, S. *Tetrahedron Lett.* **1991**, *32,* 4151.

[264] Kubiak, G.G.; Confalone, P.N. *Tetrahedron Lett.* **1990**, *31,* 3845.

[265] Knolker, H.J.; Hartmann, K. *Synlett* **1991**, 428.

[266] Moro-oka, Y.; Fukuda, T.; Iwao, M. *Tetrahedron Lett.* **1999**, *40,* 1713.

[267] Bakare, O.; Zalkow, L.H.; Burgess, E.M. *Synth. Commun.* **1997**, *27,* 1569.

[268] Barret, R.; Roue, N. *Tetrahedron Lett.* **1999**, *40,* 3889.

[269] Zhang, L.; Cava, M.P.; Rogers, R.D.; Rogers, L.M. *Tetrahedron Lett.* **1998**, *39,* 7677.

[270] Harvey, A.L. *TiPS* **1999**, *20,* 196.

[271] Henkel, T.; Brunne, R.M.; Müller, H.; Reichel, F. *Angew. Chem. Int. Ed. Eng.* **1999**, *38,* 643.